SOLID ORAL DOSAGE FORMS OF SPARINGLY SOLUBLE COMPOUNDS: ENHANCEMENT OF THEIR RELEASE PROFILES TO PREDICT BIOAVAILABILITY OF DISSOLUTION RATE LIMITED DRUGS

DARREN WAYNE MATTHEWS

Doctor of Philosophy

ASTON UNIVERSITY

December 2006

Aston University

Solid oral dosage forms of sparingly soluble compounds: enhancement of their release profiles to predict bioavailability of dissolution rate limited drugs

Darren Wayne Matthews

Doctor of Philosophy

2005

Two drugs, troglitazone and atovaquone, were selected based upon them being poorly soluble in aqueous media and being relatively lipophilic. These drugs were incorporated into solid dispersions, of various drug to polymer ratios, to improve their solubility. Three polymers were chosen to be the carrier in the solid dispersions; two gastric soluble polymers hydroxypropyl methylcellulose, polyvinylpyrrolidone and one enteric polymer, hydroxypropyl methylcellulose phthalate. Dissolution runs, in Fasted State Simulated Intestinal Fluid (FaSSIF), were performed upon the drugs, physical mixtures and the solid dispersions. The results showed that incorporation of the drug into the solid dispersion enhanced the dissolution of both drugs, the enhancement was more pronounced with troglitazone. Increasing the polymer:drug ratio and the polymer used had an effect upon the dissolution of the drugs. Physical characterisation of the dispersions showed that troglitazone was more compatible with the polymers than atovaquone.

Examination of the dissolution of troglitazone in various gastric media yielded the information that the selection of dissolution medium is important. Exposure of the troglitazone dispersions to gastric medium prior to dissolution in FaSSIF showed that there are advantages to using an enteric polymer. A computer model was derived in an attempt to predict the *in vivo* performance of the dispersions.

The influence of the carrier upon the dissolution of the drugs from a solid dispersion was investigated. It was shown that the polymers improved the dissolution rate of troglitazone when pre-dissolved. Investigation into the ability of each polymer at preventing the recrystallisation of the drug from a supersaturated solution found that polymers helped slow down the rate of re-crystallisation. Two methods were investigated, ultra-violet spectroscopy and micro-viscometry, to analyse the dissolution of the polymers. This showed that the troglitazone dispersions were, to some extent, controlled by the dissolution rate of the polymer, whereas the atovaquone dispersions were less controlled by the polymer dissolution.

Dedicated to Paul Michael Matthews (1978 – 1990)

You are 'always on my mind'

Acknowledgements

I would like to express my thanks to Professor Bill Irwin for his supervision, guidance, and patience. I also wish him happy and relaxing retirement. I am also thankful to Dr Barbara Conway for all the work she has done in ensuring that this thesis has been completed, without her advice and patient checking this would not have been completed. I would also like to thank Dr Hanna Batchelor for her advice, and the encouragement I have received from her. I would like to thank James Butler for his input, ideas and ensuring I always had the materials necessary. Dr Phil Neale and Dr John Hempenstall for their guidance, advice. Also a big thank you to Dr Angus Forster for helping me obtain some results, and for supplying me with some of my results at short notice. GlaxoSmithkline and the Biotechnology and Biological Sciences Research council for their financial support. I would like to express extreme gratitude to Chris Bache, and Jiteen Kansara for all the work that they put in during my time at Aston, ensuring that the equipment was working and that glassware etc. was clean and usable, so thank you very much I was more grateful than you can imagine (and I know I was not the easiest of people to have in the laboratory.)

Of course I would like to make a special mention to my fellow students, who made my time at Aston enjoyable and productive. Those people are as follows (and in no particular order): Sarah David, Sarah Atkinson, Andrew Ingham, and Afzal Mohammed. If it was not for you guys I may not have made it.

I would like to express my gratitude to Dr Mark Pellett for his patience whilst I have been writing up, and for giving me the chance to prove myself in industry. Following that I would like to say thank you to Chris Harrison, Chris Roper, Andrew Durber, Vicky Foot and Graham Baggaley for helping me settle in to Portsmouth whilst I have been writing up.

I would like to put a special mention to certain friends who are not connected to my work, but have a special place during this time. Firstly Ryan Noble, who has kept me grounded and sane during this period. Secondly Yulia Semanova, whose friendship and generosity have helped me through. Thirdly a special thank you to Asia, whose gentle encouragement over the last few months has helped me complete this; it is my turn to help you.

Finally, I would like to say a big thank you to my mother, Lesley Mapstone, for all her nagging over the last few years. If I am honest at this point you are always proved correct. Also thank you to my father William Matthews, for your support over the last few years. Finally thank you to Leanne Matthews, Malcolm Mapstone and Jackie Matthews.

Contents

List of Figures

List of tables

1 Introduction

1.1 Oral drug delivery systems

1.1.1 Anatomy and physiology of the stomach

The stomach has a characteristic J-shaped arrangement and is located in the left upper part of the abdomen, just below the diaphragm. The stomach, which connects the oesophagus and the duodenum, has four main functions. These functions are as follows:

1. To act as a holding area for recently eaten food.
2. To process this food into liquid chyme, from which the nutrients are far more easily absorbed in the small intestine.
3. To act as a regulator to the delivery of this chyme to the small intestine.
4. To produce acid in order to kill off any bacteria that is found on the food, and provide the correct pH for the enzyme pepsin to work.

1.1.1.1 Anatomy of the stomach

Through receptive relaxation, the stomach can adapt to hold increasing amounts of food, with it being able to accommodate volumes between 0.5 to 4 litres (Curtis and Barnes 1994). It is divided into three major regions: fundus, body and the pylorus region (figure 1-1). The curved uppermost part of the structure is the fundus. This region of the stomach provides slow continuous contractions, which has the effect of applying steady pressure to the gastric contents pushing them towards the pylorus region. Below this is located the largest part of the stomach, the body. The main role of this region is to act as reservoir for all the ingested food and liquids. The lowest area of the stomach is the pylorus region, which can be subdivided into the pyloric antrum, pyloric canal and pyloric sphincter. The pyloric antrum connects the body of the stomach to the pyloric canal, which in turn connects to the pyloric sphincter. The pyloric sphincter has two main functions. The first is to prevent large solid masses from leaving the stomach before suitable reduction in the particle size has been achieved. The second is to prevent reflux of the intestinal fluid,

which could damage the stomach lining. The ability of the pyloric sphincter to prevent the reflux of intestinal fluids has been shown to be affected by administration of oral anti-inflammatory drugs (Pantoja *et al.* 1979) and by the presence of a gastric ulcer (Valenzuela and Defilippi 1976).

Figure 1-1 Schematic diagram of the stomach (reproduced from Fox, 1996)

1.1.1.2 Histology of the stomach

The stomach wall can be divided into three main regions, the mucosa, the submucosa and the muscularis (figure 1-1).

The mucosa surface is a thick, vascular, glandular layer which is arranged in folds called rugae. The outer layer of the mucosa is lined with a single layer of columnar epithelial cells called the mucus cells. These epithelial cells also extend downwards to form gastric pits, which punctuate the mucosa (there are roughly 3.5 million of these gastric pits) (figure 1-2). Each gastric pit serves four columns of secretory cells called gastric glands. The gastric glands contain several types of different cells that secrete different products (table 1-1). These include the goblet cells, parietal cells and the chief cells, whose

secretions are released into the stomach lumen. Additionally, there are also endocrine-type cells known as G cells.

Table 1-1 The cells of the stomach and their secretions

Cell Type	Secretion	Region of stomach
Goblet cells	Mucus	Both the fundus and pyloric region
Parietal cells	Hydrochloric acid/ intrinsic factor	Fundus region only
Chief cells	Pepsinogen	Both the fundus and pyloric region
G cells	Gastrin	Pyloric region only

Figure 1-2 Schematic diagram of the gastric pits and the gastric glands of the mucosa (reproduced from Fox, 1996)

The submucosa consists of connective tissue, which connects the mucosa to the muscle layer. The muscle layer within the stomach is made up of three main layers: the outer longitudinal layer, a middle circular layer and the oblique layer.

1.1.1.3 Gastric secretions

During the course of a day, the stomach will produce up to 1.5 litres of gastric fluid, and four of the main constituents have a physiological action: mucus, hydrogen ions (hydrochloric acid), pepsin, and intrinsic factor (Table 1-1). The mucus covers the surface of the mucosa, and is secreted by the columnar epithelium cells. The main functions of the mucus are to improve movement of food masses within the stomach by lubrication, and to form a highly viscous protective barrier for the epithelium. It prevents the stomach from being either digested by the proteolytic enzymes and from the acidic conditions of the lumen. The protection from the acidic conditions is achieved by secretions into the mucus of bicarbonate ions, which meet with hydrogen ions diffusing from the lumen. This in turn sets up a pH gradient from pH 1-2 in the lumen to pH 6-7 at the cell surface (Williams and Turnberg 1981; Rees 1987; Bhaskar *et al.* 1992; and Desai and Vadgama 1992). The parietal cells secrete the hydrochloric acid into the lumen, and the main purpose of the hydrochloric acid is to convert pepsinogen into pepsin, kill any microbes and to denature proteins.

The process of gastric secretion can be broken down into three overlapping phases: the cephalic, the gastric (section 1.1.1.4) and the intestinal (section 1.1.2.3) phases. In response to the senses, taste, smell, sight and sound, the cephalic phase begins. This phase is reflex in origin and controlled by the vagus nerves. The secretions during this phase are highly acidic and rich in enzymes.

1.1.1.4 Gastric motility

The stomach has two main states, the fasted state and the fed state. The two states are self-describing; the fasted state is when the stomach is empty and the fed is after food is ingested. The type of motility pattern exhibited by the stomach depends upon which state the stomach is in. The fasted state is characterised by the migrating myoelectric complex (MMC) (figure 1-3), which provides strong contractions against the open pylorus to remove any residues left in the stomach after food digestion. The MMC consists of four distinct

phases which last from 60 – 120 minutes, and any of these phases can be interrupted by the introduction of food. In phase 1 there is only a small amount of activity, characterised by weak contractions. It is during phase 2 that the intensity of the contractions increases and the residues begin to be emptied from the stomach. The intensity of the contractions reach their peak during phase 3, expelling large particles (1.0 mm) that cannot usually go through the pylorus. During phase 4, the intensity of the contractions reduces back to the resting phase.

Figure 1-3 Diagrammatic representation of the MMC (reproduced from Washington *et al.* 2001)

As soon as food is introduced to the body, the secretion of gastric fluids begins. The greatest amount of secretory action lasts for about an hour after the ingestion of a meal. As the food enters the stomach, the fundus expands by relaxing the muscular wall, in order to compensate for the volume of ingested food. The stretch receptors are activated by this relaxation in the smooth muscle which in turn increases the amount of gastrin secreted. This increase in gastrin stimulates vigorous smooth muscle contractions within the

stomach. These contractions, which are characterised by a peristaltic wave, begin in the mid-body as shallow waves and they deepen and the velocity increases as they near the duodenum. These contractions serve to mix and propel the gastric contents, which are pushed ahead of the contractions, towards the gastroduodenal junction. This build up of the gastric contents increases the pressure within the antrum, and some of the gastric contents are evacuated into the duodenum. Before all the contents are evacuated the increase in the velocity of the peristaltic wave within this region, means that the wave overtakes the gastric contents. The result of this is that the majority of the contents are repulsed back into the stomach. This process is termed 'retropulsion' and it serves to mix the gastric contents and mechanically reduce the particle size of solids (Sanford, 1982). The process is shown in figure 1-4.

Figure 1-4 Diagrammatic representation of the process of 'retropulsion' (reproduced from Washington *et al.* 2001)

1.1.2 Anatomy and physiology of the small intestine

1.1.2.1 Anatomy of the small intestine

The small intestine, the longest section of the gastrointestinal (GI) tract, consists of three regions (figure 1-5); the duodenum (first 20-30cm), the jejunum (2.5 metres) and the ileum (3.5 metres). These areas are distinct by their properties. The duodenum is the only region that contains Brunner's glands, which produce an alkaline solution (consisting of bicarbonate) which neutralises the acidic gastric pH. The jejunum is the region where the majority

of absorption occurs, being the region that contains the most amount of villi. The ileum is characterised by the presence of Peyer's patches.

Figure 1-5 The locations of the three main regions of the small intestine (Blum patient and family learning centre, 2006)

1.1.2.2 Small intestine histology

The arrangement of the endothelium enhances the ability of the small intestine to absorb molecules by enhancing the surface area to 200 m^2 (figure 1-6). The surface area is enhanced by the folds of Kerckring, villi and microvilli.

The folds of Kerckring are a particularly prominent feature of the duodenum and the jejunum and are formed by the folding of the endothelium. Within the two regions they can protrude up to 8 mm into the lumen, and increase the surface area threefold.

The mucosa contains approximately five million villi, and these are located in the duodenum and the jejunum. The actual shape of the villi is dependent upon the region of the intestine; duodenal villi are shorter and broader than

those found within the jejunum. This difference allows for a functional difference between the two regions, the longer and thinner villi of the jejunum provide a larger surface area which is advantageous as the majority of absorption occurs within the jejunum.

Figure 1-6 How the folding of the endothelium increases the surface area of the small intestine (Washington *et al.* 2001)

1.1.2.3 Small intestine physiology – secretions and motility

1.1.2.3.1 Secretions into the small intestine

There are three main secretions into the small intestine: from glands found in the small intestine, pancreatic secretions, and biliary secretions.

Glands

There are two main types of glands found within the small intestine; the Brunner's glands (discussed in section 1.1.2.1) and the intestinal cells. The intestinal cells secrete mucus and a few enzymes, and are found all through the small intestine.

Pancreatic secretions

The pancreatic secretions consist of two major parts, alkaline fluid and enzymes. The pH of the chyme released from the stomach controls the aqueous and bicarbonate secretions from the pancreas. The secretion of the enzymes from the pancreas is determined by the level of fat and protein entering the small intestine.

Figure 1-7 The intestinal villus (reproduced from Fox, 1996)

Biliary secretions

It is the liver that secretes the bile necessary for the digestion and absorption of lipids, and also aids the dissolution of hydrophilic drugs (section1.2.4). The bile is composed of a mixture of bile salts, phospholipids, cholesterol and

bilirubin. The two main bile salts in humans are cholic acid (figure 1-8) and chenodeoxycholic acid (figure 1-8), both of which are derivatives of cholesterol. It can be seen from figure 1-8 that both bile salts have polar and non-polar regions; this allows the bile salt to have both a hydrophilic and hydrophobic face (figure 1-8). Such molecules are termed amphipathic, and are dealt with in more detail in section 1.2.2.2. The amphipathic nature of the bile salts allows it to perform two main functions; the first is the emulsification of the fat content of the food, making small fat droplets. The second is to assist the absorption of fatty acids, cholesterol and other fatty acids, by forming mixed micelles with the fatty acids, with the hydrophobic regions solubilising the fatty acids.

Figure 1-8 Structure of A) chenodeoxycholic acid (Wikipedia 2006), B) cholic acid (Wikipedia 2006), and C) a side on of cholic acid showing the hydrophobic and hydrophilic face (adapted from Newarkbioweb, 2006)

Volume

Over the course of 24 hours there is approximately 1-2 litres of pancreatic juice secreted into the duodenum. The amount of bile secreted into the intestine equals up to 600 ml a day (Diem and Lenter 1974). In addition to

these secretions the intestine secretes up to 1 litre of water, as a component of the mucus. The majority of this secretion occurs after the ingestion of a meal (Dressman *et al.* 1998). Using perfusion studies Dillard *et al.* (1965) showed that the volume of fluid present in the intestine is between 120 – 350 mL in the fasted state. However, it was shown in a study by Fordtran and Locklear (1966) that the volume can increase up to around 700 – 800 ml after the ingestion of a meal. This was also found to be dependant upon the meal type, if a hypotonic meal is eaten (in the study it was a meal of steak and water) the amount of fluid found in the intestine could be as low as 500 ml. this is due to there being net absorption of the water from the meal across the mucosa into the intestinal cells (Dressman *et al.* 1998).

1.1.2.3.2 Composition of secreted intestinal fluids

Table 1-2 pH in the small intestine in humans, in both fed and fasted states (adapted from Dressman *et al.* 1998). pH was measured using a pH sensitive Heidleburg capsule (Evans *et al.* 1988, Dressman *et al.* 1991 and Russell *et al.* 1993)

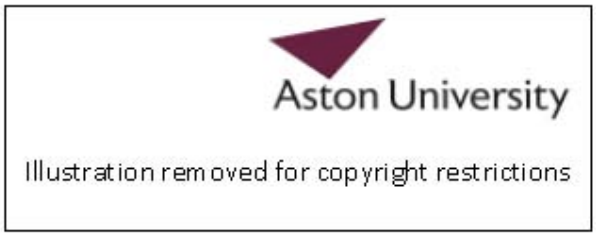

pH

As outlined in section 1.1.2.3.1, the pancreas secretes bicarbonate ions into the intestine in response to the acidic fluid coming from the stomach. This has the effect of neutralising the stomach acid, thus increasing the pH in the

intestine. Studies investigating the pH in the intestine have shown that there is a difference between the pH of the intestinal fluids in the fasted state compared to that of the fed state (table 1-2). The pH of the fasted state is on average a pH unit higher than that found in the fed state, when measured from the mid-duodenum to the ileum (Dressman *et al.* 1998). The decrease in pH that is experienced in the fed-state is due to the ingested meal buffering the effect of the carbonate ions.

Surfactants

As described in section 1.1.2.3.1, the liver secretes bile salts into the intestine, which have the effect of lowering the surface tension of the intestinal fluid, thus improving the wetting of drugs. It has been found that the fasting bile salt concentration in the intestine is about 3 – 5 mM (van Berge Henegouwen and Hofmann, 1978; Peters *et al.* 1980; Tangerman *et al.* 1986; and Marzio *et al.* 1988). This concentration, along with the secreted lecithin, is sufficient to form mixed micelles (section 1.2.2.3).

It is found that in the fed state the level of bile salts increases when compared to the fasted state. The mean concentration of bile salts increases to about 15 mM in the proximal small intestine. This increase in the bile salt concentration is due to the release of two hormones (secretin and cholecystokinin (CCK)) from the duodenum, in response to the acidic chyme entering the small intestine. These hormones have the effect of stimulating secretion of bile salts and stimulating the gall bladder to contract (Fox, 1996).

1.1.2.3.3 Small intestine motility patterns

In the fed state, the small intestine displays two main forms of contraction: segmental and peristaltic contractions, with segmental contraction being more frequent. Segmental contractions occur when a segment of the small intestine (about two centimetres in length) contracts and the sections next to it remain relaxed. This then reverses, so that the contracted part relaxes and the relaxed parts contract. This gives an overall effect of mixing up the chyme within the lumen, and allows for more contact of the food with absorbing

surface of the GI tract.

1.1.2.3.4 Small intestine transit times

The actual transit time of a meal in the small intestine has provoked some controversy. It was reported by Kerlin and Phillips (1983) that there is a differential transit time for different components. There was evidence to suggest that residues of a meal left the intestine within 2 – 12 hours. Malagelada *et al.* (1984), though, could not find any difference in the intestinal transit times between various meals.

In a review by Davis *et al.* (1986) it was stated that the actual transit time of a dosage form is four hours. This was independent of the type of dosage form (pellet, solution or a single unit) and whether the intestine was in the fed or fasted state. However, the fed or fasted state of the GI tract does affect the action of a dosage form. It was shown by Hunter *et al.* (1982) that during the fasted state a digested formulation exits the stomach in the form of a bolus, the consequence of this is that the drug is poorly dispersed in the small intestine. Feinblatt and Ferguson (1956) found that the dispersal of a pelleted drug was increased in the fed state. This was due to the drug dispersing within the food during its time in the stomach. This mixing of the drug is particularly important for those drugs that have a low solubility or a low permeability through the endothelium. It was also shown that a monolithic formulation (*i.e.* one designed to not disintegrate) is expelled during phase three of the MMC (figure1-3). As the administration of a drug is not synchronised to any phase of the MMC the exit time can be very erratic, ranging from a few minutes to 3 hours. These formulations are then carried through the small intestine as a single unit, thus reducing mixing with intestinal fluids (Washington *et al.* 2001).

Figure 1-9 Fate of a tablet after oral administration (reproduced from Aulton 2002)

1.1.3 Fate of oral delivery systems in the GI tract

Figure 1-9 shows an outline of the possible fate of an orally administered tablet. As shown, a tablet has to go through several steps before the drug can enter the systemic circulation. The steps can all be described as being rate processes, with some steps being faster than others. The slowest rate, as expected, is known as the rate-determining step for the delivery of the drug. So, for a sparingly soluble drug, it is generally accepted that the dissolution of the drug into the intestinal fluids is the rate-determining step. For a sparingly soluble drug there are various methods by which the solubility or dissolution rate can be increased (section 1.3). There are many factors that can influence the rate and extent at which a drug enters the systemic system, these can be

classed by the following three categories: physico-chemical (section 1.2), physiological (section 1.2) and formulation (section 1.3).

There are other factors that can also affect the systemic concentration of a drug, that are not to do with the physico-chemical properties. One such factor is the degradation of the drug in the intestinal fluid (drugs that show this effect include insulin (Iwanaga *et al.* 1997); this would create a scenario where there would be less of the drug available for absorption into the systemic system. There is also the scenario where the drug can be metabolised and eliminated before distribution of the drug in the systemic system thus lowering the systemic concentration.

Different dosage forms can be used to deliver the drug orally, some examples are as follows: liquids, suspensions, soft gelatin capsules and hard gelatine capsules. There are different implications, with regard to the delivery of the drug, associated with each delivery system. For example, when a liquid formulation is used the drug is presented to the GI tract in solution, thus leading to faster therapeutic response. This bypasses the need for tablet disintegration, and the subsequent dissolution of the exposed drug particles. Even if the drug precipitates out in the gastric environment (*i.e.* due to the acidic conditions) the resulting crystals will have a very small particle size and wetted sufficiently for rapid dissolution to occur in the intestine. In the instance of a soft gelatin capsule the drug is again already in solution, the gelatine shell rapidly dissolves in the gastric juices releasing the contents of the capsule. Depending on the nature of the fill material of the capsule the drug is either emulsified with the gastric fluid, or solubilised by the fill.

1.2 Factors affecting drug dissolution and solubility

1.2.1 Thermodynamic fundamentals behind solubility and dissolution

Prior to any review on the main factors that affect the solubility and the dissolution of a substance, thermodynamic background to the process should be described. The first aspect of note when a solute dissolves into a solvent is that, although an increase in volume occurs, the expected increase in

volume is not achieved (Aulton 2000). This therefore indicates that that there is some form of inter-molecular attraction occurring between the solute and the solvent molecules. In order for this process to occur in a spontaneous manner the change in Gibbs free energy (ΔG) must be of a negative value. The Gibbs free energy of a system is described by equation 1-1; where ΔH is the change in enthalpy of the system (the amount of heat absorbed or evolved during the process), T is the temperature of the system, and ΔS is the change in entropy (measure of disorder) of the system.

Equation 1-1

$$\Delta G = \Delta H - T\Delta S$$

If the above equation 1-1 was applied to an ideal solution, one where no intermolecular interactions occurred, then it would be expected for ΔH to be 0. This would mean that the ΔG would be totally reliant on TΔS.

As previously outlined, in a real solution there are intermolecular interactions between solute and solvent. During a process such as dissolution it is expected that the entropy of a system will be positive; this means that the TΔS term of equation 1-1 would be expected to be positive in the majority of cases. The follow on from this is that for a process to occur spontaneously ΔH would have to be negative, or if it is positive it has to be less than TΔS.

Equation 1-2

$$\Delta H = \Delta H_{cl} + \Delta H_{solv}$$

The term ΔH is made up of two components, defined in equation 1-2; the change in crystal enthalpy (ΔH_{cl}), the energy absorbed when the crystal structure of a substance is broken apart, and the enthalpy of solvation (ΔH_{solv}), the energy absorbed when the solute molecules are absorbed into the solvent. ΔH_{cl} is always positive and ΔH_{solv} is negative, and it is generally found that ΔH_{cl} is greater than ΔH_{solv}; therefore this means that in most cases

ΔH is positive. This means that during the process of dissolution heat is absorbed and the process is endothermic.

ΔG from equation 1-1 is a measure of how much energy is available for the work to be performed (in this case the dissolution of a drug into a solvent). As the drug dissolves into the solvent ΔG decreases, until it reaches 0. When $\Delta G = 0$ the system is said to be at equilibrium, and there is no more energy left in the system for dissolution to occur. The saturated solubility of a drug, therefore, can be considered as an equilibrium between the dissolved and undissolved drug.

1.2.2 Factors affecting the solubility of solids in liquids

As described in section 1.2.1, the amount of energy available to the system effectively controls the solubility of a drug. The factors that control the amount of energy available are reviewed.

1.2.2.1 Temperature

The way in which temperature can affect the solubility of a drug can be described by Le Chatelier's principle – 'If a dynamic equilibrium is disturbed by changing the conditions, the position of equilibrium moves to counteract the change.'

An increase in temperature is a change in conditions which will disturb the established equilibrium. The effect of increasing temperature increases the $T\Delta S$ term, from equation 1-1, this has the effect of reducing the effect ΔH_{cl} has upon the dissolution of a drug. This is because, even though there is a temperature change ΔH_{cl} will remain constant. Examination of equation 1-1 shows that if $T\Delta S$ is increased and ΔH_{cl} held constant he ΔG value will be reduced (allowing more energy into the system).

In the converse situation a substance that dissolves *via* an exothermic route will display reduced solubility in a solution at higher temperature. Shown in figure 1-10 is the effect of temperature on the solubility of some compounds. This diagram shows compounds that display both exothermic and

endothermic properties.

Figure 1-10 The solubility of various substances in water, showing the dependence of their solubility on temperature (reproduced from Aulton 2000)

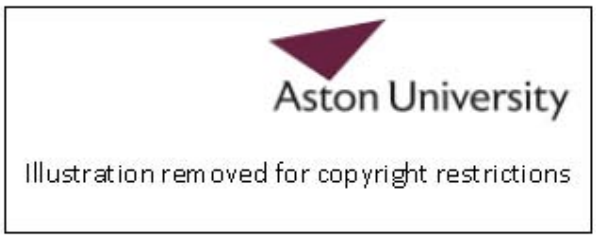

1.2.2.2 Wettability of the drug powder

Wettability describes the degree with which water (or another liquid) will spread across a surface, thus it indicates how much of a given surface will be covered by the given liquid. It is commonly expressed as an angle (contact angle), with the lower the angle the higher the wettability (figure 1-12). It is an important factor to consider for the dissolution of drugs, as the lower the contact angle the higher the surface area of the drug exposed to the dissolving liquid (it is discussed in section 1.2.3 the importance of surface area for dissolution). Before describing how the wettability of a powder can affect the solubility, it is necessary to consider theory behind the interfaces that are formed during the process of drug dissolution. For pharmaceutical powders, generally only two interfaces are considered solid/air (S/A) and

solid/liquid (S/L). It is the properties at these interfaces that can determine the solubility of a drug in a given solute, and knowledge of this behaviour can be exploited for enhancement of the performance of a drug.

In order to examine the effects that occur at an interface it is useful to consider a liquid in equilibrium with its vapour phase (thus there is a liquid/vapour interface). A liquid in this state will adopt a spherical formation, this minimises the surface to volume ratio. In order to achieve this formation the molecules at the surface are at a higher free energy than those in the bulk of the liquid, and this is due to the attraction forces that are applied to these molecules. Those molecules found in the bulk of the drop are surrounded by the same molecules, so thus are subjected to the same attractive force from all directions. This though is not the case with the molecules found at the interface as they are not surrounded by equal molecules, and so therefore not subjected to equal forces. They are in fact subjected to a net inward attraction; this places the molecules at the surface under a stress which is commonly referred to as surface tension. There is also another term used to refer to the forces acting at the interface, and that is the surface free energy – this refers to the change in free energy required to maximise the surface area at an interface.

In terms of applying this theory to dissolving drugs, three interfaces are formed for a partially immersed solid, and these are at the L/A (liquid/air), S/L and S/A (shown in figure 1-11). This type of wetting is known as immersional wetting, and this is the initial wetting that occurs with a solid when it is initially placed into a liquid. The important angle to consider is the one the solid makes at the L/A interface, the smaller this angle the easier the solid is to wet. The process of immersional wetting is described fully by equation 1-3.

Equation 1-3

$$-\Delta G_i = \gamma_{SA} - \gamma_{SL} = \gamma_{LA} \cos \theta$$

where γ is the surface tension at the interface.

From this equation if γ_{SA} is > γ_{SL} then $\theta<90°$ and the immersional wetting is spontaneous. If the reverse is true, and $\theta<90°$ then the process of immersion is not spontaneous and work is required to immerse the powder.

Figure 1-11 The process of immersion wetting, showing the three interfaces that are formed during this process; *i.e.* S/A, L/A, S/L

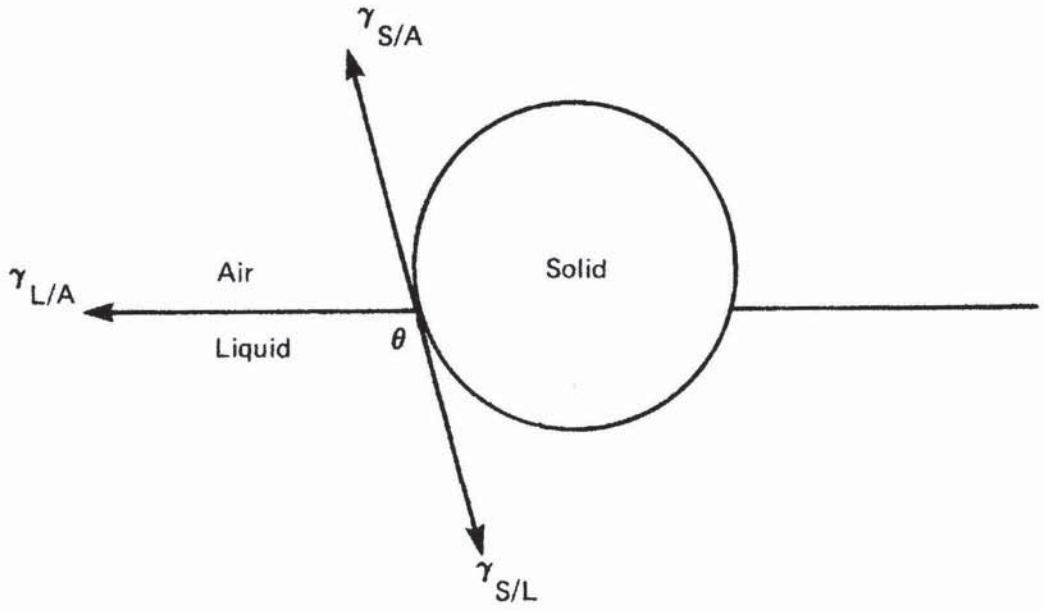

The next stage in the wetting procedure is described as spreading wetting, and this is where the liquid spreads across the surface of the solid. This is influenced by the angle that the solid makes with the liquid, this angle is known as the contact angle. It is shown in figure 1-12 how the contact angle influences the spreading wetting. The smaller the contact angle the more solvent there is in contact with the solid, thus there is more wetting occurring. Whereas, if the contact angle increases, less of the solvent is in contact with the solid, thus not much wetting occurs.

Figure 1-12 The influence of contact angle upon the spreading wetting of a solid by a solvent; a) showing a solid easily wet by the solvent, b) showing a solid that is not easily wet by the solvent. (adapted from Aulton, 2000) (L/V – Liquid/vapour (air) and S/V – solid/vapour (air))

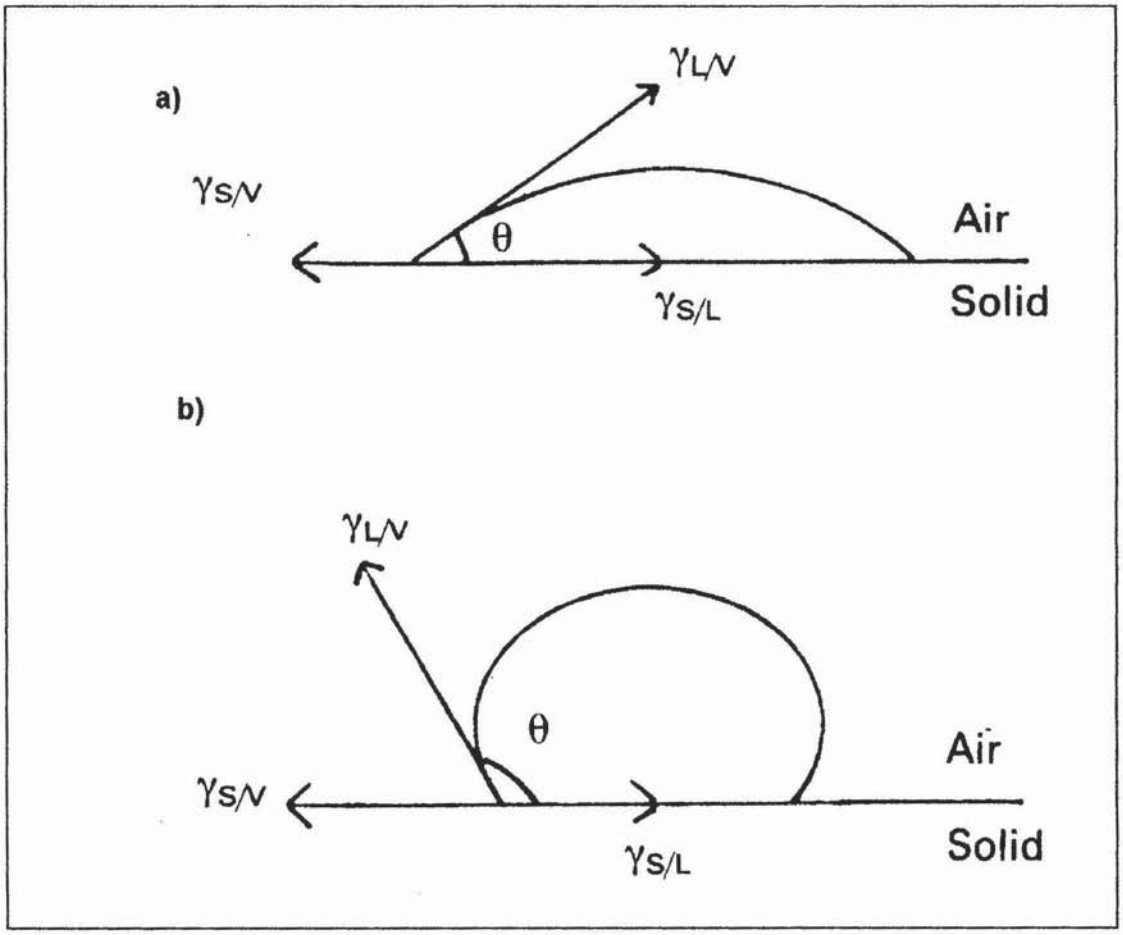

Therefore, in order to improve the dissolution of a drug in a given solvent (e.g. water) it is necessary to improve the wetting of the drug, and try and lower the contact angle so that it is nearer zero. Modification of the surface or the crystal structure of the drug are not simple methods of lowering the contact angle, so therefore a surface active agent (or surfactant) can be added to the solvent (Florence and Attwood 1988). A surfactant is a substance that can reduce the tension at a given surface.

Surfactants commonly consist of two main components, a lyophobic group (hydrophilic) and a lyophilic group (hydrophobic). Molecules with such dual nature are termed amphipathic. Due to this dual nature, it is favourable for these compounds to organise themselves at a phase boundary, aqueous/non-

aqueous for example, with the lyophobic region interacting with the aqueous phase and the lyophilic region interacting with the non-aqueous phase (as shown in figure 1-13).

Figure 1-13 The orientation of surfactant molecules at a phase boundary (reproduced from Aulton, 2000).

This accumulation of the surfactants at the phase boundary causes an expansion at the boundary which in turn reduces the surface and interfacial tension at the L/A interface. Secondary to this, the surfactants can also adsorb to the surface of a hydrophilic powder, thus reducing the solid/liquid interface. This then reduces the contact angle, and thus improves the ability of a solvent to wet a particular solid powder.

1.2.2.3 Solubilisation

As outlined in section 1.2.2.2, the addition of a surfactant in low concentrations can help lower the surface tension of a solvent and thus improve the wettability of a powder. There is a second mechanism by which surfactants can help improve the solubility of hydrophobic compounds, and that is through solubilisation. When a surfactant is added to a solvent at a particular concentration (the critical micelle concentration (CMC)), the surfactant can form what are called micelles.

A micelle is where the surfactant aggregates together to give (in aqueous media) a structure where there is a hydrophobic core and the outer part is hydrophilic. The main reason behind the formation of these micelles is the

achievement of a state of minimum free energy. The free energy, enthalpy and entropy are all related by equation 1-1. In these surfactant systems, it is the change in entropy that determines the free energy.

Figure 1-14 Diagram of Hartley's micelle, showing the polar groups on the outside, and the hydrophobic core (reproduced from Aulton, 2000)

The entropy change is caused by the effect the surfactants have upon the structure of water. Due to the hydrogen bonding present in water, water has a reasonably high degree of structure. Upon the addition of a surfactant two effects can occur. The hydrophilic region of the surfactant will cause disruption to the water structure, but this disruption is compensated by the fact that the ionic regions can form ionic interactions with the water molecules. The other effect involves the hydrophobic region of the surfactant, with the dissolution of this region being resisted by the water. This causes the water molecules to form clusters around this region. This change in alignment of the water molecules causes a negative entropy change; to counteract this change, the hydrophobic regions withdraw from the aqueous phase. This is achieved by the molecules orientating themselves at an interface, so that the hydrophobic region associates with the non-aqueous phase. As the concentration of the surfactant increases, this orientation at the interface becomes inadequate to achieve the state of minimum free energy. At a specific concentration of the surfactant (the CMC), the surfactants remove their hydrophobic regions from the aqueous phase by self aggregation. The aggregates that are formed are termed micelles, and in an aqueous solution

they consist of a hydrophobic core and the polar groups are on the outside as shown in figure 1-13 (which allows for the solubility in the water to be maintained).

Micelles can also be formed from non-ionic surfactants, non-ionic surfactants primarily consist of a hydrocarbon chain and oxyethylene side chains chains. The micelles that are formed from such surfactants, in aqueous media, have a hydrophobic core, which is surrounded by a layer of the oxyethylene groups, which is termed the palisade layer (Aulton, 2005). These oxyethylene chains hydrogen bond with the surrounding water molecules, thus producing hydrated micelles.

This hydrophobic core of the micelles has the properties of a liquid hydrocarbon, and thus can dissolve materials that are considered insoluble in water. Increase in solubility is attributed to micelle formation, as after the CMC the increase in drug that is dissolved increases exponentially with the increase in surfactant concentration (Aulton, 2005).

1.2.2.4 Effect of pH

If the drug in question is a weak acid or weak base, then an equilibrium exists between drug in the ionised and unionised state. This is represented (for both a base and acid) by equations 1-4 and 1-5 below:

Equation 1-4

$$HA \rightleftharpoons H^+ + A^-$$

Equation 1-5

$$B + H^+ \rightleftharpoons HB^+$$

The dissociation constant for the weak acid (K_a) is defined by equation 1-6:

Equation 1-6

$$K_a = \frac{[H^+][A^-]}{[HA]}$$

Taking logarithms of both sides of the equation yields equation 1-7:

Equation 1-7

$$\log K_a = \log [H^+] + \log [A^-] - \log [HA]$$

Reversal of the symbols in this equation yields equation 1-8:

Equation 1-8

$$-\log K_a = -\log [H^+] - \log [A^-] + \log [HA]$$

The –log K_a, like pH, can be represented by the symbol pK_a, so equation 1-8 can be written as:

Equation 1-9

$$pK_a = pH + \log[HA] - \log [A^-]$$

or

Equation 1-10

$$pK_a = pH + \log \frac{[HA]}{[A^-]}$$

The terms [HA] and [A^-] in equation 1-10 can be described by the terms C_u and C_i, where C_u represents the concentration of the unionised drug and C_i represents the concentration of ionised drug. When these terms are utilised the equation (1-11) is termed as the *Henderson-Hasselbalch equation*.

Equation 1-11

$$pK_a = pH + \log \frac{C_u}{C_i}$$

As is seen by equation 1-11, there will be varying amounts of unionised drug at different pHs for drugs that can be ionised (*i.e.* this occurs only for acidic or basic drugs, and not for neutral drugs). So at a high pH there will be more ionised drug, for an acidic drug. At this high pH it is expected that the solubility of the weakly acidic drug will be higher due to the ionised species being more readily hydrated by the water molecules.

Equation 1-11 can be modified so actual solubilities at specific pH can be calculated. If the total solubility of the drug of the drug is represented by S, and the solubility of the unionised form represented by S_0, it can be written:

Equation 1-12

$$S = S_0 + (\text{concentration of ionised species})$$

The subsequent rearrangement of equation 1-6, with the substitution of S_0 for [HA], and $S\text{-}S_0$ for $[A^-]$, yields:

Equation 1-13

$$\frac{K_a}{[H^+]} = \left\{\frac{S - S_0}{S_0}\right\}$$

Taking logarithms yields:

Equation 1-14

$$pH - pKa = \log\left\{\frac{S - S_0}{S_0}\right\}$$

A similar derivation is obtained for weak bases:

Equation 1-15

$$pH - pKa = \log\left\{\frac{S_0}{S - S_0}\right\}$$

Equation 1-14 shows that the solubility of a weakly acidic drug will increase exponentially with increasing pH above the pKa. Equation 1-15 shows the reverse situation that as the pH decreases below the pKa the solubility of a weakly basic drug will increase exponentially.

1.2.2.5 Crystal characteristics – polymorphism, amorphous and solvates

It is possible to vary the conditions of the crystallisation of some substances so that the constituent molecules align themselves differently in relation to the original lattice. These different crystalline structures are called polymorphs, and due to this they have different lattice energies. This in turn has an influence on the solubility of the substance. The influence of the lattice energy upon the solubility of a substance is described by equation 1-2 by the term

ΔH_{cl}. Examination of equations 1-1 and 1-2 indicates that a polymorph with a low ΔH_{cl} will yield a higher free energy than a polymorph with a high ΔH_{cl}. This means that the polymorph with the lower ΔH_{cl} is expected to be more soluble than the other. The downside of this is that the polymorph with the low ΔH_{cl} is considered to be metastable and will eventually convert to the more stable form upon storage.

Those polymorphs with higher lattice energy, and thus more stable, are generally found to have higher melting points (Shibata *et al.* 1983; Behme *et al.* 1985). The melting point of a polymorph can be a good indicator to the solubility of each form, with the melting point of the polymorph being inversely proportional to the solubility of the form.

As well as having different crystal structures, it is possible for the compound to have no crystal structure, and exist in an amorphous state. This of course will reduce the lattice energy to zero, thus increasing the free energy of the system further. A simple method of preparing an amorphous drug is through the utilisation of solid dispersions, to attempt stabilisation of the amorphous form (Chiou and Riegelman, 1971, and Mosharraf *et al.* 1999), and these will be described in section 1.3.2.

1.2.3 Factors affecting the dissolution rate of drugs – *in vitro*

A simple equation to describe the dissolution of a substance is the Noyes-Whitney equation (equation 1-16). This describes the dissolution of substance when there is the absence of a chemical reaction between the solute and solvent, and the diffusion of the solute across the static boundary layer is the slowest step (Aulton 2000).

Equation 1-16 Noyes-Whitney equation describing the dissolution process

$$\frac{dm}{dt} = kA(C_s - C)$$

where dm/dt is the rate of dissolution, A is the surface area, C_s is the concentration of solute required to make a saturated solution, C is the

concentration at time t, and k is the dissolution rate constant.

Surface area (A)

From equation 1-16, it is noticeable that an increase in the surface area of a drug will increase the dissolution rate. The available surface area of a drug for dissolution is affected by three main factors: the particle size, the dispersion of the powder in the dissolution medium, and the porosity of the particles.

The available surface area is inversely proportional to the particle size, so therefore reducing the particle size of a drug should increase the dissolution rate. Studies on the drug griseofulvin, which is a drug where the dissolution rate is the limiting factor to bioavailability, show how particle size can affect the dissolution rate of the drug. Studies have been conducted that investigated the bioavailability of micronised griseofulvin *versus* a larger particle size. The results showed that similar blood levels were obtained for the micronised drug when only 50% of the dose of the larger particles was employed (Atkinson *et al.* 1962). Further studies highlight this effect for griseofulvin and an unnamed drug, where it was shown that the dissolution rate increased as the particle size decreased (Lin *et al.* 1968). It was also observed in this study that particle size reduction can also cause a reduction in dissolution rate, as the micronised drug actually showed a slower dissolution rate than the un-milled drugs. This was attributable to the drug having a higher affinity for other drug particles than with the dissolution medium. The outcome of this attraction is that the drug can form agglomerates which are larger than the un-milled drug particles. The main interactions that can influence this attraction are Wan der Vaals interactions, and in the case of charged particles electrostatic interactions can occur. Some of the factors that contribute to this are as follows; surface morphology, surface roughness and surface hydrophobicity (Eve *et al.* 2002). It can be understood by this that hydrophobic drugs would be the more likely to be affected by such an effect.

A further part of the study conducted by Lin *et al.* was to add a small amount of surfactant (0.05% w/v lysolecithin) to the original dissolution medium, in

order to provide better dispersal of the particles in the dissolution medium. The first result of note from doing this was that the dissolution rates were in the order of the particle size for both drugs (i.e. micronised > 20/40 mesh> 12/16 mesh for griseofulvin). Also, the micronised drug, when dispersed in the original dissolution medium, formed large agglomerates, whereas when the lysolecithin was added the particle size obtained was as expected. This, of course, is attributed to the improvement in wetting, which is obtained through the addition of a surfactant into the dissolution medium (section 1.2.2.2). The effects of surfactant addition to dissolution medium will be discussed in more depth in section 4.2.

Reduction in particle size has also been used to attribute the increase in dissolution rates experienced by eutectic mixtures, which form very fine crystals upon formation; this is discussed in more depth in section 1.3.2.1.

Saturated solubility (C_s)

From equation 1-12, it is noticeable that a higher saturated solubility of a drug within a given dissolution medium will yield a higher dissolution rate. The factors that affect the saturated solubility of a drug in a given dissolution medium are outlined comprehensively in section 1.2.1.

Concentration (C)

The volume of the dissolution medium affects this parameter with regard to the dissolution rate. The equation predicts that as C nears C_s, the dissolution rate slows down; therefore using a large volume of dissolution medium would mean that it is less likely for C to near C_s. It is therefore common to conduct dissolution experiments under what is termed 'sink' conditions. In this condition, the value of C can be considered negligible compared to the saturated solubility. It is generally accepted that the maximum value of C should be 10 times less than C_s value. When a dissolution experiment is conducted under 'sink' conditions the term (C_s-C) can be simplified to the term C_s.

However, there are dissolution experiments are performed that aim to model

the physiological conditions of either the stomach or the intestine. In these instances physiological relevant volumes of dissolution medium are employed. As stated in section 1.1.2.3.1 typical volumes of intestinal fluids found *in vivo* are 120 -300 ml in the fasted state and up to approximately 800 ml in the fed state. These volumes do not take into account any co-administered fluids with the dosage form, as it is typical to have some form of drink to aid the taking of a tablet. Typically around 200 ml of fluid is co-administered with a dosage form (Dressman *et al.* 1998), this would mean that for a dissolution test aiming to mimic the *in vivo* conditions around 500 ml of dissolution media would be required for the fasted state and 1 litre for the fed state. In these conditions, it can be rare to achieve 'sink' conditions, especially in the case of sparingly soluble drugs. If 'sink' conditions were required for the dissolution test one method that has proved effective is to add a surfactant to the dissolution medium (Anderberg *et al.* 1988), this would increase the solubility of the drug in the given media (section 1.2.2.3).

1.2.3.1 Intrinsic dissolution rate (IDR)

The IDR is related solely to the solubility of a drug within a given media, and it differs from the general rates that are obtained from dosage forms in that the exposed surface area is kept constant. This rate is, therefore, unaffected by formulation effects. The IDR is, however, found to be affected by two main parameters, the diffusion of the drug in the given medium and the thickness of the diffusion layer

The IDR is found to be proportional to the diffusion of the drug in a given medium. This in turn means that it is indirectly proportional to the viscosity of the dissolution medium. The other factor that controls the diffusion of the drug in the given medium is the size of the molecule – the larger the molecule, the slower the diffusion, thus the lower the IDR.

The IDR is also indirectly proportional to the thickness of the diffusion layer. The thickness of the diffusion layer is controlled by the hydrodynamics of the system. With an *in vitro* system this is controlled by the following factors; stirrer rate, stirrer position, viscosity of the medium, shape of the vessel and

volume of the medium present.

1.2.4 Factors affecting the dissolution rate of drugs – *in vivo*

The dissolution of a drug in an *in vivo* system can be also described using the Noyes-Whitney equation. The Noyes Whitney equation, with the Nernst-Brunner and Levich modifications is shown in equation 1-17, here k has been substituted by D/δ, (Attwood and Florence, 1988). This form of the equation is considered to be more appropriate when describing dissolution *in vivo* as it identifies more of the parameters involved in dissolution than the unmodified version (Dressman and Reppas, 2000). This format of the equation allows for the examination of the physiological factors that affect the dissolution of a drug in the GI tract. Table 1-3 summarises the physiological factors that affect the dissolution of drugs within the GI tract.

Equation 1-17 Noyes-Whitney equation, based on the Nernst-Brunner and Levich modifications (reproduced from Dressman *et al.* 1998)

$$\frac{dX_d}{dt} = \frac{AD}{\delta}(Cs - X_d/V)$$

Where A is the surface area of the drug, D is the diffusion co-efficient of the drug, δ is the effective diffusion boundary layer thickness, C_s is the saturated solubility, X_d is the amount of drug already in solution and V is the volume of medium.

Table 1-3 Physiological factors that affect the different aspects of the Noyes Whitney equation in the GI tract

Factor	Physiological factor affecting parameter
Surface area	Surfactants in gastric juice and bile
Diffusion co-efficient	Viscosity of the luminal contents
Boundary layer thickness	Motility patterns and flow rate
Solubility	pH, buffer capacity, bile and food components
Amount of drug dissolved	Permeability
Volume of medium	Secretions and co-administered fluids

1.3 Methods for enhancing the solubility of drugs

1.3.1 Overview of formulation techniques and associated problems

Table 1-4 Table showing various formulation techniques used to improve the solubility of sparingly soluble drugs (adapted from Dressman and Luner 2000)

It is shown in sections 1.1 and 1.2 that the solubility or the dissolution rate can have a major impact upon the amount of drug available for a pharmaceutical effect. There have been various strategies employed to enhance the dissolution rate or the solubility of sparingly-soluble drugs (*i.e.* a drug is considered to be sparingly soluble if the highest dose is not soluble in 250 ml of aqueous media over a pH range of 1 – 7.5 (FDA, 2000)), these are listed in table 1-4. How polymorphs and particle size reduction have been used in formulations of sparingly-soluble drugs is described in sections 1.2.2.5 and1.2 .3 respectively.

1.3.1.1 Complexation

The formation of a complex with a water soluble complexation agent has been shown to enhance the dissolution of sparingly soluble drugs, and among the commonest complexation agents used are the cyclodextrins. The main principle behind cyclodextrin complexes is that the core of the cyclodextrin is hydrophobic: this can then bind to the hydrophobic region of the drug forming a complex (Florence and Attwood 1988). These complexes are soluble in the fluids in the GI tract, and after dissolution the drug is liberated from the complex where absorption can occur. Thus an important property of the complex is that it is reversible.

Pitha and Pitha (1985) demonstrated how the use of cyclodextrin complexes can increase the solubility of sparingly soluble drugs. A range of steroids were shown to have an increased solubility in an aqueous solution of cyclodextrins. The resulting solutions were then freeze-dried with the solid being compressed into tablets. Dissolution of these tablets showed a marked improvement over the dissolution of the steroid in water when compared to a tablet prepared with the steroid and a cellulose mixture.

1.3.1.2 Prodrugs

The definition of a prodrug is a 'bio-reversible chemical derivative of the active parent drug', meaning that the reconversion site maybe physico-chemical or biochemical in nature (Fleisher *et al.* 1996). The idea behind a prodrug, for solubility enhancement, is that the parent drug's structure is altered, by the addition of a solubilising progroup to the molecule with the aim to exert two possible effects. The first effect is to reduce the melting point of a drug (so in theory affecting the crystal structure, thus reducing the lattice energy and increasing the solubility), the other is to introduce an ionising group to the molecule. Examples of such groups include phosphate esters, amino acid esters or choline esters. The reconversion of the prodrug back to the parent drug is usually designed to occur at a specified physicochemical region or at a site specific enzyme.

An example of how this approach has been used to improve the dissolution of

drug is with the drug mebendazole. The absorption of mebendazole is found to be dissolution rate limited (Dawson *et al.* 1985). Studies conducted on N-alkoxycarbonyl prodrugs found that the aqueous solubility of the mebendazole increased from 1.7×10^{-6} M (for the parent drug) up to 2.7×10^{-5} M (for the ethoxy derivative). These derivatives worked by decreasing the melting point of the mebendazole from 290 °C to 165 °C (ethoxy derivative) (Nielsen *et al.* 1994). Bioavailability studies showed that the derivatives enhanced the oral bioavailability, relative to the mebendazole, by 4 – 13 fold (Nielsen *et al.* 1994).

1.3.2 Solid dispersions

1.3.2.1 History and theory of solid dispersions

Presenting a drug as a molecular dispersion was first described in 1961 when Sekiguchi and Obi compared the behaviour of sulphathiazole, in the form of a eutectic mixture, and ordinary sulphathiazole in man. It was found in this study that there was a greater absorption of the sulphathiazole when in the form of the eutectic mixture. The eutectic mixture (in its simplest form) consists of two compounds that are miscible in the liquid state but not in the solid state. They are prepared by melting the two compounds and then rapidly cooling them. If this is done at composition E (figure 1.15) both compounds crystallise out simultaneously, if this is performed at other compositions the compounds will crystallise out at different rates. The resulting product is a mixture of fine crystals of both components. Once these mixtures (if prepared from a slightly soluble drug and a highly soluble carrier) are dissolved in an aqueous medium, the carrier will dissolve quickly releasing fine crystals of the drug. This enhances the available surface area of the drug, so giving the overall effect of increasing the dissolution rate (Sekiguchi and Obi 1961, and Goldberg *et al.* 1965).

Figure 1-15 Phase diagram for the formation of eutectic mixtures (the T on each y axis represents temperature, E represents the eutectic point)

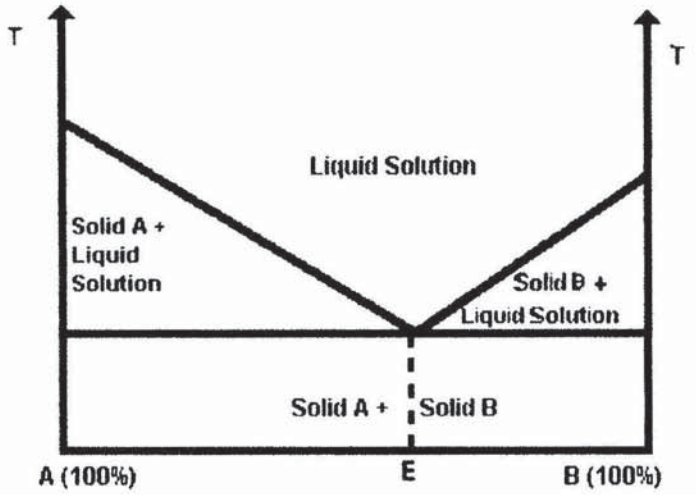

Figure 1-15 shows a system where components A and B are completely insoluble within each other in the solid state. In practice it is found that there is some solid state solubility for all two-compartment systems (Goldberg *et al.* 1965), however the level of solubility is not always considered significant. If the solubility of one component in the other is significant however (represented by the α and β regions in figure 1-16) then it can be said that a solid solution is formed. The term solid dispersion is used to describe either the eutectic mixtures or the solid solutions. Solid dispersions can be classified by two main methods: how the two components are miscible and how the solvate molecules are distributed in the solvent molecules. There are two categories in which the solvate and solvent molecules can be miscible, and these are known as continuous or discontinuous solid solutions. In a continuous solid solution all components are miscible at any ratio, and there are none of these reported as yet in the literature. In the case of discontinuous solid solutions the miscibility of the components is limited, as shown in figure 1-16. The α and β regions of the phase diagram show the regions of where a true solid solution would be found. It was suggested by Goldberg *et al.* (1965) that a solubility of 5% of one component in the other can be considered a solid solution. It is reported, however, that the detection of solid solutions below the 5% level is possible (Chiou & Riegelman 1971). On a practical level, the application of the 5% limit causes formulation problems, doses of a 50 mg

drug with only 5% solubility would be not suitable for solid solution formation, as the amount of excipient results in a large dosage form.

Figure 1-16 Phase diagram for the formation of solid solutions

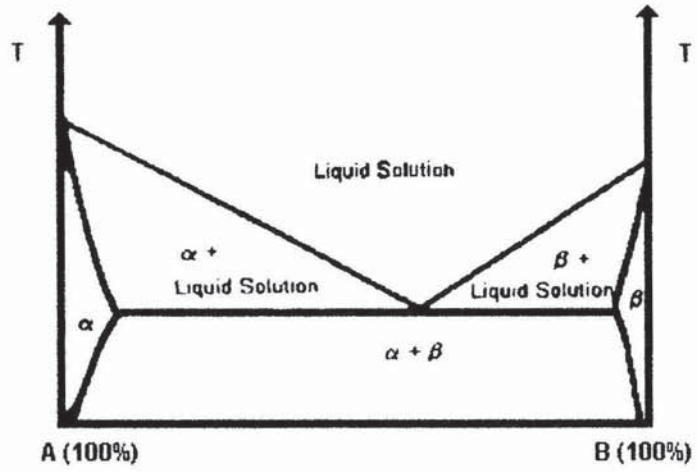

The second method for classification of solid dispersions, *i.e.*; how the solvate molecules are distributed in the solvent molecules, is broken down into three main categories; substitutional, interstitial and amorphous. Substitutional solid dispersions are classically crystalline, and the solute molecules replace the solvent molecules in the crystal lattice. This sort of structure depends on the size of the two molecules involved; the size of the solvent molecule must not differ by more than 15% from that of the solute molecules (Shriver *et al.* 1995).

In the case of interstitial solid dispersions, the solute is found in the spaces between the solvent molecules in the crystal lattice. Again the size of the molecules dictate the formation of these solid dispersions; the solute molecules must have a molecular diameter no larger than 0.59 of the solvent molecules diameter. This has then been calculated that the volume of solute can be no more than 20% of that of the solvent (Leuner and Dressman 2000).

The final type of classification is the amorphous form, and within these dispersions the solute molecules are dispersed molecularly but irregularly within the carrier (Leuner and Dressman 2000). This is where the solute is dissolved into a glassy solvent; these glass solutions are usually homogenous. These offer an advantage over the traditional solid solutions, in

that there are no strong lattice bonds. This negates a major barrier to dissolution, thus theoretically making dissolution quicker. When preparing dispersions of this type it is possible that some of the drug is not completely dissolved in the glassy solvent, and that pockets of drug in the amorphous state may exist (Sertsou *et al.* 2002).

One of the main limitations of solid dispersions is the physical instability due the amorphous drug re-crystallising (Serajuddin, 1999). There are many examples in the literature where the amorphous drug has re-crystallised during storage (Ford and Rubenstein, 1978). The study of nifedipine-nicotinamide-HPMC solid dispersions stored at various conditions (30°C/60% RH, 40°C/75% RH) found that after 1 month the amorphous nifedipine converted to the crystalline state (Suzuki and Sunada, 1998). This had the effect of significantly lowering the dissolution rate. However, a study investigating the stabilisation of amorphous ketoconazole with PVP K25 found that there was no re-crystallisation of the drug upon storage when there was elevated humidity (25°C/52% RH) (Van de Mooter *et al.* 2001). However, seeding the dispersions with crystalline ketoconazole (4.1% w/w) converted 77% of the amorphous drug back to crystalline ketoconazole.

1.3.2.2 Methods of preparation

There are two main methods used to prepare a solid dispersion, the hot-melt method and the solvent method.

The hot-melt method was first utilised by Sekiguchi and Obi (1961) in order to prepare the original eutectic mixtures that opened up the field. On a basic level, it involves the melting and mixing of the drug and polymer followed by cooling. The rate of cooling has an effect on the composition of the dispersion, in terms of molecular dispersion of the drug within the matrix. If the rate of cooling is rapid enough a situation can arise where the drug is supersaturated within the carrier, that is to say the drug molecules are kept within the carrier matrix upon sudden solidification (Ford, 1986). This degree of supersaturation is dependent upon the rate of cooling, which in turn effects the resulting dispersion; therefore this can be optimised to produce the required dispersion.

This then led to the development of several methods to achieve rapid cooling. One of these methods included snap cooling onto stainless steel plates to aid rapid heat loss (Sekiguchi *et al.* 1964). This had one drawback in that grinding was required to produce the end product. The process of grinding can cause alterations in the dispersions' properties (Forster *et al.* 2001). This was overcome by Kanig (1964) by spraying the hot-melt onto a cold surface. Spraying had the advantage of creating small pellets that did not require grinding. There are, however, other problems associated with the hot-melt method that caused the method to lose popularity. One of these problems is the miscibility of the drug and polymer in the molten state. Another of the problems is that thermal degradation of the drug can occur if too high a temperature is required to melt the carrier. Due to these limitations, the solvent method became popular during the 1970s and 1980s; in recent years the hot melt method has advanced with the use of hot melt extrusion technology in order to manufacture dispersions. This method has advantages over both the traditional melting method and the solvent method. In comparison to the melting method melt extrusion only heats the components for a short period of time, therefore reducing the risk of thermal degradation (Leuner and Dressman 2000). The melt extrusion method has both a health and safety and an environmental advantage over the solvent method, as it does not involve the use of potentially harmful solvents.

The solvent method was first developed by Tachibani and Nakumara (Ford, 1986); they dissolved β-carotene and polyvinylpyrrolidone into chloroform. The solvent was then removed by film casting over mercury. A more common way to remove the solvent is to evaporate the solvent using a variety of methods, either rotary or static evaporation, or spray drying. Dispersions prepared in this way are termed co-evaporates. Removal of the solvent is now achieved by other methods, including spray-drying and freeze-drying (Ford, 1986).

Another method for preparing solid dispersions, using solvents, is to dissolve the drug and carrier into a solvent and then add a second solvent, in which both the polymer and drug are insoluble, to the solution, the dispersion then

precipitates out. This technique was first used by Simonelli *et al.* (1969), who termed the product a co-precipitate.

The main problem associated with the solvent method is that a solvent system is needed to dissolve the carrier and drug. In recent times, the solvent method has lost some of its popularity due to environmental concerns as vast quantities of solvent can be required (Leuner and Dressman, 2000).

1.3.2.3 Proposed mechanisms for the enhancement in dissolution obtained by solid dispersions

The enhanced dissolution rate afforded by solid dispersions has been attributed to many different factors. For the eutectic mixtures that were first prepared (Sekiguchi and Obi 1961) enhancement was attributed to the decrease in particle size (section 1.2.2.1). This, however, was discounted when a eutectic mixture of chloramphenicol-urea was prepared, and the rate of dissolution of the eutectic mixture was found to be the same as the pure drug (Sekiguchi *et al.* 1964). It was found in this study, however, that there was an increase in dissolution rate of the drug when higher proportions of urea were employed (20% chloramphenicol, 80% urea). The phase diagram for the chloramphenicol-urea mixtures indicated that, at this ratio, the mixture existed as an α-solid solution. It was proposed that when the urea in the α-solid solution dissolved the chloramphenicol was presented to the solvent in a molecular state, thus increasing the dissolution rate (Goldberg *et al.* 1965). This idea was expanded when further studies of the chloramphenicol-urea system were carried out (Goldberg *et al.* 1966). It was shown that the presence of urea increased the solubility of chloramphenicol, a seven-fold increase was observed over a range of 0-60% (w/v) urea. It should also be noted that the solubility of the α-solid dispersion was the same as a physical mixture at the same ratio. The dissolution results yielded a different picture with the α-solid dispersion having a dissolution rate more than double that of the physical mixture. This difference was attributed the physical state of the drug in the solid solution, *i.e.* the vastly reduced particle size. It has since been found that the dissolution rate can change even if the particle size

remains constant (Sjökvist and Nyström 1988).

When the drug is contained within a solid dispersion it is dissolved into the carrier (this dependant upon the carrier concentration), therefore some or all of the drug is in an amorphous form, and this means that there is no crystal structure to disrupt. The energy required to break up the crystal structure is not needed, and therefore, not a limitation (Taylor and Zografi, 1997).

It has been shown that even non-surface-active carriers can improve the wettability of a drug (Chiou and Reigelman, 1971). This is favourable as it reduces the contact angle, which in turn increases the available surface area for dissolution. Once the drug is dissolved in the medium from the solid dispersion, the solution formed can become supersaturated and the drug can precipitate back out. There is some evidence that shows that the polymer can inhibit this precipitation, holding the drug in solution (Simonelli *et al.* 1976; Hilton and Summers, 1986; Usui *et al.* 1997). There is also evidence to suggest that if the drug does precipitate out of the solution, that it precipitates as a metastable polymorph. This metastable polymorph can be highly soluble compared to the original polymorph of the drug, thus it goes back into solution; this has been shown with indomethacin (Ford and Rubinstein, 1978; Hilton and Summers, 1986).

Another mechanism is the possibility that the release of the drug could be related to the behaviour of the carrier or the drug itself. This mechanism was first proposed by Craig (2002), in which he termed the mechanisms carrier-controlled or drug-controlled dissolution. Before the mechanism can be discussed in detail the historical background needs to be presented. This mechanism finds its roots in the models proposed by Higuchi *et al.* (1965) and Higuchi (1967). These models describe the possible fates of two compartment systems, and the model makes the assumptions that the dissolution of both components is diffusion-controlled and that the dissolution surface is non-disintegrating. Figure 1-17 shows the three possible scenarios that can occur at the solid/liquid boundary during dissolution. These depend upon the amounts of each component within the system. If constituent A is the

more rapidly dissolving component, then this would form the dissolving surface, and *vice-versa* for B.

Figure 1-17. The dissolution of a two component system (where N represents the proportion of each component, D represents the diffusing coefficients in the dissolving medium and C represents the solubility in the dissolving medium (subscripts A and B refer to the two components)(reproduced from Craig 2002)

By applying this relationship to solid dispersions, if the drug was the major component then it would form a drug-rich dissolving surface, thus controlling the dissolution (Corrigan, 1985). The model proposed in the study states that neither the dissolution rate of component A or component B from the binary system can be higher than the dissolution rate of the component alone. This means that any increases in the dissolution rate are due to either complex formation or the dissolution surface is a disintegrating surface. Equation 1-18 shows how the dissolution rate for component B can be calculated when component A is the faster dissolving component.

Equation 1-18 - Equation for the calculation of the dissolution rate of component b (where G is the dissolution rate, N is the proportion of each component, a and b refer to the two components)

$$G_b = \frac{N_b \times G_a}{N_a}$$

In the case of high polymer loadings, it was proposed that the drug would still form a controlling drug layer at the dissolving surface, but there would not be

enough drug to support this layer. This leads to the drug becoming dispersed within the polymer. Thus polymer dissolution is not hindered and the drug release becomes controlled by the carrier.

Using equation 1-18 it is possible to calculate the dissolution rate of the drug, from a solid dispersion with high drug loading, by assuming the polymer is the faster dissolving compartment. This model was used with a degree of success, predicting the dissolution rate of eight different systems: bendroflumethazide:PEG (1:20 and 1:10), barbituric acid:PEG (1:30 and 1:10), hydroflumethiazide:PEG (1:20 and 1:10) and phenobarbital:PEG (1:30 and 1:50) (Corrigan 1986). This then led to theory that if the drug is present as the minor component within the solid dispersion then the dissolution of the drug is controlled by the dissolution of the polymer. The argument for carrier-controlled dissolution was enhanced further when ten drugs were found to possess similar dissolution rates when incorporated into PEG 6000 solid dispersions (Dubois and Ford 1985). It was also found in this study that when the drug content was plotted against the dissolution rate, a linear relationship was observed. The range of this linear relationship was variable between drugs, indicating that carrier-controlled dissolution only dominates up to a certain concentration and this depends upon the drug (0-2% w/w for phenylbutazone and 0-15% w/w for paracetamol).

There is however some evidence that suggests carrier dissolution is not the only mechanism occurring. During studies in which the particle size of griseofulvin released from the dispersions was measured (Sjökvist and Nyström 1988), it was found that the dissolution rate enhancement was related to the particle size of the released drug, especially for the solvent method. In the study by Sjökvist and Nyström (1988) polyethylene glycol was used as a carrier for griseofulvin. In this study it was found that the griseofulvin existed as a fine particulate within the PEG matrix. It was found that as the drug concentration was increased the particle size of the drug within the dispersions increased, this led to the decrease in particle size. It is felt that this mechanism will not be evident in the work that will be undertaken in this study as the dispersions will be prepared by spray drying, which has

been shown to result in the drug being in the amorphous state (Jung *et al.* 1999). There was also an investigation into relating the physical properties of alkyl *p*-aminobenzoates (PABAs) to the dissolution rate (Sjökvist-Saers and Craig, 1992). It was found that there was a linear relationship between the solubility of the pure PABAs and their intrinsic dissolution rate. The same relationship was found for the PABAs when incorporated into a dispersion. It must be stated that for dispersions prepared with a high drug loading, the dissolution rate was independent of the composition. This led to the suggestion of a mechanism other than carrier-controlled dissolution. This is due to the properties of the drug having an effect upon the overall dissolution which should not occur with true carrier-controlled dissolution (Craig 2002).

For dispersions with low drug loadings, there are two possible mechanisms controlling the release of the drug: one in which the dissolution of the carrier controls the dissolution of the drug, from now on termed carrier-controlled dissolution, and another in which the physical properties of the drug appear to control the rate of dissolution, from now on termed drug-controlled dissolution. A model that possibly explains these observations was proposed by Craig (2002) (figure 1-18). The first stage of the model is the same for both mechanisms, at this point a carrier rich dissolving surface forms. It is this surface that the drug must pass through to be released into the bulk phase. The next phase of the mechanism is the dissolution of the drug into the carrier diffusion layer, from there the drug is released into the bulk medium. It is second phase, the dissolving of the drug into the dissolving surface, which is critical in deciding which mechanism occurs. It was stated by Craig (2002) that in the case of carrier-controlled dissolution the drug dissolves into the carrier quickly, this results in the drug being molecularly dispersed within the diffusion layer. The viscosity of the dissolving surface is high enough to cause the subsequent diffusion of the drug through this layer to be very slow. Therefore, the controlling factor to the release of the drug is the dissolution of the polymer. Conversely in the drug controlled release the particles dissolve slowly into the diffusion layer, so are released into the bulk medium as solid particles. Consequently the properties of the drug control the dissolution rate, *i.e.* particle size and physical form, in the drug-controlled dissolution

mechanism. There are other possible explanations that have been put forward that offer potential explanations to why dispersions with a high carrier loading may go through either mechanism. One of theories discussed previously in this section is that the carrier can improve the wetting of the drug (Chiou and Reigelman, 1971). It would, therefore, be expected that if a carrier significantly improves the wetting that the drug will dissolve quicker into the carrier diffusion layer, so enabling carrier-controlled dissolution to occur.

Figure 1-18 Diagrammatic representation of the polymer controlled dissolution mechanism of a solid dispersion (a) where the drug diffuses into the polymer and the drug controlled mechanism (b) where the drug is released intact into the dissolution medium (Craig, 2002)

It is has also been proposed that the physical nature of the drug within the solid dispersion could have an effect on deciding which mechanism occurs (Sertsou *et al.* 2002a). If the drug is completely in the amorphous state then the drug is already molecularly dispersed, thus providing a larger surface area for the dissolution of the drug into the diffusion layer. This would therefore provide a more rapid dissolution rate of the drug into the carrier, thus the carrier controlled dissolution mechanism would be utilised. This is further supported by further work performed by Sertsou (2002b), in this study it was found that those dispersions where the drug was fully incorporated into the

solid dispersion (*i.e.* fully amorphous) had levels of dissolution, after 5 five minutes, ten-fold higher than those dispersions where the drug was not fully incorporated into the dispersion. This theory is supported by model proposed by Corrigan (1985), as it was stated in this model that the ratio of carrier to drug can be a deciding factor on the eventual mechanism. The model states that if there is a large difference in the solubilites of the two components, then the range of carrier:drug ratios at which carrier controlled dissolution will occur becomes very small and occurs only at very high carrier loadings. The likelihood is that all of the factors play a part in deciding upon which mechanism is the more likely, at this time a full mechanism which enables a clear prediction of how a drug will behave in a solid dispersion is as yet unclear. What is also apparent from the studies discussed is that more understanding about how the carrier and drug behave together is required.

1.3.3 The effect of surfactants on the release of drugs from solid dispersions

As already outlined (section 1.3.2.1) one of the major problems with solid solutions is the potential for the drug to re-crystallise from the amorphous phase due to moisture, heat etc. This will affect the dissolution and the overall quality of the product.

The incorporation of a surfactant into a solid dispersion has been used to obtain the following two different effects: the enhancement of the stability of solid dispersions (Mura *et al.* 1999) and the more widely investigated enhancement of solubility (Sjökvist *et al.* 1991, and Sheen *et al.* 1995). The main surfactants that have been used to obtain both these effects have been polysorbate 80 and sodium dodecyl sulphate (SDS); with Mura *et al.* (1999) using both to study dissolution enhancement and stability, Sjökvist *et al.* (1991) using SDS to study dissolution enhancement and Serajuddin (1990) using polysorbate 80 to study dissolution enhancement.

It was reported that the complete dissolution of poorly soluble drugs from a PEG:polysorbate 80 mixture was achieved, in contrast with incomplete dissolution from PEG-only solid dispersions (Serajuddin, 1990). This suggested there is some promise in the utilisation of surfactants within solid

dispersion for the further enhancement of drug dissolution. It was also reported in the same study that the incorporation of the surfactant into the dissolution medium did not have the same effect, with the dissolution of the drug being comparable to the PEG-only solid dispersions. It was, therefore, concluded that it is the local concentration of surfactant that is the driving factor behind this enhancement.

Following on from this study, these systems were investigated from a structural point of view (Morris *et al.* 1992) and examining the miscibility of the binary mixture of PEG:polysorbate 80 (Tejwani *et al.* 2000). The X-Ray Powder Diffraction (XRPD) and the Differential Scanning Calorimetry (DSC) data indicated that the incorporation of polysorbate 80 in large quantities (20, 50, 70 % w/w) into the PEG actually had no effect on the PEG crystal structure (Morris *et al.* 1992). Therefore, it does not interact with the polymer used, but instead incorporates itself into the amorphous regions of the PEG solid dispersion (see figure 1-19). This would enable this system to be an effective carrier for a solid dispersion; this is due to the structure of PEG (which is an effective carrier without the addition of a surfactant) being un-affected by the surfactant, and the size of the amorphous region of the vehicle being enhanced (figure 1-19) thus allowing more drug to be incorporated in the amorphous phase (resulting in an enhanced dissolution (section 1.2.1)).

The miscibility of these carriers was then investigated, with the results indicating that with low molecular weight PEGs – polysorbate 80 mixtures two phases were formed, with polysorbate 80-rich globules being present (Tejwani *et al.* 2000). It was postulated that the findings of Morris *et al.* (1992) (that the polysorbate 80 was found in the amorphous phase), could be due to the immiscibility of the two components in the solid state. The conclusion from this study was that care should be taken at the pre-formulation stage when utilising this carrier to ensure complete miscibility.

SDS:PEG systems, as well as polysorbate systems, have also been investigated with reference to solid dispersions. A study showed that the incorporation of SDS into the solid dispersion had a dramatic effect upon the

dissolution of 10% w/w griseofulvin from PEG 3000 solid dispersions (Sjökvist *et al.* 1991). It was found that when the SDS was added to the dispersion, 100% dissolution of the griseofulvin into water was achieved within five minutes, whereas the dispersion with no SDS only achieved less than 50% dissolution of griseofulvin after 15 minutes. The same pattern was found for dispersions with varying concentrations of griseofulvin (3% and 20% w/w griseofulvin). The dissolution of 10% dispersions with 1% SDS was then studied in dissolution media containing varying amounts of SDS. It was found that the dissolution of the griseofulvin from these dispersions was independent of the dissolution medium, leading to a two-tiered conclusion; 1) that wetting of the surfactant during release outweighs the effect of changes in the dissolution medium, and 2) that there must be some other physical structure due to the presence of SDS in the solid dispersion. The first conclusion was supported by the measurement of the carrier dissolution (measured by the disintegration time of a tablet of the dispersions), which showed that the incorporation of the SDS into the dispersion also increased the dissolution rate of the carrier. Solid state investigation of the dispersion was also carried out, with the XRPD showing that the presence of a griseofulvin phase slowly diminished with more SDS added to the dispersion. At levels of 2% SDS, it was found that no crystalline griseofulvin was present within any of the dispersions (at any % w/w fraction of griseofulvin). This led to the conclusion that the incorporation of the surfactant into this system increased the solubility of griseofulvin into the PEG, thus forming a solid solution. The DSC data also supported theory that a solid solution was formed when SDS is incorporated. It is found that there was a decrease in the ΔH of the melting endotherm for PEG when increasing SDS was incorporated into the solid dispersion (see table 1-18). This indicated that there had been some form of phase change occurring within the dispersion. Further investigations were performed upon these griseofulvin:PEG dispersions, involving solid state ^{13}C NMR (Aldén *et al.* 1993). It was found in the ^{13}C NMR traces that for the dispersion without SDS the spectrum were essentially a superimposition of griseofulvin and PEG; this indicates that there is no interaction between the two components. In the griseofulvin:SDS:PEG dispersions it was found that there were some changes in the griseofulvin peaks; three CH_3 peaks were found (implying

three different surroundings), and the methoxy and C-O carbons were strongly influenced by the formation of the solid solution. This indicates that there are interactions occurring between the polymer and the griseofulvin. Supporting XRPD data showed that the griseofulvin in the griseofulvin:PEG dispersion was present in the crystalline form, whereas when 2% of SDS was added, it appeared that all the griseofulvin was incorporated in the solid solution. The postulated mechanism was that the griseofulvin is bound to small aggregates of the surfactant, this hydrophilic complex then dissolves into the PEG structure (Aldén *et al.* 1992).

A comparative study of the effects of inclusion of an anionic surfactant and a non-ionic surfactant on the dissolution of solid dispersions was conducted (Mura *et al.* 1999). The study investigated naproxen dispersions with PEG 4000, 6000 and 20,000, with (and without) the incorporation of either SDS or polysorbate 80. The study again found that the addition of a surfactant to the dispersion increased the dissolution of the drug when compared to dispersions without the surfactant. The proposed mechanism for the improvement by the surfactants, was that they acted as a wetting agent in the micro environment around the drug. Dispersions incorporating SDS were more effective at increasing the dissolution rate, and the amount of drug dissolved. This was attributed to the SDS having higher solubilising power, as it was found in that the solubility of naproxen was higher in SDS solution than in polysorbate 80 solutions. It was also attributed to the SDS being more hydrophilic than the polysorbate 80, this is due to the anionic structure of the SDS making the molecule more polar and so more hydrophilic. This means the SDS dissolves into the dissolution medium quicker than the non-ionic surfactant, thus influencing the surface tension quicker. It has also been shown by Aldén *et al.* (1993) that the fact that the SDS is charged helps it interact better with the PEG, forming an aggregate. In contrast the non-ionic surfactant did not interact with the PEG, due to there being no charge on the molecule. As discussed previously the SDS forms an aggregate with the griseofulvin as well, which due to the interaction between the SDS and the PEG means that more griseofulvin is incorporated in the solid dispersion.

Table 1-5 Effect of griseofulvin and SDS concentration in the PEG solid dispersions upon the heat of fusion of griseofulvin. The lower the heat of fusion the more griseofulvin there is incorpated in the solid solution (reproduced from Sjökvist, 1991)

Figure 1-19 Schematic diagram of the crystalline-amorphous structures of a) PEG and b) PEG-polysorbate 80 mixture (reproduced from Morris *et al.* (1992))

Another aspect of the study conducted by Mura *et al.* (1999) was to investigate whether these surfactants could stabilise the solid dispersion. As described in section 1.3.2.1, the long term stability of solid dispersions is one of the major obstacles restricting their widespread use in products. The effect of aging on the dispersions was investigated using XRPD, DSC and dissolution testing. Solid state examination of the prepared systems yielded the information that the amorphous nature of the solid dispersion had been enhanced by the presence of the surfactant. This can support the proposal put forward by Sjökvist *et al.* (1991) that the surfactant enables more of the drug to be incorporated into the solid solution. There was very little effect upon thermal characteristics for the solid dispersions after storage for 30 months under ambient conditions, except an increase in the heats of fusion for all the dispersions. This was suggested to be due to an increase in crystallinity of the solid dispersion and this effect was more pronounced in the SDS dispersions. It was found that there was no significant change in the dissolution properties of the solid dispersions after storage. The implication of this is that the addition of a surface active agent, whilst enhancing the performance of the dispersion, offers no major advantage in stabilising the solid dispersion against the effect of aging.

1.3.4 Marketed solid dispersions

Although there is a lot of research that has been dedicated to the area of solid dispersions, only a few products have in fact made it to the market place. Three products that have made it are a griseofulvin in polyethylene glycol (Gris-PEG, Novartis), a nabilone in PVP (Cesamet, Lilly) (Serajuddin 1999) and troglitazone prepared as a solid dispersion with PEG and PVP (Nicolaides *et al.* 1999). It has been suggested that the following factors have influenced the reasons behind why solid dispersions have not been a commercial success: a) the methods of preparation, b) the scale up of the manufacturing process, c) the formulation of them into dosage forms, d) the reproducibility of the physicochemical parameters, and e) the physical and chemical stability of the carrier and drug (Serajuddin 1999)

1.4 *In vivo in vitro* correlations (IVIVC)

1.4.1 Bio-pharmaceutical classification system (BCS)

Figure 1-20 Diagrammatic representation of the bio-pharmaceutics classification system

CLASS I **HIGH SOLUBILITY HIGH**	**CLASS II** **LOW SOLUBILITY HIGH**
CLASS III **HIGH SOLUBILITY LOW**	**CLASS IV** **LOW SOLUBILITY LOW**

The bio-pharmaceutics classification system (BCS) was originally proposed in 1995 by Amidon *et al.* and seeks to classify pharmaceutical products into four main categories (figure 1-20). The original aim of the system was to correlate the *in vitro* drug dissolution to the *in vivo* bioavailability. The model utilises drug permeability and drug solubility to achieve this aim. It was believed these two parameters are the two main aspects that control the absorption of drug through the gut wall. The actual limits that can be applied to the drugs have been under some discussion since the system was originally proposed. The original limits were based upon deriving certain parameters for the drug candidate - Dissolution Number (Dn), Dose Number (Do) and Absorption Number (An). The dissolution number is described as the ratio between the intestinal residence time and the dissolution time (equation 1-19), the dose number is described as the ratio of dose concentration to drug solubility (equation 1-20) and the absorption number is described as the ratio between

absorptive time and intestinal residence time (equation 1-21). For class II drugs it is found that the dissolution number is low (<1) and the absorption number and dose number are generally high.

Equation 1-19 The dissolution number for a drug (Dn – dissolution number, T_{si} – intestinal residence time, and T_{diss} – dissolution time)

$$Dn = \frac{\langle T_{si} \rangle}{\langle T_{diss} \rangle}$$

Equation 1-20 The dose number for a drug (Do – dose number, M – dose, V_0 – volume of water taken with dose, and C_s – solubility of drug)

$$Do = \frac{M / V_0}{C_s}$$

Equation 1-21 The absorption number for a drug (An – absorption number, T_{si} – intestinal residence time, and T_{abs} – absorptive time)

$$An = \frac{\langle T_{si} \rangle}{\langle T_{abs} \rangle}$$

A simpler approach to determine the solubility class of a drug is to utilise the dose:solubility ratio (Dressman and Fleisher 1986). This method has a weakness in that drugs can experience either an equilibrium or a kinetic problem, leading to a false interpretation. Two drugs have been discussed in the literature that highlight this difference: griseofulvin and digoxin. Both drugs are known to have dissolution rate limited absorption, with griseofulvin having a solubility of 15 µg/ml and digoxin 20 µg/ml. The main difference is that the dose of griseofulvin is 500 mg and digoxin is 0.25 mg. Applying the dose:solubility ratio means that to dissolve the whole dose of griseofulvin 33 litres of fluid would be required, and for digoxin 12.5 ml. In the case of griseofulvin there would be insufficient media within the GI tract (studies have shown that the total amount of fluid entering the intestine over a 24 hour

period is 5 – 10 litres (Dressman *et al.*, 1998). For digoxin, there is enough medium to dissolve the whole dose, the main problem is that the dissolution rate is too slow to allow sufficient dissolution. This leads to the problem that sufficient drug is not in solution for absorption at the optimum points in the GI tract.

1.4.2 Development of an *in vitro in vivo* correlation (IVIVC)

It is now widely accepted that out of the four classifications, it is the class II drugs that are the most suitable for development of an IVIVC (Löbenberg and Amidon 2000). Although this can only be achieved by using a well designed and discriminatory dissolution test that can mimic sufficiently the conditions found within the GI tract. This is due to the dissolution of the drug product being the rate determining step for the bioavailability of a drug (section 1.3.1). Therefore there is a necessity to develop *in vitro* dissolution tests that better predict the *in vivo* performance of a drug (Dressman *et al.* 1998).

1.4.3 The use of bio-relevant dissolution medium to simulate the intestinal contents

As stated in section 1.4.1, class I drugs are those that dissolve readily into aqueous media over a pH range of 1-8, therefore it is not expected that the dissolution of the drug will be the limiting factor to the overall bioavailability. As an indication of the bio-equivalence of the formulations of a class I drug it is suggested that a one point dissolution test should be sufficient (85% of drug dissolved within 15 minutes) (FDA 1997).

Table 1-6 Composition of the Fasted State Simulated Intestinal Fluid (FaSSIF)

Constituent	Concentration
KH_2PO_4	0.029 M
NaOH	qs pH 6.8
NaTaurocholate	5 mM
Lecithin	1.5 mM
KCl	0.22 M
Distilled water	qs 1L
Osmolarity = 280 – 310 mOsm Buffer capacity 10 ± 2 mEq/L/pH	

This is not the case for class II drugs for which the rate limiting factor for absorption is the dissolution of the drug (section 1.4.1), and as in section 1.2, the dissolution of these drugs is affected by many different factors. These factors include pH, surfactant concentration, and the volume available for dissolution (Galia *et al.* 1998). It was proposed that a meaningful test for such drugs should use a dissolution medium that mimics the constituents of intestinal fluids in both the fed and fasted states. This led to the development of two new dissolution media, the fasted state simulated intestinal fluid (FaSSIF), and the fed state simulated intestinal fluid (FeSSIF); whose composition is shown in tables 1-6 and 1-7 respectively. The compositions of these media seek to mimic the concentrations found *in vivo* (1.1.2.3.2). As discussed in section 1.1.2.3.2, the pH of intestinal fluid is controlled by bicarbonate, this has been substituted with potassium di-hydrogen phosphate (FaSSIF) or acetic acid (FeSSIF) as the bicarbonate is unstable in the presence of oxygen and therefore could cause fluctuations in the pH values (Dressman and Reppas 2000). Sodium taurocholate was selected as the representative bile salt as cholic acid has been found to be the most prevalent bile salt in intestinal fluids, and the taurine conjugate has a low pK_a so there would be no risk of precipitation. The lecithin concentration was decided based on physiological data which suggests that the bile salt:lecithin ratio is between 2:1 – 4:1 (Dressman et al. 1998).

Table 1-7 Composition of the Fed State Simulated Intestinal Fluid (FeSSIF)

Constituent	Concentration
Acetic acid	0.144 M
NaOH	qs pH 5
NaTaurocholate	15 mM
Lecithin	4 mM
KCl	0.19 M
Distilled water	qs 1L
Osmolarity = 485 – 535 mOsm Buffer capacity 76 ± 2 mEq/L/pH	

1.4.4 Designing a prognostic dissolution test with bio-relevant dissolution media

In the development of a bio-relevant dissolution test other factors, other than the test medium, need to be considered, *i.e.* the volume of the media required, and the duration of the test.

Volume of media

The factors affecting the dissolution of drug were described in section 1.2.4, and as seen from equation 1.6 the volume of dissolution medium present will affect the dissolution rate. So in a bio-relevant dissolution test it is important to mimic the volume of intestinal fluid as closely as possible. In a perfusion study performed by Dillard *et al.* (1965) the volume of fluid found in the human intestine, in the fasted state, varied from 120 ml – 350 ml (this was dependent upon the perfusion rate used).

The volume of fluids available for the dissolution of a drug in the intestine has been found to be not only dependent upon the secretions and water flux across the gut wall but also on volume of fluids ingested (Dressman et al. 1998). This, therefore, needs to be considered in the development of a bio-relevant dissolution test, as generally with orally administered products water is co-administered. It is suggested in the literature that when using FaSSIF fluids, 500 ml of dissolution medium should be used, this corresponds to 250 ml of co-administered fluids, and 250 ml of secretions (Dressman and Reppas, 2000).

Duration of dissolution test

As in section 1.1.2 the mean transit time for a dosage form is between 1-4 hours, so therefore to allow for 1-2 hours for drug absorption, dissolution of the drug should be complete within one hour (Dressman et al. 1998).

1.4.5 Predicting the *in vivo* behaviour from the *in vitro* parameters

With the development of the biopharmaceutics classification system (section 1.4.1) coupled with the increasing use of high throughput methods for drug discovery the hunt for a model to predict the bioavailability of these potential

drug molecules has intensified (Norris *et al.* 2000). Such a model should have the following properties (Grass 1997):

- Use a very simple experimental preparation.
- Be easy to perform large numbers of tests.
- Be predictive of results in humans

There have been three main approaches utilised to try and obtain a model that will be able to achieve these aims: mathematical modelling based upon the physico-chemical properties of a drug, linking the results from *in vitro* absorption studies of a drug with pharmacokinetic parameters of the drug and the development of computer simulations based upon the dissolution and absorption of a drug.

1.4.6 Mathematical modelling of dissolution data – comparing profiles and obtaining a rate

In section 1.4.4 the value of dissolution testing as a prognostic tool for the establishment of an IVIVC was described. In order for dissolution testing to be used in this manner, there has to be some method of comparing the obtained dissolution profiles for their similarity. One of the simplest ways of achieving this is to compare the dissolution of a test batch to a reference batch at a single time point. This form of comparison is only workable with rapidly dissolving products (typically a class 1 drug), so for sparingly soluble products it is suggested that dissolution profiles are generated (FDA, 1997). This is due to products which may have different dissolution profiles up to that point, which in turn could have an impact upon the pharmacokinetics (Adams *et al.* 2001). It is a far more difficult prospect to model than just one time point, and there have been several models proposed in the literature. There are two main methods by which this can be achieved; either by the model-independent method or the model-dependent method (there is a third method that was classified as ANOVA-based methods by Polli *et al.* (1997), but these can be classed as model independent (Adams *et al.* 2001)).

The two methods that are accepted by the FDA as a means of comparing the

similarity of dissolution profiles are the f_1 (the difference factor) and the f_2 (the similarity factor) test (equation 1-22 and 1-23) proposed by Moore and Flanner (1996). These two tests are examples of a model independent method. The difference factor calculates the percentage error between the time points of each curve, when the overall percentage error is 0 then the curves are considered identical with a proportional increase as the error increases. It is considered that the dissolution profiles are similar if the difference factor is between 0 and 15 (Adams *et al.* 2001).

Equation 1-22 Calculation of the F_1 value

$$f_1 = \left\{ \frac{\sum_{t=1}^{n} |R_t - T_t|}{\sum_{t=1}^{n} R_t} \right\} * 100\%$$

where, R_t is the percentage drug dissolved for the reference product at time t, T_t is the percentage drug dissolved at time t for the test product.

The similarity factor is a logarithmic transformation of the sum of squared error, and is a measurement of the similarity of the percentage dissolution between the two curves. It is considered that that the dissolution profiles are similar if the similarity factor falls between 50 and 100 (Adams *et al.* 2001). It is also advised to not include any time points where the dissolution is above 85%, since the number of these points can have an impact on the similarity factor thus possibly giving a wrong impression (Shah *et al.* 1998).

Equation 1-23 calculation of the F_2 value

$$f_2 = 50 * \log\left\{ \left[1 + \left(\frac{1}{n} \right) \sum_{t=1}^{n} (R_t - T_t)^2 \right]^{-0.5} * 100 \right\}$$

Other examples of model independent methods are the ratio test procedures, which include testing the ratio between area under the curve (AUC), mean dissolution time and ratio of percentage dissolved (Polli *et al.* 1997).

The other category, the model-dependent methods, rather than directly comparing the two profiles, allow for the derivation of model parameters that can then be statistically compared. These models achieve this by using some form of curve fitting procedure, from the curve these parameters can be obtained – for example the slope in a zero order model equals the dissolution rate. Below are two examples of model-dependent methods, with a brief description:

Hixson-Crowell cube-root law

This model was derived by Hixson and Crowell to describe the dissolution of uniformly sized particles. The model expressed the dissolution rate based upon the cube root of the weight of the particle. This relationship assumes that the radius of the particle is not constant throughout dissolution (equation 1-24, m_0 represents the initial weight, m represents amount dissolved, and K is the cube root dissolution rate ((weight)$^{1/3}$time^{-1}).

Equation 1-24 Hixson-Crowell cube root law

$$m_0^{1/3} - m^{1/3} = Kt$$

Higuchi square-root rate law

This model has been used to describe the dissolution of a drug from an insoluble matrix, as the square root of a time-dependent process based upon Fickian diffusion (Gohel *et al.* 2000). It is described as shown by equation 1-25, where Q_t represents the amount of drug dissolved at time t, k_H is the release rate constant.

Equation 1-25 Higuchi square-root rate law

$$Q_t = k_H \sqrt{t}$$

The dissolution models that have been described all rely on the drug concentration increasing with time in order for them to be successful; this sort of data is known as monotonic (Valsami *et al.* 1999). There are, however, occasions when non-monotonic dissolution data is encountered, especially in

the case of solid dispersions. In the dissolution of solid dispersions the following type of profile can be obtained; there is an initial, rapid, increase of the drug concentration in solution until a maximum is obtained (at this maximum, the drug is generally in the supersaturated state). This is then followed by a slow decline in the concentration of the drug in solution until a plateau is reached. There are very few methods that adequately model such data, with the model dependent models failing to linearise the data, and there are generally not enough adequate data points for either an f_1 or f_2 test. One such model was proposed by Valsami (1999) and relies on a population growth model of dissolution (equation 1-26). In this model the mass dissolved is not defined by time but rather fractions of the dose dissolved at generations.

Equation 1-26

$$\Phi_{n+1} = \Phi_n + r(1- \Phi_n)(1 - \Phi_n X_0 / \theta)$$

with X_0 is the dose, θ is the amount of drug in solution corresponding to the saturation solubility, r is a proportionality constant, and Φ_n, Φ_{n+1} are the fraction of dose at generations n and n+1. In order to compare dissolution profiles the following two dimensionless parameters can be derived: r (denotes the maximum fraction of dose dissolved) and θ/X_0 (denotes the fraction of dose in solution at the plateau point). One weakness of this model is that, unlike the majority of the other models, it fails to derive a dissolution rate based upon the data presented.

1.4.6.1 Mathematical models for predicting the *in vivo* performance of a drug

One early mathematical model that sought to predict the GI absorption of a poorly soluble drug was a mixing tank model (Dressman and Fleisher 1986). This model took into account such dissolution parameters as initial particle radius, dose, diffusivity and boundary layer thickness. The model required the solving of three differential equations to describe the whole process of the GI absorption. In order to validate the method simulations of both griseofulvin, and digoxin were performed. The aim of these simulations was to test the model validity in predicting the absorption of the two drugs based upon the particle size (for assessing how the dissolution rate influences the absorption)

and how the physiological conditions of the GI tract can control the absorption. The model proved very useful for the prediction of how the particle size affects the absorption of the drugs and how the poor solubility of a drug can limit the extent of absorption.

A simpler method was used to calculate the absorption potential of drug (Dressman *et al.* 1985). This is a dimensionless parameter that acts as an approximation to predict the oral absorption of a drug. The absorption potential of a drug is calculated using the model shown in equation 1.27. As can be seen from the model many variables that are thought key to the absorption of a drug are included (*e.g.* solubility, octanol-water partition coefficient). There was a reasonable correlation between the absorption potential and the pharmacokinetic parameter F (the fraction of the dose absorbed *in vivo*). There are some issues with the model when concerned with sparingly soluble drugs, firstly the solubility is based upon the aqueous solubility. As in section 1.4.3, the intestinal fluids contain agents capable of aiding the wetting and subsequent dissolution of such compounds, the intrinsic solubility of the drugs is the solubility of a drug in water, so does not take into account the potential effects of natural wetting agents. Finally it is only suitable as a first approximation, as it gives no idea to the actual pharmacokinetic properties of a potential drug compound.

Equation 1-27 Calculation of the absorption potential of drugs

$$AP = \log\left(P \cdot F_{non} \cdot \frac{S_0 \cdot V_L}{X_0} \right)$$

Where AP = absorption potential, P = partition co-efficient, F_{non}= fraction of drug unionised, S_0 = intrinsic solubility, V_L = volume of luminal contents and X_0 = dose administered.

1.4.6.2 Permeability models

Relating permeability data to correlate with the fraction absorbed is useful to establish permeability models. One such study correlated the permeability of compounds through the intestinal wall of rats (perfusion study) with the F value for various drugs (Amidon *et al.* 1988). It was again found that a good

correlation was achieved between the two parameters. The limitations of this model were acknowledged by the authors, and this was that the dose:solubility ratio (section 1.4.1) was not utilised in this model. The way that this would affect the model is that it is expected that for low solubility drugs, the amount of drug at the absorbing surface would be low, whereas in the experiments the amount of drug at the absorbing surface would be high. This would result in an overestimation of the permeability. This work pre-dated the biopharmaceutics classification system, and it would therefore be expected to be useful for the prediction of class I and III drugs. This model sought to predict the *in vivo* performances of drugs based upon their permeability through the intestinal wall. Since the advent of the biopharmaceutics system the aim has been towards predicting the *in vivo* performance of a drug using *in vitro* dissolution testing, the reasons and methods to achieve this are outlined in section 1.4.3. As already seen the weaknesses that were shown up in the permeability models were their failure to compensate for weakly soluble drugs (whose formulation can affect various parameters), and the actual linking of the data with pharmacokinetic parameters (except the fraction absorbed). This has led to the development of human perfusion studies, which allow for the direct analysis of drug absorption *in vivo* (Lennernas 1998). Human perfusion studies are now required by the FDA (2000) for the determination of the permeability class of a drug. It is recommended that the use of cultured monolayers of epithelial cells should only be used for a drug that is transported passively. This is because the proteins that mediate active transport are missing and this could therefore understate the absorption of a drug, thus giving a drug the wrong BCS class (FDA 2000).

This has led to the development of various models to try and obtain this aim, ranging from the development of computer simulations, to practical laboratory methods (from now on known as *in silico* and *in vitro* methods).

An *in vitro* model has recently been proposed that takes into account both the dissolution and permeability characteristics of drug (Kobayashi *et al.* 2001). The model also incorporates the change in pH that is experienced by a dosage form when transferred from the stomach to the intestine. The main

advantage of such a system is that, unlike the early studies based on the substance permeability (Dressman *et al.* 1985 and Amidon *et al.* 1988), this model compensates for low solubility drugs having very low amounts of drug at the absorbing surface. The model proved useful in predicting the variability in the bioavailability of the poorly soluble drug abendazole, which has proved to display variable *in vivo* data. The weaknesses of this model were acknowledged by the authors: one of these was that only 3 mg of drug was tested in 3 ml of dissolution media. This means that the effects of a potential dosage form could not be examined. This model, like the early permeability studies, is very useful in determining how a drug is likely to respond *in vivo* but with the addition of dissolution as a parameter. What it does not do is allow for a prediction of the plasma-time curve for a potential drug candidate.

1.4.6.3 Computational methods

In order to develop a model to predict the plasma-time curve is has become necessary for researchers in the area to develop computer based models. Different approaches have been utilised to develop such models; using the obtained permeation, using the predicted performance of the drug in the intestine (Wilson *et al.* 1991, Grass, 1997 and Nicolaides et al. 2001) and finally using a heterogeneous tube model (Kalampokis *et al.* 1999). There are now many software packages available that allow for the development of such models. Examples include general modelling programs such as STELLA, and the more specific *in silico* programs like GastroPlus®. The advantages of such programs are that once a model is developed, screening of analogues of compounds and various formulations can take place based upon some simple physicochemical properties. One very comprehensive model was developed using the software STELLA (Grass, 1997). The permeability and solubility parameters of the model drugs in all areas of the GI tract (e.g. jejunum and ileum) were taken into account. The model also considers the various physical aspects of the small intestine; such parameters include the surface area and the fluid dynamics. In order to derive the *in vitro* data, permeability studies were performed using tissue from various areas of the intestine (*e.g.* jejunum tissue, and the ileum). The complex nature of this model means that it would probably have very little practical use as a screening tool. This is due to the

amount of background work involved, the diffusion studies at various parts of the intestine, and solubility studies at various pHs. The other problem associated with the model in its current state is that it is not optimised for the administration of solid oral dosage forms, although it was stated by the author the model could be adjusted to take this into account.

Another approach in developing a computational method for the prediction of the plasma-time curve is to link the *in vivo* performance of the drug with the performance of the drug within the intestine. One such model has been proposed that links the *in vitro* dissolution rate with the plasma time-curve (Nicolaides et al. 2001*)*. The main aim of this model was to investigate whether the differences measured with *in vitro* dissolution testing could be seen in the simulated plasma time-curve. The investigation also aimed to specify the conditions under which the prediction could be achieved. The first aspect in the development of the model was to describe the *in vivo* dissolution of the drug. The *in vitro* dissolution was performed in one of the following dissolution media: FaSSIF, FeSSIF, milk or the USP simulated intestinal medium, using a range of different drugs. The FaSSIF and FeSSIF as discussed in section 1.4.3 contain bile salts at physiological levels, with the FeSSIF fluid containing 3 times the amount of taurocholate. In comparison the USP simulated intestinal fluid contains no bile salts, and is a pH 6.5 buffer. Milk is a medium that has been suggested as an appropriate dissolution media for representing the fed state, this is because it contains an appropriate ratio of fat:carbohydrate:protein (Dressman *et al.* 199) The biorelevant dissolution medium had already been shown to be able to be discriminating when the *in vitro* data was compared to the *in vivo* plasma-time (Galia, 1999). It was then necessary to apply a dissolution model to the *in vitro* dissolution tests, it was chosen to use one based upon the Noyes-Whitney equation (equation 1-16) and the other was a first order equation (Nicolaides et al. 2001). There were no restrictions applied to the absorption of the drug into the plasma, and it was assumed that 100% available drug was absorbed into the plasma. To achieve the correct levels of absorbed drug, the concentration was multiplied by the bioavailability constant (F), which is a measure of the percentage of drug absorbed. To complete the model the elimination and

distribution of the drug were included.

The resulting model was successful in predicting the plasma-time curve, when the f_1 similarity test was applied (prediction of the plasma profile was possible (9.6 < or = f1 < or = 34.2) in seven out of eleven cases (Nicolaides et al. 2001)). However, there is no indication as to how well the obtained pharmacokinetic parameters (T_{max}, AUC and C_{max}). It was found that the bio-relevant dissolution media provided the best results when combined with the Noyes-Whitney dissolution model. This was attributed to the presence of the bile salts within the biorelevant dissolution media which enabled better wetting of the drugs. The main concern with this model is that it relies on the fraction absorbed to describe the amount of drug absorbed. The fraction absorbed value, for sparingly soluble drugs, can be variable based upon the formulation applied. The usual way to calculate the F value is to calculate the AUC of one product with the AUC of another (generally the oral against the parental).

The data obtained from the Nicolaides model does show that it is possible to obtain a prediction of the plasma-time curve, but only if some of the pharmacokinetic data is available. Other models that have used the behaviour of the drug in the intestine have also found similar promising results. One such model was developed to predict the behaviour of sustained release products (Wilson *et al.* 1991), so used the gastric residence times instead of the dissolution time.

1.5 Drug Profiles

1.5.1 Troglitazone

The drug troglitazone was developed as an oral anti-diabetic drug, and it works by improving insulin sensitivity and responsiveness. It is found to be effective in the treatment of both insulin-dependent and non-insulin-dependent diabetes mellitus. However, in 1998 it was reported troglitazone was responsible for hepatocellular injury, this lead to increased plasma levels of liver enzymes, and some patients, who used troglitazone suffered severe or fatal liver damage. This lead to the withdrawal of troglitazone from the market

(Parker, 2002).

Figure 1-21 shows that troglitazone has 4 asymmetric carbons, and thus exists in 4 different stereoisomers. It has been found that troglitazone exists in equal amounts of these four stereoisomers (Suzuki *et al.* 2002).

Troglitazone is an ideal candidate as a class II drug, as it is found to be sparingly soluble, having a solubility of ca. 10 µg/ml in water (Suzuki *et al.* 2004). Calculation of the dose:solubility ratio shows that it would require at least 20,000 L of water to dissolve the amount of troglitazone found within one tablet, which is 200 mg. It has also been found that troglitazone is rapidly absorbed through the gut wall, with an absolute bioavailability of 40 – 50% (Parker 2002). Troglitazone is also a weakly acidic drug, having pK_a of 6.5 and 12.0 (Nicolaides *et al.* 2001), so therefore its solubility is dependent upon the pH of the solvent.

Studies of troglitazone in FaSSIF fluid show that with the presence of the natural bile salts there is an enhancement in the dissolution of the drug when compared to compendia dissolution medium (Galia 1999). It was hypothesized that this increase was due to the presence of the bile salts found in FaSSIF, which are not present in the compendia dissolution medium. It was also found that dissolution was quicker and occurred to a greater extent in FeSSIF than FaSSIF. This difference between the dissolution in the FaSSIF and FeSSIF can be explained by the levels of taurocholate found within the two media. In FeSSIF the level of taurocholate is above the CMC, whereas in FaSSIF it is below this value (Levis *et al.* 2003). This correlates with what has been found *in vivo*, where the amount of drug absorbed in the fed state increased by 30 – 80% compared to the fasted state (Galia 1999).

The pharmacokinetics of troglitazone have been found to be variable, with the tmax occurring between 2-3 hours, and the T1/2 ranges between 7.6 – 24 hours (Parker 2002).

Figure 1-21 Molecular structure of troglitazone

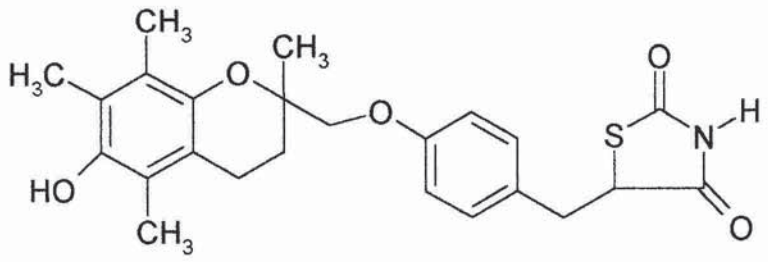

Troglitazone

1.5.2 Atovaquone

Atovaquone (shown in figure 1-22) has been generally used as an anti-malarial drug. Atovaquone is also an ideal candidate to study as a class II drug, as it is a sparingly soluble drug, having a solubility of 0.43 µg/ml in water (Nicolaides *et al.* 2001). Calculation of the dose:solubility ratio shows that almost 2 million litres of SIF would be required to dissolve the dose of drug supplied in one tablet, which is 250 mg. It can be predicted that atovaquone would be absorbed through the gut wall as it is very lipophilic, having a log P of 5.1 (Nicolaides *et al.* 2001). Atovaquone is non-ionic, so its solubility is not affected by the pH of the solvent.

Studies examining dissolution of 250 mg Wellvone® tablets in FaSSIF show that dissolution is enhanced compared to USP SIF, thus indicating that the presence of natural bile salts affect the dissolution of atovaquone (Galia 1999). When the FaSSIF results are compared to the dissolution of atovaquone in FeSSIF, a further enhancement in dissolution is experienced. This follows what is found *in vivo*, as for a 500 mg dose of atovaquone the absolute bioavailability has been determined to be approximately 10% in the fasted state and 30% in the fed state (Dressman and Reppas 2000).

Figure 1-22 Molecular structure of atovaquone

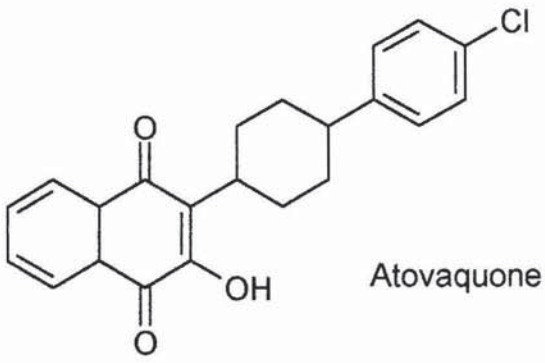

Atovaquone

1.6 Aims and objectives

- The first objectives were to determine a) how different polymers affect the dissolution of a sparingly soluble drug from a solid dispersion, and b) how the polymer concentration affected the dissolution of the drug from the solid dispersions. This was followed by assessing whether similar relationships were found when a different drug was used with the same polymers at the same ratios.

- The next objective was to establish a suitable mathematical method to assess the differences found in the dissolution of the drugs from the solid dispersions. As discussed in section 1.4.6 there are many different models that have been used to compare dissolution profiles, and to model the data obtained from the data. It was stated that the current models for assessing the similarity of dissolution profiles are unable to assess super-saturated dissolution data, *i.e.* they do no compensate for the recrystallisation of the drug during the test.

- The effect of the paddle speed was investigated to establish what effect agitation of the dissolution medium had upon the dissolution of the solid dispersions. A further aim of this study was to investigate whether any discrimination of the dissolution profiles found using the FaSSIF was dependent upon the paddle speed.

- It was an aim of the study to investigate the use of bio-relevant dissolution media as a predictor of the *in-vivo* performance. This was to

be achieved by investigating the effects on the dissolution of troglitazone from some of the proposed gastric dissolution media. It was then intended to investigate how the pre-exposure to gastric fluid affected the dissolution of the solid dispersions in the intestinal fluid. It is proposed that a system will be developed that allows for the change from a gastric to an intestinal medium. Finally based upon the data obtained from the dissolution results, in FaSSIF, a computer simulation of the *in vivo* performance will be developed. For this model comparison of the dissolution of the prepared solid dispersions with market producted will be required.

- The final aim of this work is to investigate how the carrier influences the dissolution of the drug from the dispersion. As discussed in section 1.3.2.3 there are many different theories as to the possible mechanism behind the release of the drug from a solid dispersion; these include improved wetting of the drug by the carrier, inhibition of the crystal growth of the drug by the polymer, and finally the release of the drug is controlled by the dissolution of the polymer. It is the aims to investigate to what extent these effects affect the release of troglitazone from a solid dispersion.

2 Materials and methods

2.1 Ultra-Violet Spectroscopy (UV)

2.1.1 Experimental

2.1.1.1 Equipment

A unicam UV-Visible spectrometer, equipped with the vision software V3.40 was used to analyse the results. Matched pairs of UV quartz cells were used.

2.1.1.2 Method

- Scan speed – Interstellar scan
- Data interval – 1.0 nm
- Lamp change – 325.0 nm
- Bandwidth – 2.0 nm
-

Samples were prepared by rinsing the quartz cell twice with distilled water and then rinsing twice with the solution under analysis.

Before any sample analysis was undertaken a baseline scan was obtained using a blank solution of the solvent in which the substance under analysis was dissolved into so that any interference could be accounted for. Samples were then scanned from 190 – 300 nm to determine λ_{max}.

2.2 HPLC assay of Troglitazone

2.2.1 Introduction

The method used to analyse the troglitazone was adapted from a method by Galia (2000). To adapt the method to measure the intended rage such parameters as the detector sensitivity were varied. The intended range selected was based upon data obtained by Galia (2000) on the dissolution of troglitazone in FaSSIF.

All the developed methods underwent a performance check; this was to show that the method was repeatable, and that there was no day to day variance.

2.2.2 Experimental

2.2.2.1 Materials

Troglitazone was supplied by GlaxoSmithKline (Ware, UK). Acetonitrile and orthophosphoric acid were obtained from Aldrich (Poole, UK). All materials were pharmaceutical, analytical or HPLC grade as appropriate.

2.2.2.2 Equipment

The HPLC system consisted of a WISP 712 auto injector, a Waters 490E ultraviolet detector, and a Waters 600E system controller and was fitted with an Erma degasser ERC-3312. The results were collected and integrated using JCL6000 for Windows 2.0 Chromatography Data System, supplied by Jones Chromatography UK.

2.2.2.3 Methods

2.2.2.3.1 Method 1

Standards were prepared to encompass a range of 0.005 - 0.2 $mgml^{-1}$; this range was based upon the dissolution data obtained from Galia (2000). All standards were prepared from a stock solution and diluted using a solvent mixture (60:40 acetonitrile:water). All standards were injected once and the peak areas were then used to construct a calibration curve using Microsoft Excel®.

The chromatographic conditions were:

- Injection volume - 20 μl
- Mobile phase - acetonitrile:water:orthophosphoric acid (60:40:0.008)
- Wavelength - 230 nm
- AUFs - 0.375 abs
- Flow rate - 1.0 ml min^{-1}
- Run time - 7 min
- Column - Techsphere ODS 5μm 150mm x 4.6mm ID

To performance check the method, five samples of a known concentration (0.075 mg ml^{-1}) were prepared in a solvent mix (60:40 acetonitrile:water). These samples were then analysed using the HPLC method detailed in this section. This was repeated over three days, and on each day fresh samples and standards were prepared. To asses the repeatability of the method the relative standard deviation (RSD) was calculated for the results each day, and for all the results obtained over the testing period. The target RSD was ≤ 2%, this is the value stated in the United States Pharmacopoeia (USP,1995). The data for this performance check can be found in appendix 3.

2.2.2.3.2 Method 2

Due to the poorly soluble nature of troglitazone (section 1.5.1) it was considered necessary to develop a more sensitive analytical method. For this method the calibration range encompassed 0.5 – 10 $\mu g ml^{-1}$. The rest of the method was as detailed in section 2.2.2.3.1.

The chromatographic conditions were:

- Injection volume - 75 µl
- Mobile phase - acetonitrile:water:orthophosphoric acid (60:40:0.008)
- Wavelength - 230 nm
- AUFs - 0.1 abs
- Flow rate - 1.0 ml min^{-1}
- Run time - 7 min
- Column - Techsphere ODS 5 µm 150 mm x 4.6 mm ID

To performance check the method, five samples of a known concentration (5.5 µg ml^{-1}) were prepared in a solvent mix (60:40 acetonitrile:water). These samples were then analysed using the HPLC method detailed in this section. This was repeated over three days, and on each day fresh samples and standards were prepared. To asses the repeatability of the method the relative standard deviation (RSD) was calculated for the results each day, and for all the results obtained over the testing period. The target RSD was ≤ 2%, this is

the value stated in the United States Pharmacopoeia (USP,1995). The data for this performance check can be found in appendix 4.

2.2.2.4 Sample Data

Sample chromatograms can be found in appendix 1.

The data from the performance check of the method shows that suitable repeatability was obtained, with no day to day variance for both methods (appendices 3 and 4).

Figure 2-1 Sample calibration curve for troglitazone. Results are the mean of three replicates, error bars ± SD

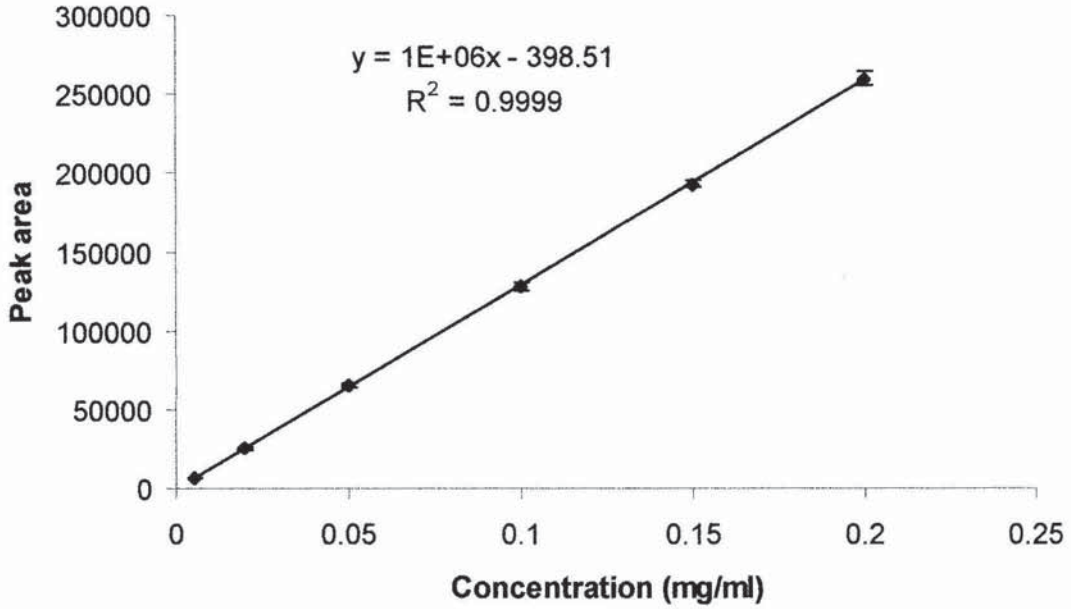

2.3 HPLC Assay of Atovaquone

2.3.1 Introduction

The method used to analyse the troglitazone was adapted from a method by Galia (2000). To adapt the method to measure the intended rage such parameters as the detector sensitivity were varied. The intended range selected was based upon data obtained by Galia (2000) on the dissolution of troglitazone in FaSSIF.

All the developed method underwent a performance check; this was to show

that the method was repeatable, and that there was no day to day variance.

2.3.2 Experimental

2.3.2.1 Materials

Atovaquone was supplied by GlaxoSmithKline (Ware, UK). Acetonitrile and trifluoroacetic acid were obtained from Aldrich (Poole, UK). All materials were pharmaceutical, analytical or HPLC grade as appropriate

2.3.2.2 Equipment

The HPLC system consisted of a WISP 712 auto injector, a waters 490E ultraviolet detector, and a Waters 600E system controller and is fitted with an Erma degasser ERC-3312. The data was collected and integrated using JCL6000 for Windows 2.0 Chromatography Data System, supplied by Jones Chromatography.

2.3.2.3 Method

Standards were prepared to encompass a range of 0.005 - 0.2 mg ml^{-1}; this range was based upon the dissolution data obtained from Galia (2000). All standards were prepared from a stock solution and diluted using a solvent mixture (60:40 acetonitrile:water). All standards were injected once and the peak areas were then used to construct a calibration curve using Microsoft Excel®.

- Injection volume - 100 μl
- Mobile phase - acetonitrile:water:THF (60:40:0.008)
- Wavelength - 254 nm
- AUFs - 0.01 abs
- Flow rate - 1.5 ml min^{-1}
- Run time - 12 min
- Column - Techsphere ODS 5 μm 150 mm x 4.6 mm ID

To performance check the method, five samples of a known concentration

(3.5 μg ml^{-1}) were prepared in a solvent mix (60:40 acetonitrile:water). These samples were then analysed using the HPLC method detailed in this section. This was repeated over three days, and on each day fresh samples and standards were prepared. To asses the repeatability of the method the relative standard deviation (RSD) was calculated for the results each day, and for all the results obtained over the testing period. The target RSD was ≤ 2%, this is the value stated in the United States Pharmacopoeia (USP,1995). The data for this performance check can be found in appendix 5.

2.3.2.4 Sample Data

Sample chromatograms can be found in appendix 2.

The data from the performance check of the method shows that suitable repeatability was obtained, with no day to day variance (appendix 5).

Figure 2-2 Calibration curve for Atovaquone HPLC assay. Results are the mean of three replicates, error bars ± SD

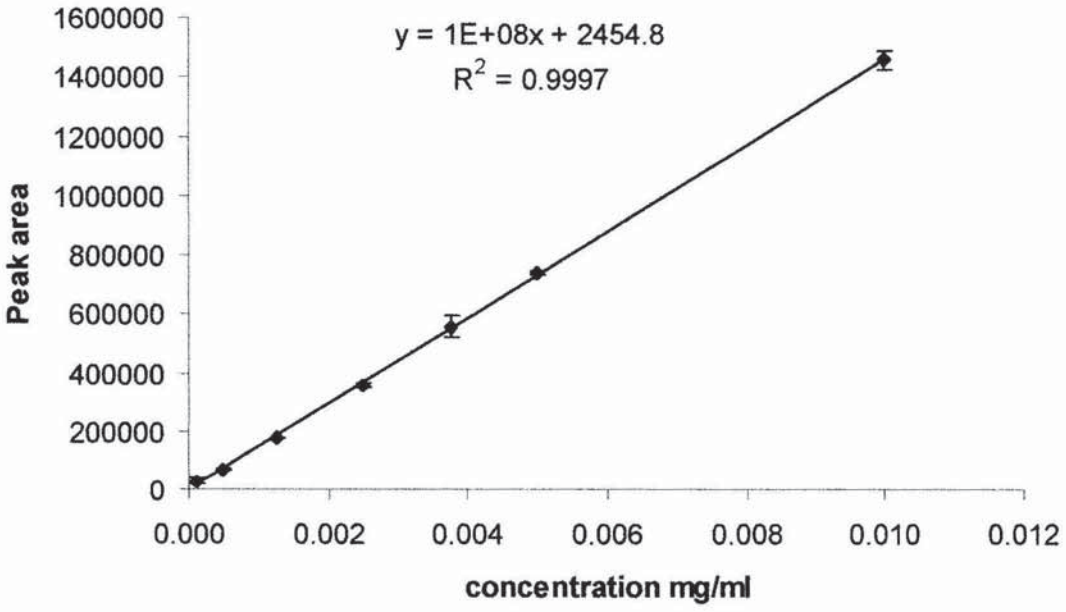

2.4 Spray drying

2.4.1 Introduction

As discussed in section 1.2.2.2, there are two main methods for the preparation of solid dispersions; the solvent method and the fusion method.

For the purpose of this study, the method to be used was the solvent method. One of the main problems associated with the solvent method is the removal of the solvent; one quick method of achieving this is to spray-dry the solution.

The spray drying process involves the liquid being atomised into small droplets, which are sprayed into a heated spray chamber. This spray chamber then provides a large surface area in which the small droplets can dry into solid particles.

Some of the advantages include:

- Short residence time at elevated temperature.
- Drying time is rapid
- Particle size can be controlled

Disadvantages

- Bench-top spray driers give low yields (typically 30 – 50 %)

2.4.1.1 The use of spray drying for solid dispersion formulation

There have been a few studies demonstrating the use of a spray drier in the preparation of solid dispersions. All these studies showed that the resultant solid dispersion produced the drug in the amorphous state (Jachowicz and Nurenbürg 1997, and Jung *et al.* 1999). Arias *et al.* (1995) compared the preparation of solid dispersions by the spray drying method to the hot melt method. It was found that there was an advantage to the spray drying method. The spray dried solid dispersions, for all prepared ratios, gave an increased dissolution rate compared to the melt method. This was attributed to the fact that there is closer contact between the drug and the carrier when the spray drying method was used; this led to stronger interactions between the drug and carrier. Also the spray drying technique producing more of the drug in the amorphous state.

2.4.2 Experimental

2.4.2.1 Materials

HPMC (Pharmacoat 603) and HPMCP (HP-55) were supplied by R.W Unwin (Welwyn, UK). PVP (K-30) was supplied by ISP Europe (Tadworth, UK). Dichloromethane and ethanol were supplied by Aldrich (Poole, UK). Atovaquone and troglitazone were supplied by GlaxoSmithKline (Ware, UK).

2.4.2.2 Equipment

The spray drier used was a Büchi 190 mini dryer, and a Gallenkamp vacuum oven.

2.4.2.3 Method

Dispersions were prepared with the following amounts of polymer: 9, 17, 23, 50, 71, 83 and 91% (w/w). Appropriate amounts of drug and polymer, relating to the concentration of polymer required, were dissolved into a solvent mixture of dichloromethane:ethanol (75:25). Dissolved mixtures were then spray dried using the following settings:

- Outlet temperature - 75°C
- Inlet temperature - 106°C
- Flow rate - 10 ml min^{-1}
- Atomising air - 600 l hr^{-1}
- Aspirator - 100%
- Vacuum - 40 – 45 mbar

Troglitazone has two melting points, the first is at 122.56°C and the second is at 160.00°C (Suzuki *et al.* 2002), and the atovaquone melting point was shown in DSC studies to be 220.64°C (section 3.1.4.1). this means that degradation of the drugs due to the spray drying should not be an issue.

The resulting dispersions were then placed overnight in a vacuum oven, with the vacuum set to 100%, and the temperature at 40°C.

The samples were then analysed to ensure that the required ratio of drug to polymer was obtained (see section 3.1.2.3).

To prevent degradation from humidity, dispersions were stored in a desiccator, and disposed of after three months of manufacture.

2.5 Investigating the uniformity of the solid dispersions

2.5.1 Introduction

A method was developed with the sole purpose of ensuring that theoretical drug concentration of the dispersion is maintained, and that the drug is homogeneously distributed within the dispersions.

2.5.2 Experimental

2.5.2.1 Materials

Solid dispersions were prepared as detailed in section 2.4. Acetonitrile was obtained from Aldrich (Poole, UK).

2.5.2.2 Equipment

As detailed in section 2.4.2.2.

2.5.2.3 Method

50 mg of each dispersion was dissolved in 100 ml acetonitrile:water (60:40); 5 ml of this stock was withdrawn and diluted to 10 ml with acetonitrile:water (60:40). These samples were the analysed using the HPLC method detailed in section 2.2.2.3.1 (for troglitazone samples) or 2.3.2.3 (for atovaquone samples).

2.6 Dissolution

2.6.1 Experimental

2.6.1.1 Materials

Sodium taurocholate and lecithin were supplied by GlaxoSmithKline (Ware, UK). Sodium Hydroxide and potassium dihydrogen phosphate were obtained from Aldrich (Poole, UK).

2.6.1.2 Equipment

The dissolution equipment consisted of a Hanson SR6 dissolution bath, fitted with a Validata control unit; it was also equipped with 1 litre round bottomed flasks and paddles that conform to USP apparatus II.

2.6.1.3 Method

The paddle speed for dissolution was typically 75 rpm (unless stated differently), and the bath temperature was 37°C. The FaSSIF was prepared to the composition described in table 1-6. The volume of dissolution medium used was typically 500 ml (unless stated in the method).

Samples were weighed out so that the mass of drug was constant, for troglitazone this would be 200 mg (section 1.5.1), and atovaquone 250 mg (section1.5.2). The samples were then tipped into the bath and the weighing boats washed with 10 ml of the dissolution media (taken from the flask before-hand) and returned to the flasks.

Sampling was carried out at 5, 10, 15, 20, 30, 45, 60 and 90 minutes. This was achieved by drawing 5 ml of the medium from the flask using sampling rods (that conform to the USP specifications). These rods were fitted with a 10 μm frit to prevent undissolved particles from being removed. The samples were then filtered using a 0.45 μm cellulose acetate filter, with the first 2 ml being discarded, into a HPLC vial. This was replaced with 5 ml of fresh dissolution media.

2.7 Differential Scanning Calorimetry (DSC)

DSC is used to determine thermal properties of substances, for example the melting point (mp), and the glass transition temperature (T_g). It is because of these properties that it has been used extensively in the science of solid dispersions. As discussed in section 1.2.2 it is expected that within a solid dispersion made with an amorphous polymer that the drug will be found in the amorphous state. The use of DSC potentially allows for the amount of drug in the amorphous state to be quantified (Sertsou *et al.* 2002). This is achieved by

comparing the expected ΔH of the pure drug melt peak with any possible melt peak found within the solid dispersion.

2.7.1 Experimental

2.7.1.1 Materials

Solid dispersions were prepared as detailed in section 2.4

2.7.1.2 Equipment

DSC data were obtained using a Perkin-Elmer Diamond DSC, equipped with Pyris software.

2.7.1.3 Method

Between 5-10mg of each sample were weighed into aluminium sample pans, which were then crimped with a lid with a drilled hole of a diameter of 0.3mm. The sample pan was then placed into the furnace, with a blank pan in the other furnace. The following method and conditions were used for each run:

- Purge gas - Nitrogen
- Heating rate - 10°C/min

The resulting results were then processed using the Pyris software. The melting points of each peak were derived by measuring the onset temperature. Glass transitions were measured using the half Cp extrapolated function.

2.8 X-Ray Powder Diffraction (XRPD)

2.8.1 Experimental

2.8.1.1 Materials

Solid dispersions were prepared as detailed in section 2.4

2.8.1.2 Equipment

XRPD was performed on a Phillips X'pert MPD.

2.8.1.3 Method

Samples were prepared by putting approximately 300 mg of powder into the designed die, which was then inserted onto the instrument. The following parameters were then used:

- Count time – 1 s
- Step size – 0.04° 2θ
- Source – Ni filtered Cu-kα radiation (40 kV and 50 mA)
- Scanning range – 0 – 25° 2θ

3 Dissolution and physical characterisation of solid dispersions

3.1 Dissolution and subsequent modelling

3.1.1 Introduction

The USP describes four main methods with which dissolution testing can be performed: apparatus I – Rotating Baskets, apparatus II – rotating paddles, apparatus III – reciprocating cylinders and apparatus IV – flow through cell systems. The apparatus I and II are the most commonly used as they are robust enough to investigate the dissolution properties of a wide range of drugs.

As outlined in section 1.4.6 it is necessary to use a method to statistically compare the dissolution profiles, either by a model-dependent or a model-independent method. As the data shown in this chapter shows some examples of non-monochromatic dissolution data for troglitazone and atovaquone dispersions (the HPMCP 50% and above samples show the best examples), the models that were described in section 1.4.6 can be considered inappropriate. The exception to this is the model described by Valsami (1999) (section 1.4.6), which is quoted to be specifically for non-monochromatic data. However, it was decided not to use this model; this is due to there being no indication of the time at which the plateau or the maximum occurs therefore not giving any indication to the shape of the curve from the data alone. It was felt important in this instance to see this indication to the shape of the curve in the data as not all the curves show this precipitation. It is therefore intended to use a model-independent method, using the AUC. The AUC has been used by Polli *et al.* (1997) to describe differences between dissolution profiles, here the ratio between the AUC of the test product and the reference product, at different time points, was calculated.

It was highlighted in section 1.3.2.3 that it is possible that the dissolution rate of the chosen carrier can influence the dissolution rate of the drug. It has been shown in the literature that the dissolution rate of two different drugs can be similar from the same polymer (Dubois and Ford 1985). It has also been found

that the dissolution rate of a drug can be manipulated by the choice in carrier. The second purpose of this experiment, therefore, is to assess the way in which the different polymers affect the dissolution of both atovaquone and troglitazone.

3.1.2 Experimental

3.1.2.1 Materials

See sections 2.2.2.1, 2.4.2.1 and 2.6.1.1 for details of the materials used.

3.1.2.2 Equipment

Dissolution was performed using the equipment described in section 2.6.1.2. Analysis was performed on the HPLC system described in section 2.2.2.2. DSC analysis was performed on the equipment as described in section 2.7.1.2. XRPD analysis was performed on the equipment as described in section 2.8.1.2. Spray drying was performed using the equipment detailed in section 2.4.2.2.

3.1.2.3 Method

Solid dispersions were prepared at various ratios of drug:polymer (1:10 (91% polymer), 1:5 (83% polymer), 1:2.5 (71% polymer), 1:1 (50% polymer), 2.5:1 (29% polymer), 5:1 (17% polymer) and 10:1 (9% polymer)) using either troglitazone or atovaquone with either HPMCP, PVP or HPMC, using the method described in section 2.4.2.3. These ratios were selected as they allowed for the investigation of effects of high and low polymer loading. They were subsequently tested for homogeneity using the method described in section 2.5.2.3. The FaSSIF was made up to the concentrations given in table 1-6. To simulate the expected volume found *in-vivo* 500 ml of dissolution media was for each experiment.

Dissolution testing was performed as described in section 2.6.1.3. For all dissolution testing the samples under examination were added as a free powder.

HPLC analysis was performed as described in section 2.2.2.3.1 and 2.3.2.3

the only difference being that all samples were diluted in equal proportions with acetonitrile. The cumulative mass of drug dissolved at time t was calculated using the equation shown in equation 3-1.

Equation 3-1

$$Mt_{(n)} = V_r \cdot \left(\left(\frac{P_a - C}{m} \right) * 2 \right) + V_s \sum_{p-1}^{n-1} C_p$$

- Mt - Current cumulative mass at time t
- V_r - Volume of receiver
- V_s - Volume of sample
- C_p - Previous measured concentrations
- P_a - Peak area of current sample
- C - Intercept of calibration chart
- m - Slope of calibration chart
- n - Time point

The AUC for each dissolution profile was calculated using the PK functions for Excel add in (Usansky *et al.* 1999). ANOVA tests were performed using Graphpad's Instat 3 software package. Polynomial curves were fitted to the dissolution data using Microsoft Excel® (example spreadsheet located in appendix 3).

DSC analysis was performed as described in section 2.7.1.3. The main thermal properties investigated were the glass transition, melting endotherms and recrystallisation exotherms. The melting endotherms, and recrystallisation exotherms were analysed by integrating the peaks and recording the onset. Glass transitions were integrated using the half Cp extrapolation method on the Pyris software.

XRPD analysis was performed as described in section 2.8.1.3.

3.1.3 Results and discussion

3.1.3.1 Dissolution and solid state characterisation of troglitazone

Figure 3-1 Dissolution of troglitazone from physical mixtures with HPMCP. Results are the mean of three replicates, error bars ± SD

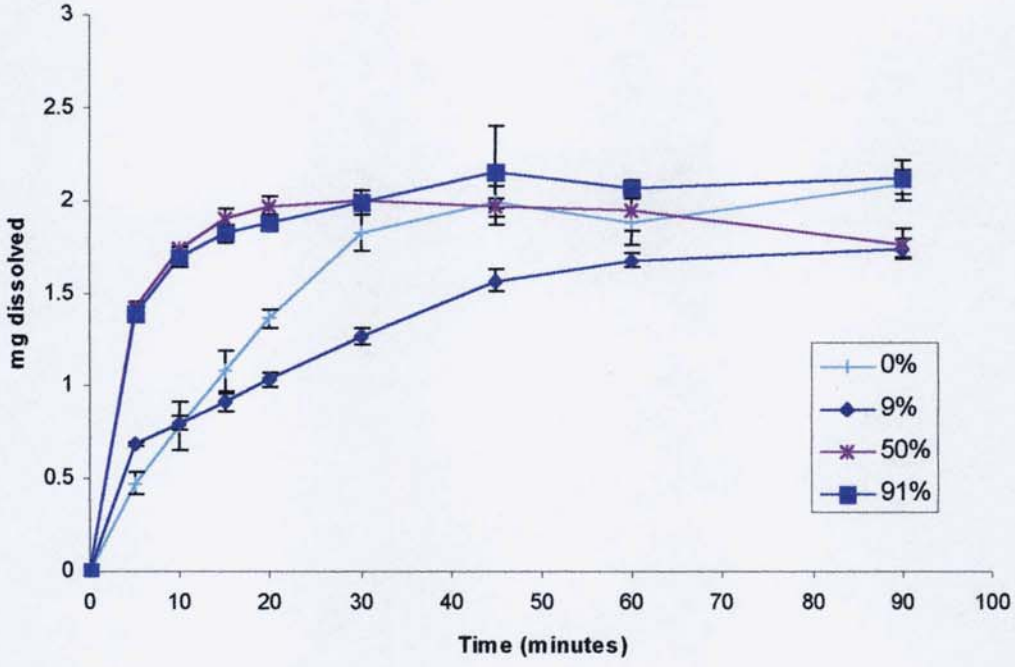

It is seen from figures 3-1 to 3-3 that troglitazone, when in the powder form, obtains a dissolution of less than 2.5 mg/ 500 ml which corresponds to 5 µg/ml. This is lower than solubility of troglitazone in water found by Suzuki *et al.* (2004), which was 10 µg/ml. This could be due to two reasons; 1) troglitazone is less soluble in FaSSIF than in water, and 2) the troglitazone has not reached a saturated solubility during the dissolution test. It is unlikely that troglitazone is less soluble in FaSSIF than in water, firstly it would be expected that the presence of surfactants in the FaSSIF should aid the dissolution (via the mechanism discussed in section 1.2.2.2, and secondly it has been shown that there is a large increase in the dissolution of troglitazone in FaSSIF when compared to aqueous buffer solutions at pH 6.5 (Galia 1999). Unfortunately it was not possible to ascertain the saturated solubility in FaSSIF, due to the rapid degradation of FaSSIF during a solubility test. The rapid degradation of the FaSSIF was evident in two ways; firstly when the FaSSIF was stored for more than 1 day, at room temperature, a white

precipitate appeared which was accompanied by a distinct change in the odour. The second way in which the degradation was evident was the appearance of several new peaks in the HPLC analysis of the solubility samples, some of which overlapped with the peak of the active ingredient. The solubility tests were performed by placing 1 gram of product in 20 ml of FaSSIF which were then stored at 37°C. It was then intended to test the solutions on subsequent days until a plateau value was established. An alternative method for measuring the saturated solubility in FaSSIF has been shown in the literature which takes only 2 hours to perform. Levis *et al.* (2002) placed excess drug into 50 ml of FaSSIF, this mixture was then stirred using an overhead stirrer at 300 rpm. Samples were then taken at regular intervals over a two hour period, resulting in the amount of drug dissolved achieving a significant plateau, which represented the saturated solubility. To fully clarify the differences a dissolution study was conducted in water, and it was found that there was no significant dissolution of troglitazone over 90 minutes (*i.e.* the HPLC assay was not sensitive enough to detect the troglitazone). This indicates that the FaSSIF increases the dissolution of troglitazone, and that the lower solubility experienced is most probably to do with the physical properties of the powder (*i.e.* particle size and wettability).

The effect of incorporating troglitazone into physical mixtures is also shown in figures 3-1 to 3-3. It is seen that the physical mixtures offer no major improvement on the maximum dissolution of troglitazone, and in fact, especially in the cases of PVP and HPMC, the addition of the polymer inhibited the dissolution. This was an expected result, as it is seen from the literature that the incorporation of sparingly soluble drugs into binary physical mixtures does not offer any enhancement in the dissolution of the drugs studied (Paradkar *et al.* 2004). It is flet that this inhibition of troglitazone dissolution could be caused by the enhancement of the local viscosity around the troglitazone particles during dissolution, this would have to be confirmed using a technique like microviscometry (section 5.1.3). However, figure 3-1 shows that increasing the HPMCP content of the mixture leads to an increase in the dissolution of the drug. It is postulated that this is due to the HPMCP being more efficient at wetting troglitazone; this is discussed in more depth in

section 5.2.

Figure 3-2 Dissolution of troglitazone from physical mixtures with HPMC. Results are the mean of three replicates, error bars ± SD

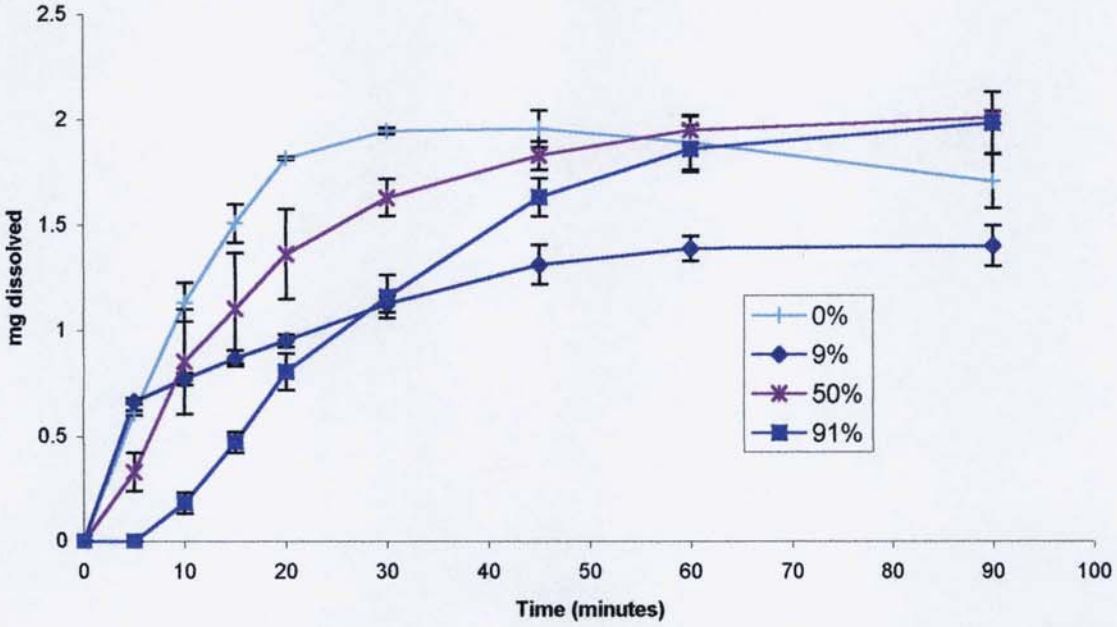

Figure 3-3 Dissolution of troglitazone from physical mixtures with PVP. Results are the mean of three replicates, error bars ± SD

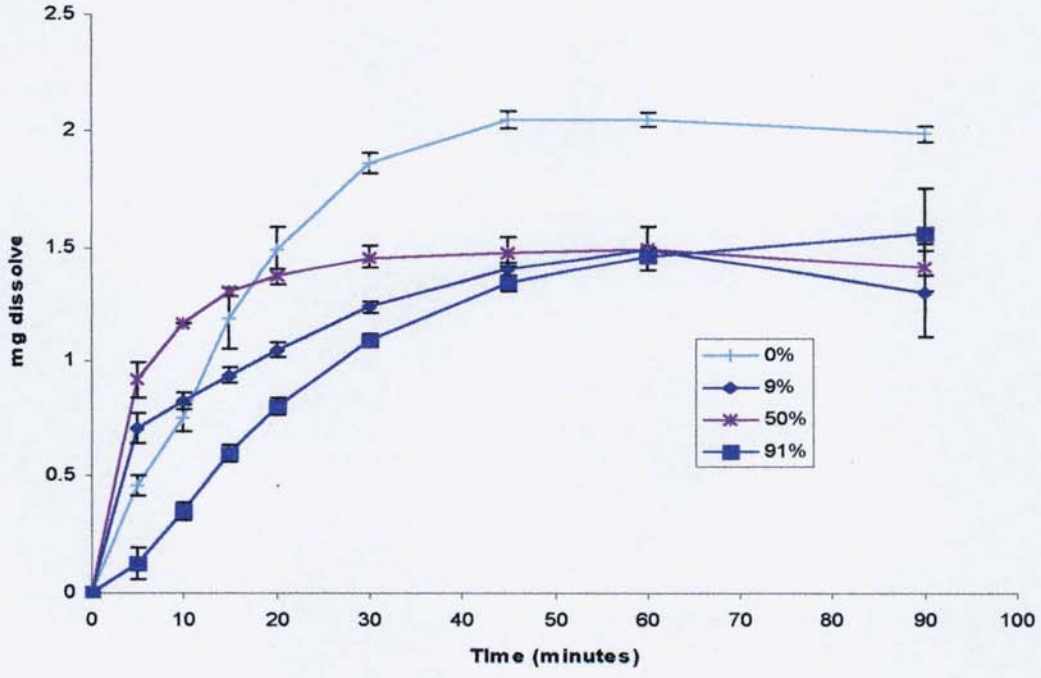

Figure 3-4 DSC trace of pure troglitazone

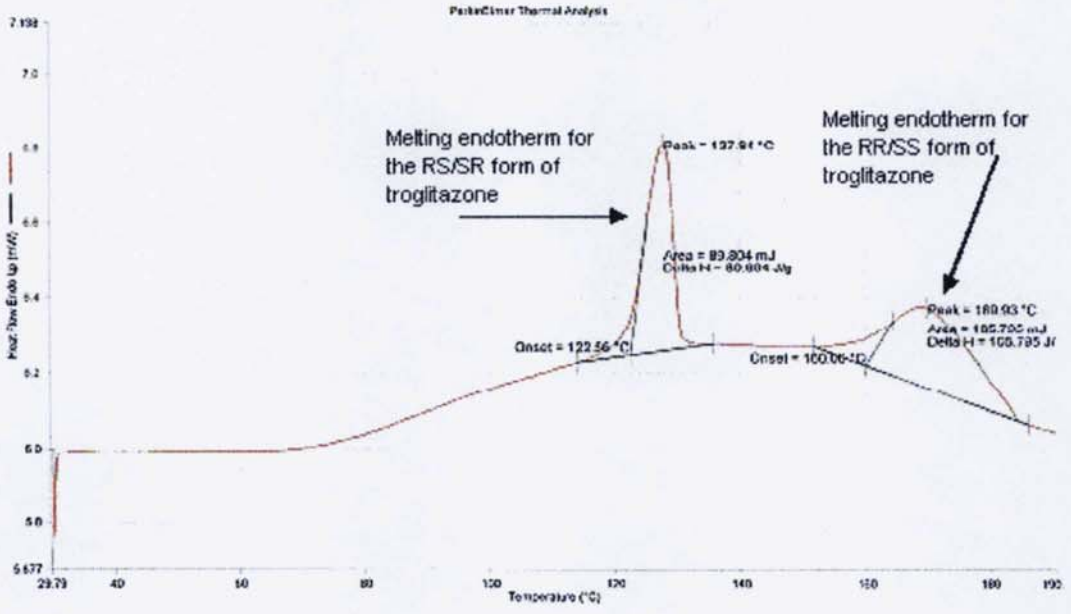

Figure 3-5 XRPD trace of pure troglitazone

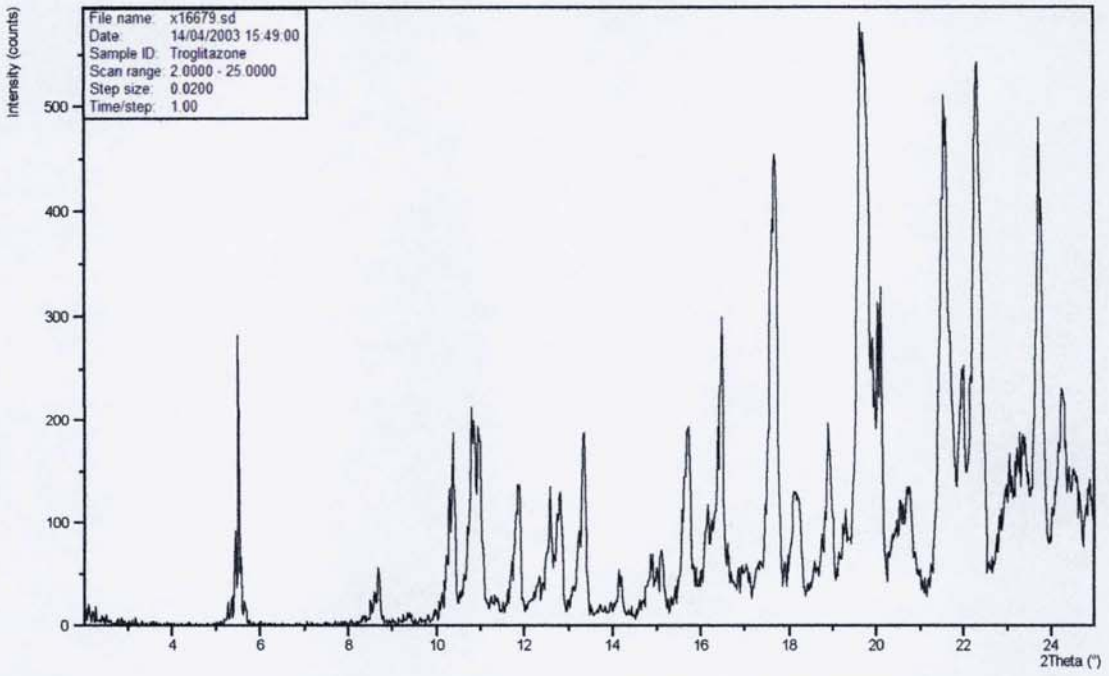

Figure 3-4 shows that troglitazone has two distinct melting endotherms, one at 122.56°C and the other at 160.00°C. It was stated in section 1.5.1 that troglitazone exists in four optical isomers, of equal amounts, and that there is a diastereomeric relationship between the isomers (RS/SR and RR/SS). It

was shown by Suzuki *et al.* (2002) that the peak found at 122.56°C represents the RR/SS form and the RS/SR form is represented by the peak at 160.00°C. Solubility testing, in pH 9 borate buffer, upon each isomer yielded the information that there is a difference in the solubilities of the optical isomers, with the RS/SR form having a slightly higher solubility. Upon quench cooling of the troglitazone drug substance, to make it amorphous it was found that a large increase in solubility was experienced; with a rise from 7µg/ml to 125 µg/ml for the RR form, 11.9 µg/ml to 87.3 µg/ml for the SR form, 12.8 µg/ml to 89.0 µg/ml for the RS form and 5.2 to 120 for the SS form. XRPD was also carried out upon the troglitazone, with the same characteristics peaks being found as shown in figure 3-5, *i.e.* the doublet peak between 10 -11°.

Figure 3-6 shows the effect of heating upon spray-dried troglitazone, it can be seen that within this profile that troglitazone has a glass transition temperature of 55°C, the presence of a glass transition temperature indicates that spray drying cause troglitazone to exist in the amorphous state. Further evidence that the troglitazone, post spray drying, is in the amorphous state can be seen in figure 3-7 where none of the characteristic XRPD peaks seen in figure 3-2 are present. Also as heating progresses the troglitazone does eventually recrystallise, resulting in a melt endotherm at 168.77°C, this indicates that only the RS/SR forms have recrystallised. Examination of the ΔH of the recrystallised troglitazone with that of the untreated troglitazone indicates that not all of this form has recrystallised. One interesting fact is that the melting endotherm has split into two peaks, the melting point of the first peak is higher than would be expected for the RR/SS form, it could well be that during the recrystallisation a metastable polymorph was formed. The ΔH of the untreated troglitazone (160°C) is 105.79 J/g compared to that of the spray dried troglitazone which is 37.05 J/g. The outcome of this is that troglitazone is relatively stable when in the amorphous state. It was suggested by Suzuki *et al.* (2002) that the presence of these four isomers leads to increased stability of the troglitazone when in the amorphous state, by the action of one diastereomer blocking the attachment of the other diastereomer to its solid state surface.

Figure 3-6 DSC trace of spray-dried troglitazone

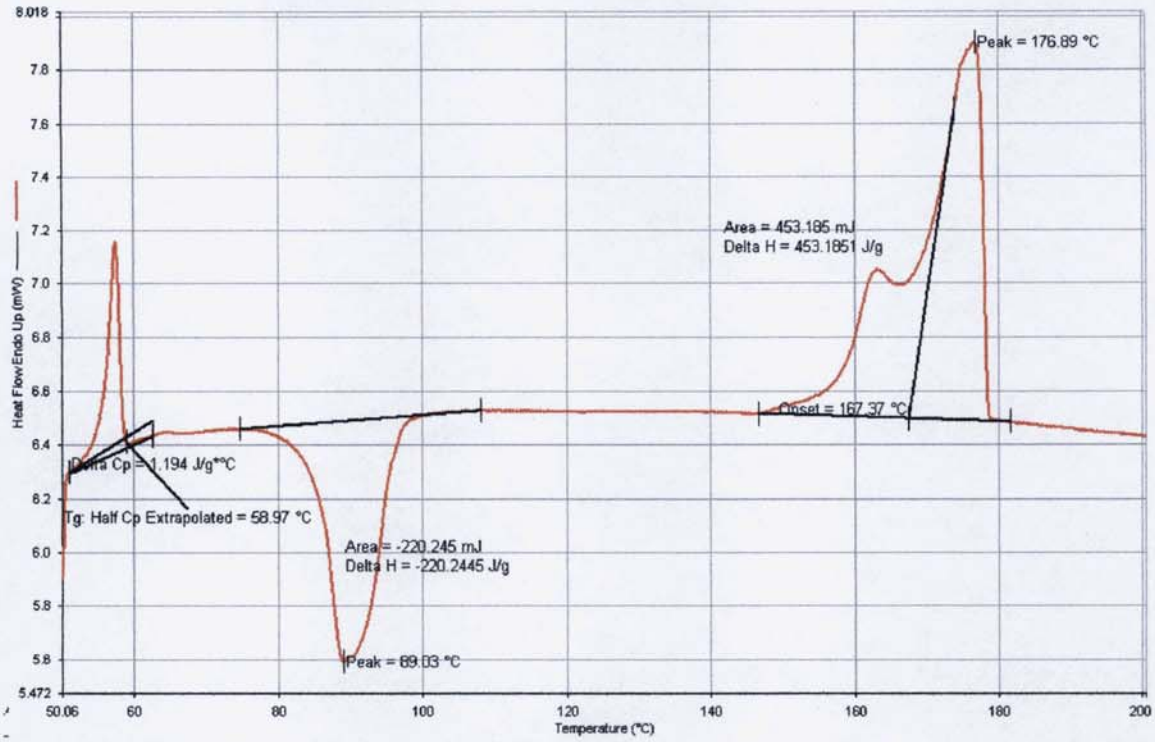

Figure 3-7 XRDP trace of spray dried troglitazone

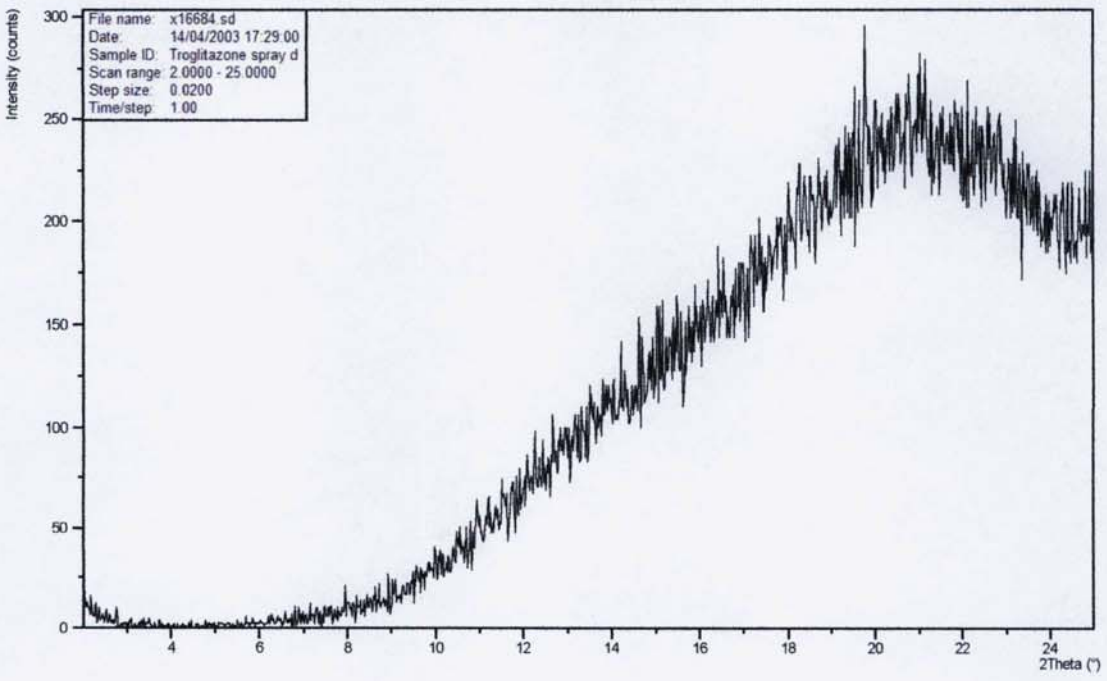

3.1.3.2 The effect of incorporating troglitazone into a solid dispersion on the degree of supersaturation

Figures 3-8, 3-9, and 3-10 show three main aspects; that as expected the dissolution of troglitazone is improved by the incorporation into a solid

dispersion (1.3.2), secondly that the amount of polymer appears to have a large impact upon the dissolution of troglitazone (this is discussed in more depth in sections 3.1.3.3, 3.1.3.4 and 3.1.3.5), and finally the dissolution of troglitazone is affected by the polymer used to form the solid dispersion (discussed in more depth in sections 3.1.3.6 and 3.1.3.7). It is also noticeable that the HPMCP dispersions experience a large amount of recrystallisation/precipitation after the peak level of troglitazone is dissolved. Table 3-1 shows the degree of enhancement in the dissolution of troglitazone when incorporated into the various solid dispersions. This was calculated by dividing the peak concentration of troglitazone dissolved (during dissolution) from a dispersion, by the peak amount of free troglitazone dissolved during dissolution (figure 3-2). The effect that the concentration and type of polymer has upon the dissolution of polymer can be seen in table 3-1. As the amount of polymer in the dispersion increases, the 'degree of enhancement' increases until it reaches a peak value (71% for both HPMC and PVP, 83% for HPMCP), where after the 'degree of enhancement' decreases. The fact that the degree of enhancement firstly increase and then starts to decrease for all the polymers is an expected result, and discussed in more depth in sections 3.1.3.3 (HPMCP), 3.1.3.4 (PVP) and 3.1.3.5 (HPMC).

Table 3-1 The degree of enhancement obtained when the peak mass dissolved from the solid dispersions is compared to troglitazone alone

Amount of polymer in dispersion	Degree of enhancement		
	HPMCP	HPMC	PVP
9%	9.16	16.78	26.88
17%	11.30	23.58	32.19
29%	29.58	18.49	39.09
50%	54.53	36.15	43.47
71%	69.24	43.04	47.64
83%	70.64	8.06	15.22
91%	50.98	7.19	37.96

Figure 3-8 Dissolution of troglitazone from HPMCP solid dispersions at various concentrations of HPMCP (w/w). Results are the mean of three replicates, error bars ± SD.

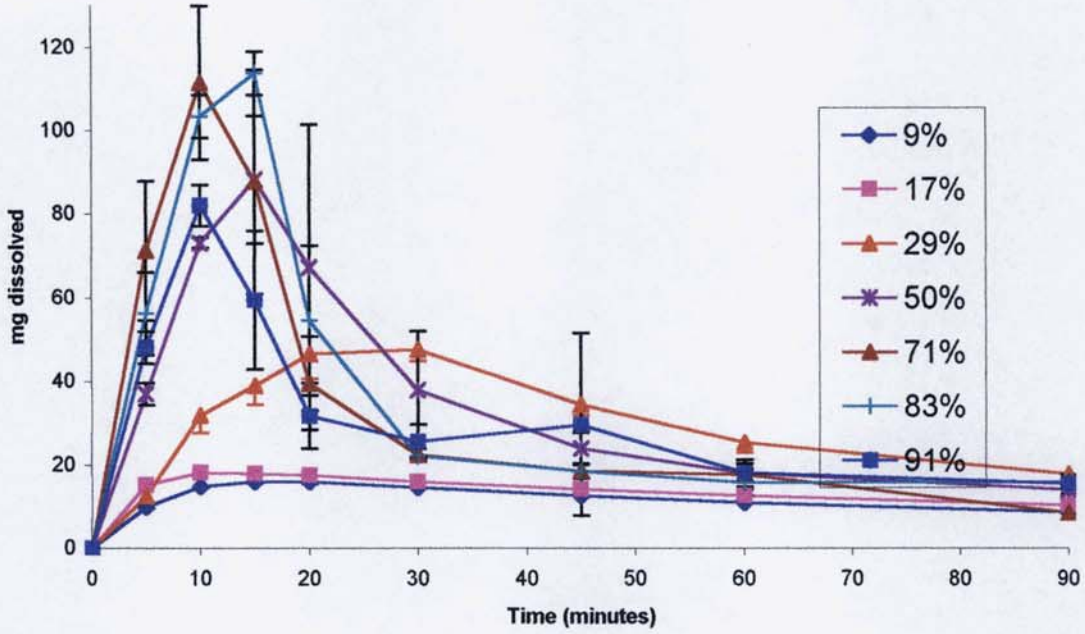

Figure 3-9 Dissolution of troglitazone from PVP solid dispersions at various concentrations of PVP (w/w). Results are the mean of three replicates, error bars ± SD.

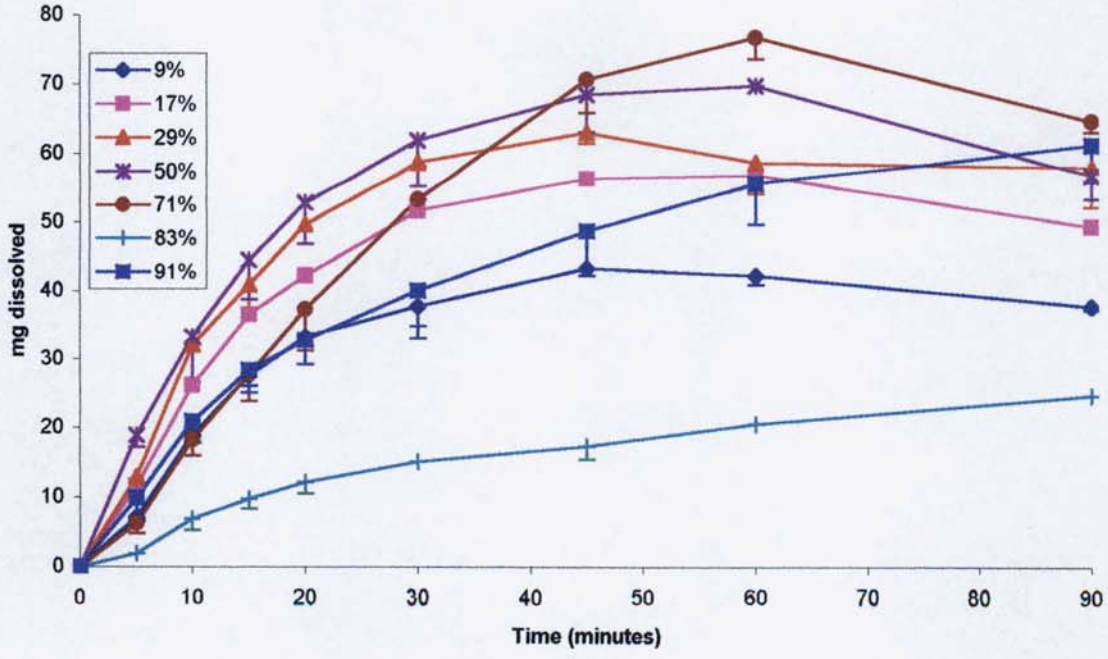

Figure 3-10 Dissolution of troglitazone from HPMC solid dispersions at various concentrations of HPMC (w/w). Results are the mean of three replicates, error bars ± SD.

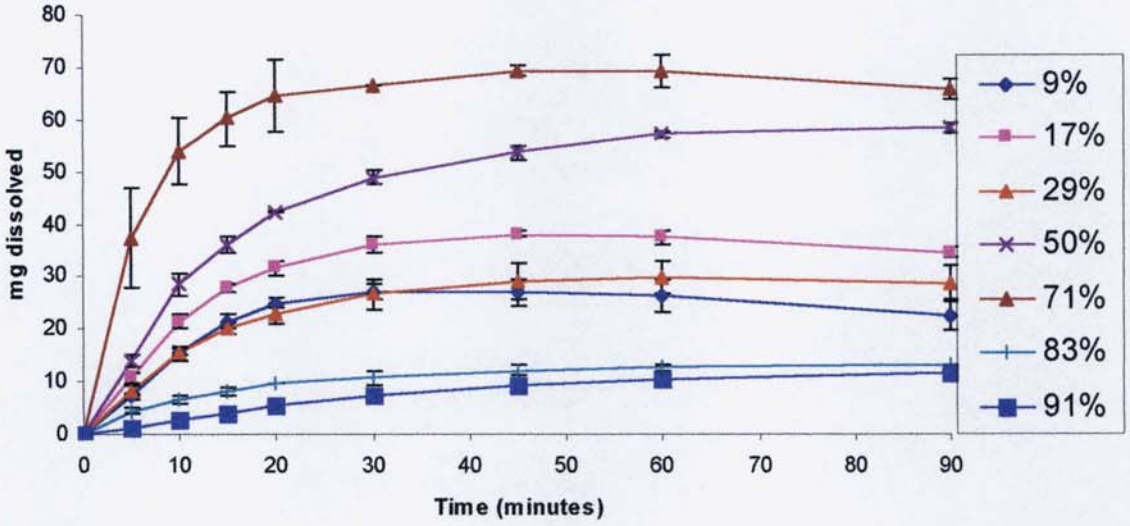

This data also gives an indication of the extent the choice of polymer has upon the dissolution of troglitazone. It is seen that at the lower concentrations of polymer, PVP (9, 17 and 23% polymer) is the most effective at increasing the peak amount of troglitazone dissolved. Whereas, from 50% polymer concentration onwards, HPMCP is the most effective polymer at increasing the amount of troglitazone dissolved. It is seen in figures 3-8, 3-9 and 3-10 that different concentrations of each polymer have a major impact upon the peak amount of drug dissolved. Calculation of the degree of enhancement, therefore, allows a quantitative method to assess the size of these differences. From these data, however, it is not possible to get any indication of the profile data (i.e. there is no time data), and there is no indication as to profile similarity. In order to address this, the AUCs at 20 and 90 minutes were calculated (table 3-2) and compared using an ANOVA test, followed by a Tukey analysis, the result of these analyses can be found in tables 3-3 to 3-22.

3.1.3.3 Effect of HPMCP concentration upon the dissolution of troglitazone

From the data shown in table 3-3, there is a major change between the behaviour of the solid dispersions, over the first 20 minutes, when the HPMCP

concentration reaches 50% (w/w) concentration. The differences between the AUC of those dispersions with 50% (w/w) and above HPMCP, compared to those that are below 50% are considered highly significant (in the majority of cases $p < 0.001$). This fits with one of the proposed mechanisms for the release of drugs from solid dispersions. It has been proposed that in dispersions of high drug loadings, during the dissolution process, the properties of the drug itself control the dissolution of the dispersions. This is because the surface of the dispersion is drug-rich, ensuring that the dispersion below is not wetted. This means that the wetting of the dispersion is controlled by the drug rather than the carrier, thus the dissolution would be expected to be slower (Ford 1986). Above 50% polymer content it is expected that the surface of the dispersions would be polymer-rich, so therefore the dissolution of the polymer controls the dissolution of the dispersion. It is, also noticeable from the results that at a HPMCP concentration of 91% (w/w) the profile is not as significantly different from that of the 29% dispersion ($p < 0.05$). It is proposed in section 5.4.6 that this is due to the dissolution of the HPMCP being slightly slower from the 91% dispersion than when it is incorporated in the 71% dispersion.

Table 3-2 The AUC_{20}, AUC_{90} and the polynomial rate of the troglitazone solid dispersions. Results are the mean of three replicates, ± SD

% Polymer	AUC_{20} ($mg.ml^{-1}.min$)			AUC_{90} ($mg.ml^{-1}.min$)			Polynomial rate (mg/min)		
	HPMCP	PVP	HPMC	HPMCP	PVP	HPMC	HPMCP	PVP	HPMC
9	243 ± 5	351± 18	282 ± 16	1071 ± 16	3150 ± 117	2075 ± 173	2.10	0.99	1.02
17	300 ± 15	442 ± 65	379 ± 18	1237 ± 29	3872 ± 555	2913 ± 98	4.48	1.23	1.58
29	510 ± 68	447 ± 60	276 ± 19	2695 ± 32	3999 ± 895	2253 ± 234	2.71	2.71	1.42
50	1160 ± 175	616 ± 77	497 ± 19	2945 ± 656	4599 ± 1050	4282 ± 65	6.50	4.30	3.14
71	1452 ± 312	355 ± 37	918 ± 137	2664 ± 290	4986 ± 297	5513 ± 470	11.57	0.89	10.33
83	1503 ± 72	121 ± 22	111 ± 22	2925 ± 151	1456 ± 155	870 ± 200	10.59	0.20	1.30
91	1028 ± 132	378 ± 43	53 ± 6	2459 ± 198	3978 ± 647	822 ± 195	3.51	1.31	0.20

Table 3-3 Results of the Tukey analysis of the AUC_{20} of the HPMCP dispersions (shaded boxes indicate no significant difference)

%Polymer	% Polymer						
	9	17	29	50	71	83	91
9							
17	>0.05						
29	>0.05	>0.05					
50	<0.001	<0.001	<0.01				
71	<0.001	<0.001	<0.001	>0.05			
83	<0.001	<0.001	<0.001	>0.05	>0.05		
91	<0.001	<0.001	<0.05	>0.05	<0.05	<0.05	

Examination of figure 3-8 shows that, from visual inspection, the profiles for the 50%, 71%, 83% and 91% are indeed similar, but the peak release of troglitazone from the 29% dispersion is lower than the other dispersions. It is for these dispersions that undertaking an ANOVA for the AUC_{20} is necessary, as this does show differences between the 29% (w/w) dispersion compared to the other dispersions (table 3-3). Using these both these values to compare the dissolution profiles gives a description of the behaviour of these dispersions over time – showing that the dispersions containing more than 50% (w/w) polymer release troglitazone quicker than from the 29% (w/w) dispersion. It has been shown for solid dispersions that contain HPMCP that increasing the polymer concentration increases the amount of drug dissolved (Kai *et al.*, 1996, and Sertsou 2002). This has been put down to two possible reasons: 1) that a coarser dispersion of particles is found with dispersions made at high drug loading, or 2) that in the dispersion with a high polymer loading there is more drug incorporated into the solid solution. It has been shown that the implication of this increase in the *in vitro* dissolution leads to more drug absorbed *in vivo*. Kai *et al.* (1996) examined the release of drug from the solid dispersion through oral administration in beagles and it was found that the 1:5 (drug:HPMCP) dispersion provided better

bioavailability (larger AUC and C_{max})than the 1:3 dispersion.

Table 3-4 Results of the Tukey analysis of the AUC_{90} of the HPMCP dispersions (shaded boxes indicate no significant difference)

%Polymer	% Polymer						
	9	17	29	50	71	83	91
9							
17	>0.05						
29	<0.05	<0.05					
50	<0.01	<0.05	>0.05				
71	<0.05	>0.01	>0.05	>0.05			
83	<0.01	<0.05	>0.05	>0.05	>0.05		
91	<0.01	<0.01	>0.05	>0.05	>0.05	>0.05	

What has not been reported before for HPMCP dispersions is the decrease in the amount of drug released from the solid dispersions as the polymer concentration increases. Tables 3-3 and 3-4 show that the dissolution of troglitazone from the 91% HPMCP dispersion is significantly different from those of lower polymer content. Table 3-2 shows that the difference is that the 91% dispersion has less dissolution than the 50%, 71% and 83% dispersions. It is postulated that this difference is due to the local viscosity increases that would be generated with higher polymer content. This could be confirmed by measuring the viscosity of the solution during dissolution, by using microviscometry (section 5.1.3)

Figure 3-11 DSC trace of HPMCP HP-55

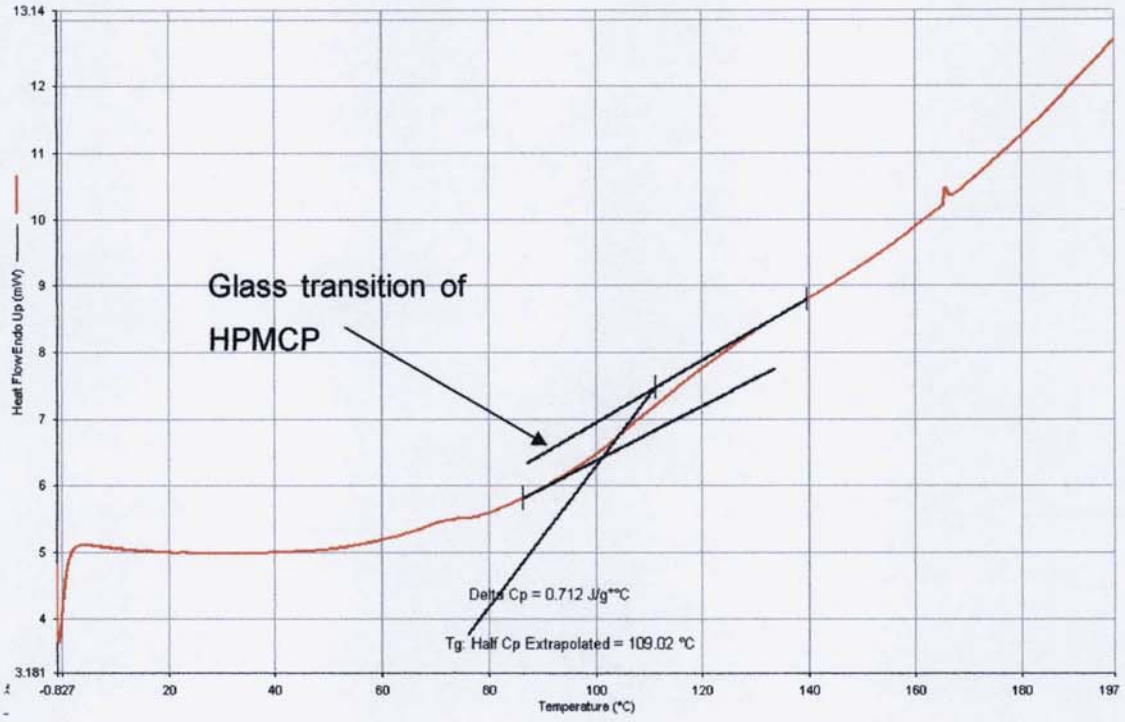

It is seen from figures 3-12 to 3-15 that increasing the concentration of HPMCP in the solid dispersions has a large effect upon thermal characteristics of the solid dispersions. At the lower polymer loading (figure 3-12) the profile is very similar to that of troglitazone spray-dried alone (figure 3-6), *i.e.* there is a recrystallisation preceding a melting endotherm at 172°C, which is comparable to that of spray dried troglitazone. The main difference in the profiles is that ΔH of the melting endotherm in figure 3-12 is a lot lower than that of spray dried troglitazone alone (230 J/g compared to 453 J/g). This indicates that not all the troglitazone has crystallised during the heating process. The consequence of this is that it can be said that some of the troglitazone is incorporated in the HPMCP in the form of a solid solution, and the rest of the troglitazone is freely dispersed in the amorphous form (Sertsou 2002). When the higher polymer dispersions are considered (figures 3-13 to 3-15) it can be seen that in all cases no drug recrystallises under heating, and that there are two glass transition phases

present. It is felt that the lower temperature glass transition temperature represents troglitazone, and that the higher temperature glass transition temperature represents HPMCP. As the polymer concentration increases, the glass transition temperature of both components increases. This is indicative of an interaction between the two components. It has been proposed that changes in phase temperatures, when binary mixtures are used, indicates an interaction between the two components (Smith 1982). The fact that there are two glass transition temperatures indicates that there are two phases present within the solid dispersion, rather than one which would be expected with a true solid solution. It is also worth noting that the XRPD traces (figures 3-16 to 3-18) show no evidence of crystalline material being present in the solid dispersions.

Figure 3-12 DSC trace of the troglitazone dispersion with 17% HPMCP

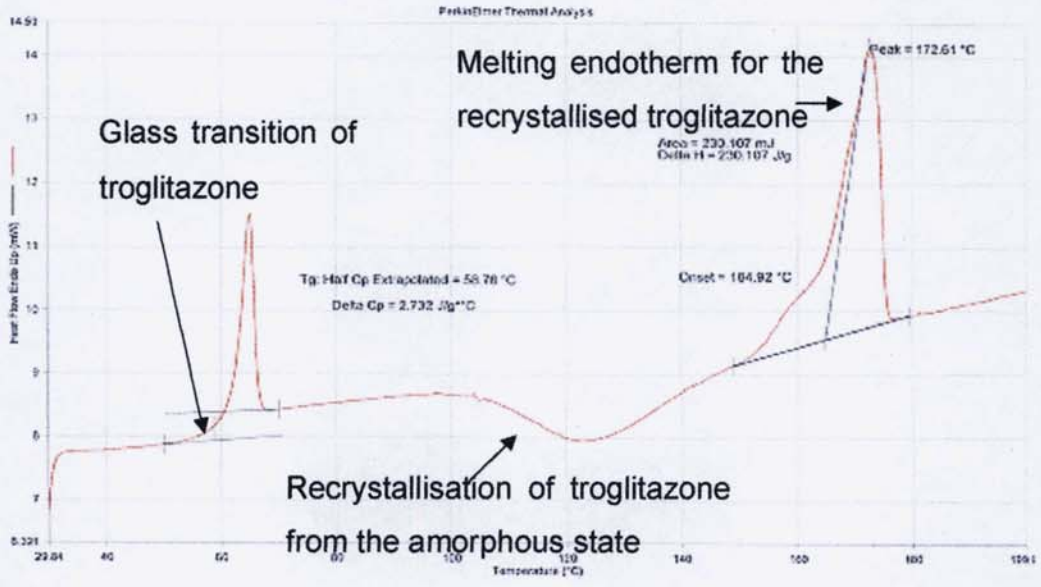

Figure 3-13 DSC trace of the troglitazone dispersion with 50% HPMCP

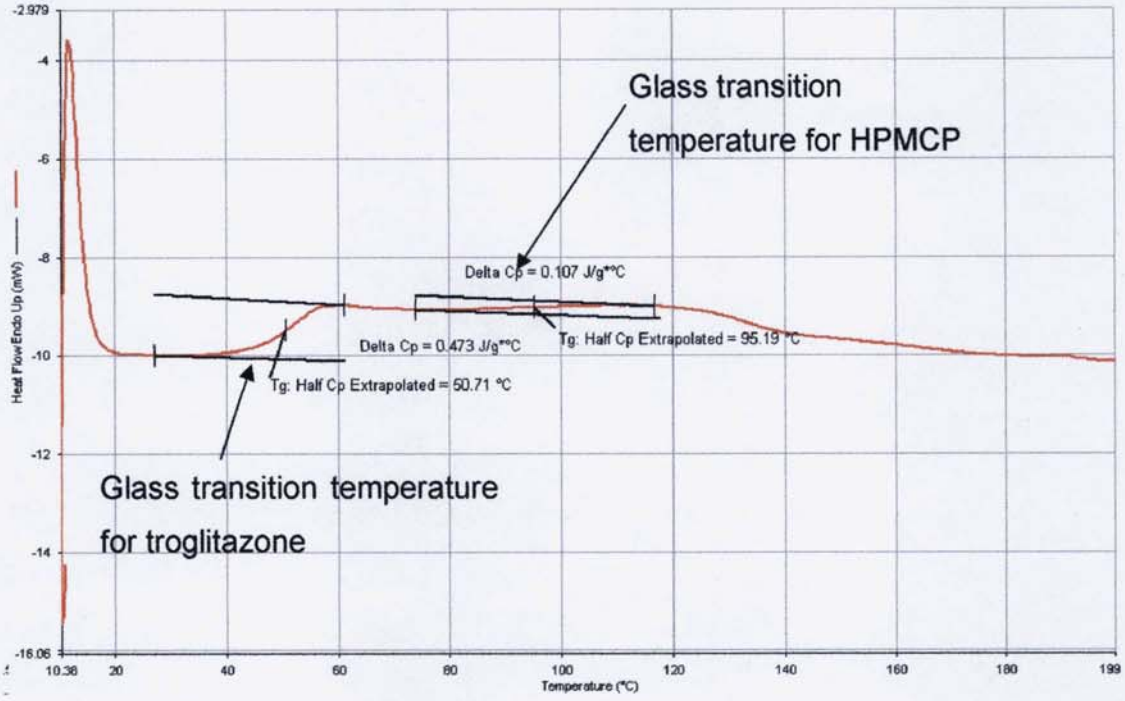

Figure 3-14 DSC trace of the troglitazone dispersion with 71% HPMCP

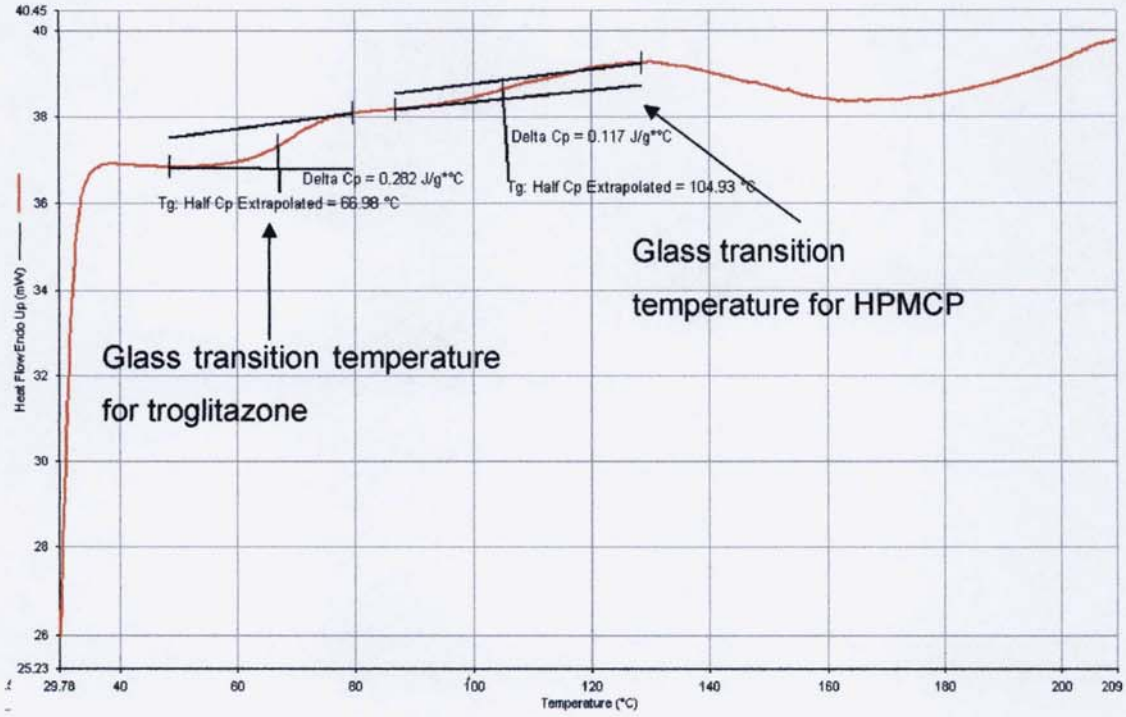

Figure 3-15 DSC trace of the troglitazone dispersion with 83% HPMCP

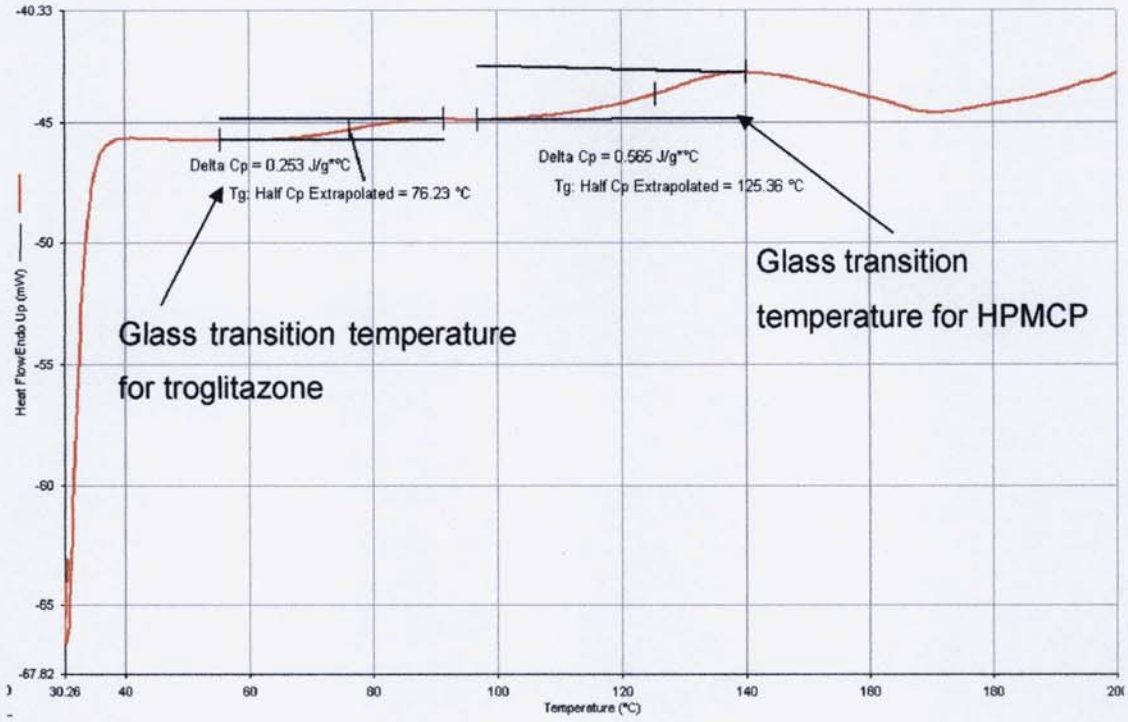

Figure 3-16 XRPD trace of the troglitazone dispersion with 17% HPMCP

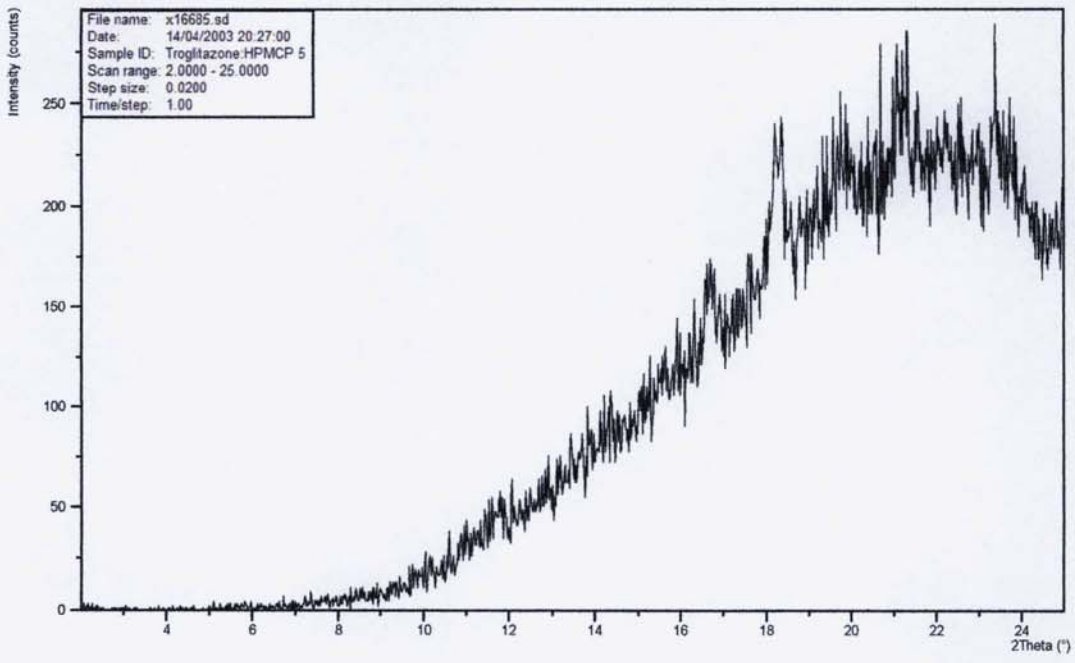

Figure 3-17 XRPD trace of the troglitazone dispersion with 50% HPMCP

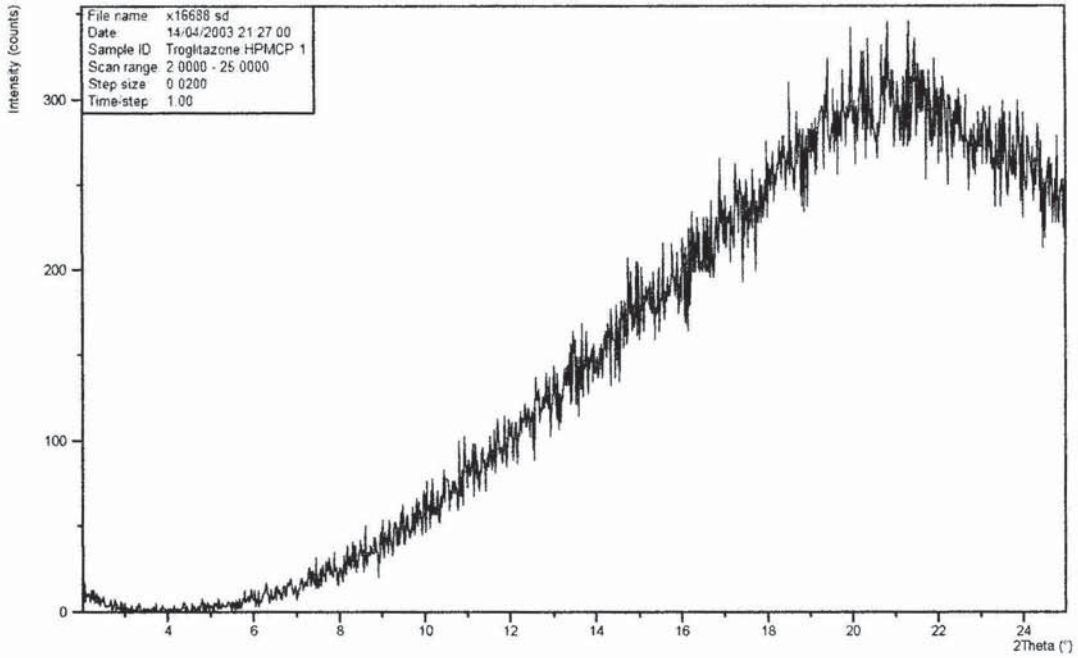

Figure 3-18 XRPD trace of the troglitazone dispersion with 91% HPMCP

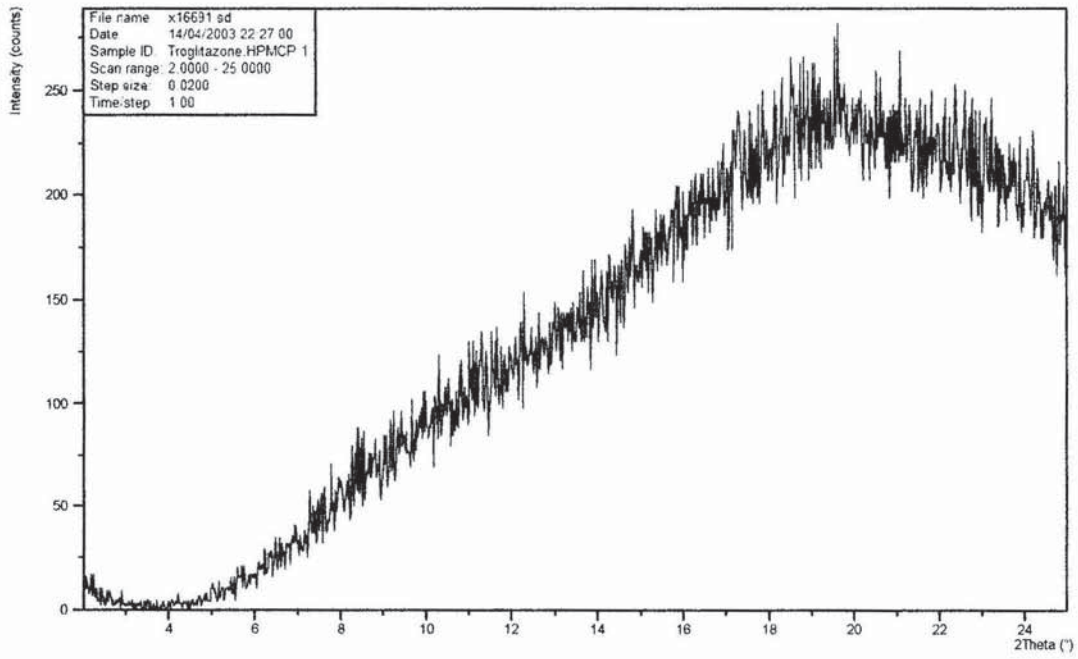

3.1.3.4 Effect of PVP concentration upon the dissolution of troglitazone

Tables 3-5 shows that increasing PVP concentration has a very different effect to

that seen with the HPMCP dispersions. The performance of the PVP dispersions, over the first 20 minutes, peaks at the 50% (w/w) dispersions, with the 9,17, 29, 71 and 91% dispersion all not significantly different from each other ($p>0.05$). Examination of the AUC data in table 3-2 shows that the lower PVP concentration dispersion (9, 17, 29% (w/w)) do in fact have relatively high AUC_{20} values (ignoring the 50% dispersion); this indicates that the amount of polymer has very little impact upon the early dissolution of troglitazone from a PVP dispersion.

These findings compare favourably with those of Tantishaiyakul *et al.* (1996), where dispersions of PVP:piroxicam were prepared at different ratios. It was found that as the PVP concentration increased there was a slow increase in the dissolution rate up to the 4:1 ratio, which was followed by a decrease in dissolution rate as PVP content increased. This also concurs with findings made by Ford (1986) and Akbuga *et al.* (1988). There are several possible reasons why this could be the case with PVP dispersions; one is the local viscosity of the carrier during dissolution (Tantishaiyakul *et al.* 1999), another is the possible presence of crystalline regions within the dispersion (Leuner, 2000) and finally the leaching of the polymer during dissolution to form polymer-rich layers around the drug particles (Pandit and Khakurel, 1984). The most plausible reasons for the observations from this study are those proposed by Tantishaiyakul *et al.* (1999) and Pandit and Khakurel (1984). The idea that crystalline regions are probably not the cause in the instance of troglitazone is because it can be seen from figure 3-4 that troglitazone is amorphous in nature after spray-drying. XRPD data of the 17% and 50% dispersions, figure 3-23 and 3-24, also show that there is no evidence of crystalline regions within the PVP dispersions. There is also no evidence in the 91% solid dispersion of any crystalline regions. With regards to the local viscosity influencing the dissolution, it has been shown that for grades of PVP with a higher molecular weight (i.e. leads to a higher viscosity (Walking, 1994)) the release of the drug is slower compared to those of a low molecular weight (Hilton and Summers 1986, Tantishaiyakul 1999). This would, therefore,

correspond that an increase in viscosity can reduce the dissolution of a drug from PVP dispersions.

Table 3-5 Results of the Tukey analysis of the AUC_{20} of the PVP dispersions (shaded boxes indicate no significant difference)

%Polymer	% Polymer						
	9	17	29	50	71	83	91
9							
17	>0.05						
29	>0.05	>0.05					
50	<0.001	<0.05	<0.05				
71	>0.05	>0.05	>0.05	<0.001			
83	<0.001	<0.001	<0.001	<0.001	<0.001		
91	>0.05	>0.05	>0.05	<0.001	>0.05	<0.001	

Examination of the results of the ANOVA for the AUC_{90} of the PVP dispersions (table 3-14) shows that the concentration of PVP within the dispersion has very little impact upon the release of troglitazone. In the majority of cases the difference between the AUC_{90} for is considered not significant ($P>0.05$). The only case this is not true for is the 83% (w/w) dispersion, which from the obtained data the dissolution is severely impeded (figure 3-9).

The effect of increasing the polymer concentration upon the physical structure of the PVP:troglitazone dispersions can be seen in figure 3-20. It can be seen that for the lower polymer concentration dispersions that troglitazone recrystallises out, and like the HPMCP dispersions, the ΔH for the melting endotherm is less than that found for spray dried troglitazone. The ΔH for this 9% dispersion is in fact less than that for the HPMCP 17% dispersion. As the polymer concentration is increased the dispersions appear as amorphous with no recrystallisation of troglitazone. What is also apparent in the case of the PVP dispersions is that there is only one clear glass transition temperature present in the dispersions between 17% and 71% PVP, thus indicating the drug and polymer are in one

phase for these dispersions.

Table 3-6 Results of the Tukey analysis of the AUC_{90} of the PVP dispersions (shaded boxes indicate no significant difference)

%Polymer	% Polymer						
	9	17	29	50	71	83	91
9							
17	>0.05						
29	>0.05	>0.05					
50	>0.05	>0.05	>0.05				
71	<0.05	>0.05	>0.05	>0.05			
83	>0.05	<0.01	<0.01	<0.001	<0.001		
91	>0.05	>0.05	>0.05	>0.05	>0.05	<0.01	

The 91% and 83% dispersion do show more than one thermal event; in the case of the 83% dispersion there are clearly two glass transitions and some apparent melting endotherm (at around 150 °C). The two glass transition temperatures are also present in similar positions in the 91% dispersion. The two glass transitions, in both dispersions, are at higher temperatures than expected for PVP (figure 3-19), this is not expected with solid dispersions. It is shown in the literature that the glass transitions for solid dispersions falls between that of the carrier and the drug, with the tendency for the glass transition temperature to move towards that of the carrier as the polymer concentration increases (Hino and Ford 2001). This could indicate that in these dispersions there is an interaction occurring between the two components other than the incorporation of the drug in to a solid solution, the nature of which has not been established. The sort of interaction that could occur could be hydrogen bonding causing cross-linking. Cross-linking within the polymers has been shown to increase the tg (Hidalgo *et al.* 1999 and Hoursten *et al.* (1999)). The methods that have been employed to investigate hydrogen bonding interactions, within solid dispersions, are attenuated total reflection Fourier transform infra-red spectroscopy (ATR-FTIR) (Tantishaiyakul *et al.* 1999) and solid state Carbon 13 nuclear magnetic resonance (NMR) spectroscopy

(Schachter *et al.* 2004). When using ATR-FTIR it has been shown that the wavenumber of a peak, corresponding to the chemical group involved in the hydrogen bonding interaction, will shift when it is involved in a hydrogen bond (Tantishaiyakul *et al.* 1999). The same applies to the solid state carbon13 NMR, the carbon atom that is influenced by the interaction will shift its position. This observation could establish why these two dispersions (83 and 91% polymer) undergo reduced dissolution, as it has been shown that crosslinked PVP tends to swell rather than erode during dissolution (Grassi *et al.* 2001).

Figure 3-19 DSC trace of PVP K30

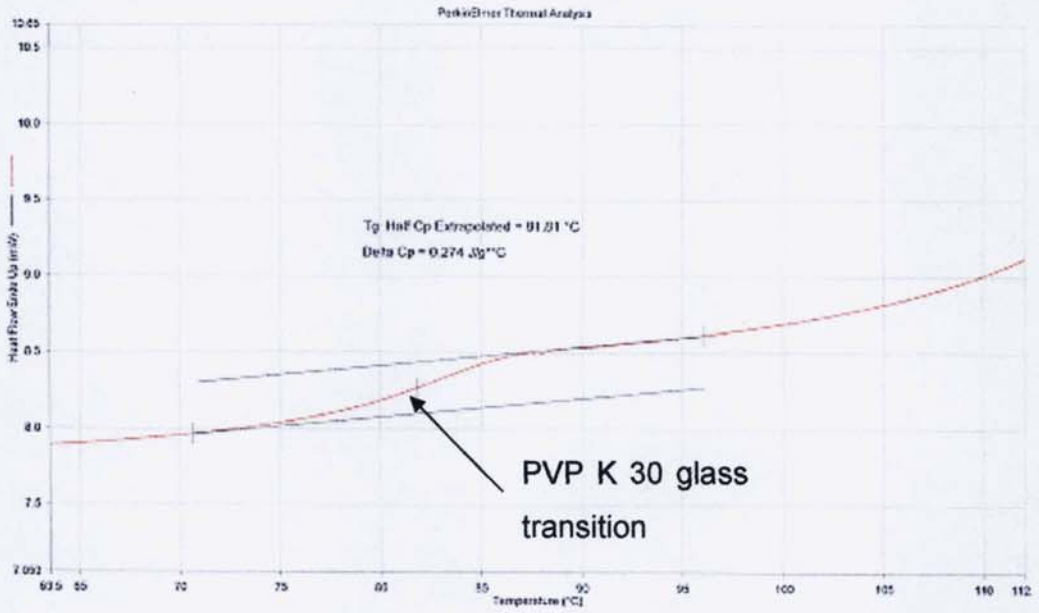

Figure 3-20 DSC traces of PVP:Troglitazone dispersions (key: 9% PVP, 17% PVP, 50% PVP, 71% PVP, 83% PVP, 91%)

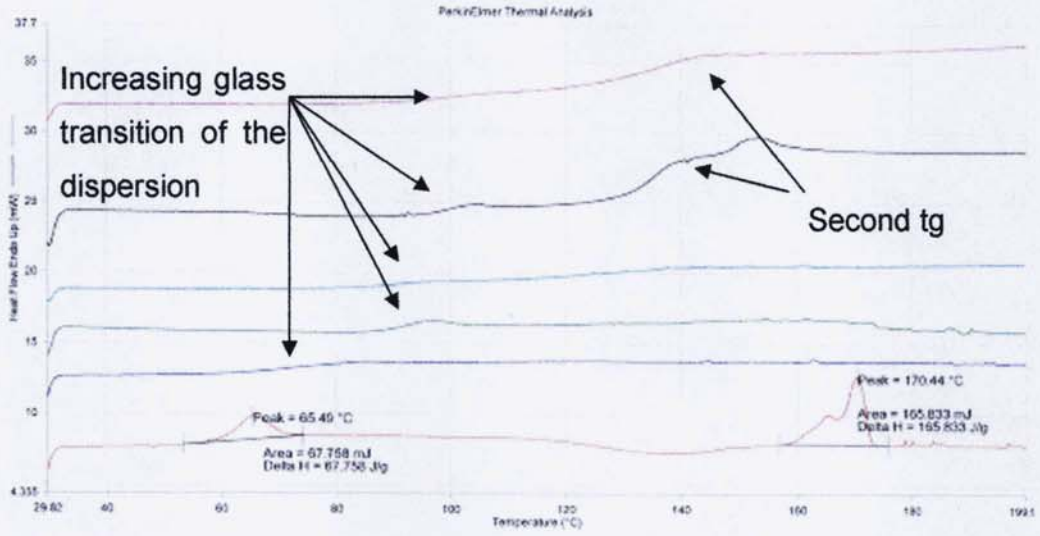

Figure 3-21 DSC trace of the troglitazone dispersion with 9% PVP

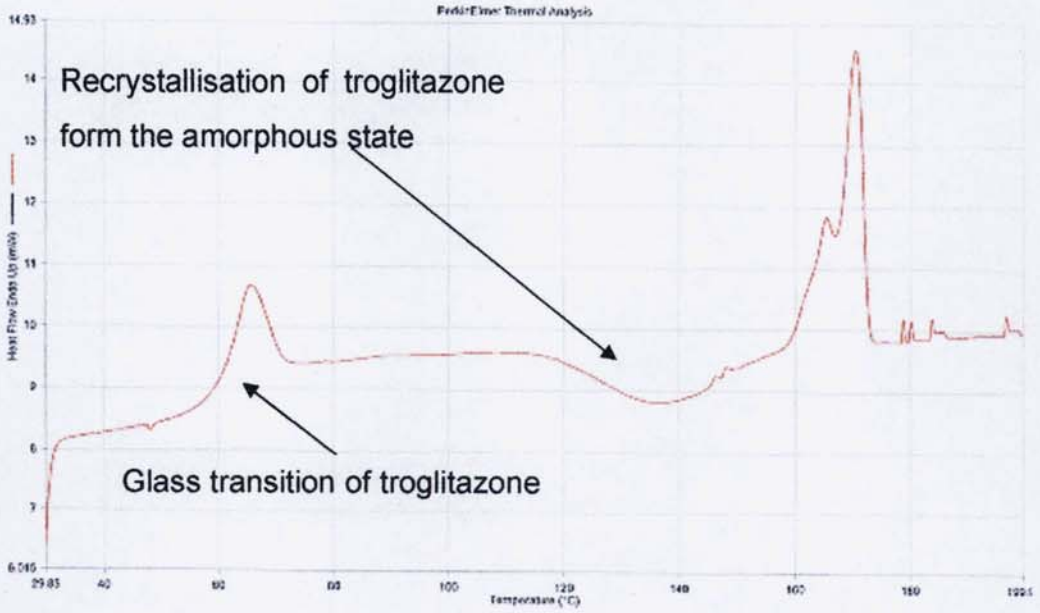

Figure 3-22 DSC trace of the troglitazone dispersion with 91% PVP

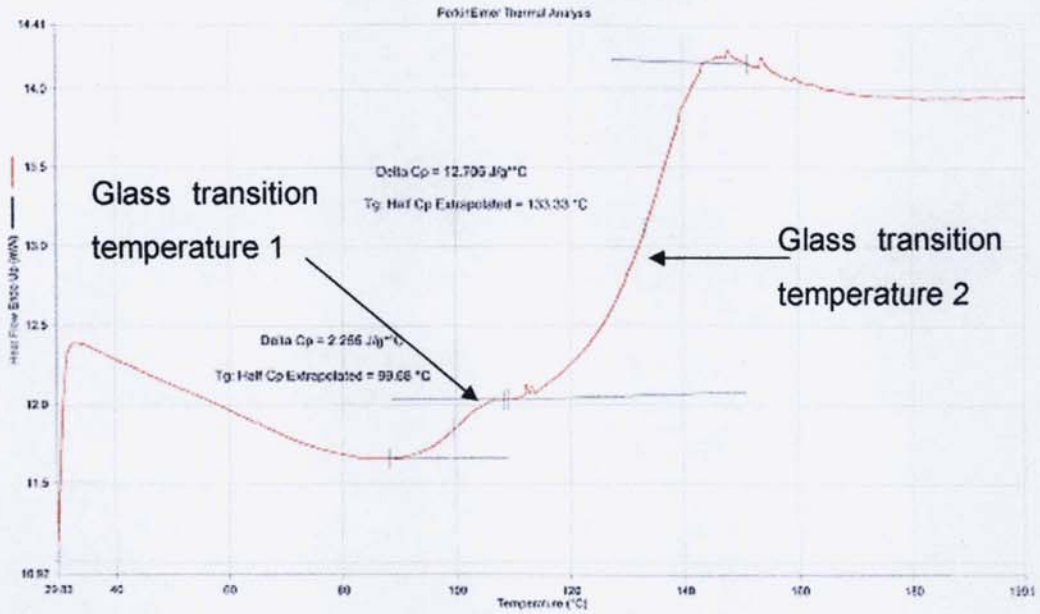

Figure 3-23 XRPD trace of the troglitazone dispersion with 17% PVP

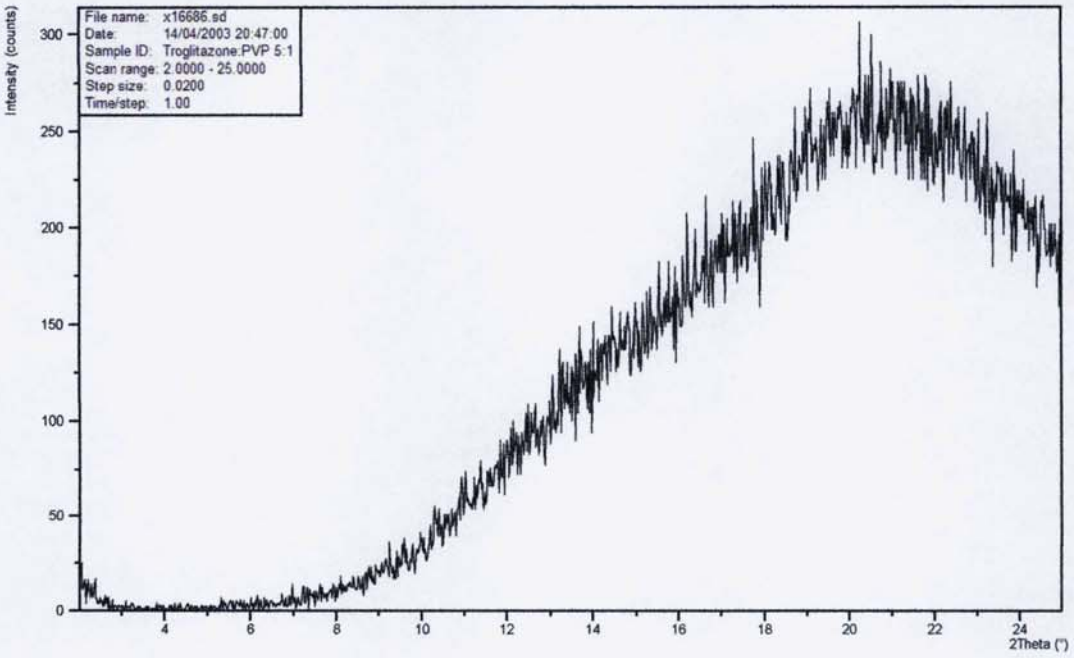

Figure 3-24 XRPD trace of the troglitazone dispersion with 50% PVP

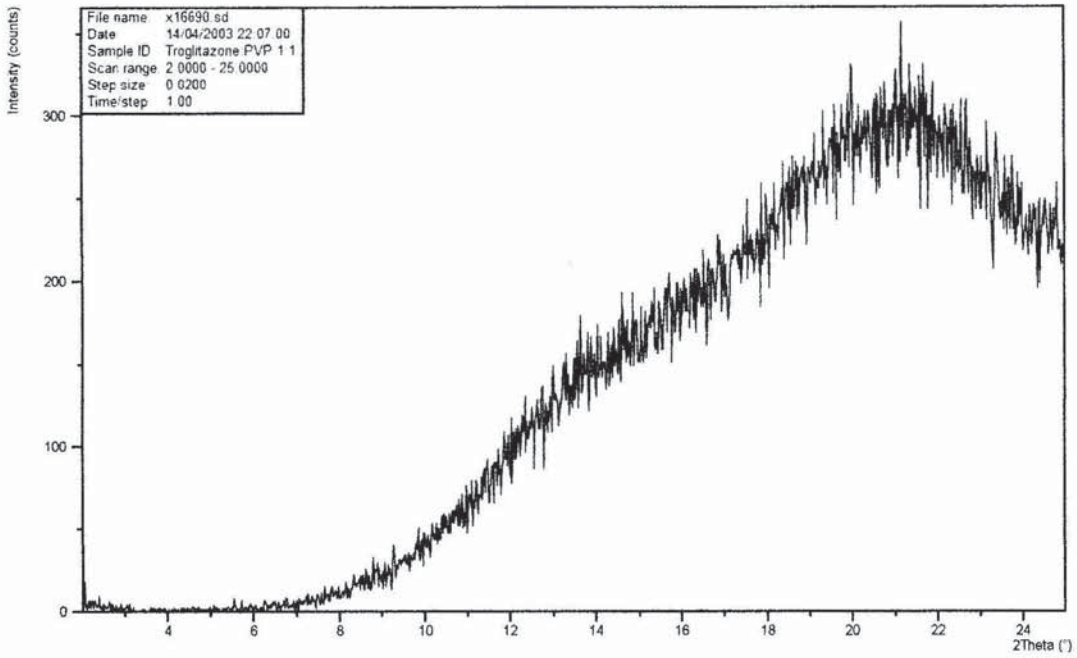

3.1.3.5 Effect of HPMC concentration upon the dissolution of troglitazone

For dissolution of HPMC dispersions over the first 20 minutes, it can be seen from tables 3-2 and 3-7 that there appear to be three distinct regions within the range of polymer concentrations. The first region encompasses those dispersions with a high drug loading (9, 17, 29 % (w/w)), the second region involves the middle concentrations (50 and 71% (w/w)) and the final is those dispersions with a high polymer loading (83 and 91% (w/w)). The first region is characterised by the three dispersions showing no significance differences in their release of troglitazone over twenty minutes ($p>0.05$ in all cases). This, therefore, shows that the level of HPMC within the dispersions at these concentrations has very little impact upon the dissolution of the dispersion, as predicted by theory of drug-rich surfaces. The second region shows similar behaviour to the HPMCP dispersions, in that the dissolution increases significantly between the 50 and 71% dispersions. The distinction between the AUC_{20} of the high drug loaded dispersions compared to the 50% dispersion is not as clear as in the case of HPMCP dispersions (in this instance $p<0.01$, rather than <0.001). The major

change in behaviour occurs with the 71% (w/w) dispersion, which is significantly different to all the other dispersions. The third region is characterised by a sudden and large reduction in the AUC_{20}. This decrease was observed with the HPMCP dispersions, but the decrease was not as dramatic. It is postulated that when the polymer concentration reaches this level, the overall dissolution of the dispersion is controlled by that of the polymer (Ford 1984). Investigation into the polymer dissolution showed that for the 91% dispersion the dissolution of the polymer was very slow (section 5.4.6). Visual inspection showed that the 83% and 91% HPMC troglitazone dispersions formed a gelatinous layer on top of the dissolution medium; this reduction in the wetting of the polymer will have the effect of reducing the dissolution of the polymer from the solid dispersion.

Table 3-7 Results of the Tukey analysis of the AUC_{20} of the HPMC dispersions (shaded boxes indicate no significant difference)

%Polymer	% Polymer						
	9	17	29	50	71	83	91
9							
17	>0.05						
29	>0.05	>0.05					
50	<0.01	>0.05	<0.01				
71	<0.001	<0.001	<0.001	<0.001			
83	<0.05	<0.001	<0.05	<0.001	<0.001		
91	<0.01	<0.001	<0.01	<0.001	<0.001	>0.05	

The choice of polymer concentration, when using HPMC, has quite a large impact upon the release of troglitazone. There are only three dispersions where the dissolution profiles have been considered similar: 29% vs 9%, 29% vs 17% and 91% vs 83%. Further examination of table 3-2 and figure 3-10 shows that the concentration of HPMC is more important than for both HPMCP and PVP dispersions. Too much HPMC added to the dispersion (83% and 91% (w/w)) inhibits dissolution, whereas too little HPMC (9% and 17% and 29% (w/w) results

in a very slow and incomplete dissolution. From these data it can be seen that 71% (w/w) of HPMC is the optimum level tested for dissolution enhancement.

Table 3-8 Results of the Tukey analysis of the AUC_{90} of the HPMC dispersions (shaded boxes indicate no significant difference)

%Polymer	% Polymer						
	9	17	29	50	71	83	91
9							
17	<0.01						
29	>0.05	>0.05					
50	<0.001	<0.001	<0.001				
71	<0.001	<0.001	<0.001	<0.001			
83	<0.001	<0.001	<0.001	<0.001	<0.001		
91	<0.001	<0.001	<0.001	<0.001	<0.001	>0.05	

Thermal analysis for the HPMC dispersions is not as straight forward as found with the PVP and HPMCP dispersions. It is seen in figure 3-26 the DSC analysis of all the HPMC dispersions, that all the dispersions are amorphous in their nature. This is confirmed by the absence of any of the characteristic peaks for troglitazone in the XRPD analysis (figures 3-5, 3-30 and 3-31). What is not seen, unlike with the PVP or HPMCP dispersions, is either the presence of a second glass transition temperature, or any movement in the glass transition temperature. Closer examination of the 9%, 17% and 50% dispersions (figures 3-27, 3-28 and 3-29) show that the glass transition temperature, of what is believed to be troglitazone, has shown no change with increasing polymer concentration. This indicates that within these dispersions there is present troglitazone that, although amorphous, is not interacting with the HPMC, this could be the region of free amorphous drug that wasas predicted by Sertsou (2002).

Figure 3-25 DSC trace of HPMC (Pharmacoat 603)

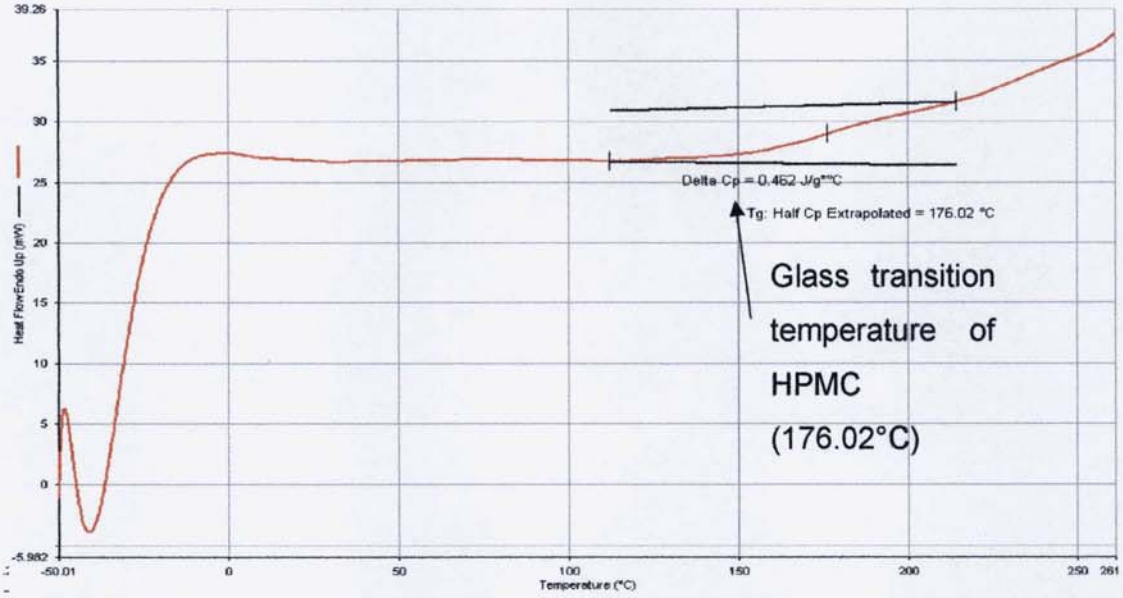

Figure 3-26 DSC traces of HPMC:troglitazone dispersions (key: 9% HPMC, 29% HPMC, 50% HPMC, 71% HPMC, 83% HPMC, 91% HPMC

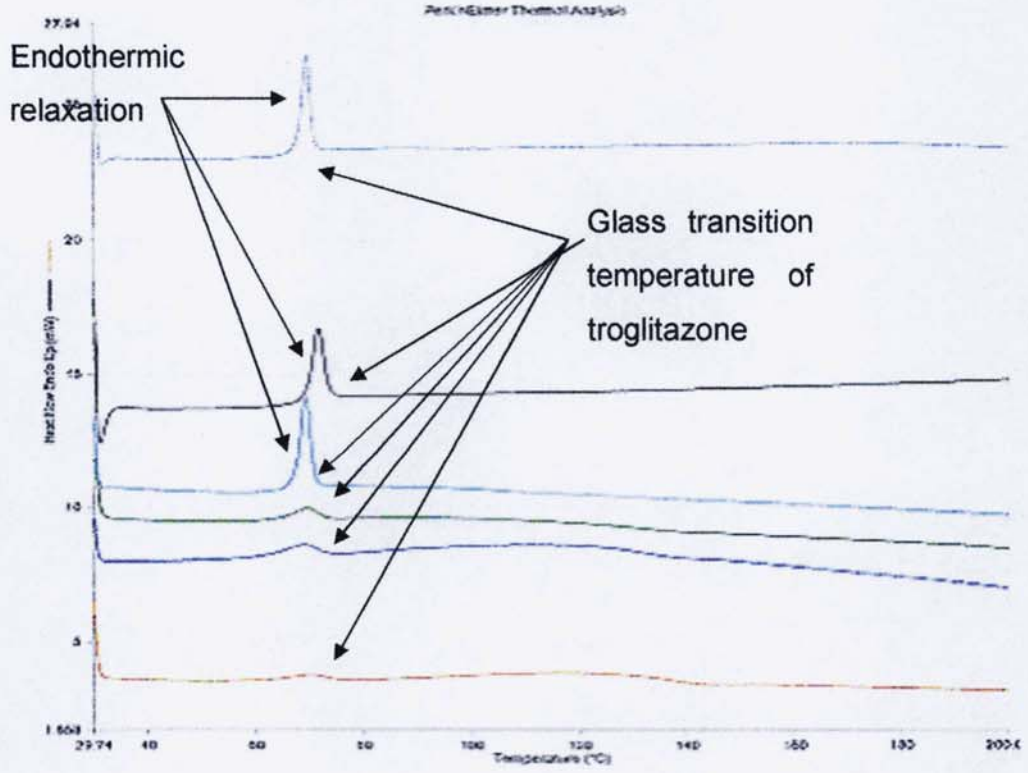

Figure 3-27 DSC trace of the troglitazone dispersion with 9% HPMC

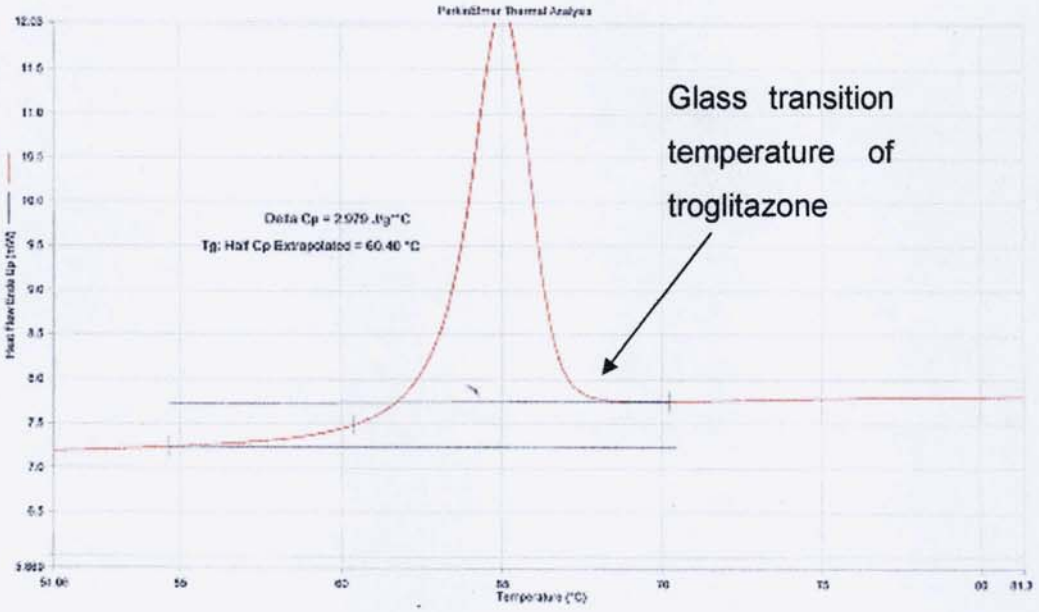

Figure 3-28 DSC trace of the troglitazone dispersion with 29% HPMC

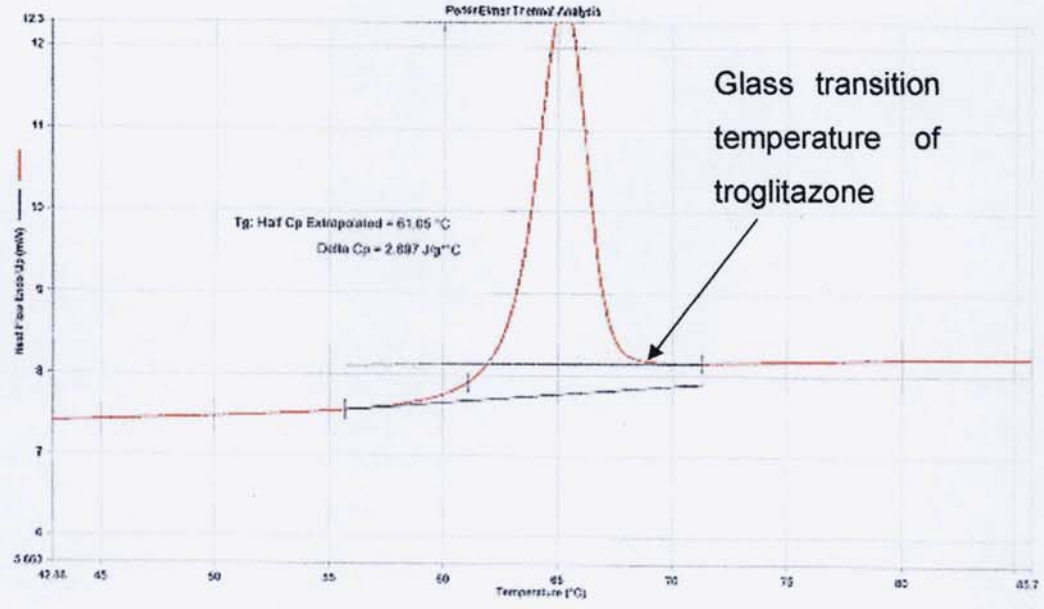

Figure 3-29 DSC trace of the troglitazone dispersion with 50% HPMC

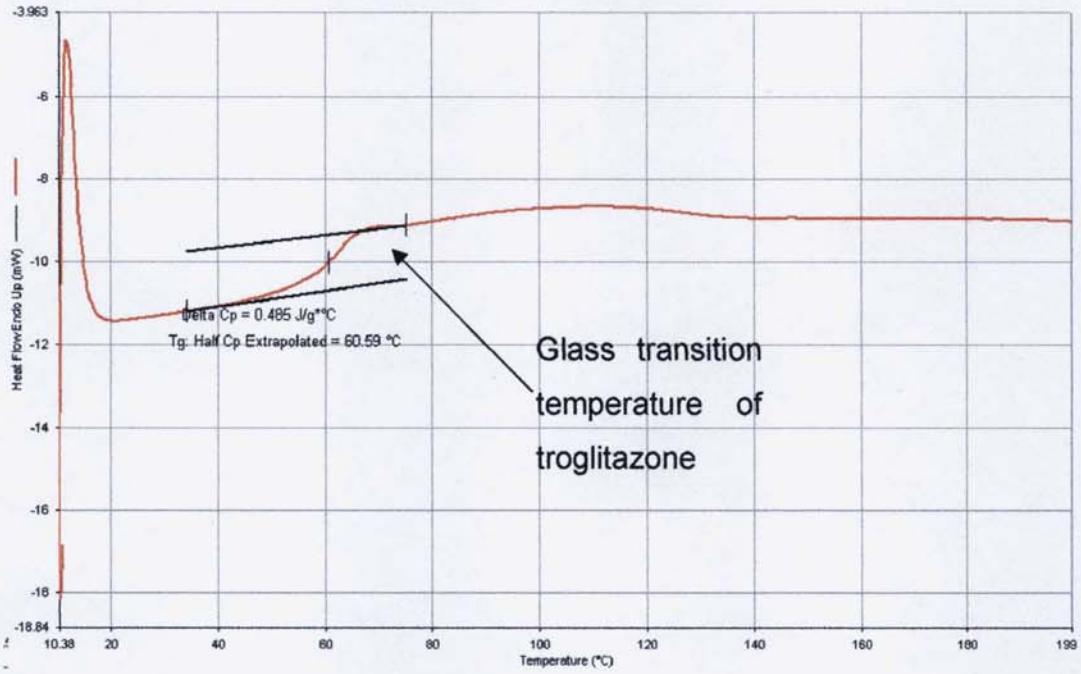

Figure 3-30 XRPD trace of the troglitazone dispersion with 9% HPMC

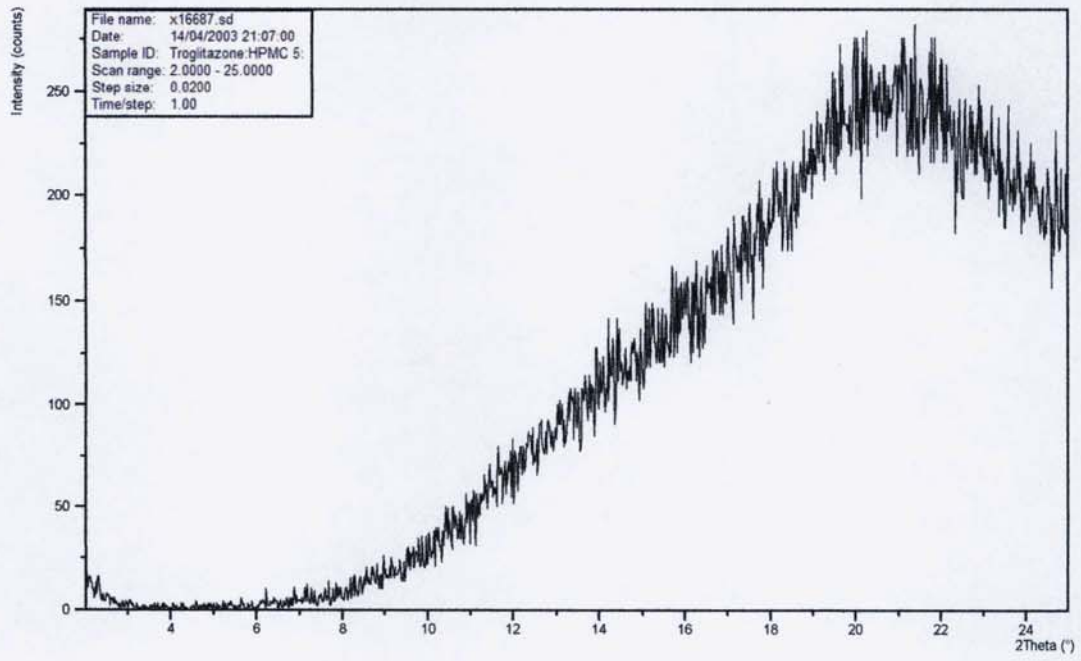

Figure 3-31 XRPD trace of the troglitazone dispersion with 50% HPMC

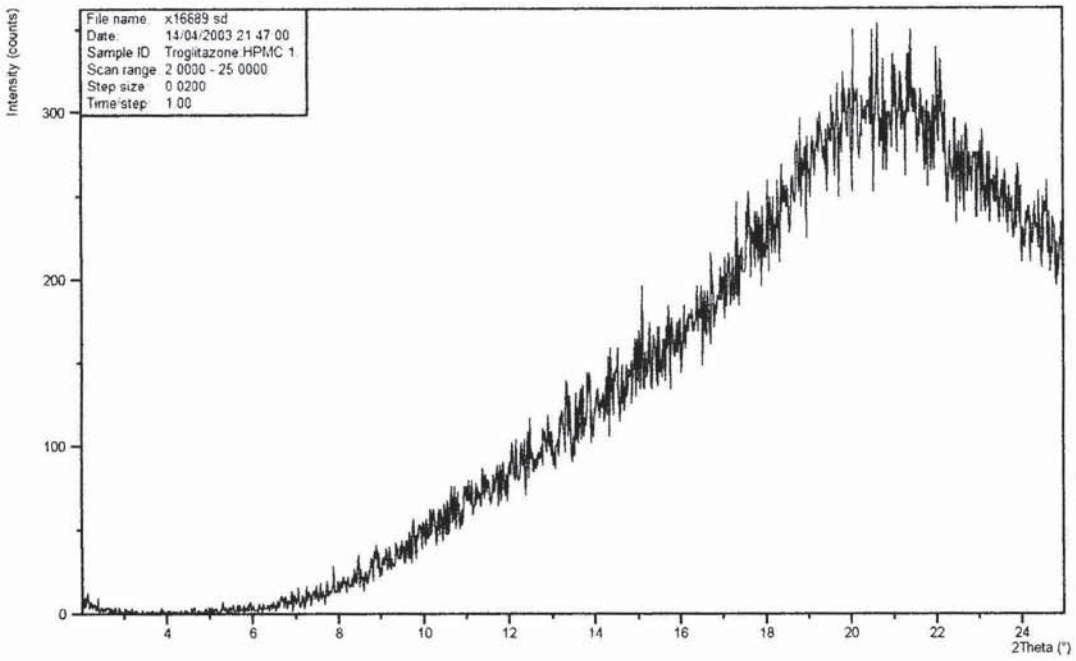

3.1.3.6 Effect of polymer selection upon the dissolution of troglitazone over the first 20 minutes

The way in which the different polymers affect the dissolution of the troglitazone is assessed in tables 3-9 to 3-15, which displays the ANOVA results along with the mean difference (in AUC_{20}). It is noticeable from these data that at the low polymer concentrations (9 and 17% (w/w)) PVP gives the greatest enhancement of the dissolution of troglitazone, over the first 20 minutes. At this level of polymer, it is the HPMCP dispersions that give the least degree of enhancement in dissolution of troglitazone. At the 29% (w/w) concentration the profiles of the HPMCP and PVP dispersions are considered not significantly different from each other. For the 50% concentration and above, the HPMCP dispersions consistently give the highest release of troglitazone. Therefore using an HPMCP with troglitazone has a highly significant effect upon the release of troglitazone over the first 20 minutes of dissolution compared to that of PVP and HPMC.

Table 3-9 Results of the Tukey analysis of the AUC_{20} of the 9% dispersions (shaded boxes indicate no significant difference, bracketed figure indicates the mean difference x v y)

Polymer		Polymer		
		HPMCP	PVP	HPMC
Polymer	HPMCP			
	PVP	<0.001 (108.13)		
	HPMC	<0.05 (38.45)	<0.01 (-69.68)	

Table 3-10 Results of the Tukey analysis of the AUC_{20} of the 17% dispersions (shaded boxes indicate no significant difference, bracketed figure indicates the mean difference x v y)

Polymer		Polymer		
		HPMCP	PVP	HPMC
Polymer	HPMCP			
	PVP	<0.05 (141.75)		
	HPMC	>0.05 (78.50)	>0.05 (-63.25)	

Table 3-11 Results of the Tukey analysis of the AUC_{20} of the 29% dispersions (shaded boxes indicate no significant difference, bracketed figure indicates the mean difference x v y)

Polymer		Polymer		
		HPMCP	PVP	HPMC
Polymer	HPMCP			
	PVP	>0.05 (-63.62)		
	HPMC	<0.01 (-234.05)	<0.05 (-170.43)	

Table 3-12 Results of the Tukey analysis of the AUC_{20} of the 50% dispersions (shaded boxes indicate no significant difference, bracketed figure indicates the mean difference x v y)

Polymer		Polymer		
		HPMCP	PVP	HPMC
	HPMCP			
	PVP	<0.01 (-544.31)		
	HPMC	<0.001 (-663.11)	>0.05 (118.80)	

Table 3-13 Results of the Tukey analysis of the AUC_{20} of the 71% dispersions (shaded boxes indicate no significant difference, bracketed figure indicates the mean difference x v y)

Polymer		Polymer		
		HPMCP	PVP	HPMC
	HPMCP			
	PVP	<0.01 (-1096.90)		
	HPMC	<0.05 (-533.96)	<0.05 (562.89)	

Table 3-14 Results of the Tukey analysis of the AUC_{20} of the 83% dispersions (shaded boxes indicate no significant difference, bracketed figure indicates the mean difference x v y)

Polymer		Polymer		
		HPMCP	PVP	HPMC
	HPMCP			
	PVP	<0.001 (-1382.40)		
	HPMC	<0.001 (-1391.60)	>0.05 (-9.22)	

Table 3-15 Results of the Tukey analysis of the AUC_{20} of the 91% dispersions (shaded boxes indicate no significant difference, bracketed figure indicates the mean difference x v y)

Polymer		Polymer		
		HPMCP	PVP	HPMC
	HPMCP			
	PVP	<0.001 (-650.02)		
	HPMC	<0.001 (-974.93)	<0.01 (324.91)	

The choice of polymer has a significant impact upon the release of troglitazone from a solid dispersion over ninety minutes (tables 3-16 through to 3-22). Even at the lower polymer concentrations (9 and 17%), where the dissolution is considered to be drug-controlled, there are significant differences in the dissolution (3-16 and 3-17) between the different polymers. At these lower concentrations it is seen that the PVP dispersions significantly out-perform both the HPMC and HPMCP. It is difficult, with the data obtained, to categorically say why this is the case. It hypothesised; however, that there is more troglitazone dissolved into the PVP (at these low ratios) than there is in the HPMC and HPMCP dispersions. Work performed by Hino and Ford (2001) showed that it is possible to calculate how many drug molecules are bound to an individual polymer residue. This was done by finding the point at which there is no crystalline drug in the polymer film. The hypothesis here is that more troglitazone molecules bind to one residue of PVP than with HPMC or HPMCP. This would mean that at the low polymer loadings there is more troglitazone incorporated into the PVP solid dispersions than there is in the HPMC and HPMCP dispersions. This shows that even at such low concentrations, the choice of polymer can still be an important factor for seeking an enhancement in the dissolution of troglitazone. This could be an important factor when the formulation of a sparingly soluble drug is considered, and the mass of the excipient is an important factor. As although an optimum enhancement is not obtained at such a low concentration of polymer, there is a degree of enhancement that could lead to an overall improvement in the bioavailability.

It is seen, however, as the polymer concentration increases, the superior performance found with PVP dispersions, at the lower concentrations, is reduced. The AUC_{90} of the PVP dispersion with the 29% and 50% (tables 3-18 and 3-19) is not significantly different to the HPMCP dispersions, and the 50% dispersion is not significantly different to that of HPMC dispersions. Also at a concentration of 71% there is no significant difference between the AUC_{90} of PVP and HPMC. There is, however, a significant difference between the dispersions at 71% between HPMCP and PVP (or HPMC and HPMCP), with the HPMCP having a reduced AUC_{90}. This is a reversal for the 71% HPMCP dispersion; the AUC_{20} at this concentration was significantly larger than either the PVP or HPMC dispersion (table 3-10), this change in the rank order is due to the large amount of precipitation that occurs on dissolution with this dispersion (figure 3-7).

The DSC and XRPD analysis (sections 3.1.3.2, 3.1.3.3 and 3.1.3.4) show that all the dispersions contained no crystalline material, and are therefore amorphous in nature. It is also shown from the data for spray-dried troglitazone that this material is also amorphous in its nature, but has a tendency to crystallise out upon heating in the DSC. To prevent this re-crystallisation from occurring during a DSC analysis faster scan rates can be utilised. Hyper-DSC is a technique that allows scan rates of up to 600°C/min to be achieved, and it has been shown that at such scan rates the recrystallisation of amorphous compounds during a DSC run can be inhibited (McGregor *et al.* 2004). At these scan rates the re This re-crystallisation is not present in all dispersions above 50% (w/w) polymer, and in the some instances (PVP and HPMC dispersions) there is only one glass transition temperature detected. The presence of only one implies that the drug is fully incorporated into the solid dispersion and dissolution would be expected to be quicker and more complete from such dispersions. However, this is not found to be the case, with the HPMCP dispersions clearly showing more than one glass transition temperature, but having a higher peak dissolution value (table 3-1) and more rapid dissolution (3-2). It is believed that the rate and extent of troglitazone

dissolution from these three carriers is not simply governed by what is seen from the physical structures, and that further mechanisms are involved which control these parameters. It has been alluded to that small differences found between the dissolution of solid dispersions, as seen with the HPMC and PVP dispersions (50% and 71%), are due to differences in wetting of the solid dispersions, this aspect is discussed in depth in section 3.1.3.6.

Table 3-16 Results of the Tukey analysis of the AUC_{90} of the 9% dispersions (shaded boxes indicate no significant difference)

Polymer	Polymer			
		HPMCP	PVP	HPMC
	HPMCP			
	PVP	<0.001 (2079.70)		
	HPMC	<0.001 (1004.00)	<0.001 (-1075.80)	

Table 3-17 Results of the Tukey analysis of the AUC_{90} of the 17% dispersions (shaded boxes indicate no significant difference)

Polymer	Polymer			
		HPMCP	PVP	HPMC
	HPMCP			
	PVP	<0.001 (2634.50)		
	HPMC	<0.01 (1676.10)	<0.05 (-958.43)	

Table 3-18 Results of the Tukey analysis of the AUC_{90} of the 29% dispersions (shaded boxes indicate no significant difference)

Polymer	Polymer			
		HPMCP	PVP	HPMC
	HPMCP			
	PVP	>0.05 (1304.70)		
	HPMC	>0.05 (-441.62)	<0.05 (-1746.3)	

Table 3-19 Results of the Tukey analysis of the AUC_{90} of the 50% dispersions (shaded boxes indicate no significant difference)

Polymer		Polymer		
		HPMCP	PVP	HPMC
Polymer	HPMCP			
	PVP	N/A[1]		
	HPMC	N/A[1]	N/A[1]	

1 p>0.05 therefore curves are considered identical

Table 3-20 Results of the Tukey analysis of the AUC_{90} of the 71% dispersions (shaded boxes indicate no significant difference)

Polymer		Polymer		
		HPMCP	PVP	HPMC
Polymer	HPMCP			
	PVP	<0.001 (2322.20)		
	HPMC	<0.001 (2849.40)	>0.05 (527.22)	

Table 3-21 Results of the Tukey analysis of the AUC_{90} of the 83% dispersions (shaded boxes indicate no significant difference)

Polymer		Polymer		
		HPMCP	PVP	HPMC
Polymer	HPMCP			
	PVP	<0.001 (-1468.90)		
	HPMC	<0.001 (-2055.00)	<0.05 (-586.02)	

Table 3-22 Results of the Tukey analysis of the AUC_{90} of the 91% dispersions (shaded boxes indicate no significant difference)

Polymer		Polymer		
		HPMCP	PVP	HPMC
Polymer	HPMCP			
	PVP	<0.001		
	HPMC	<0.001	<0.05	

3.1.3.7 Effect of polymer selection upon the dissolution rate after fitting with a polynomial curve fit

The final parameter that was calculated for the dispersions was the polynomial rate constant, an example of the curve fitting is shown in figure 3-32. A polynomial fit is a curved trend line usually used when the data fluctuates, such as in the case of the supersaturated data obtained for the dissolution of the solid dispersions. From the equation of the fit the figure shown in red font (figure 3-32) can be used to describe the initial rate of dissolution. This number is equivalent to m in the equation 'y = mx +c', and can also be calculated by drawing a tangent to the curve from t=0 (figure 3-33).

Figure 3-32 An example of the fit obtained from applying a polynomial fit to the dissolution data (0-20 minutes), the figure shown in red is the derived rate (example shown is the 50% HPMC dispersion)

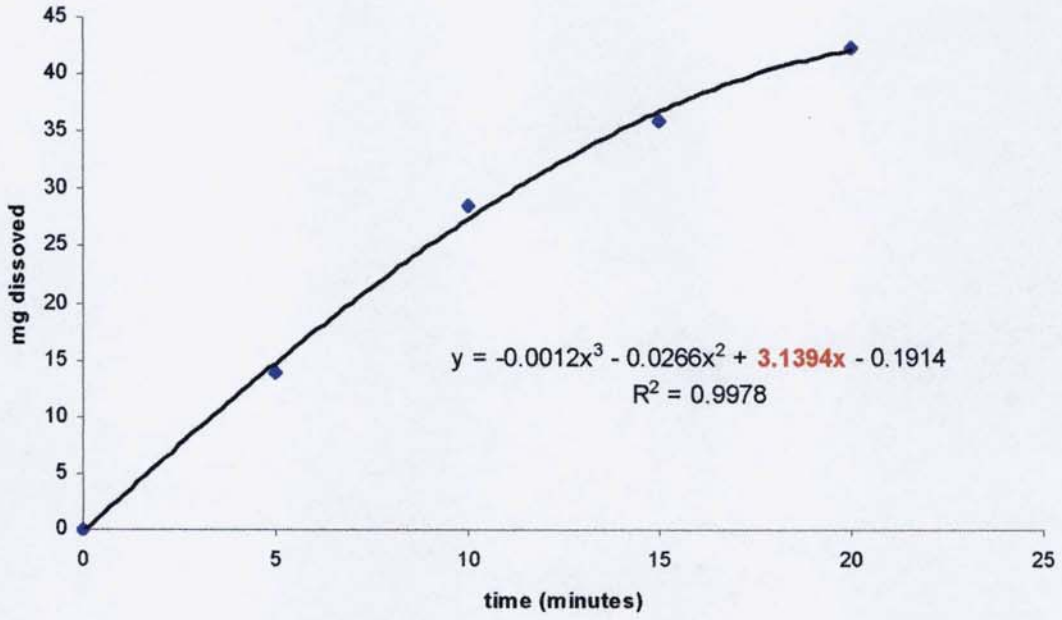

Figure 3-33 Showing the plot of data over the first minute of dissolution based upon the polynomial rate

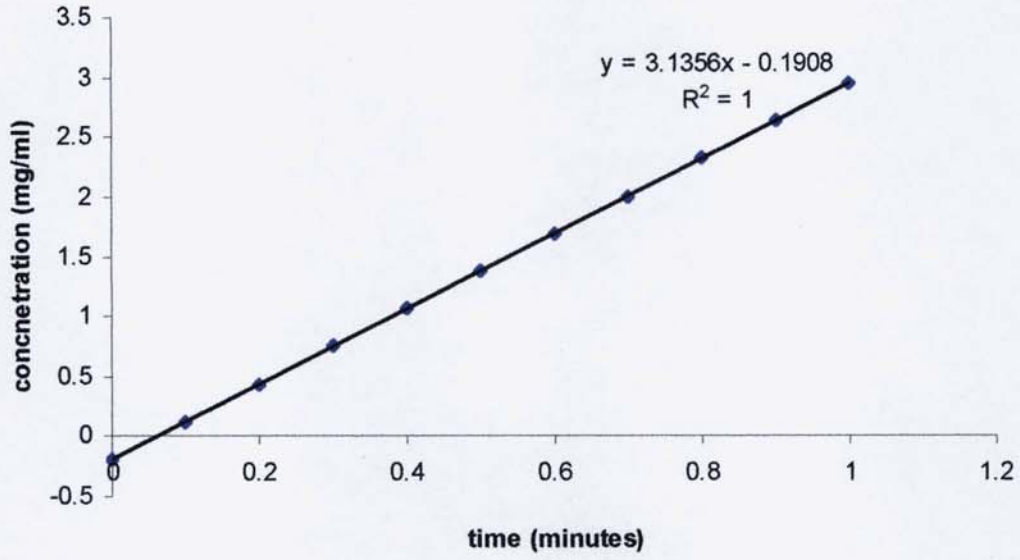

As shown, polynomial curve fitting of the dissolution profiles allows for the derivation of an initial rate of dissolution, the initial dissolution rate of pharmaceutical powders has been linked to the wettability of the powder (Lippold and Ohm, 1986). It was shown that powders with increasing wettability had a higher effective surface area, which in turn led to faster dissolution rates. Figure 3-34 shows how the initial dissolution rates of the solid dispersions change as the polymer concentration increases. It is seen that as the polymer concentration increases the dissolution rate increases, until peak dissolution rate is achieved (50% w/w for both HPMC and PVP dispersions, and 71% w/w for the HPMCP dispersion). This means that as the polymer concentration increases the wettability of the solid dispersion increases. Lheritier *et al.* (1995) showed that increasing the level of carrier in a solid dispersion lowered the contact angle, thus increasing the wettability of the solid dispersion. This was attributed to the carrier forming a film around the drug particles, thus reducing the hydrophobicity of the dispersion. It is also shown in figure 3-34 that the dissolution rate decreases, after a peak value (50% for PVP, 71% for both HPMC and HPMCP), the possible reasons for the decrease in dissolution have been detailed in sections 3.1.3.2 –

3.1.3.4.

Figure 3-34 Change in polynomial dissolution rate of troglitazone dispersions as the polymer concentration changes

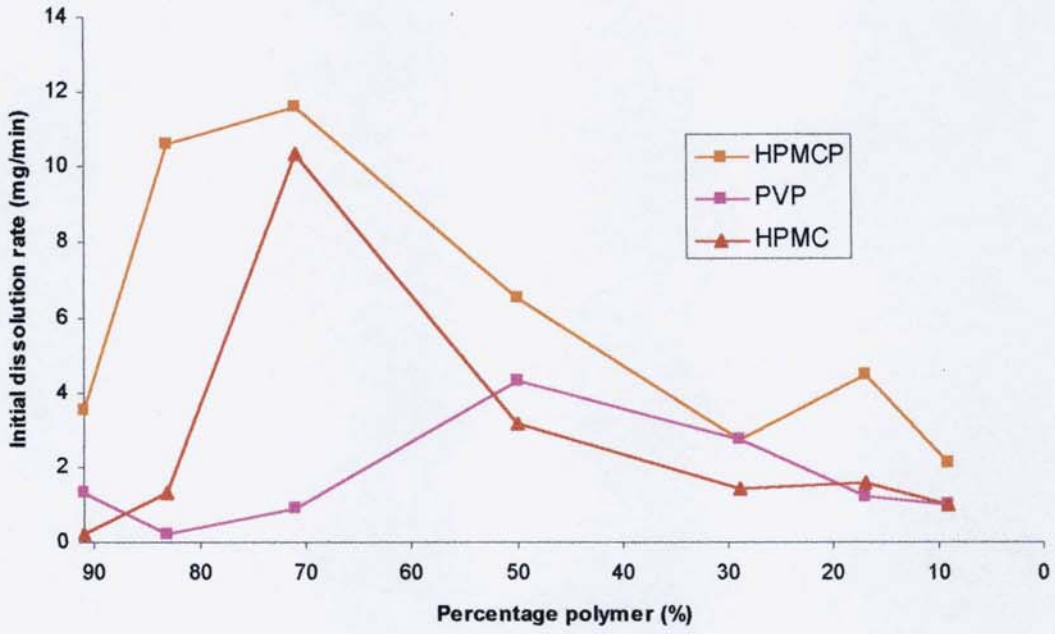

The plot of the polynomial dissolution rates versus the percentage polymer (figure 3-34) shows a similar pattern to that described by Ford (1984), figure 3-35. In this schematic diagram the area marked A is said to be an area where dissolution is carrier-controlled, so for the HPMCP, and HPMC dispersions this area includes dispersions up to 71% (w/w), and for PVP up to 50% (w/w). It is predicted that in region A the largest increases in dissolution rate are experienced, which is the case in all the polymers examined. It is proposed that after the maximum dissolution rate the released drug particles begin to form agglomerates which are harder to dissolve (Ford and Rubenstein, 1977; Ford and Rubenstein, 1978). Figure 3-34 shows that there are differences in the dissolution rates, between polymers at a given ratio above 50% w/w, in the regions where release from the solid dispersions is polymer controlled is expected (A/B). As this curve is derived from initial rates it can be said that the polymer selection has an impact upon the wetting of the solid dispersion. If the mechanism for improved wetting, provided by Lheritier *et al.* (1995), is used then

it can be said that the HPMCP is wetted better in the FaSSIF fluid than either the PVP or the HPMC. Section 5.3.1 discusses the dissolution of the polymers, where it was found that the HPMCP, alone, had a quicker dissolution rate than the HPMC.

Figure 3-35 Schematic diagram showing the effect of polymer concentration upon the dissolution rate of solid dispersions (reproduced from Ford 1986)

What is evident from this work is that the AUC_{20}, the AUC_{90} and the polynomial rate have been practical methods of highlighting quantitatively the differences between the dissolution profiles of the various troglitazone dispersions. Using this approach, it has become clear that polymer selection is an important factor for

the development of a troglitazone solid dispersion. It is possible to develop a solid dispersion that gives a very rapid release by using an enteric polymer, HPMCP, The enteric polymer approach has also highlighted that the concentration of polymer is not always an important factor (as in the case of PVP), thus allowing less excipient to be used.

3.1.4 Atovaquone

3.1.4.1 Dissolution and characterisation of atovaquone

Figure 3-36 Dissolution of atovaquone in FaSSIF. Results are the mean of three replicates, error bars ± SD

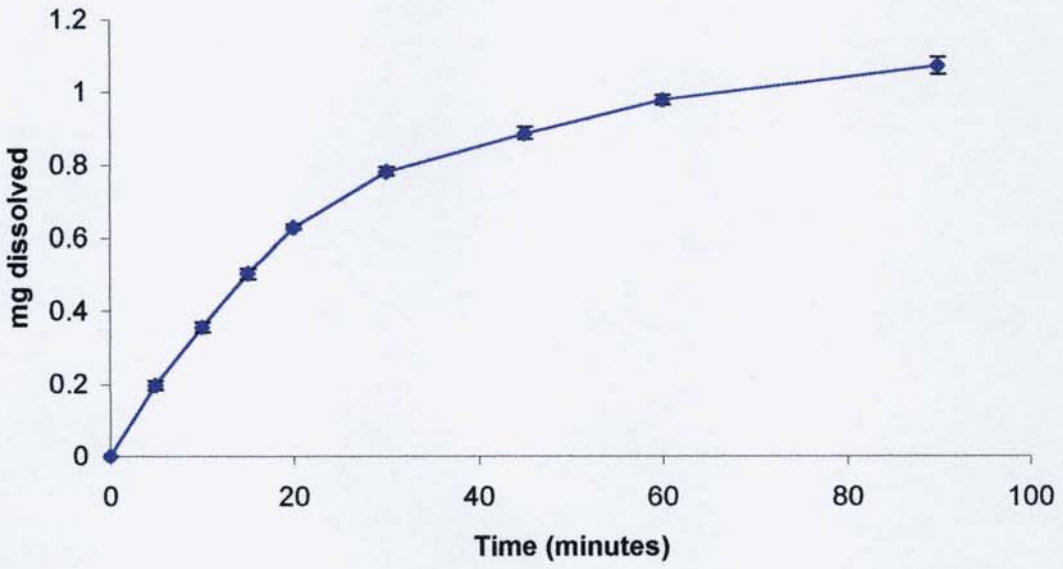

Figure 3-36 shows the dissolution profile that was obtained for the dissolution of atovaquone in FaSSIF alone, and it is seen that approximately 1 mg of atovaquone dissolved in 500 ml of FaSSIF over a period of 90 minutes. This corresponds to a solubility of 2 µg/ml, which, unlike troglitazone, is higher than the solubility found in water, which was 0.43 µg/ml (section 1.5.2). This shows that the solubility of atovaquone is enhanced by the presence of the natural surfactants (*i.e.* lecithin and sodium taurocholate) found in the FaSSIF. As with troglitazone, a true solubility value for atovaquone in FaSSIF was not established, due to the instability of the FaSSIF over extended time periods

(section 3.1.3.1). The dissolution of physical mixtures of atovaquone and each polymer was performed; unfortunately no data could be obtained as the HPLC method was not sensitive enough to detect any dissolved atovaquone. This, therefore, indicated that, like troglitazone, the presence of the polymers co-dissolving with the drug inhibited the dissolution of the drug. This has been attributed to the local viscosity around the particles during the initial stages of dissolution.

Figure 3-37 shows that atovaquone has one distinct melting endotherm at 220.64° C, and the ΔH of this melting is 77.883 J/g. Spray drying of atovaquone had no effect upon the structure of atovaquone (result not shown), and the ΔH and melting point did not change. It was also found that upon spray-drying no re-crystallisation occurred, thus indicating that atovaquone, post spray-drying, remained in the crystalline state. This shows that atovaquone is either not easily converted to the amorphous state, or that it rapidly returns to the crystalline state upon storage.

Figure 3-37 DSC trace of atovaquone

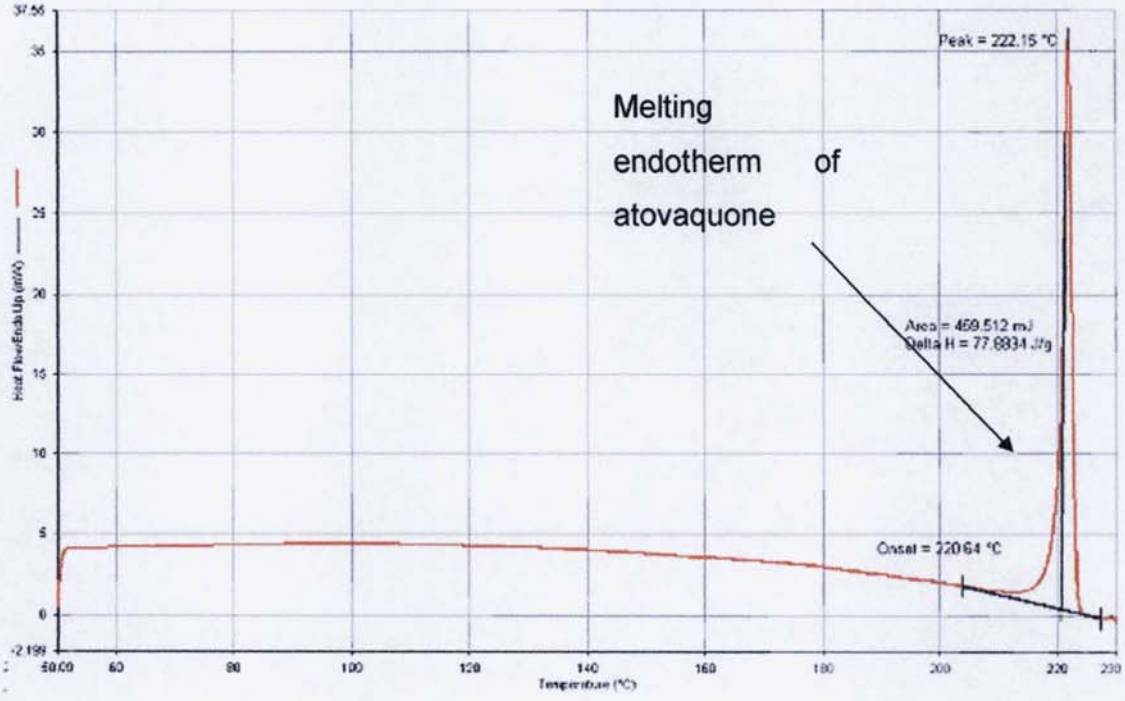

3.1.4.2 The effect of incorporating atovaquone into a solid dispersion on the degree of super-saturation

Figure 3-38 Dissolution of atovaquone from HPMCP dispersions. Results are the mean of three replicates, error bars ± SD

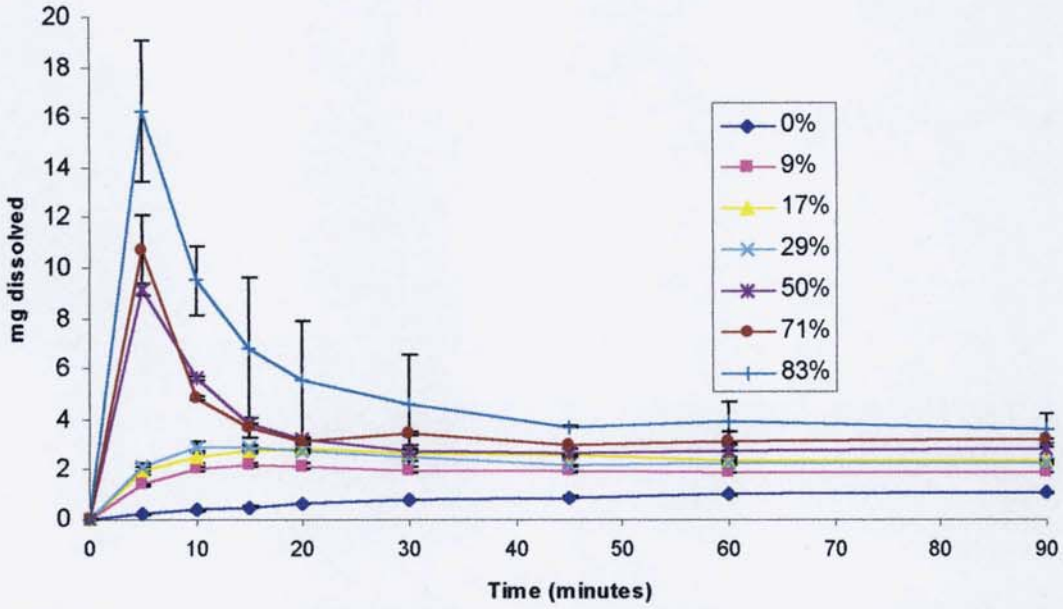

As outlined in section 3.1.1 the dissolution of atovaquone from solid dispersions using the three polymers (HPMCP, PVP and HPMC) was also studied, figures 3-38, 3-39 and 3-40. Table 3-23 displays the 'degree of super-saturation' for these dispersions. It is shown that as the polymer concentration is increased, for all polymers, there is an increase in the 'degree of supersaturation'. Like the troglitazone preparations a large enhancement is found when a threshold value is passed (50% for HPMCP, 71% for HPMC and 50% for PVP). At the low concentrations of polymer, 9, 17, 29% polymer, this enhancement is insignificant for all the polymers, with a rise of just 0.03 from the 9% to the 17% dispersions (in the case of PVP dispersions). The threshold value for the PVP and HPMCP dispersions appears to be between 29% and 50% (w/w), where the degree of supersaturation more than doubles in both cases (table 3-23). In the case of HPMC it is not until 71% w/w of polymer is used that such an increase is

experienced.

Figure 3-39 Dissolution of atovaquone from PVP dispersions. Results are the mean of three replicates, error bars ± SD

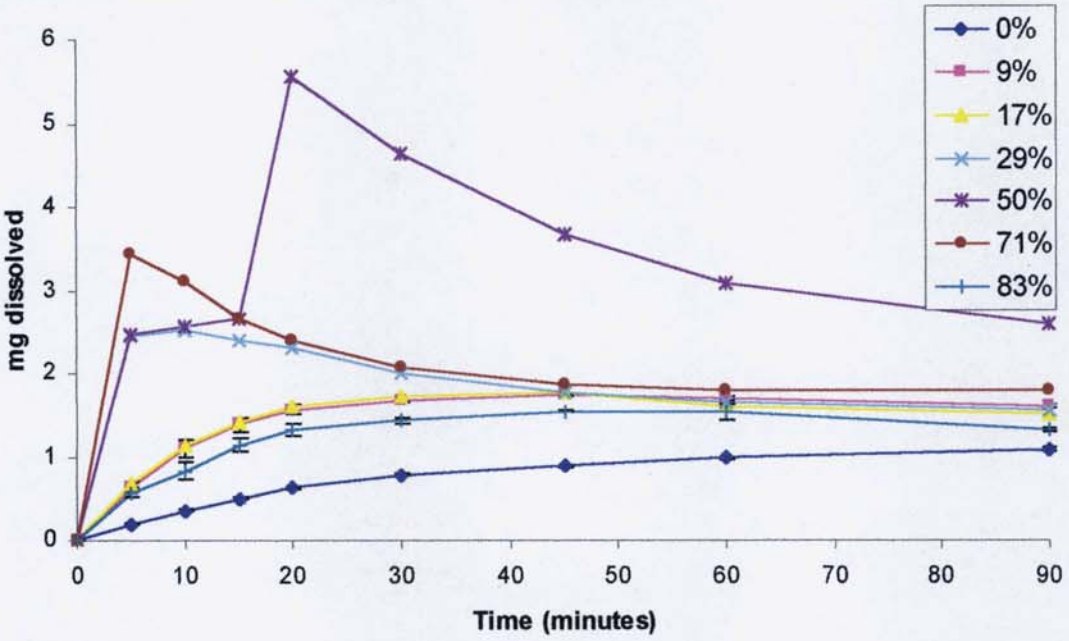

In the case of HPMCP the 'degree of supersaturation', continues to rise for all formulations. This indicates that the polymer is aiding the dissolution of the atovaquone. With the PVP samples it is observed that the degree of supersaturation decreases after the threshold value, back to a supersaturation value comparable with the 9% w/w dispersion. This indicates that rather than enhancing the dissolution of atovaquone, PVP in high concentrations inhibits dissolution. As discussed previously, it is postulated that at high polymer loadings the release of drug is dependent upon the polymer dissolution (Ford 1986; Craig, 2002). If the dissolution of these dispersions follows this mechanism it can be proposed that there is poor dissolution of the PVP from such dispersions. It has also been proposed that the dissolution of a drug from a solid dispersion could be controlled somewhat by the physical structure of the dispersion (Sertsou, 2002), and this is examined in more depth in section 3.3. The 'degree of supersaturation' in the HPMC dispersions plateaus after the threshold value has been obtained; this data conflicts what was found with troglitazone – in which an

83% w/w HPMC dispersion resulted in a reduction in the dissolution. This means that it is possible that even at these high concentrations of polymer, the drug could possibly still influence the wetting of the polymer.

Figure 3-40 Dissolution of atovaquone from HPMC dispersions. Results are the mean of three replicates, error bars ± SD

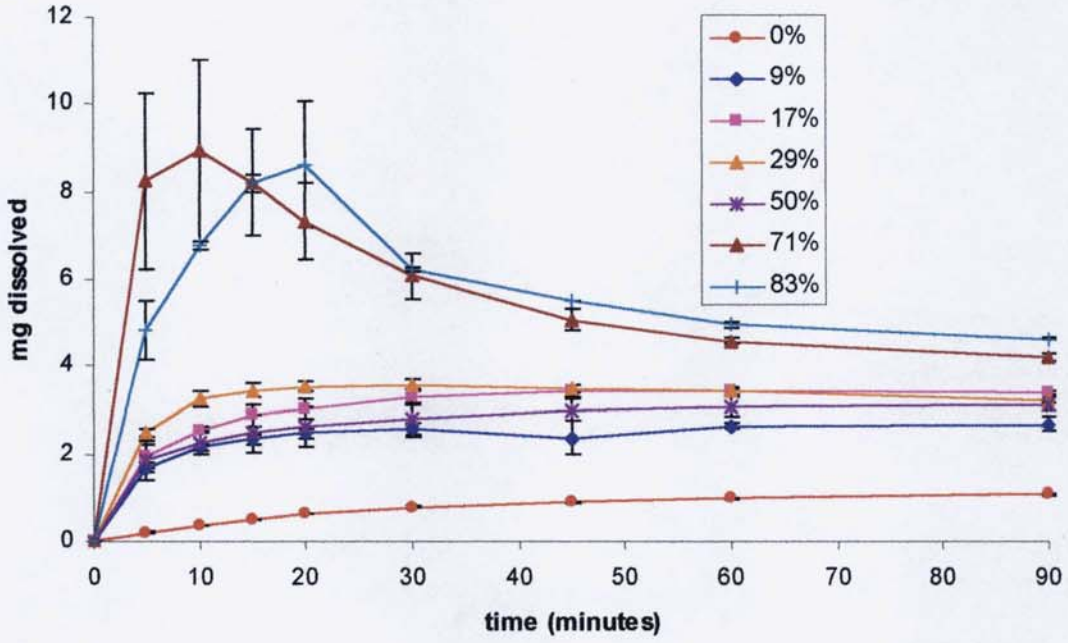

Table 3-23 The degree of supersaturation obtained when the peak mass dissolved from the solid dispersions is compared to that of atovaquone

% polymer	Polymer		
	HPMCP	HPMC	PVP
9%	2.07	2.50	1.62
17%	2.62	3.22	1.65
29%	2.70	3.31	2.36
50%	8.54	2.92	5.20
71%	10.02	8.35	3.21
83%	15.16	8.06	1.65

3.1.4.3 Effect of HPMCP concentration upon the dissolution of atovaquone

It has been shown that the amount of HPMCP within a dispersion has an impact on the peak amount of atovaquone dissolved from a solid dispersion (figure 3.38, table 3-23), this, though, gives little information on how the amount of HPMCP influences the rate at which it releases atovaquone. Tables 3-24 and 3-25 show that as the amount of HPMCP is increased, the amount of atovaquone dissolved over the first 20 minutes is also increased. Table 3-25 shows that at the low concentrations of HPMCP (9, 17, 29% w/w) the effect of increasing HPMCP is not significant ($P>0.05$ between all dispersions). This shows that that it is the physical properties of the drug controlling the dissolution of the solid dispersion (Craig 2002). The AUC_{20} from dispersions containing 50% w/w and above are all significantly different from each other ($P<0.001$, except in the case of 50% vs 71%); this indicates that there is some other mechanism involved in the dissolution of atovaquone from these dispersions compared to those of low polymer concentration.

Table 3-24 Results of the Tukey analysis of the AUC_{20} of the HPMCP:atovaquone dispersions (shaded boxes indicate no significant difference)

%Polymer	% Polymer					
	9	17	29	50	71	83
9						
17	>0.05					
29	>0.05	>0.05				
50	<0.001	<0.001	<0.001			
71	<0.001	<0.001	<0.001	>0.05		
83	<0.001	<0.001	<0.001	<0.001	<0.001	

It is seen, from tables 3-24 and 3-25, that increasing the HPMCP concentration within the atovaquone dispersions enhances the dissolution of atovaquone. It is seen from the 9% dispersion through to the 83% dispersion that there is a steady increase in the AUC_{90}. Tukey analysis, following ANOVA, indicates that in the

majority of cases the increase can be considered extremely significant (the exceptions being the 29% compared to the 17% dispersion, and the 71% compared to the 50% dispersion). One of the possible reasons behind such an increase could be due to the enhanced wetting of the dispersion, due to the increase in HPMCP concentration; this is supported by the increase in the initial dissolution rate (table 3-27). The other probable explanation is that at the higher polymer ratios the drug is in the amorphous form, so no energy is required to break the crystal lattice. The DSC data, however, shows that the atovaquone is not strongly incorporated into a solid dispersion, as even at the higher polymer concentrations the atovaquone can recrystallise upon heating (figures 3-43 and 3-46). This is evidence that whilst the drug is in an amorphous form it is not incorporated in a solid solution (Sertsou *et al.*, 2000), which has been shown to have a significant effect upon the dissolution of the drug from a solid dispersion.

Table 3-25 Results of the Tukey analysis of the AUC_{90} of the HPMCP:atovaquone dispersions (shaded boxes indicate no significant difference)

%Polymer	% Polymer						
		9	17	29	50	71	83
	9						
	17	<0.01					
	29	<0.01	>0.05				
	50	<0.001	<0.001	<0.001			
	71	<0.001	<0.001	<0.001	>0.05		
	83	<0.001	<0.001	<0.001	<0.001	<0.001	

The dissolution of atovaquone, at the higher polymer ratios is consistent with what has been described before in the literature for HPMCP dispersions, in that there is rapid initial dissolution of the drug followed by a rapid recrystallisation (Kai *et al.*, 1996, and Sertsou 2002). The atovaquone dispersions are following what is considered the normal behaviour for such dispersions. What is evident is that although an improvement in dissolution is found using the solid dispersion approach with atovaquone and HPMCP, it is only at the very high polymer

proportion that this improvement is realised, *i.e.* the 83% dispersion. Using the 83% dispersion would correspond to having 1.25 grams of excipient (considering the dosage to be 250 mg), which would be an excessive amount for a solid dosage form (Sertsou 2002). It is, therefore felt that the solid dispersion route for atovaquone with HPMCP would not be an appropriate route for a formulation.

3.1.4.4 Effect of PVP concentration upon the dissolution of atovaquone

In the case of the PVP dispersions, a different pattern emerges and the two distinct regions (as found with the HPMCP dispersions) are not evidenced when polymer concentration is considered. In the instance of the HPMCP dispersions there is a distinct boundary between the low polymer concentration dispersions and the high polymer concentrations. With the PVP dispersions there are again two distinct regions, the first contains the very low polymer concentration dispersions (9 and 17% w/w) and the very high polymer concentration dispersion (83% w/w), the second contains the intermediate dispersions (29, 50 and 71% w/w). It is seen that the PVP begins to exert an effect, over the first twenty minutes, upon the dissolution of atovaquone at only 29% w/w, and that any further increases have only a minimal effect upon the dissolution.

Table 3-26 Results of the Tukey analysis of the AUC_{20} of the PVP:atovaquone dispersions (shaded boxes indicate no significant difference)

%Polymer	% Polymer						
		9	17	29	50	71	83
	9						
	17	>0.05					
	29	<0.001	<0.001				
	50	<0.001	<0.001	>0.05			
	71	<0.001	<0.001	>0.05	>0.05		
	83	>0.05	>0.05	<0.001	<0.001	<0.001	

Table 3-27 The AUC_{20}, AUC_{90} and the polynomial rate of the atovaquone dispersions. Results are the mean of three replicates, ± SD

% Polymer	AUC_{20} (mg.ml^{-1}.min)			AUC_{90} (mg.ml^{-1}.min)			Polynomial rate (mg/min)		
	HPMCP	PVP	HPMC	HPMCP	PVP	HPMC	HPMCP	PVP	HPMC
9	33. ± 1.2	19.5 ± 1.3	37.1 ± 1.5	168.3 ± 2.2	136.2 ± 1.9	216.4 ± 5.2	0.38 ± 0.04	0.14 ± 0.02	0.56 ± 0.04
17	43.1 ± 0.9	20.2 ± 1.3	44.4 ± 4.3	217.7 ± 4.1	134.9 ± 2.1	280.6 ± 12.4	0.66 ± 0.03	0.16 ± 0.02	0.66 ± 0.13
29	46 ± 2.2	42.6 ± 9.7	54.9 ± 2.2	206.9 ± 8.3	165.9 ± 14.8	293.9 ± 8.8	0.58 ± 0.04	0.98 ± 0.31	0.79 ± 0.03
50	101.0 ± 0.3	52.5 ± 2.	39.4 ± 7.8	295.6 ± 8.0	301.4 ± 5.9	248.5 ± 25.8	4.79 ± 0.23	0.88 ± 0.29	0.64 ± 0.17
71	104.1 ± 8.4	52.0± 1.2	145.3 ± 27.2	328.6 ± 9.0	185.0 ± 3.9	499.9 ± 41.7	6.49 ± 1.00	1.47 ± 0.03	3.07 ± 0.83
83	177.7 ± 24.7	20.2 ± 1.3	120.5 ± 5.7	490.6 ± 21.5	134.9 ± 2.0	483.9 ± 22.7	8.69 ± 1.69	0.16 ± 0.02	1.59 ± 0.53

Over 90 minutes a similar pattern emerges as to that seen at 20 minutes, again the 9%, 17% and 83% dispersions are considered similar. This time, however the 29%, 50% and 71% dispersions are considered significantly different from one another, table 3-27 also shows that 50% dispersion has the largest AUC_{90}. It is shown in table 3-23 that as the polymer concentration increases from 29% to 71% the degree of supersaturation increases (from 29 – 50%) then decreases (50% - 71%). These results indicate that increasing the concentration of polymer has less of an effect upon the dissolution of atovaquone than the HPMCP (section 3.1.3.9), and there is only any significant improvement when 50% or 71% of the dispersion is polymer.

As discussed in section 3.1.3.4 it is expected to find a rise in the dissolution rate of the drug from PVP dispersions, as the polymer concentration increases. It is found, however, that once a peak dissolution performance is obtained further increases in PVP concentration only serve to lower the dissolution of the drug, this was also found with the PVP:atovaquone dispersions (based upon the AUC_{20} and AUC_{90} data). This peak in dissolution was found to occur when the polymer concentration was 50%. It is, therefore considered that the PVP:atovaquone dispersions are behaving in a manner that would be expected from what is shown in the literature. The degree of enhancement, though, compared to the dissolution of the drug alone is a lot smaller than would be expected from such dispersions.

Table 3-28 Results of the Tukey analysis of the AUC_{90} of the PVP:atovaquone dispersions (shaded boxes indicate no significant difference)

%Polymer	% Polymer					
	9	17	29	50	71	83
9						
17	>0.05					
29	<0.01	<0.01				
50	<0.001	<0.001	<0.001			
71	<0.001	<0.001	<0.05	<0.001		
83	>0.05	>0.05	<0.01	<0.001	<0.001	

3.1.4.5 Effect of HPMC concentration upon the dissolution of atovaquone

As shown from the 'degree of super-saturation' data (table 3-23) HPMC appears to have very little influence upon the dissolution of atovaquone from a solid dispersion until polymer concentration reaches 71%. This is mirrored in the AUC_{20} data shown in table 3-29 and 3-30. It is seen from the Tukey analysis that the concentration of polymer has very little effect upon the dissolution of atovaquone between 9 – 50% polymer content. It could, therefore, be assumed that between these ratios the dissolution of the polymer is not the main controlling factor behind the dissolution. When dissolution from dispersions containing over 50% polymer is considered, it is seen that there is further enhancement in the dissolution of atovaquone, with both the 71% and 83% dispersion being significantly different to the other dispersions ($p<0.001$). It is therefore assumed that the polymer is having some effect upon the dissolution of the drug from these two dispersions. However, the dissolution of both the 71% and 83% dispersion is not entirely controlled by the dissolution of the polymer. This is because data shown in section 3.1.4.6 shows that not the entire drug is fully incorporated into the solid dispersion.

Table 3-29 Results of the Tukey analysis of the AUC_{20} of the HPMC:atovaquone dispersions (shaded boxes indicate no significant difference)

%Polymer	% Polymer						
		9	17	29	50	71	83
	9						
	17	>0.05					
	29	>0.05	>0.05				
	50	>0.05	>0.05	>0.05			
	71	<0.001	<0.001	<0.001	<0.001		
	83	<0.001	<0.001	<0.001	<0.001	>0.05	

Table 3-30 Results of the Tukey analysis of the AUC_{90} of the HPMC:atovaquone dispersions (shaded boxes indicate no significant difference)

%Polymer	% Polymer					
	9	17	29	50	71	83
9						
17	<0.05					
29	<0.05	>0.05				
50	>0.05	>0.05	>0.05			
71	<0.001	<0.001	<0.001	<0.001		
83	<0.001	<0.001	<0.001	<0.001	>0.05	

3.1.4.6 Effect of polymer selection upon the dissolution of atovaquone

Tables 3-31 to 3-36 show the impact that the different polymers have upon the dissolution of atovaquone from solid dispersions over the first 20 minutes. It is seen even at the low polymer concentrations (9 and 17% w/w) that the choice of polymer does have some impact upon the dissolution of the atovaquone. The PVP dispersions, at both 9% and 17% w/w, are considered to result in significantly different dissolution to those composed of HPMCP and HPMC. This, therefore, suggests that dissolution from these dispersions is not solely controlled by the physical properties of the drug, as previously discussed, and that the polymer does exert some control over the dissolution of atovaquone. HPMCP and HPMC at these concentrations have a similar influence upon the dissolution of atovaquone. As the polymer concentration increases above 50% there is still a significant difference between the dissolution of atovaquone from the dispersions. This therefore shows that polymer selection does have some effect upon the dissolution of atovaquone. This observation, together with the fact that for each polymer the concentration has a significant effect upon dissolution over the first 20 minutes (sections 3.1.4.2 -3.1.4.4), indicates that the initial dissolution of atovaquone occurs, to some extent, via a carrier-controlled mechanism. If it was solely a drug controlled mechanism, the choice of polymer and amount of polymer would have little effect upon the dissolution of atovaquone (Craig 2002), this is discussed in more depth in section 3.1.4.7.

Table 3-31 Results of the Tukey analysis of the AUC_{20} of the 9% atovaquone dispersions (shaded boxes indicate no significant difference)

Polymer	Polymer		
	HPMCP	PVP	HPMC
HPMCP			
PVP	<0.001 (-13.71)		
HPMC	<0.05 (3.81)	<0.001 (17.52)	

Table 3-32 Results of the Tukey analysis of the AUC_{20} of the 17% atovaquone dispersions (shaded boxes indicate no significant difference)

Polymer	Polymer		
	HPMCP	PVP	HPMC
HPMCP			
PVP	<0.001 (-22.92)		
HPMC	>0.05 (1.29)	>0.001 (24.21)	

Table 3-33 Results of the Tukey analysis of the AUC_{20} of the 29% atovaquone dispersions (shaded boxes indicate no significant difference)

Polymer	Polymer		
	HPMCP	PVP	HPMC
HPMCP			
PVP	N/A		
HPMC	N/A	N/A	

Table 3-34 Results of the Tukey analysis of the AUC_{20} of the 50% atovaquone dispersions (shaded boxes indicate no significant difference)

Polymer	Polymer		
	HPMCP	PVP	HPMC
HPMCP			
PVP	<0.001 (-48.57)		
HPMC	<0.001 (-61.61)	<0.001 (13.03)	

Table 3-35 Results of the Tukey analysis of the AUC_{20} of the 71% atovaquone dispersions (shaded boxes indicate no significant difference)

Polymer		Polymer		
		HPMCP	PVP	HPMC
	HPMCP			
	PVP	<0.05 (-52.06)		
	HPMC	<0.05 (40.27)	<0.001 (92.34)	

Table 3-36 Results of the Tukey analysis of the AUC_{20} of the 83% atovaquone dispersions (shaded boxes indicate no significant difference)

Polymer		Polymer		
		HPMCP	PVP	HPMC
	HPMCP			
	PVP	<0.001 (-157.53)		
	HPMC	<0.01 (57.18)	>0.001 (100.35)	

The choice of polymer has quite a large impact upon the dissolution of the atovaquone over 90 minutes, especially at the lower concentrations of polymer. The results of the Tukey analysis of these dispersions show that the eventual dissolution is significantly different after 90 minutes. When the dispersions contain 50% w/w polymer and above, the choice of polymer becomes less important, as at 50% w/w the PVP and HPMCP dispersion are considered similar, and at 83 % w/w the HPMC and HPMCP dispersions are considered similar. The polynomial rates in table (3-26) show that atovaquone has a faster dissolution rate when used in HPMCP dispersions (50% and above) compared to either the PVP and HPMC dispersions. This shows that the polymer selection is is having an effect upon the initial dissolution of atovaquone. This is further evidence to suggest that the drug-controlled mechanism is not the sole controlling mechanism for the dissolution of atovaquone from the dispersions (this is discussed further in section 3.1.4.7).

Table 3-37 Results of the Tukey analysis of the AUC_{90} of the 9% atovaquone dispersions (shaded boxes indicate no significant difference)

Polymer	Polymer		
	HPMCP	PVP	HPMC
HPMCP			
PVP	<0.001 (-32.09)		
HPMC	<0.001 (48.07)	<0.001 (80.16)	

Table 3-38 Results of the Tukey analysis of the AUC_{90} of the 17% atovaquone dispersions (shaded boxes indicate no significant difference)

Polymer	Polymer		
	HPMCP	PVP	HPMC
HPMCP			
PVP	<0.001 (-82.77)		
HPMC	<0.001 (62.90)	<0.001 (145.66)	

Table 3-39 Results of the Tukey analysis of the AUC_{90} of the 29% atovaquone dispersions (shaded boxes indicate no significant difference)

Polymer	Polymer		
	HPMCP	PVP	HPMC
HPMCP			
PVP	<0.01 (-41.01)		
HPMC	<0.001 (86.98)	<0.001 (127.99)	

Table 3-40 Results of the Tukey analysis of the AUC_{90} of the 50% atovaquone dispersions (shaded boxes indicate no significant difference)

Polymer	Polymer		
	HPMCP	PVP	HPMC
HPMCP			
PVP	>0.05 (5.80)		
HPMC	<0.05 (-47.14)	<0.05 (-52.94)	

Table 3-41 Results of the Tukey analysis of the AUC_{90} of the 71% atovaquone dispersions (shaded boxes indicate no significant difference)

Polymer		Polymer		
		HPMCP	PVP	HPMC
Polymer	HPMCP			
	PVP	<0.001 (-143.55)		
	HPMC	<0.001 (171.32)	<0.001 (314.87)	

Table 3-42 Results of the Tukey analysis of the AUC_{90} of the 83% atovaquone dispersions (shaded boxes indicate no significant difference)

Polymer		Polymer		
		HPMCP	PVP	HPMC
Polymer	HPMCP			
	PVP	<0.001 (-355.67)		
	HPMC	>0.05 (-6.66)	>0.001 (349.01)	

Figure 3-41 shows the DSC trace of the 9% HPMC dispersion, with atovaquone, and it is seen from this trace that the majority of the atovaquone is still in a crystalline state. The ΔH for the melt endotherm is of a similar magnitude to that of atovaquone alone (9 J/g compared to 77 J/g) and it is also seen that the melt temperature has not been altered by the incorporation of atovaquone with HPMC (219°C compared 220°C). This indicates that there is no interaction between atovaquone and the HPMC, as it is predicted that when interactions occur the melting temperature and peak shape tend to change (Smith 1982). There is, however, with the dispersion an enhancement in dissolution compared to atovaquone alone, by a factor 2.07 (table 3-23). The same pattern is experienced when the polymer concentration is increased (figure 3-42), the melting endotherms for the PVP and HPMC dispersions show no alterations in the melting temperature and the ΔH, again indicating no interaction. DSC results for HPMCP dispersions does show that there is some form of interaction between the atovaquone and the polymer, as the onset melt temperature and the peak shape has altered (figure 3-42).

However, the ΔH of the melting endotherm is still comparable to that of atovaquone alone. Therefore, it is believed that the mechanism of increased dissolution, in the lower polymer loading dispersions, is via particle size reduction as predicted by Sekiguchi and Obi (1961) and within these dispersions the atovaquone is dispersed within the polymer in small crystalline regions, of a very small particle size.

Figure 3-41 DSC trace of an atovaquone dispersion with 9% HPMC

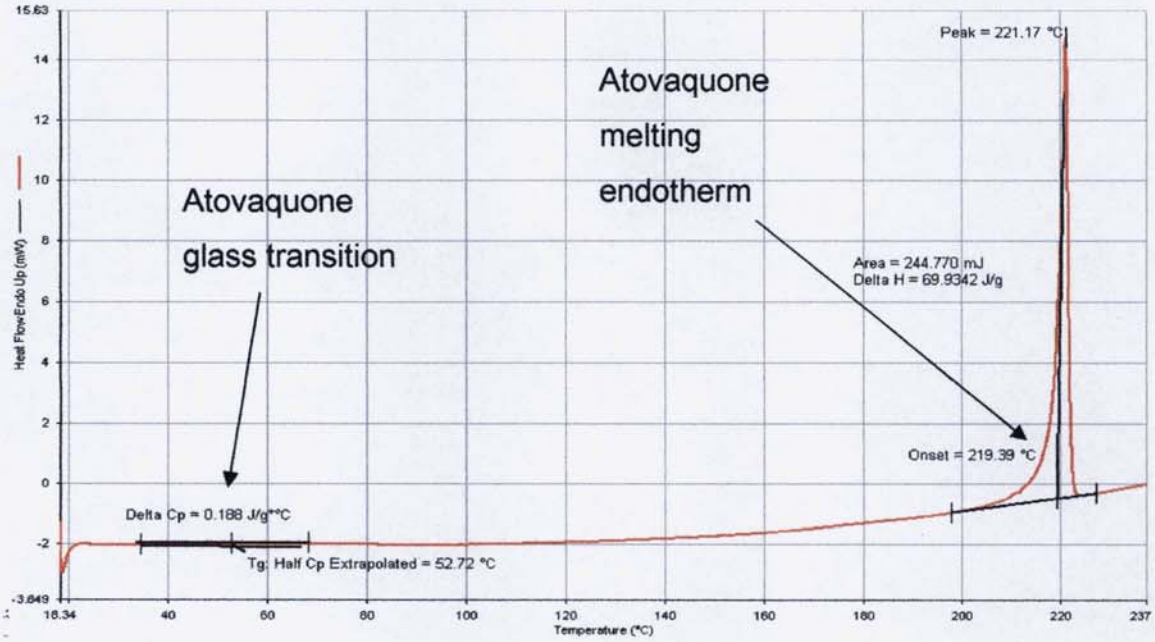

Figure 3-42 DSC traces of atovaquone dispersions with 17% polymer (key: PVP, HPMCP, HPMC)

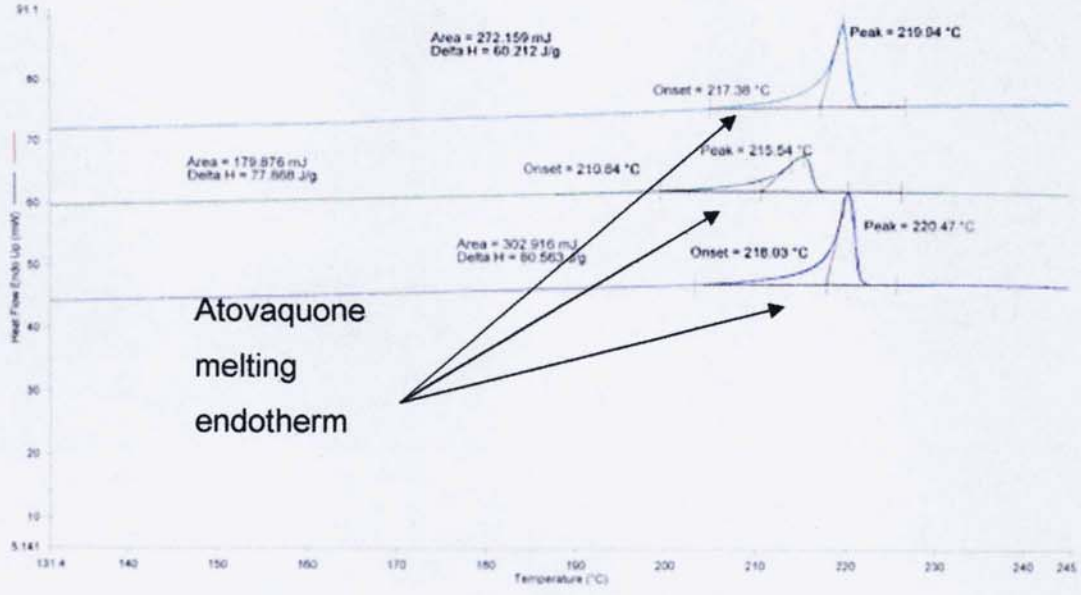

When the higher polymer loading dispersions are considered a different picture emerges (figures 3-43 to 3-46). Here it is seen that upon heating atovaquone crystallises out from the 50% dispersions (figures 3-43 and 3-44), and that the ΔH and the melting temperature have altered. Firstly the recrystallisation indicates that atovaquone is now present in an amorphous form within the dispersion (the XRPD data shown in figure 3-47 shows this for the 50% HPMC dispersion), secondly the reduction in the ΔH value shows that the entire drug content has recrystallised out from the amorphous phase. It is seen that the ΔH values for both the HPMC and the HPMCP are the same; this therefore indicates that within these dispersions the same amount of drug has recrystallised out. Regarding the structure of these two dispersions, it is hypothesised that there is some drug incorporated into the solid dispersion and that there are regions of amorphous drug dispersed within the carrier, as predicted by Sertsou (2002). The fact that these two dispersions are similar in structure does not explain why the dissolution of these two dispersions is significantly different (after both 20 minutes and 90 minutes, tables 3-34 and 3-40). Therefore, the differences between the behaviour of these two dispersions is better explained by the behaviour of the carrier whilst undergoing dissolution (section 5.4.6).

Figure 3-43 DSC trace of atovaquone dispersion with 50% HPMCP

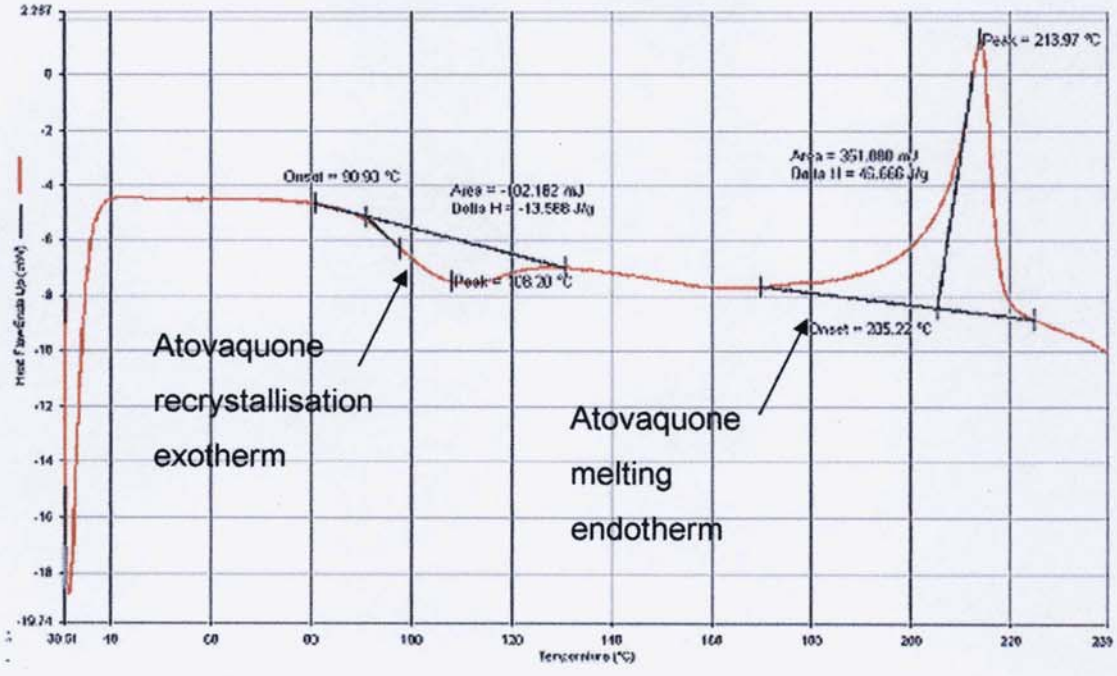

Figure 3-44 DSC trace of atovaquone dispersion with 50% HPMC

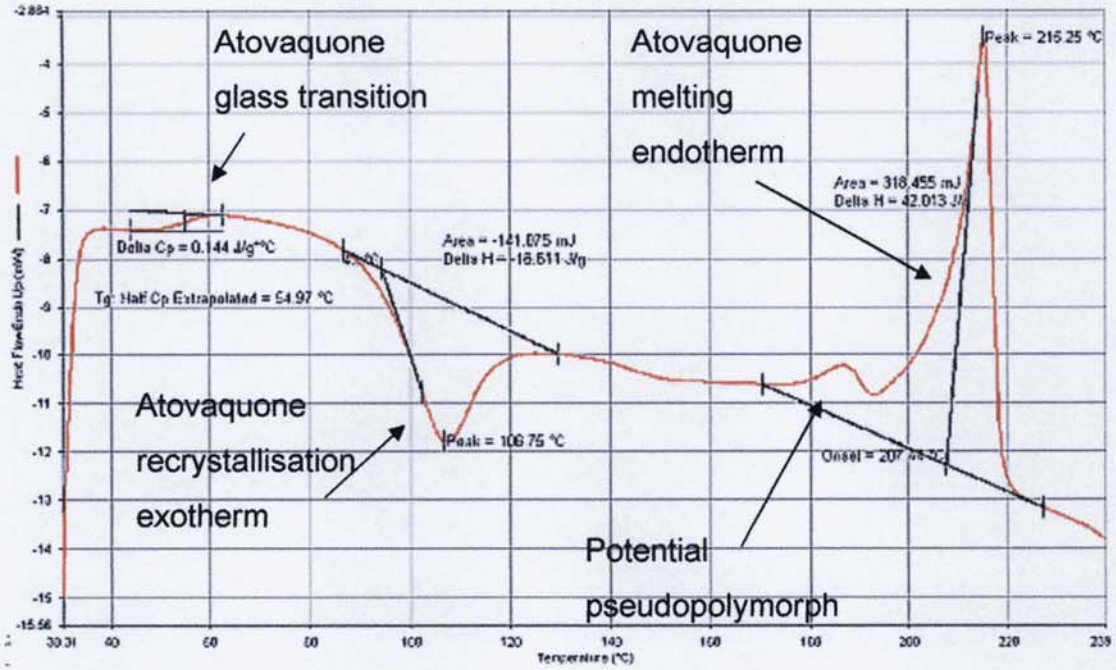

The picture that emerges with the 83% dispersions of HPMC and HPMCP is similar to that of the 50% dispersions (figures 3-45 and 3-46), that the dispersions are similar in structure. With both dispersions it is again seen that that there is a region where the drug recrystallises from the dispersion during heating, although there is no clear melt endotherm for this recrystallised drug. The fact that the melt endotherm is not so prominent in these dispersions indicates that there is either more of the drug incorporated into the polymer or that the high amount of polymer (and related high viscosity) is preventing the free amorphous regions from interacting and thus providing a region of crystalline material. The fact that the dissolution of both the 83% HPMC and HPMCP dispersions is significantly higher than of the corresponding 50% dispersions indicates that it is the former structure that is present (*i.e.* more drug is incorporated into the carrier).

What can be shown from thermal studies of the atovaquone dispersion within these carriers is that the carriers used are not compatible with atovaquone for the formulation of solid dispersions. This is based upon the fact that in both cases (HPMC and HPMCP) the drug fails to form a strong interaction with the polymers, thus limiting the amount of drug that is incorporated into the carriers as solid solutions.

Figure 3-45 DSC trace of atovaquone dispersion with 83% HPMC

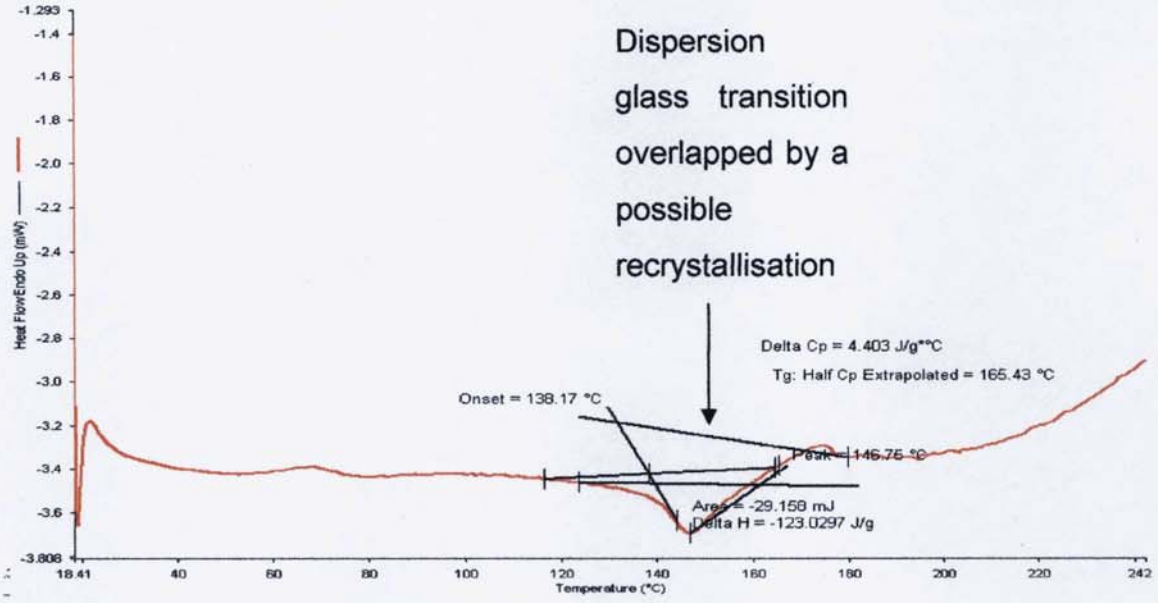

Figure 3-46 DSC trace of atovaquone dispersion with 83% HPMCP

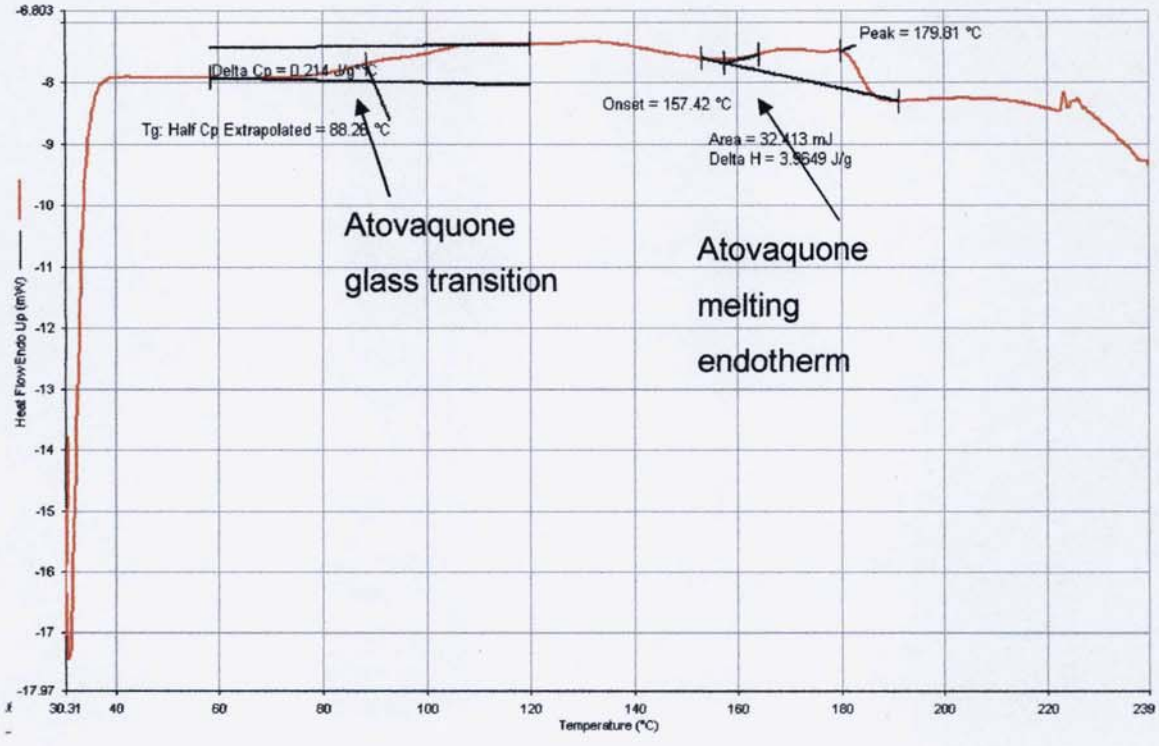

Figure 3-47 DSC trace of atovaquone dispersion with 50% HPMC

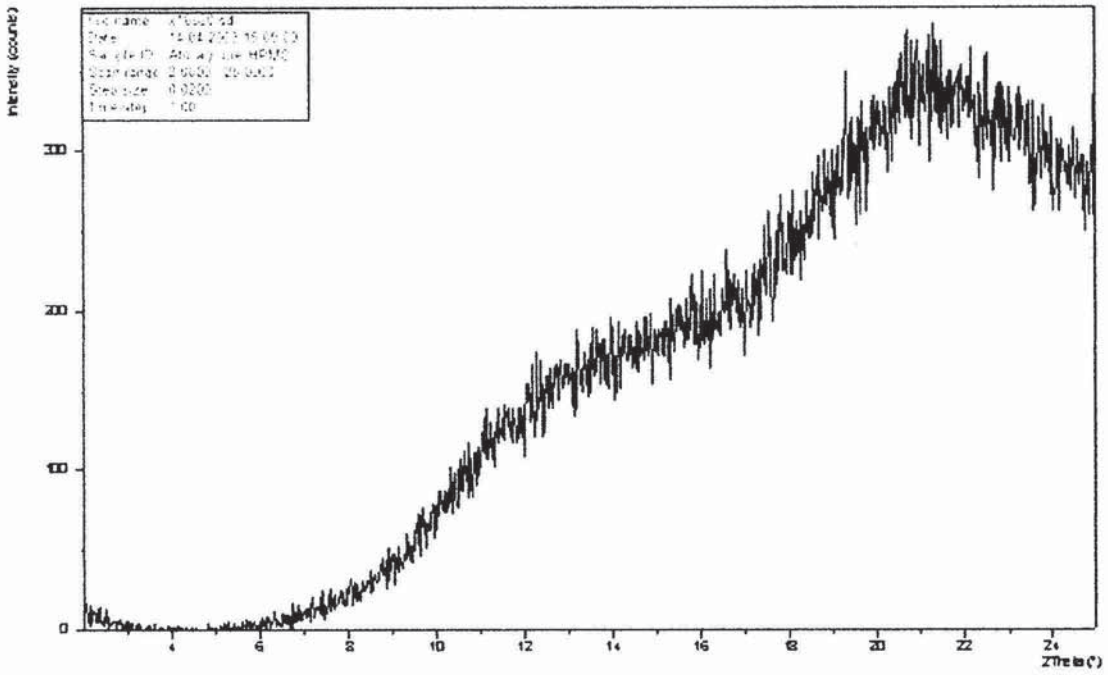

3.1.4.7 Comparison of the effect that incorporation into a solid dispersion has upon atovaquone and troglitazone

Figures 3-48, 3-49 and 3-50 show comparisons of the 'degree of supersaturation' between the atovaquone and troglitazone dispersions. It is shown that the polymers examined are far more effective at enhancing the dissolution of troglitazone than they are for atovaquone. This indicates that the polymer is not the only factor that controls the overall dissolution of the drug from the atovaquone dispersions. The mechanisms described in section 1.3.2 could offer some explanation to the differences seen between the atovaquone and troglitazone dispersions. It could be hypothesised that, in the broadest sense, the troglitazone dispersions are undergoing carrier controlled dissolution, whereas the atovaquone dispersions are undergoing drug controlled dissolution. This hypothesis is based simply on the fact the degree of supersaturation is higher for troglitazone, and as stated by Craig (2002) it is expected that there will be more dissolution with carrier-controlled dissolution. Application of the model proposed by Corrigan (1985) goes some way to supporting this hypothesis, as it was stated that the larger solubility difference between the two components the higher the polymer loading required for carrier controlled dissolution to occur. It is seen from sections 1.5.1 and 1.5.2

that there is a >10 fold difference in the solubilities of troglitazone and atovaquone. So application of this model predicts that carrier controlled dissolution would be more easily achievable with troglitazone than atovaquone (taking into account the fact that the same polymers are used for the atovaquone and troglitazone dispersions). There is evidence to suggest, however, that the choice of polymer is controlling some aspect of the dissolution of atovaquone from the dispersions (section 3.1.4.6).

The other factor that could control which mechanism was followed is the dissolution of the drug into the dissolving layer (Craig 2002). It is felt that the polynomial dissolution rates could give an indirect measurement of this, as stated in section 3.1.3.7 this gives an indication of the wetting of the drug by the polymer. It is seen from tables 3-2 and 3-25 that the troglitazone dispersions consistently have a higher dissolution rate than the atovaquone dispersions. This, therefore, indicates that the polymers are wetting the troglitazone better than the atovaquone. This could mean that troglitazone dissolves into the dissolving layer faster than atovaquone, thus facilitating carrier-controlled dissolution for troglitazone.

Figure 3-48 Comparison of the degree of supersaturation of the troglitazone:HPMCP with the atovaquone:HPMCP dispersions. Results are the mean of three replicates, error bars ± SD

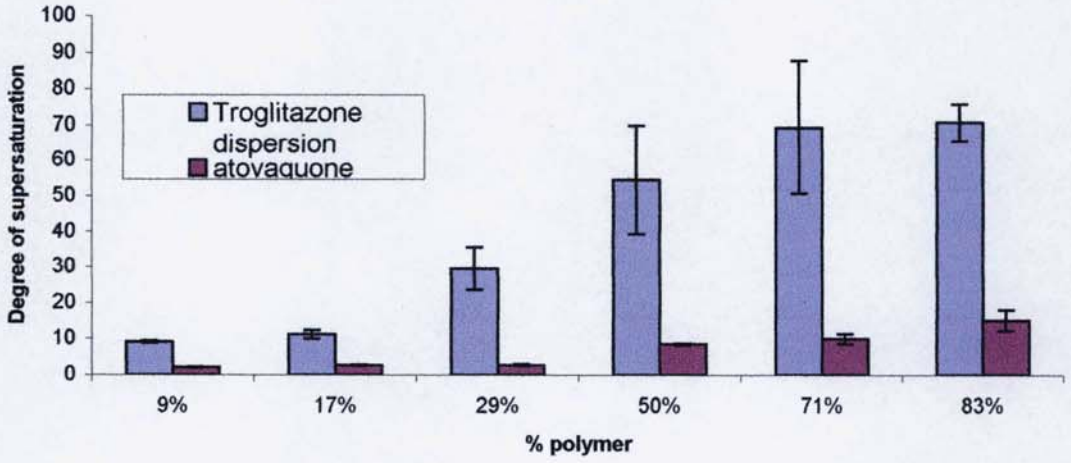

Figure 3-49 Comparison of the degree of supersaturation of the troglitazone:PVP with the atovaquone:PVP dispersions. Results are the mean of three replicates, error bars ± SD

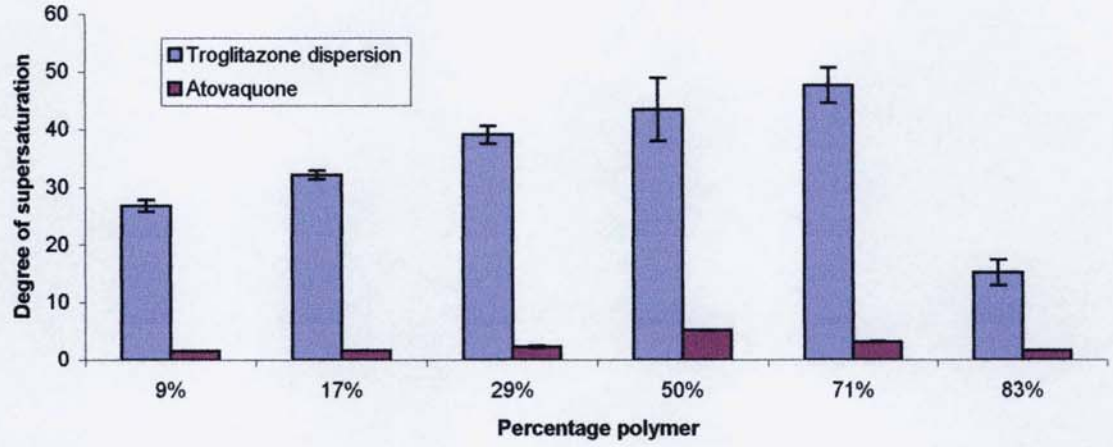

Figure 3-50 Comparison of the degree of supersaturation of the troglitazone:HPMC with the atovaquone:HPMC dispersions. Results are the mean of three replicates, error bars ± SD

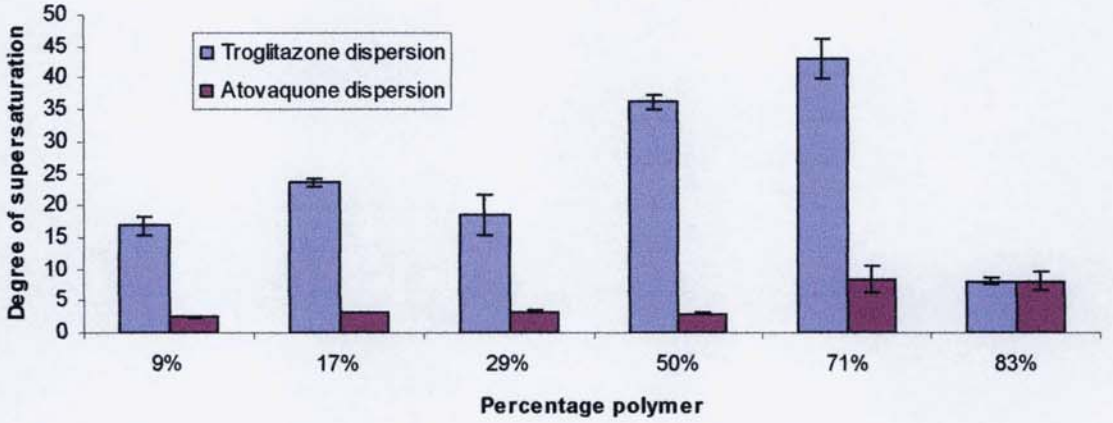

The final factor that has been hypothesised to decide which mechanism is more likely is the dissolution is the physical form of the drug within the solid dispersion. It was stated in section 1.3.2 that carrier-controlled dissolution is more likely when the drug is fully incorporated into the solid dispersion. Using the atovaquone and troglitazone 50%HPMC dispersions as an example it can be seen that there are some clear differences. Firstly from figure 3-50 it can be seen that there is an almost 10 fold difference between the degree of

supersaturation. Examination of the troglitazone:HPMC 50% dispersion (figure 3-29) shows evidence that the troglitazone within the dispersion is in an amorphous state, this is due to the absence of a melting endotherm. The DSC trace also shows that the drug is fully incorporated in the solid solution, this is due to there being no re-crystallisation of troglitazone and the presence of one glass transition temperature (Tg) (60.59°C). The fact that that there is also only one Tg present in the trace also indicates that there is only one system present within the dispersion. Examination of the corresponding atovaquone:HPMC dispersion (figure 3-44) shows a recrystallisation exotherm, thus indicating that not all of the drug is incorporated in the solid dispersion (section 1.3.2.3). There is also evidence that there is small amount of drug in the crystalline state, as the ΔH for the melting endotherm is much larger than the re-crystallisation exotherm (18.611J/g compared to 42.013 J/g). According to the work by Sertsou, (2002) there are regions of free amorphous drug within the dispersion that are not incorporated into a solid solution, due to the presence of the re-crystallisation exotherm. Sertsou *et al.* (2002) showed that the presence of a recrystallising exotherm was evidence of amorphous drug not being incorporated into the solid dispersion. Also if there is some drug in the crystal phase, it is understood that that not all the drug is fully incorporated as part of a solid solution (Chiou and Riegleman, 1971). This, therefore, indicates that it is more likely that the atovaquone dispersions will undergo drug-controlled dissolution and the troglitazone undergo carrier controlled dissolution.

The majority of the evidence suggests that the differences seen between the atovaquone and troglitazone dispersions in figures 3-48 to 3-50 are to do with the fact that the troglitazone dispersions undergo carrier-controlled dissolution and the atovaquone dispersions undergo drug-controlled dissolution. However, if the all the atovaquone dispersion dissolved via drug-controlled dissolution it would be expected that the dissolution of atovaquone from all of the dispersions would be the same, regardless of polymer. Sections 3.1.4.5 and 3.1.4.6 show that there are significant differences between the dissolution of atovaquone dispersions made at the same polymer loading but with different polymers. This means that the drug-controlled mechanism is not the

only mechanism involved for the atovaquone dispersion. It is hypothesised that maybe both mechanisms are involved, especially with the dispersions with the high polymer loading. However, it is felt that a mechanism similar to the drug-controlled dissolution mechanism dominates the dissolution of the atovaquone dispersions due to the large differences found between them and the troglitazone dispersions. It is proposed that carrier-controlled dissolution is occurring in the atovaquone dispersions, but is the minor contributor to the overall dissolution of the drug. This could be due to a small amount of the drug, which is molecularly dispersed within the polymer, being incorporated into the dissolving surface when it forms. This means that when the polymer is released into the bulk the drug is released with it, thus meaning that some of the dissolution is carrier controlled. Whilst the rest of the drug slowly dissolves into the dissolving surface, thus meaning the rest of the drug goes through the drug-controlled mechanism. It is also felt that troglitazone has a similar dual mechanism, and this is discussed in section 5.4.5.

3.2 Influence of paddle speed upon the discrimination of dissolution of dispersions

3.2.1 Introduction

It has been stated that the paddle speed is not an important factor for the preparation of a discriminating dissolution test when using the FaSSIF medium (Galia, 2000). This has been attributed to the presence of the bile salts in the dissolution medium, and this is suggested to be adequate to form a discriminating dissolution test.

It was the intention to determine whether this observation held true for the dissolution of solid dispersions in FaSSIF. The dissolution testing was performed using paddle speeds of 25 rpm, and 75 rpm. The 75 rpm paddle speed was selected as the upper speed, as preliminary testing showed that speeds above this caused a vortex to occur in the dissolution media. The speed 25 rpm was selected as it was the intention to examine an extreme difference to the 75 rpm, and this was the slowest speed the bath was capable of.

3.2.2 Experimental

3.2.2.1 Materials

See sections 2.2.2.1, 2.4.2.1 and 2.6.1.1 for details of the materials used.

3.2.2.2 Equipment

Dissolution was performed using the equipment described in section 2.6.1.2. Analysis was performed on the HPLC system described in section 2.2.2.2.

3.2.2.3 Method

Solid dispersions were prepared as described in section 2.4.1.1. Dissolution testing was carried out as described in section 2.3.1.3, except the paddle speed was set at 25 rpm. Samples were then analysed using the HPLC method described in section 2.2.2.3.2.

To ascertain the degree of discrimination between the samples, the AUC_{20}, AUC_{90} and the M_{max} (maximum drug dissolved) were calculated as described in section 3. ANOVA followed by a Tukey test were undertaken using Graphpad Instat 3.

3.2.3 Results and discussion

Figure 3-51 Dissolution of troglitazone from 9% (w/w) dispersions at 25 rpm. Results are the mean of three replicates, error bars ± SD

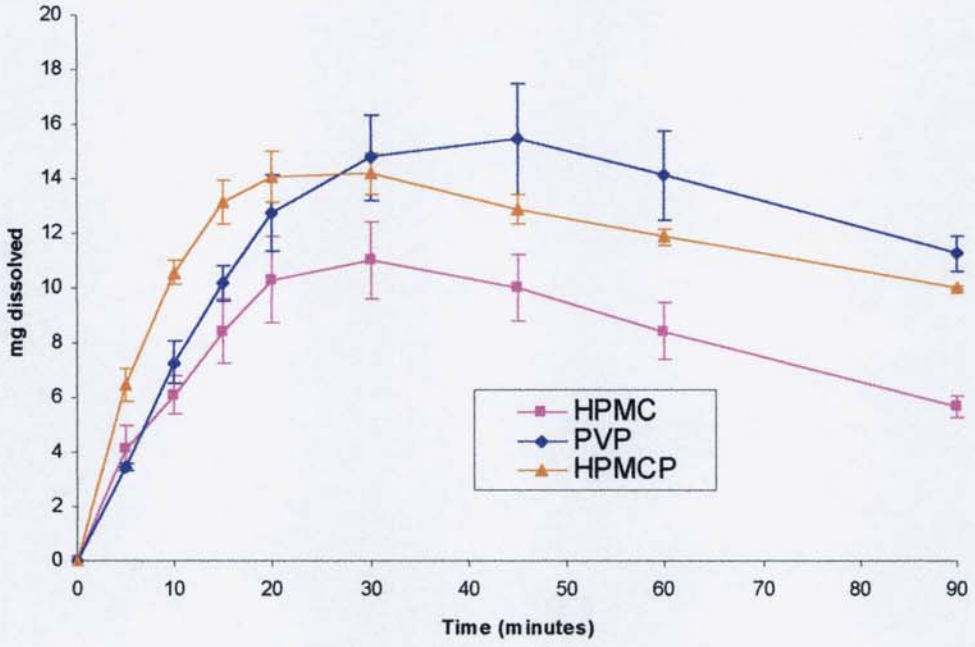

Figure 3-52 Dissolution of troglitazone from 50% (w/w) dispersions at 25 rpm. Results are the mean of three replicates, error bars ± SD

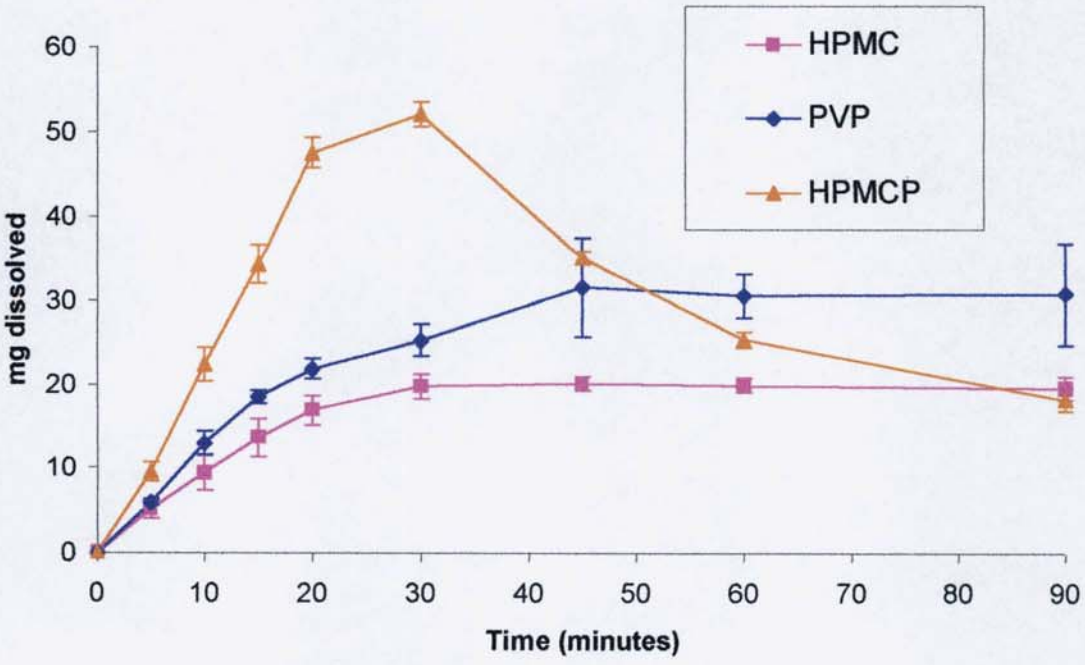

Figure 3-53 Dissolution of troglitazone from 91% (w/w) dispersions at 25 rpm. Results are the mean of three replicates, error bars ± SD

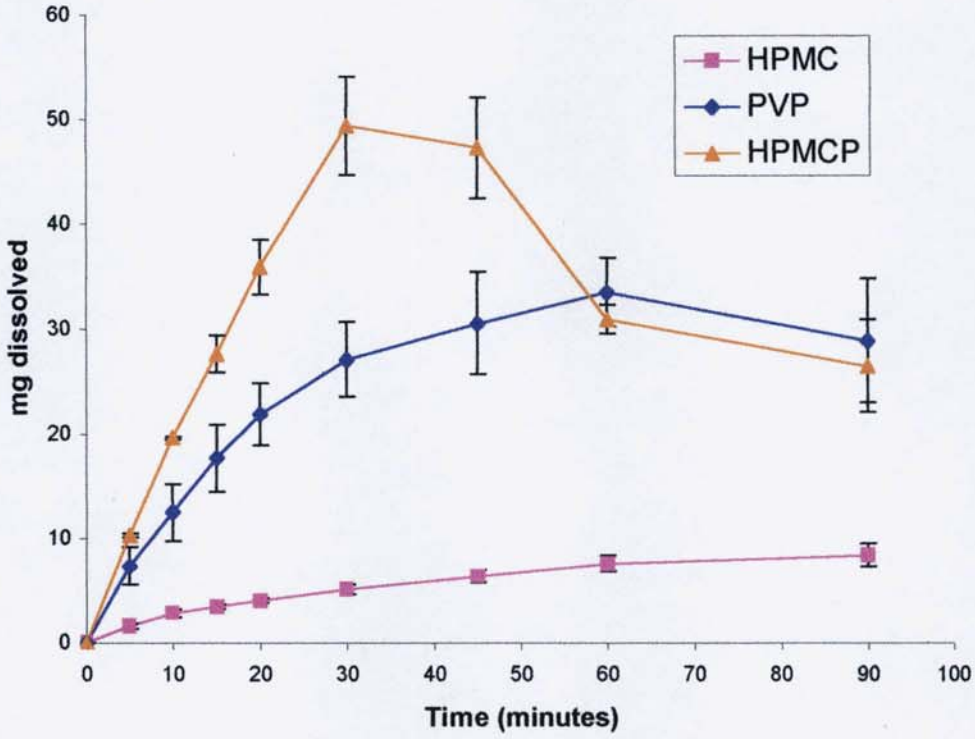

Figures 3-51, 3-52 and 3-53 show the dissolution profiles for troglitazone from the 9%, 50% and 91% dispersion (all polymers), when a paddle speed of 25 rpm is employed. It is seen from these figures that even at 25 rpm, the dispersions still enhance the dissolution of troglitazone, and each polymer has a different effect upon the dissolution of troglitazone. Table 3-43 shows the AUC data (at 20 and 90 minutes) and the maximum level of drug dissolved. From these data, a rank order for each parameter can be derived, and compared with the rank orders of these parameters derived from the dispersions from the 75 rpm dissolution test (chapter 3).

It is noticeable from the rank orders, shown in table 3-44, that there are some differences in the orders when comparing the dissolution of the dispersions at 25 rpm to 75 rpm. The main differences are that, at 75 rpm, the HPMC (50%) dispersion has more drug dissolved after 20 minutes than PVP (91%), and that the AUC_{20} for HPMCP (9%) lowest at 75 rpm, whereas it is the highest at 25 rpm. The resulting Tukey analysis of the dispersions showed that there is no significance in these changes in the order of the AUC_{20} (table 3-45).

Table 3-43 AUC_{20} and AUC_{90} and C_{max} data for the dissolution of the dispersions at 25 rpm (Results are the mean of three replicates, error bars ± SD)

Polymer in dispersion	Polymer concentration	AUC_{20} mg.ml.min	AUC_{90} mg.ml.min	M_{max} (mg)
HPMC	9%	118.90 ± 7.73	714.47 ± 58.58	11.01 ± 1.42
	50%	182.74 ± 25.16	1555.59 ± 84.18	20.07 ± 0.79
	91%	48.87 ± 4.76	521.83 ± 37.75	8.33 ± 1.08
HPMCP	9%	185.59 ± 9.04	1039.99 ± 34.79	14.18 ± 0.75
	50%	449.44 ± 54.45	2705.53 ± 102.55	51.97 ± 3.38
	91%	376.79 ± 19.89	2971.70 ± 183.19	49.58 ± 4.39
PVP	9%	136.40 ± 4.31	1103.90 ± 84.18	15.44 ± 2.04
	50%	240.84 ± 9.88	2288.89 ± 211.19	31.61 ± 5.98
	91%	215.61 ± 52.52	2304.67 ± 246.25	33.41 ± 3.25

Table 3-44 Comparison of the rank order between the AUC_{20} for the dissolution of the dispersions at either 20 rpm or 75 rpm (data for 75 rpm samples found in table 3-2)

AUC_{20} for the dispersion at 25 rpm	**AUC_{20} for the dispersions at 75 rpm**
1. HPMCP (50%)	1. HPMCP (50%)
2. HPMCP (91%)	2. HPMCP (91%)
3. PVP (50%)	3. PVP (50%)
4. PVP (91%)	4. HPMC (50%)
5. HPMC (50%)	5. PVP (91%)
6. HPMCP (9%)	6. PVP (9%)
7. PVP (9%)	7. HPMC (9%)
8. HPMC (9%)	8. HPMCP (9%)
9. HPMC (91%)	9. HPMC (91%)

Table 3-45 Results of the Tukey analysis comparing the rank order for the AUC_{20}

	p-value (25 rpm)	p-value (75 rpm)
PVP (91%) v HPMC (50%)	>0.05 (not significant)	>0.05 (not significant)
HPMCP (9%) v PVP (9%)	>0.05 (not significant)	>0.05 (not significant)
HPMCP (9%) v HPMC (9%)	>0.05 (not significant)	>0.05 (not significant)

Table 3-46 Comparison of the rank order between the AUC_{90} for the dissolution of the dispersions at either 25 rpm or 75 rpm

AUC_{90} for the dispersion at 25 rpm	**AUC_{90} for the dispersions at 75 rpm**
1. HPMCP (91%)	1. PVP (50%)
2. HPMCP (50%)	2. HPMC (50%)
3. PVP (91%)	3. PVP (91%)
4. PVP (50%)	4. HPMC (9%)
5. HPMC (50%)	5. HPMCP (50%)
6. PVP (9%)	6. HPMCP (91%)
7. HPMCP (9%)	7. HPMC (9%)
8. HPMC (9%)	8. HPMCP (9%)
9. HPMC (91%)	9. HPMC (91%)

The differences in the rank order, between the 75 rpm and 25 rpm, for the AUC_{90} is far more pronounced than for the AUC_{20}. The main difference is in the performance of the HPMCP (50% and 91%) dispersions; at 75 rpm it is noticeable that these dispersions are low in the rank order, whereas at 25 rpm they rank highly. This is due to the precipitation of the troglitazone after the dissolution of the HPMCP dispersions at 50% and 91%. At 75 rpm, the precipitation occurs after only 15 minutes of the dissolution test, whereas at 25 rpm precipitation begins after 30 minutes. Also, at 75 rpm the 50% HPMCP dispersion (for example) undergoes a decrease of 84% of the amount of drug in solution, whilst the 25 rpm the decrease is only 64%. This means that the impact of the precipitation of the drug on the AUC_{90} for the HPMCP 50% and 91% dispersions tested at 25 rpm is not as significant as in those dispersions

tested at 75 rpm.

The implications of these findings are that, although the use of FaSSIF is capable of providing a discriminatory test regardless of the paddle speed, *i.e.* differences can be seen between dissolution profiles regardless of paddle speed, some care has to be taken, with regards to solid dispersions, as to whether the results are relevant. This is because over ninety minutes the rank order of the AUC_{90} for the dispersions undergoing dissolution at 25 rpm shows differences to that of that at 75 rpm. The changing of the paddle speed also has another implication. It is shown in figures 3-54 to 3-56 that changing the paddle speed has a significant impact upon the dissolution of the dispersion, with the slower speed having an almost 100-fold lower AUC_{90}. This then poses the question as to which paddle speed is representative of the dissolution occurring *in vivo.* It was stated by Dressman *et al.* (1998) that the motility of the GI tract is highly variable and that it is very unlikely that a single paddle speed would be able to completely simulate the motility of the GI tract. Work has been performed Katori *et al.* (1995) to optimise a dissolution method for a product by altering the paddle speed. It was shown in the work by Katori *et al.* (1995) that a very low paddle speed of 10 rpm was required to mirror the *in vivo* performance of the formulations. However, Nicolaides *et al.* (2001) achieved a good correlation between the *in vitro* dissolution, of a series of drugs, with the *in vivo* performance, using a paddle speed of 100 rpm. These two studies highlight the difficulties in developing an *in vitro* dissolution test that thoroughly represents the *in vivo* performance of a formulation. It is, therefore the recommendation that animal bioavailability studies would still be required on a selection of formulations, for example one dispersion from each polymer class in order to cover any differences (*i.e.* the effect of an enteric polymer) that could be possible between the polymers *in-vivo.* Then using the *in vivo* data in conjunction with a model, such as developed in section 4.5, and a series of *in vitro* dissolution tests at different paddle speeds, a paddle speed that would represent the *in* vivo dissolution could be found.

Figure 3-54 Comparison of the AUC_{90} for the HPMCP dispersions. Results are the mean of three replicates, error bars ± SD

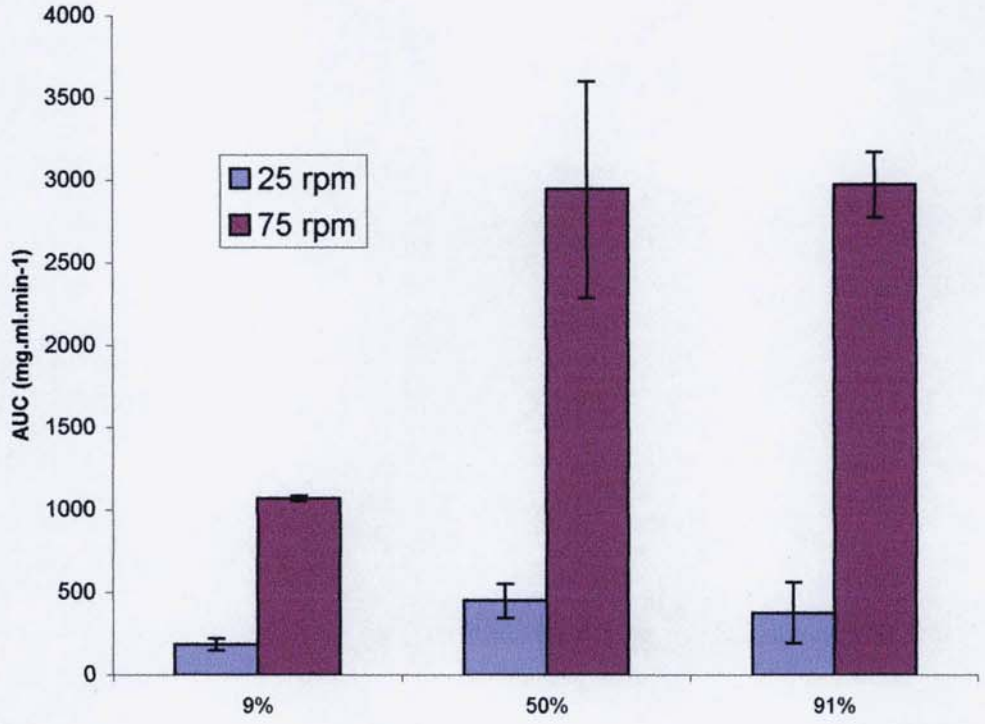

Figure 3-55 Comparison of the AUC_{90} for PVP dispersions. Results are the mean of three replicates, error bars ± SD

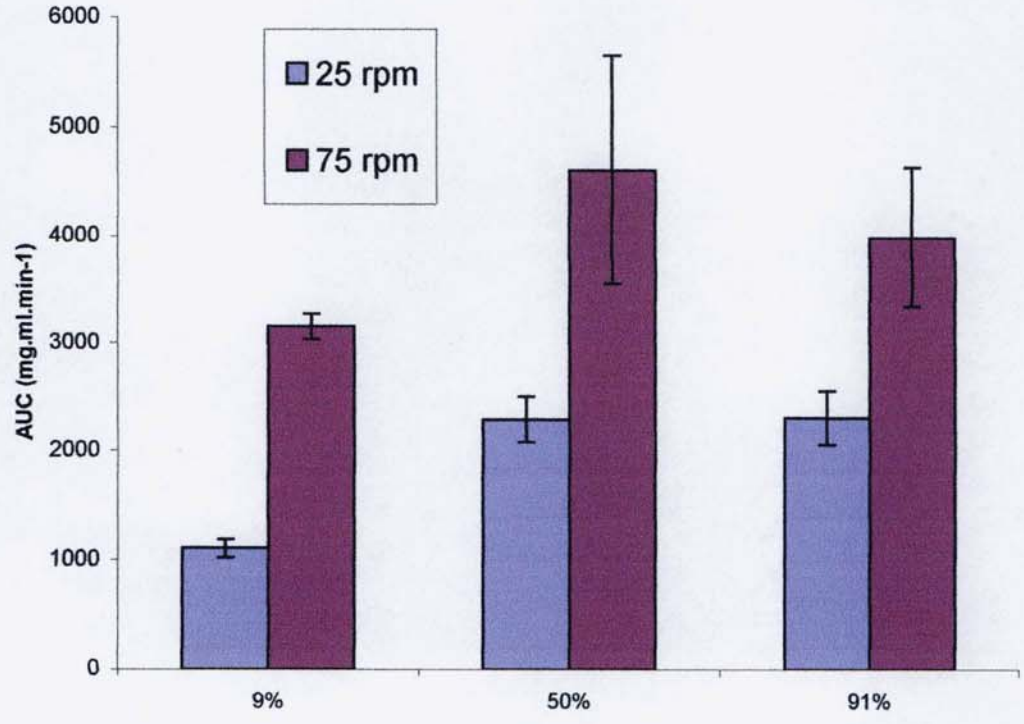

Figure 3-56 Comparison of the AUC_{90} for HPMC dispersions. Results are the mean of three replicates, error bars ± SD

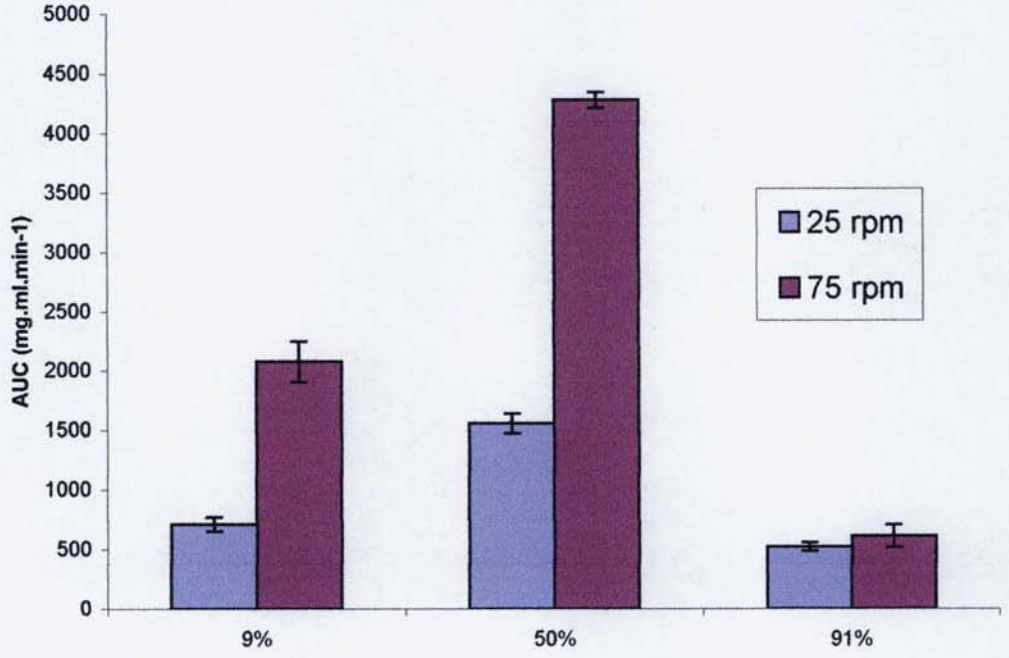

It is evident from figures 3-54, 3-55 and 3-56 that reducing the paddle speed from 75 rpm to 25 rpm has reduced the dissolution of troglitazone from the solid dispersions. This observation was not wholly unexpected, as it has been shown for griseofulvin:xylitol solid dispersion that the dissolution rate reduced when the paddle speed was reduced (Sjökvist and Nyström 1990). Work performed by Kukura *et al.* (2004) into the hydrodynamics of the apparatus II dissolution vessel can help explain these observations. This study found that increasing the paddle speed from 50 rpm to 100 rpm, for apparatus II, increased the magnitude of the strain rates experienced by the dissolution medium, it is these shear forces that control the thickness of the boundary layer thickness (*i.e.* the factor that controls the mass transfer from the dosage form to the bulk media). It is found that high strain rates lead to a thinner boundary layer. Application of this information, along with the carrier-controlled mechanism proposed by Craig (2002) allows some understanding as to why the dissolution of troglitazone from a solid dispersion will be

reduced by a slower paddle speed. In the instance of slow paddle speed, the transfer of polymer from the bulk particle to the bulk solution phase would be slower, due to the thicker boundary layer, thus the release of the drug into the bulk solution would be slower. However, the findings in this study contradict the prediction proposed by Craig (2002), whereby more rapid paddle speeds would favour drug-controlled dissolution. The drug-controlled mechanism still predicts that the dissolution of the drug will be enhanced compared to the drug alone, but not as much as the carrier-controlled model. It is felt that it may require an extreme paddle speed (*i.e.* 200 rpm) to induce this possible mechanism, as it would require a very fast transfer of polymer to the bulk liquid phase. In the case of the dispersions with high drug loading, the reduction in dissolution can be explained by the mechanism proposed by Ford (1986). In this mechanism (part d in figure 3-35) the drug forms a drug-rich boundary layer through leaching of the drug, at a lower paddle speed this layer will be thicker than at a higher paddle speed, as the transfer of drug to the bulk liquid phase would be slower.

4 Simulating and modelling the passage of the dispersion from the stomach into the intestine

4.1 The development of an *In vivo In vitro* Correlation (IVIVC)

The establishment of an IVIVC is of importance to the pharmaceutical industry from a quality perspective, as the *in vitro* test can then be used as a predictor of the *in vivo* performance of a drug. It is stated by the FDA that it is possible, for a class II drug (BCS), for an IVIVC to be developed (FDA, 1997). It is outlined in the USP XXIII Chapter <1088> that there are three levels of correlations: A, B and C.

Level A correlation: This is a predictive mathematical model for the relationship between the entire *in vitro* dissolution and the entire *in vivo* response, such as the plasma-time curve (Young *et al.* 1997).

The level B correlation: This is a predictive mathematical model that relates a particular *in vitro* parameter to that of an *in vivo* parameter, *e.g.* the dissolution rate constant to the absorption rate constant (Young *et al.* 1997).

The level C correlation: This is a predictive mathematical model that relates the amount of drug dissolved *in vitro* at a particular time to a pharmacokinetic parameter that characterises the *in vivo* performance, *e.g.* C_{max}(Young *et al.* 1997).

The guidelines for the development of an IVIVC are outlined in the USP that at least three batches, which differ in *in-vivo* performance, are available. Modification of the *in vitro* dissolution test is then performed so that those differences experienced *in vivo* are found *in vitro*.

As shown in the modified Noyes Whitney equation (section 1.2.4), the dissolution of drug is affected by several parameters: hydrodynamics of the medium, solubility in the medium and the volume of the medium. These parameters are important for the design of dissolution tests aiming at predicting *in vivo* performance (Dressman *et al.* 1998; section 1.4.4).

Alteration of the hydrodynamics of a dissolution test can be achieved by changing the paddle/basket speed. In order to achieve the maximum discrimination between samples it is suggested that mild agitation conditions should be employed for dissolution tests (Dash *et al.* 1988). A paddle speed of 50 rpm is considered to be sufficiently low agitation for a discriminating dissolution test (FDA, 1997).

The composition of the dissolution medium has also been shown to have an effect upon the discriminatory nature of the dissolution test. Dissolution of two different commercial formulations (Euglucon N® and Glukovital®), which show different *in vivo* performance, of glibenclamide (a BCS class II drug) in various dissolution media was carried out to assess which parameters affected discrimination of differences in dissolution (Löbenburg *et al.*, 2000). In the study by Löbenburg *et al.* (2000) the following media were investigated for the establishment of an IVIVC: compendial simulated intestinal fluid (SIF) (a pH 7.5 buffer without pancreatin), FaSSIF (see section 1.4.3), FeSSIF (see section 1.4.3), $FaSSIF_{slt}$ (FaSSIF with the taurocholate and lecithin removed), $FeSSIF_{slt}$ (FeSSIF with the taurocholate and lecithin removed), simulated gastric fluid (SGF) (a pH 1.5 buffer) and a pH 6.0 phosphate buffer. It was found that the FaSSIF medium provided the best correlation between the *in vitro* parameters and the *in vivo* parameters. This could be due in part to the osmolarity of the FaSSIF, it has been shown by Lane *et al.* (2006) that there is a strong link between the osmolarity of medium and the diffusion rate of a drug. It was shown that the osmolarity of FaSSIF was within the expected physiological range. Another instance where the dissolution medium has shown to be effective in discriminating between the *in vivo* performance by *in vitro* methods is in the instance of danazol tablets. Danazol shows enhanced *in vivo* absorption when it is administered in the fed state over the fasted state; the Cmax is approximately three-fold higher in the fed state. The *in vitro* dissolution was performed in four dissolution media FaSSIF, FeSSIF, compendial SIF, and water. The FaSSIF and FeSSIF fluid predicted the three-fold difference found *in vivo*. It was shown that almost no dissolution occurred in the compendial medium and water; therefore no discrimination

was measured (Dressman and Reppas 2000).

4.2 Dissolution of pharmaceuticals in the gastric fluids

As the first environment any orally delivered formulation encounters is the comparatively acidic gastric fluid, it is important to consider the effects that exposure to this environment will have on the dissolution. Various media have been used in an attempt to simulate gastric fluid, including the USP gastric medium (USP XXIII). This is a pH 1.5 buffer, thus simulating only the expected pH of the gastric medium, so therefore not taking into account the potential for gastric medium to contain surface-active compounds. The surface tension of sampled gastric fluid is between 35 – 45 $mN.m^{-1}$ (Dressman *et al.* 1998), whereas USP dissolution medium has a surface tension of >70 $mN.m^{-1}$. This, therefore, confirms the presence of a surface tension lowering agent within the gastric fluid. It was originally thought that this reduction in surface tension was due to refluxed bile salts, found in concentrations between 0 – 1 mM, from the intestinal media. There was, however, no correlation between surface tension, bile salt concentration and pH. This, therefore, indicates that the lower surface tension in the gastric fluid is not due to the refluxed bile salts alone (Efentakis and Dressman, 1995).Work performed by Vertzoni *et al.* (2005) showed that is likely that the presence of pepsin in the stomach lowers the surface tension of the gastric fluid.

Since the development of the Biopharmaceutics Classification System, the impetus to develop physiologically meaningful dissolution media has increased (Luner and VanDer Kamp 2001). It is expected that, for poorly soluble drugs, a dissolution medium that is physiologically relevant will give more meaningful results for IVIVIC determination. In the accepted compendial gastric medium there are no surface-active agents present, therefore the enhanced wetting that would be expected in gastric fluids is not experienced in the compendial dissolution medium. This means that the dissolution of sparingly soluble drugs is underestimated in compendial media. One way of attempting to simulate the wetting effects of gastric medium is to reduce the surface tension of the compendial medium. In recent years,

various gastric media have been proposed utilising various surfactants in order to reduce the surface tension to physiological levels; Sodium Dodecyl Sulphate (SDS) (Dressman *et al.* 1998), and Triton® X-100 (Galia *et al.* 1999) are some examples.

There is some evidence to suggest that the selection of surfactant for the dissolution media would have to be on a product-to-product basis. This is in part due to evidence that suggests that different surfactants have different abilities to wet drugs. Studies examining the contact angle of various surfactants upon a compressed model drug showed a lot of variability in the contact angles at the appropriate surface tension ($40mN.m^{-1}$) (Luner *et al.* 1996). It has also been stated that within dosage forms there are other factors that can mask the wetting effects of the surfactant, such as drug particle size, excipient type, surfactant concentration, thus making it difficult to understand how well a surfactant works with a particular drug (Itai *et al.*1985).

More recently studies have been undertaken that have investigated the possible use of the natural bile salts found in the gastric fluids as wetting agents. One study suggested that the wetting effects of freshly sampled gastric juice, from volunteers, showed, at a given surface tension, a difference in wettability compared to mixtures of just bile salts (Fell and Mohammad 1995). This, therefore, supported the observations made by Efentakis and Dressman (1995) that it is not just purely the bile salts that are lowering the surface tension. A recent study involved several media using taurodeoxycholic acid as the bile salt and incorporated phospholipids at physiological relevant concentration. The following parameters were then compared against media that have been previously suggested in the literature; surface tension, contact angle and adhesion tensions. It was found that for the surfactants complete wetting was achieved (contact angle = 0), whilst for the physiologically relevant media reduced contact angles were recorded but not to the same extent as the surfactants. It was therefore postulated that a surfactant system could result in different wetting abilities than would result *in vivo*. Therefore, it is considered that the use of a surfactant-based gastric medium would have to be developed on a surface

tension basis, and compared to bio-relevant dissolution media.

Recently another medium has been proposed for simulating gastric fluids that is based upon FaSSIF, called the fasted state simulated gastric fluid (FaSSGaF) (Vertzoni *et al.* 2005). This dissolution medium was developed to simulate the reduction of the surface tension using a combination of taurocholate, lecithin and pepsin. When compared to the media discussed earlier in this section (gastric media with either Triton® x-100 or gastric) it was found to give a slower dissolution rate and less of a plateau. This, therefore, gave the conclusion that using artificial surfactants can lead to an over estimation of the dissolution. This fluid consists of the following constituents:

Table 4-1 Composition of FaSSGaF (reproduced from Vertzoni *et al.* 2005)

Constituent	Concentration
NaCl	0.03 M
HCl	qs pH 1.6
NaTaurocholate	80 µM
Lecithin	20 µM
Pepsin	0.39 AU/L
Distilled water	qs 1L
Surface tension = 40 mN/m	

4.3 Evaluation of surfactants in gastric media

4.3.1 Introduction

In section 4.2, it was shown that two different surfactants have been proposed in the literature as constituents in gastric media: SDS, and Triton® X-100, with USP gastric medium. As very little published data is available comparing these media during dissolution, it was the intention to compare the influence of these media upon the dissolution of troglitazone. Pure troglitazone was chosen over the solid dispersion of the drug as it was the intention of the study to compare the effects of the different media upon a sparingly soluble drug with severely limited solubility due to the low pH (pK_a = 6.1), rather than a dispersion which is relatively soluble.

4.3.2 Experimental

4.3.2.1 Materials

Sodium dodecyl sulphate, Triton® X-100, and hydrochloric acid were obtained from Aldrich (Poole, UK). All other materials as described in section 2.2.2.1.

4.3.2.2 Equipment

Dissolution was performed using the equipment described in section 2.6.1.2. Analysis was performed on the HPLC system described in section 2.2.2.2.

4.3.2.3 Method

The USP gastric medium was prepared as described in the USP. For the preparation of the media containing a surfactant the pH 1.5 buffer was prepared, and to this the appropriate amount of surfactant was added. For the Triton® X-100 a concentration of 0.1% w/v was used (Galia *et al.* 1999), and for the SDS the concentration was 2 g/l (Dressman *et al.* 1998). The concentration of SDS and Triton® X-100 in the dissolution media was chosen because it is at this concentration where the surface tension of the media is similar to that found physiologically (Dressman *et al.* 1998, Reppas and Dressman 2000). FaSSGaF was prepared using the ingredients and concentrations described in section 4.2.

Dissolution was performed using the method described in section 2.6.1.3 with 200 mg of troglitazone added to the medium.

HPLC analysis was performed as described in section 2.2.2.3.1 or 2.2.2.3.2.

Rates derived from the polynomial curve fit (from 0-30 minutes) were used to compare the data, this was calculated as described in section 3.1.3.6.

4.3.3 Results and discussion

It would be expected that in an *in vivo* situation the dissolution of troglitazone in the gastric fluids would be severely limited due the acidic conditions that would be present. This is because, as stated in section 1.5.1, troglitazone is a weakly acidic drug, with a pK_a of 6.1. This would mean that it would be

expected that the solubility of troglitazone in the fasted state intestinal fluids (pH approximately 6.5) would be higher than in the fasted state gastric fluid (pH approximately 1.5), if pH was the only parameter considered. In section 1.2.2.2, wetting by natural surfactants was proposed as one of the other parameters which affects the solubility of a drug within the GI tract. It was also stated that the level of surfactant is higher in the intestinal fluids, than in the gastric fluids. This, therefore, means that troglitazone would be expected to have a faster dissolution rate in the simulated intestinal media than in the gastric medium. Comparison of the dissolution of troglitazone in FaSSIF with that in the gastric media containing Triton® X-100 and SDS (figures 4.1, 4.2 and table 4.1) show this to not be the case. It is found that the dissolution of troglitazone in the gastric medium is faster, and more complete than in FaSSIF. Tukey analysis of the dissolution rates of troglitazone in the three media containing surfactants showed that the difference between the dissolution of troglitazone in the SDS media compared to the Triton® X-100 is insignificant ($p>0.05$).

Figure 4-1 Dissolution of troglitazone in various gastric media. Results are the mean of 3 replicates ± standard deviation

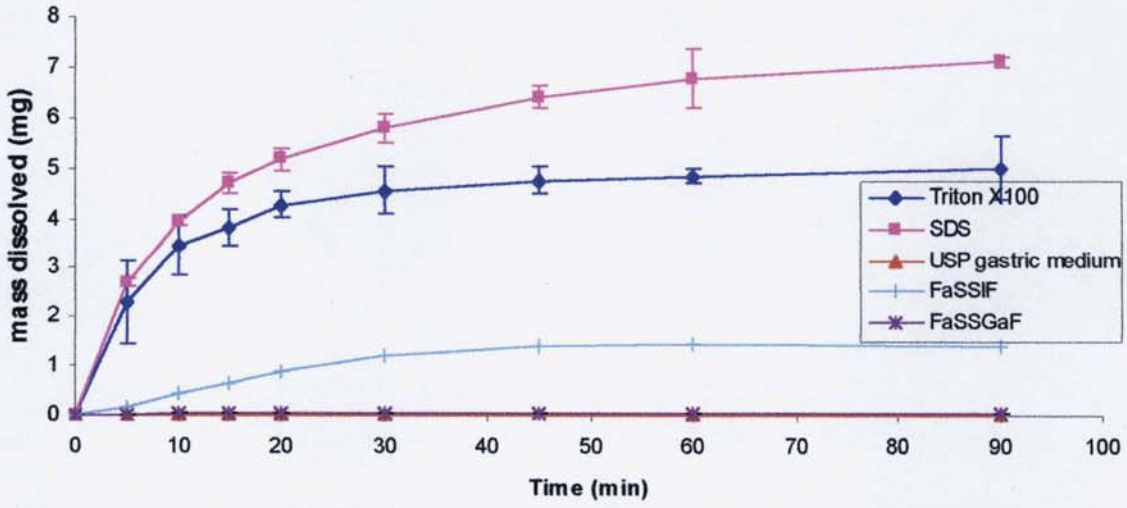

These results support the contact angle data that was obtained by Dressman *et al.* (1998), where the solutions containing the artificial surfactants showed complete wetting, whereas the natural bile salts did not display complete wetting.

Table 4-2 Polynomial rates for troglitazone in a range of gastric media (mean of 3 replicates ± S.D.)

Dissolution media	Polynomial rate (mg/min)
USP gastric fluid	0 ± 0
Triton® X-100	0.550 ± 0.188
SDS	0.628 ± 0.010
FaSSIF	0.323 ± 0.008
FaSSGaF	0.016 ± 0.001

It is also shown by the results in figure 4.1 and table 4-2 that there is a significant difference between the dissolution rates of troglitazone in the SDS medium and the Triton® X-100 medium, $p<0.05$. This indicates that the medium with SDS was superior in wetting troglitazone than that made up with Triton® X-100. It is shown in the results above, though, that obtaining a physiological relevant surface tension is not the only factor to consider when developing a physiologically relevant gastric fluid. It is felt that the differences experienced between the Triton® X-100 and the SDS media is due to the SDS being more efficient at wetting troglitazone. Work performed by Luner *et al.* (1996) shows that even though the surface tension is the same for two surfactant solutions there are other parameters that are different. It was found in this study that at a surface tension of 40 mN/m the SDS lowered the contact angle of the solution with a sparingly soluble drug more than Triton® X-100. This signifies that, in the case of the drug in the study, there is more complete wetting when SDS is used. It was also found that the SDS had higher adhesion energy than the Triton® X-100, at the same surface tension, it was concluded from this that the SDS would be more preferentially absorbed at the solid-liquid phase rather than the air liquid-phase. As outlined in section 1.2.2.2 the absorption of surfactant to a powder reduces the contact angle, and therefore allows more complete wetting. This pattern, lower contact angle and higher adhesion energy (for SDS) at the same surface tension, was also found to exist when Parafilm® (found to have similar properties to paraffin (Zografi and Yalkowsky (1974)) was used instead of a sparingly soluble drug.

The results in this study show that care should be taken when selecting/developing a gastric media for the purpose of developing a biorelevant dissolution test. It is seen that using either SDS or Triton® X-100 could vastly overestimate the dissolution of a drug in the gastric medium if used. It is recommended from these results that natural bile salt, such as taurocholate, and pepsin should be used to lower the surface tension of the media.

4.4 *In vitro* method for the simulation of a drug passing from the gastric to the intestinal fluids

4.4.1 Introduction

It was shown in section 1.1.3 that upon ingestion of an orally delivered dosage form, the first region encountered is the gastric region. The discussion in sections 1.1.1 and 1.1.2 show that conditions encountered in this region are very different to those in the small intestine. Such differences are the pH (generally between pH 1-2 in the gastric region and between pH 5-7 in the small intestine), the level of natural bile salts (higher in the intestine) and the amount of fluids (again higher in the intestine). In section 3.1 the dissolution was carried out only in FaSSIF, with no consideration of the effect that the prior exposure to a low pH environment could have upon the performance of these dispersions.

Kondo *et al.* (1994) prepared solid dispersions of a poorly soluble drug with the enteric polymer HPMCP (HP-55). To investigate the ability of the polymer to protect the drug from conditions in the gastric region, a pH-shift dissolution method was utilised. This involved the dissolution of the solid dispersion in a pH 1.2 medium. After one hour a pH-adjusting solution of potassium di-hydrogen phosphate and sodium hydroxide was added to adjust the pH to 6.5. Over the first hour, no dissolution was observed, showing that the enteric polymer inhibited the dissolution of the drug at this low pH. Following addition of the pH-adjusting solution the formulation dissolved. When the dissolution curves of the samples that were exposed to the low pH prior to dissolution at

6.5 were compared to those samples that underwent dissolution at pH 6.5 was no differences seen in the dissolution profiles. This shows that the enteric polymer inhibited release of the drug into the pH 1.2 buffer. Subsequent animal studies showed that there was almost complete absorption of the drug. This investigation involved the use of pharmacopoeial dissolution media, so there was no appreciation for the effect of the bile salts, and it was performed at a constant volume (500 ml) so it did not represent biorelevant volumes.

The FDA also have scope for the use of dissolution being performed in two different media, known as two-tiered dissolution tests (FDA, 1997). This involves performing a dissolution test within a gastric medium, then at the prescribed time, the dosage form is removed from the media and transferred to an intestinal medium. This method is only really used in special cases, to investigate the quality of an enteric coating for example. This sort of method has some limitations; one of these is that it is only really suitable for the dissolution of dosage forms that would not be expected to disintegrate within the gastric fluid, and also it would not be suitable for the dissolution of free powders.

To develop a model for gastric to intestinal dissolution test there are a number of parameters that need to be considered, in order to make it both realistic and easy to use. The four main parameters that have been identified are the composition of the gastric juice (for a full discussion on the composition of gastric and intestinal fluids see sections 4.2 and 1.4.3 respectively), the rate at which the intestinal fluid is to be added, the volume of gastric medium to be used, and length of time the dispersion is incubated in the gastric media. These parameters were identified by Dressman *et al.* (1998), as those that should be considered for the development of a dissolution test for the prediction of *in vivo* dissolution.

The volume of fluid available for the dissolution of drugs has been shown to be dependent upon the volume of fluid co-administered with the dosage form, secretions and water flux across the gut wall. When in the fasted state, the volume of fluid within the stomach can be as little as 20 – 30 ml. For most bio-

availability studies, with oral dosage forms, the average amount of fluid co-administered is about 200 – 300 ml (Dressman *et al.* 1998). It should, therefore, be considered that to fully represent the dissolution of a drug in the stomach a volume of 250 – 350 ml should be employed. Perfusion studies performed by Dillard *et al.* (1965) upon the small intestine, in the fasted state, showed that at any time there was between 150 – 350 ml of intestinal fluid. It therefore follows that, for a bio-relevant dissolution test, a volume of between 400 – 700 ml should be employed; it has been recommended by Dressman *et al.* (1998) that a volume of 500 ml should suffice for examining dissolution in the fasted state.

For the selection of a suitable gastric fluid the following exclusion criteria were applied: the gastric fluid should not affect the dissolution in the FaSSIF fluid, and the dissolution of troglitazone should be lower than found in the FaSSIF fluid. The rationale behind the criteria is that certain gastric media may enhance the dissolution of the drug in the FaSSIF (*e.g.* the addition of a strong surfactant), thus any comparison with the dissolution in the FaSSIF alone is not significant. As troglitazone is a weakly acidic drug it can be expected that there will be less dissolved in the gastric fluid than in the FaSSIF, due to the acidic nature and the lower surfactant level found in the gastric medium. One of the major issues with selecting a gastric fluid was its compatibility with the FaSSIF fluid. The exclusion criteria (section 4.1.2) stated that the gastric medium should not contain any different component to the FaSSIF that will have a significant impact on the eventual dissolution in the FaSSIF. The gastric medium contains one component that is not in the FaSSIF (excluding the HCl), and that is pepsin. The concentration of pepsin used was because it aided the lowering of surface tension of the simulated gastric fluid to the physiological level (Vertzoni *et al.* 2005).

The following considerations should be made when determining the duration of each stage of dissolution: whether the drug is to be administered in the fed state or the fasted state, and the place of optimal absorption within the GI tract (Dressman *et al.* 1998). It was discussed in section 1.1.1.4 that the emptying pattern of the stomach is dependent upon whether there is the presence of

food. The emptying of saline solutions from the stomach was investigated by Oberle *et al.* (1990). It was found to be dependent upon the motility phase for the stomach. The shortest residence times were when the stomach was in phase III ($t_{0.5}$ = 5 min (for 200 ml)), and the longest was phase I ($t_{0.5}$ = 23 min (for 200 ml)). Hunter *et al.*, (1982) found that the residence time for dosage forms of various particle sizes (1 mm – 14 mm) during the fasted state ranged from 15 – 420 min. Dressman *et al.* (1998) recommended for drugs that are administered in the fasted state, and absorbed readily in the upper small intestine a time of 30 minutes should be sufficient for a bio-relevant dissolution test in gastric medium. The transit time of a dosage form through the small intestine has been shown to be independent of the state of the GI tract (i.e. fasted or fed), and dosage form (i.e. solution or tablet) (Malagelada *et al.*, 1984). Davis *et al.* 1986 showed that the average transit time within the small intestine is between 3 – 4 hours, independent of dosage form. These results account for transport throughout the whole small intestine and not all areas are suitable for absorption. Dressman *et al.*, (1998) recommends that a time of 60 minutes should be adequate, as this allows 1-2 hours for absorption.

4.4.2 Experimental

4.4.2.1 Materials

Pepsin was supplied from Sigma Aldrich (Poole, UK). See sections 2.2.2.1, 2.4.2.1 and 2.6.1.1 for details of the materials used. Solid dispersions used in this study were as follows:

Troglitazone: 50% PVP
50% HPMCP
50% HPMC

4.4.2.2 Equipment

Dissolution was performed using the equipment described in section 2.6.1.2. Analysis was performed on the HPLC system described in section 2.2.2.2.

4.4.2.3 Method

Prior to the exchange method

- Volume selection

Dissolution was performed as described in section 2.6.1.3, with the exception that for one test the dissolution bath was set up to use only 250 ml of dissolution medium.

HPLC analysis was performed as described in section 2.2.2.3.2

- Composition of gastric fluid

Dissolution was performed as described in section 2.6.1.3. FaSSIF was prepared with (at 0.295 AU/L) and without pepsin.

HPLC analysis was performed as described in section 2.2.2.3.1

For the exchange method

For the first 30 minutes dissolution was undertaken as described in 4.4.2.3 (volume selection with 250 ml of FaSSGaF). After 30 minutes 250 ml of a concentrated form of FaSSIF was added to the dissolution vessel. The pH of one dissolution vessel for each run was tested to ensure that the pH was between 6.4 – 6.6. Dissolution was then carried out as described in section 2.6.1.3. HPLC analysis was carried out as described in sections 2.2.2.3.1 (for the intestinal phase) and 2.2.2.3.2 (for the gastric phase).

4.4.3 Results and discussion

Figure 4-2 shows the profiles obtained for the dissolution of troglitazone in FaSSGaF at 500 ml and 250 ml. Due to the difference in volume it is felt appropriate to compare the concentration in mg/ml at each time point. The result of the f2 test gave a value of 64.5 (spreadsheet found in appendix 4). This, therefore, indicates that the dissolution profiles can be considered similar (FDA 1997). It is therefore appropriate to use only 250 ml to simulate the dissolution in the gastric fluid.

Figures 4-3 shows the comparative dissolution of troglitazone from a 50% PVP dispersion in FaSSIF with and without pepsin. A dispersion of 50% was selected as at this concentration the effects of the polymer were neglible (*i.e.* with the 83% and 91% dispersions the dissolution was seen to be impeded),

whilst at the same time giving a high level of dissolution compared to the dispersions with low polymer loading. It was felt inappropriate to use any of the HPMCP dispersion to do this test, as only three data points can be used on the HPMCP dispersions for a f2 test, due to the re-crystallisation, which is not nearly enough. The inclusion of pepsin had little effect upon the dissolution of troglitazone from the 50% PVP dispersion, the f2 = 85.4 and the profiles were said to be similar.

Figure 4-2 Dissolution of troglitazone in 250 ml and 500 ml of FaSSGaF. Results are the mean of three replicates, error bars ± SD.

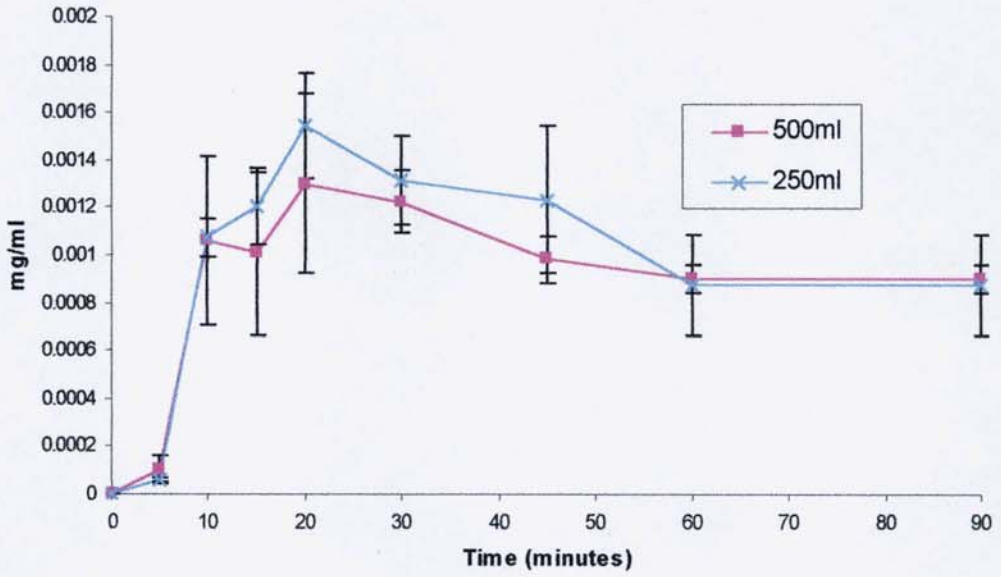

Figure 4-3 The dissolution of troglitazone from the 50% PVP dispersion in FaSSIF containing pepsin and FaSSIF without pepsin. Results are the mean of three replicates, error bars ± SD

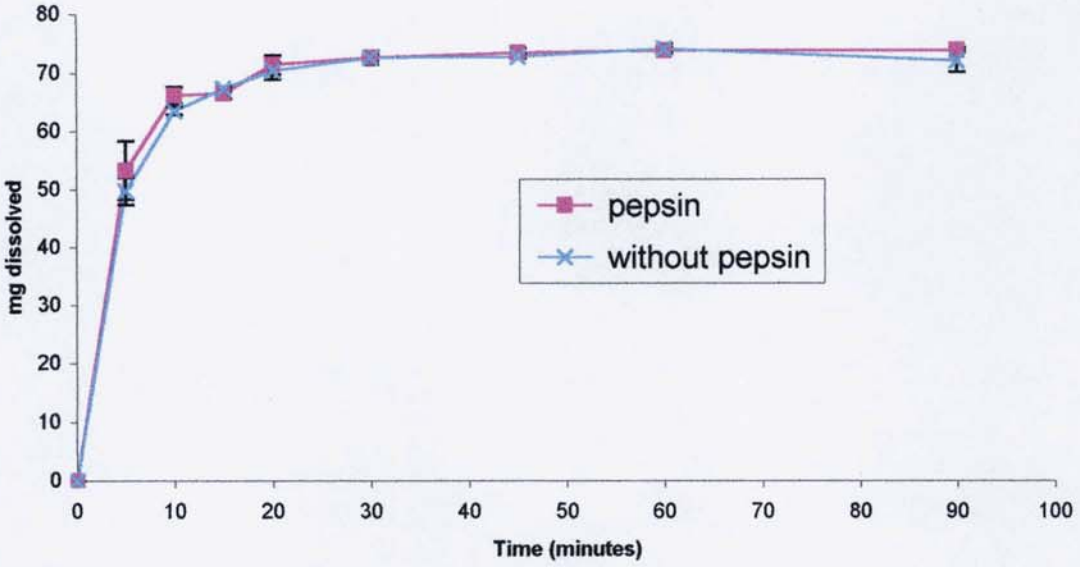

The data obtained from the exchange experiment; shown in figure 4-4 (it should be noted that the concentration is recorded in mg/ml in order to compensate for the volume difference found between the gastric and intestinal media, show that even after exposure to gastric fluid, each solid dispersion still attains a higher dissolution than that of the troglitazone. This indicates that exposure to the gastric fluid has little impact on dissolution, even if the dispersion is formed with the gastro-soluble polymers. The degree of enhancement obtained (section 3.1.3.2), in FaSSIF, is lower if the dispersions are exposed to gastric fluid (table 4-3). One of the outcomes of examining the effect of the gastric medium upon the dissolution of troglitazone in this way is that the amount of troglitazone dissolved has in fact increased significantly (from 1.45 mg/500 ml in FaSSIF alone to 4 mg/500 ml when pre-exposed to gastric medium). This increase in the troglitazone dissolution could be due to it being pre-wetted by the gastric fluid, so when FaSSIF is added to the dissolution vessel the troglitazone is already immersed in the medium, whereas when dissolution is performed in FaSSIF alone, the troglitazone has to undergo the process of immersion wetting to enable it to be available for dissolution. It has been shown that during the initial wetting, a poorly wetting drug can form loose aggregates which in turn would increase the particle size, this would result in a slower dissolution rate for the drug (Lin *et al.* 1968). The

fact that troglitazone shows higher dissolution after pre-exposure to gastric media helps explain why there are such large differences in table 4-3. As the test is a comparative test between the dissolution of troglitazone alone and from the dispersion, it follows that if the amount of troglitazone dissolved increased then the degree of enhancement would reduce.

Figure 4-4 Dissolution of troglitazone alone and from solid dispersions in media where the flow from gastric to intestinal conditions is simulated. Results are the mean of three replicates, error bars ± SD.

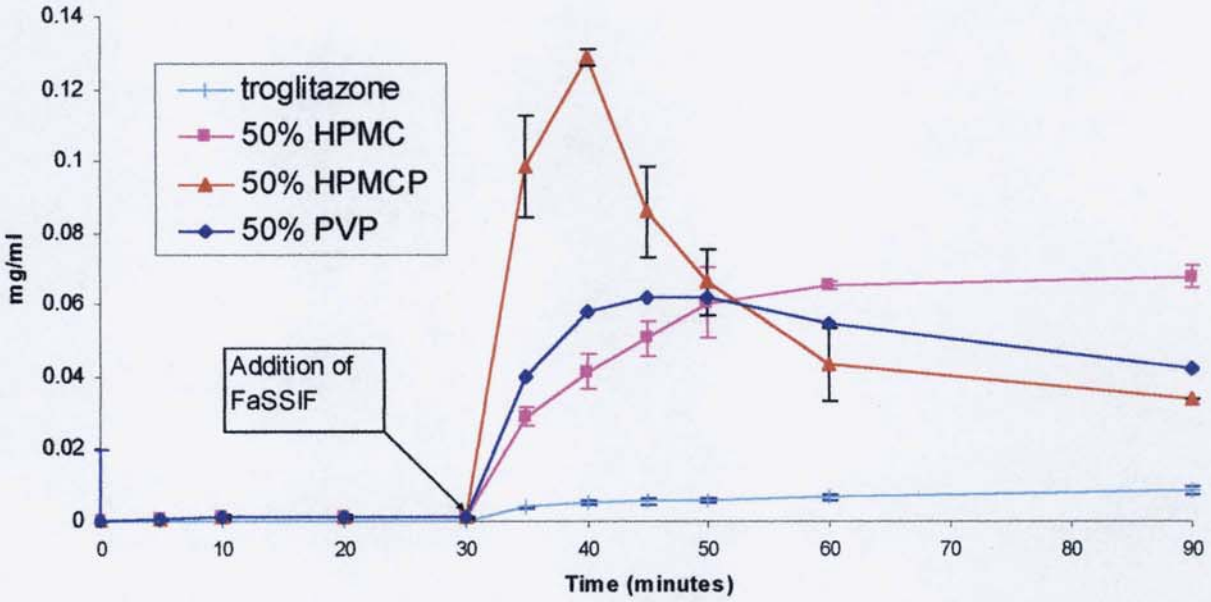

Table 4-3 Degree of enhancement of troglitazone from the dispersions when in FaSSIF of dispersions not exposed and those exposed to gastric fluid (calculated by dividing the peak dissolution from the dispersion by the peak dissolution of troglitazone)

Polymer	Degree of enhancent (FaSSIF alone)	Degree of enhancement (pre exposed to gastric)
HPMCP	54.53	16.13
PVP	43.47	7.75
HPMC	36.15	8.5

A more practical way of comparing the effects would be to compare the dissolution profiles of the dispersion in FaSSIF alone to those pre-exposed to gastric medium; this differs subtly from studying the supersaturation (as in section 3.1.3.2 the supersaturation is measure of the increase in peak dissolution achieved by the dispersions when compared to troglitazone alone). A comparison of the dissolution profiles of the troglitazone solid dispersions after they have been exposed to the gastric media to those where the dissolution was performed in just FaSSIF are shown in figures 4-5, 4-6 and 4-7 (mg dissolved was selected for the y-axis as there was no difference in the volume of dissolution media used) it is noticeable that in all cases the peak amount of drug dissolved has been reduced in those samples that have been exposed to the gastric media. The dissolution of troglitazone from the HPMCP dispersion has reduced from 87.50 mg/500 ml to 64.32 mg/500 ml, for the PVP dispersion a reduction of 60.50 mg/500 ml to 30.98 mg/500 ml was found, and from the HPMC dispersion a reduction from 55.50 mg/500 ml to 33.85 mg/500 ml was found. Considering this data it can be said that the exposure to the gastric medium has had a significant effect upon the dissolution of troglitazone from the solid dispersions. In the case of the dispersions prepared with gastric soluble polymers this drop in dissolution after pre-exposure to gastric fluid can be explained by the dispersions undergoing dissolution in the gastric fluid (Kai 1996). This dissolution of the gastric soluble dispersions, however, does not appear to disrupt the initial of release of troglitazone from the dispersions. Figures 4-5, 4-6 and 4-7 shows evidence that the initial dissolution of the solid dispersions has not been altered by prior exposure to gastric fluid, as over the first five minutes of dissolution each profile is super-imposable. It appears that the dissolution in the gastric fluid only affects the peak dissolution obtained from the gastric soluble dispersions; this is most probably due to there being less of either solid dispersion available for dissolution in the FaSSIF. This difference could have an impact upon the performance of the dispersion *in vivo*; this is supported by the findings of Kondo *et al.* (1994). It was shown that the dissolution of the drug under study from solid dispersions prepared with the gastric soluble polymer copolyvidone was similar to that from those prepared with HPMCP at pH 6.5. When the two solid dispersions were examined *in*

vivo, the HPMCP dispersions showed almost complete absorption, and displayed a higher AUC than for the copolyvidone when the dose was doubled. This was ascribed to the fact that in the stomach the copolyvidone dispersions dissolve in the gastric fluid, and thus drug subsequently crystallises out prior to absorption in the intestine so there is less drug at the site of absorption. However, in the case of the HPMCP dispersions dissolution occurs in the small intestine, therefore there would be more drug dissolved at the site of absorption, thus allowing for more absorption.

A paired t-test was performed on the AUC_{60} of each curve. For the HPMCP dispersions it is found that the difference between the amount dissolved is considered not significant ($p>0.05$). For the PVP and HPMC dispersion it is found that the difference between the amount dissolved is considered very significant ($p<0.001$). This shows, as shown by Kondo *et al.* (1994), that the use of an enteric polymer as the carrier inhibits the dissolution of the drug from the solid dispersion in the gastric fluid.

The fate of an orally administered formulation is shown in figure 1-8, and it is shown that a tablet can undergo disintegration into aggregates/ fine particles of the drug or the drug itself can undergo dissolution. Such a dissolution model, as described in this section, could be used to investigate the fate of an oral dosage form in the gastric media. From this the impact of each different mechanism, on the dissolution characteristics in the intestine can be assessed.

Figure 4-5 Comparison of the dissolution of troglitazone from 50% HPMCP solid dispersion with and without prior exposure to gastric fluid. Results are the mean of three replicates, error bars ± SD.

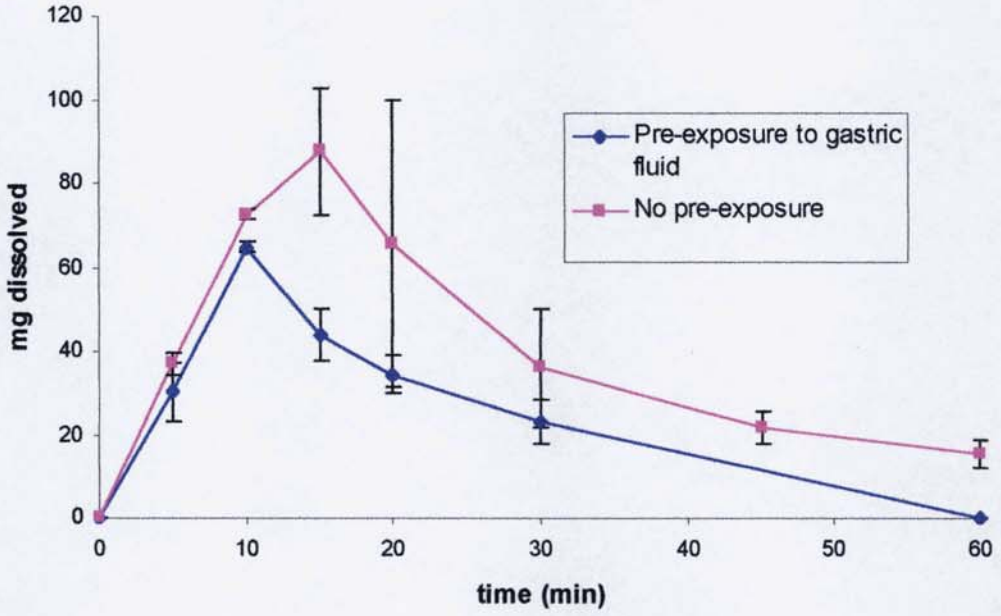

Figure 4-6 Comparison of the dissolution of troglitazone from 50% PVP solid dispersion with and without prior exposure to gastric fluid. Results are the mean of three replicates, error bars ± SD

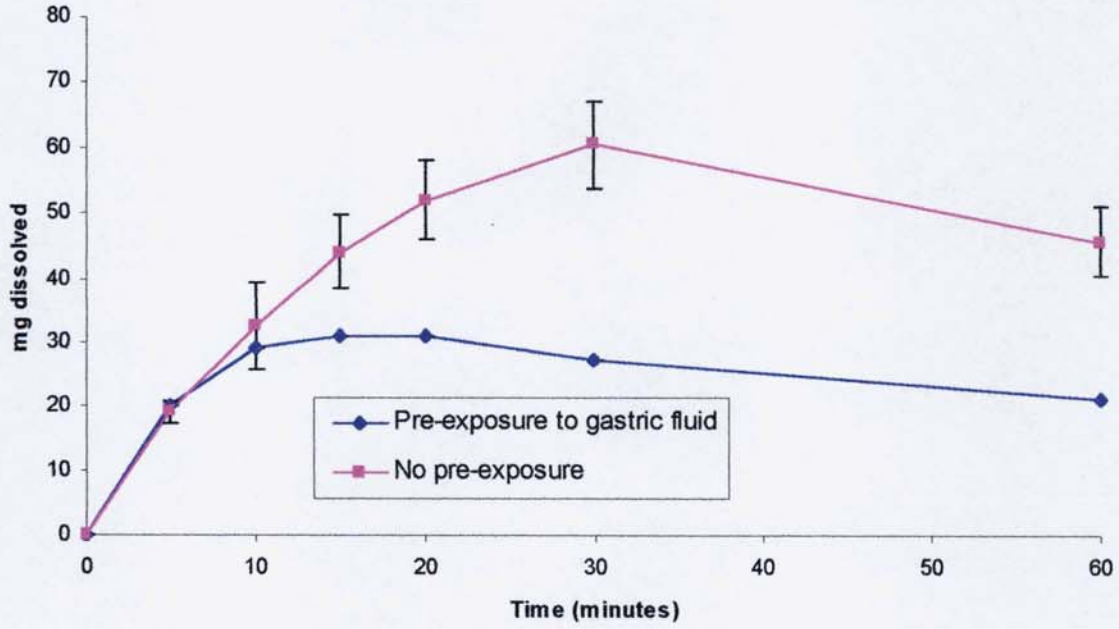

Figure 4-7 Comparison of the dissolution of troglitazone from 50% HPMC solid dispersion with and without prior exposure to gastric fluid. Results are the mean of three replicates, error bars ± SD

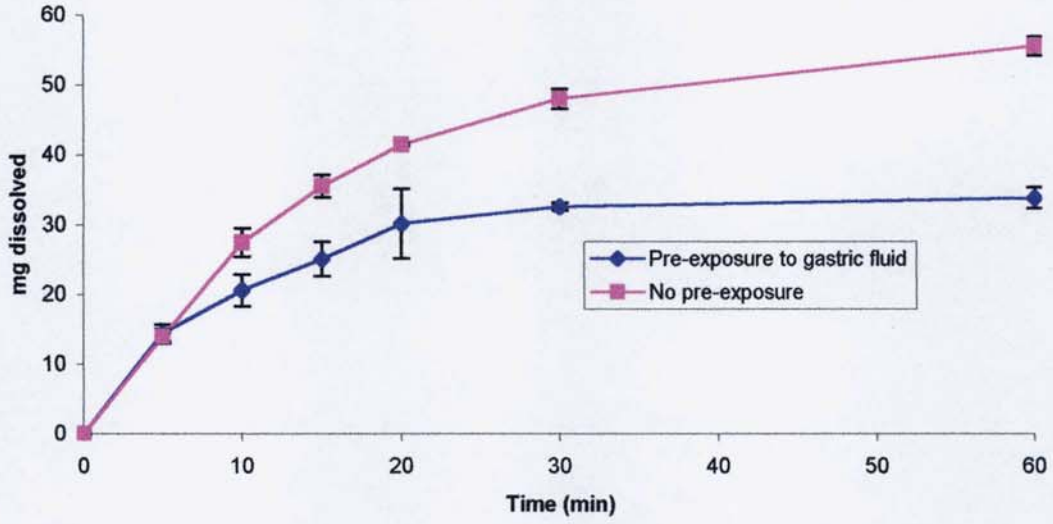

4.5 Modelling the bioavailability of troglitazone from dispersions

4.5.1 Introduction

The aim is to create a model to predict the *in vivo* behaviour of the solid dispersions in the fasted state, based upon the *in vitro* dissolution of the dispersion in FaSSIF. The modelling software used is Modelmaker 4, which is written by Cherwell Scientific, 2000.

4.5.2 Modelmaker 4, an introduction

A basic model was constructed from two main components; compartments and flow arrows. The compartments are described as being a container within the model, and are defined by what is entering and leaving. The flow arrows describe the movement of a quantity from one compartment to another. When used in conjunction with the compartments, the flows help build up a series of differential equations that describe the rate at which the quantity is moving.

Within most models it would be expected for there to be some values that will remain constant, for example the gastric emptying rate could be described as a constant. The software has the facility to determine constants, within the

program; these are known as the parameters.

The software also has the facility to compare data to already experimentally obtained results, thus allowing for the optimisation of the model. This works by the software adjusting selected parameters to reduce the standard error between the experimentally determined results and the results obtained from the model.

4.5.3 The design and assumptions made in the development of the model

The first process in designing such a model was to decide upon the critical stages and processes that would occur within the model. It was initially decided that the critical stages involved were as follows:

- Drug in the stomach
- Dissolution of the drug in the stomach
- Drug in intestine
- Drug in colon
- Dissolution of drug in the intestine
- Drug absorption into the blood
- Drug distribution and elimination

Figure 4-8 shows how the stages combine to make a flowing model, the format of this model is based on the models described by Wilson *et al.* 1991. The arrows in the diagram represent the processes that occur, and these are as follows:

- The flow from 'solid drug in stomach' to 'drug dissolved in gastric' is described by the dissolution rate of the dispersion in the FaSSGaF.
- The flow from 'solid drug in stomach' to 'solid drug in intestine' is described by the gastric solids emptying rate.
- The flow from 'solid drug in intestine' to 'drug dissolved in intestinal fluid' is described by the dissolution rate of the dispersion in the FaSSIF.
- The flow from 'drug dissolved in gastric fluid' to 'drug dissolved in

intestinal fluid' is described by the gastric liquids emptying rate.

- The flow from 'solid drug in intestine' to 'solid drug in colon' is described by the transit time in the intestine.
- The flow from 'drug dissolved in intestinal fluid' to 'drug absorbed into blood' is described by the absorption rate.
- The flow from 'drug absorbed in blood' to 'dispersed and eliminated drug' is described by the volume of distribution and the elimination constant.

Figure 4-8 Proposed schematic diagram of the model describing the passage of the drug moving from administration to elimination

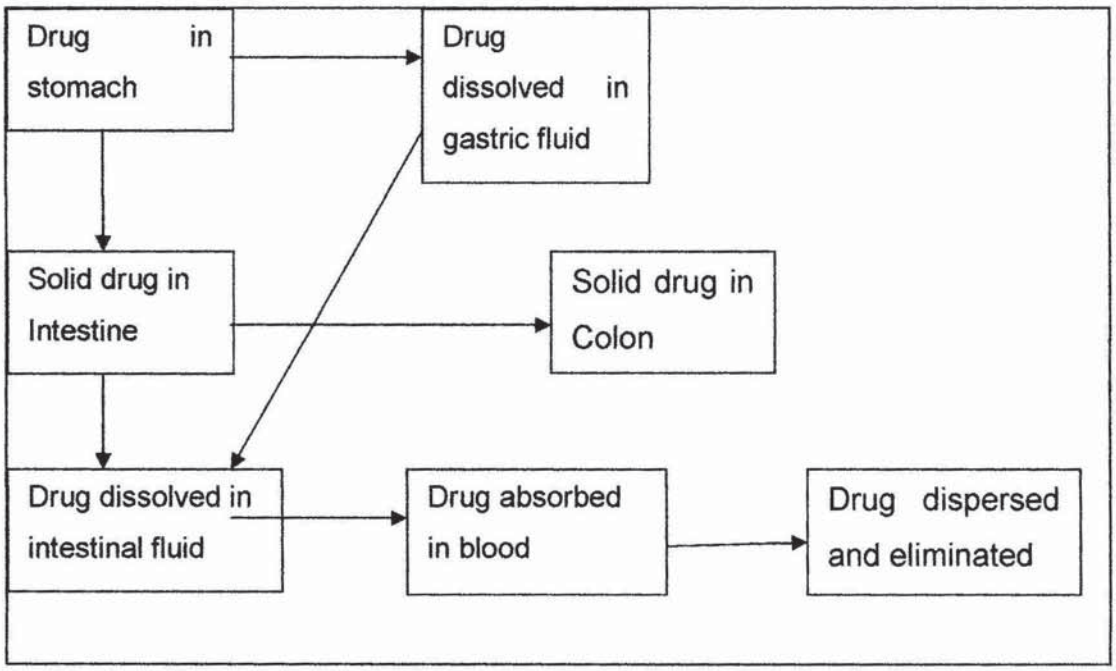

In the eventual model, shown in figure 4-9 the 'dissolution of drug in stomach' compartment has been removed from the model. The rationale behind this decision is that the dissolution and any subsequent absorption of the drugs in the stomach would be negligible. This is based upon three main factors; the first being the very slow dissolution rates experienced in the FaSSGaF (section 4.4.3), secondly the short residence time in the stomach experienced in the fasted state, and finally the barrier to absorption of drug from the stomach due to the smaller surface area of the stomach (*i.e.* there are no villi in the stomach). The first two reasons are linked to each other, in that the length of time within the stomach would dictate the amount of drug dissolved.

Based on the accepted residence times of a dosage form in the stomach, the expected length of time would be around thirty minutes (section 4.4.1). It is shown in sections 4.3 and 4.4 that the dissolution of troglitazone, from the dispersions, is minimal in FaSSGaF over this time. Thus the impact of dissolution in the stomach was considered negligible.

One issue that was not considered for the development of this model was the possibility of degradation of the drug within the GI tract. One of the main reasons that this aspect was not considered for the model is the overall complexity that would be involved. It was also felt that that this may turn the attention away from the main aim of the intended model.

The diagram displayed in figure 4-9 shows the overall flow of the model, from the initial entry into the stomach to the elimination of the drug.

Figure 4-9 Final schematic diagram of model for the movement of the drug from administration to elimination

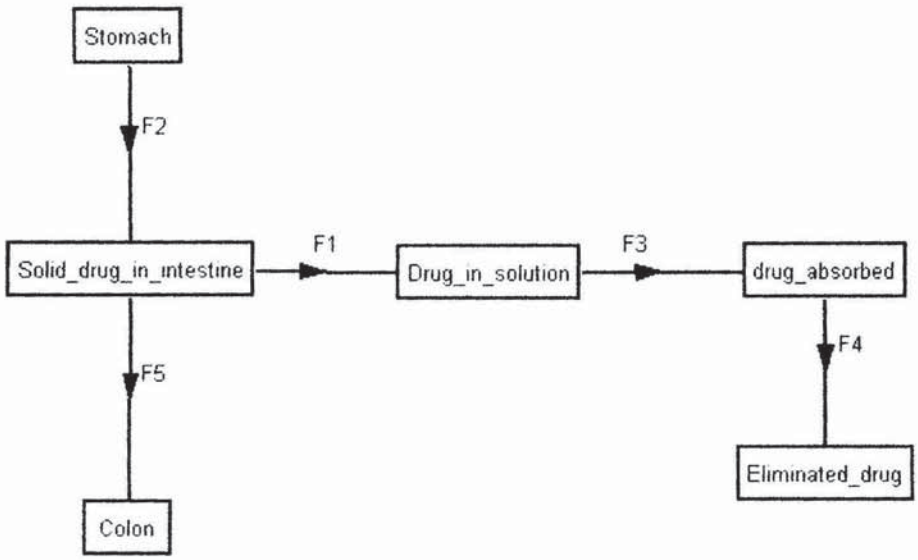

Figure 4-10 Example of the parameters used within the model

Name	Value	Optimize	Minimize	Monte Carlo	Dist Type
Main					
absorbec	1.7	☑	☐	☐	Normal ...
Eliminatec	2.816	☑	☐	☐	Normal ...
halflife	16.561	☑	☐	☐	Normal ...
V	14200	☐	☐	☐	Normal ...

4.5.4 Modelling of transit time of troglitazone through the GI tract

One of the first aspects of the model that was designed was to establish a suitable transit rate of the drug through the GI tract (flows F2 and F5 in figure 4-9). The transit rate within the GI tract can have a major impact upon the overall amount of drug absorbed into the blood (section 1.1.3). To develop this section of the model, all other stages were removed and only the flow from the stomach to the colon was considered. The times that were used corresponded to what is stated in the current literature. The times that are used in this model were suggested by Dressman et al. (1998) and they are as follows: for gastric emptying the average time is 1 hour, and the transit time of the drug in the small intestine is 3hours .

Figure 4-11 Mass of drug in each compartment as a function of time, as predicted by the model

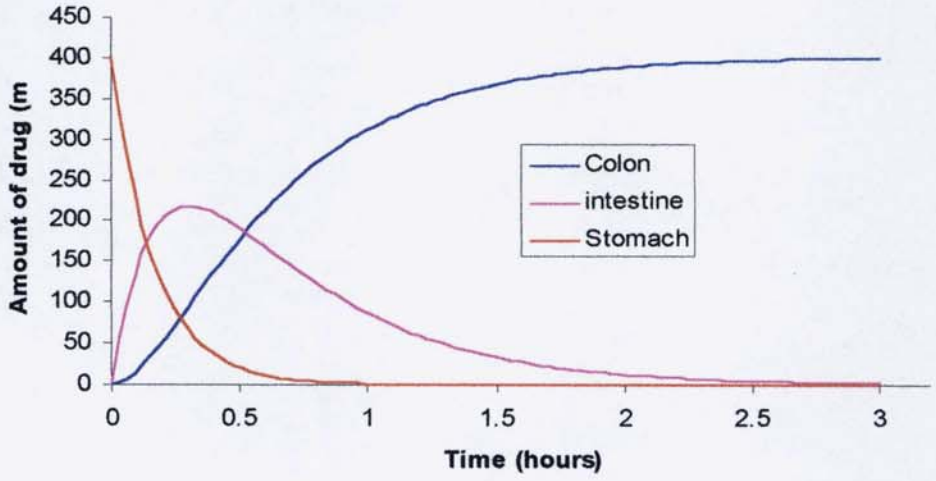

The mass of drug (mg) in each compartment as a function of time is shown in figure 4-11. It can be seen that from the graph that drug is completely emptied from the stomach within 1 hour, thus successfully simulating the physiological time.

4.5.5 The introduction of the dissolution kinetics to the model

It has been proposed that the following factors are the main driving forces behind drug dissolution within the GI tract (for a list and explanation see section 1.2): surface area of the drug, diffusivity of the drug, boundary layer thickness, solubility, amount of drug already dissolved and volume of the solvent available. Due to the design of the *in vitro* dissolution test these parameters have been accounted for, *i.e.* by using 500 ml of dissolution media, and the use of biorelevant dissolution media.

Previous methods used to describe the dissolution of the dispersions, within this study, have relied on fitting polynomial curves to the dissolution profiles to describe the dissolution rate (section 3.). As described earlier this was due to the precipitation from the supersaturated systems, and the fitting of a linear model to such profiles is difficult. This is a problem that has been encountered in a previous attempt to develop an in-silico model for a troglitazone solid dispersion (Nicolaides *et al.*, 2001).

The previous methods for comparing the dissolution of the dispersions (polynomial fit) were not appropriate for the development for this model. The two main requirements of a potential model are that it should be able to describe the dissolution as a function of time, and secondly the proposed model should take into account that the mass of drug available for dissolution is reducing over time. The polynomial fit, which proved suitable in section 3.1.37 at giving an indication to the wetting properties of the polymers, was inappropriate because it does not take into account the amount of drug remaining for dissolution. Unsuccessful attempts were made to develop such a model, this though unveiled a series of other problems. The rate derived from the polynomial fit is the initial dissolution rate (section), which is a very fast rate, so this overestimated the dissolution (figure 4-12). When the amount

of drug dissolved is calculated using the polynomial derived rate it is seen that there is a large discrepancy between the actual and calculated *in vitro* data (figure 4-12).

Figure 4-12 Comparison of the actual dissolution of the HPMC 71% (w/w) with that calculated from the polynomial rate. Results are the mean of three replicates, error bars ± SD.

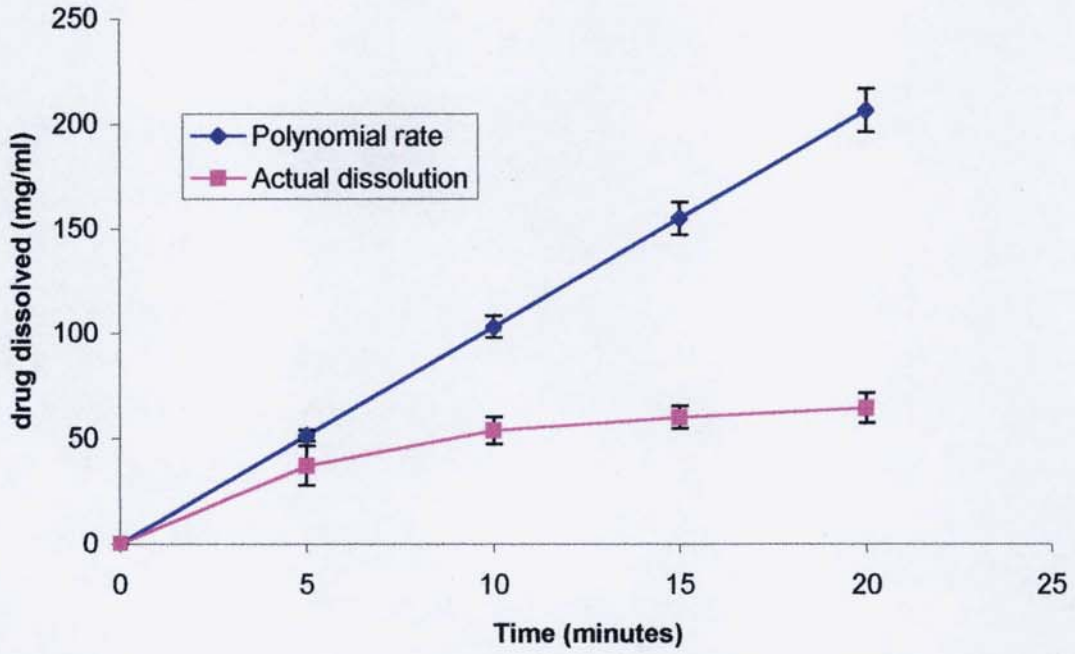

It was, therefore, decided to fit the data to the Hixson-Crowell dissolution model (equation 1-24). The reason why this model was chosen to describe the kinetics is that it fits the set criteria for the model, *i.e.* it describes the dissolution as a function of time, and it takes into account mass available for dissolution. Figure 4-13 shows how the kinetics were incorporated into the model.

The model does not describe the precipitation that occurs with the HPMCP dispersions. This omission is justified by the very fact that troglitazone is a class II drug, in the BCS. This means that the bioavailability of troglitazone is limited by its dissolution and not the absorption, and it has been described that troglitazone is rapidly absorbing (Parker 2002). Kai *et al.* (1996) showed, for a rapidly absorbing drug, that any re-crystallisation that occurs *in vitro*,

after dissolution from a solid dispersion, has very little impact on the *in vivo* performance.

Figure 4-13 Equation describing the dissolution kinetics of the drug in the model

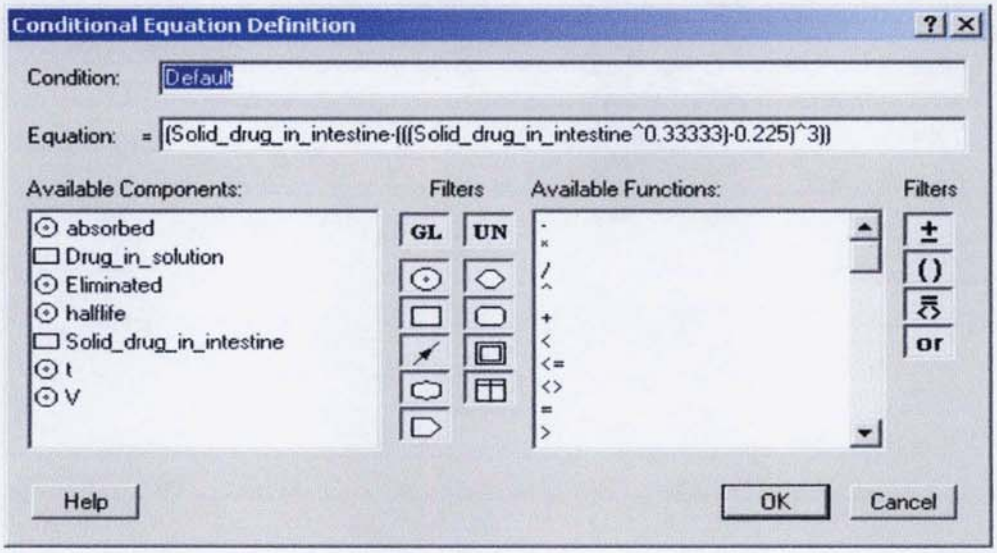

4.5.6 Simulation of the absorption and elimination of the drugs

The equations used in the F3 and F4 (Figure 4-13) were adapted from those used by Wilson *et al.* (1991) to describe both the absorption of the drug through the intestine and the elimination of the drug. Figures 4-14 and 4-15 show the equations that were used in the final model.

Figure 4-14 Equation describing the flow from 'drug in solution' to 'drug absorbed'

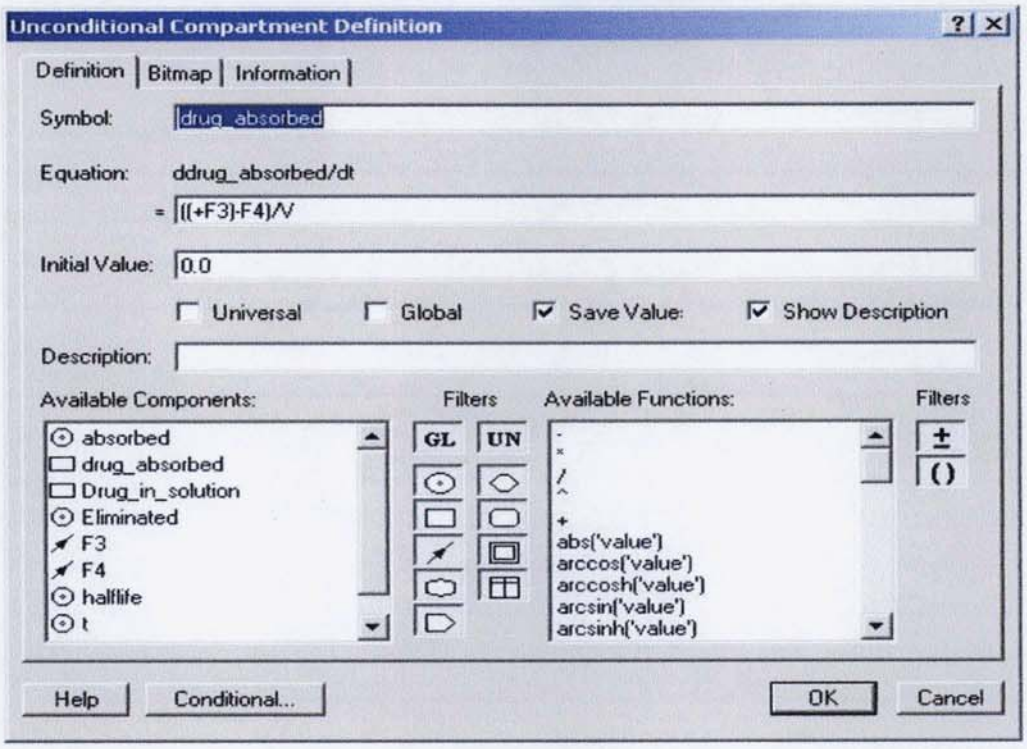

Figure 4-15 Equation describing the flow from 'drug absorbed to 'drug eliminated'

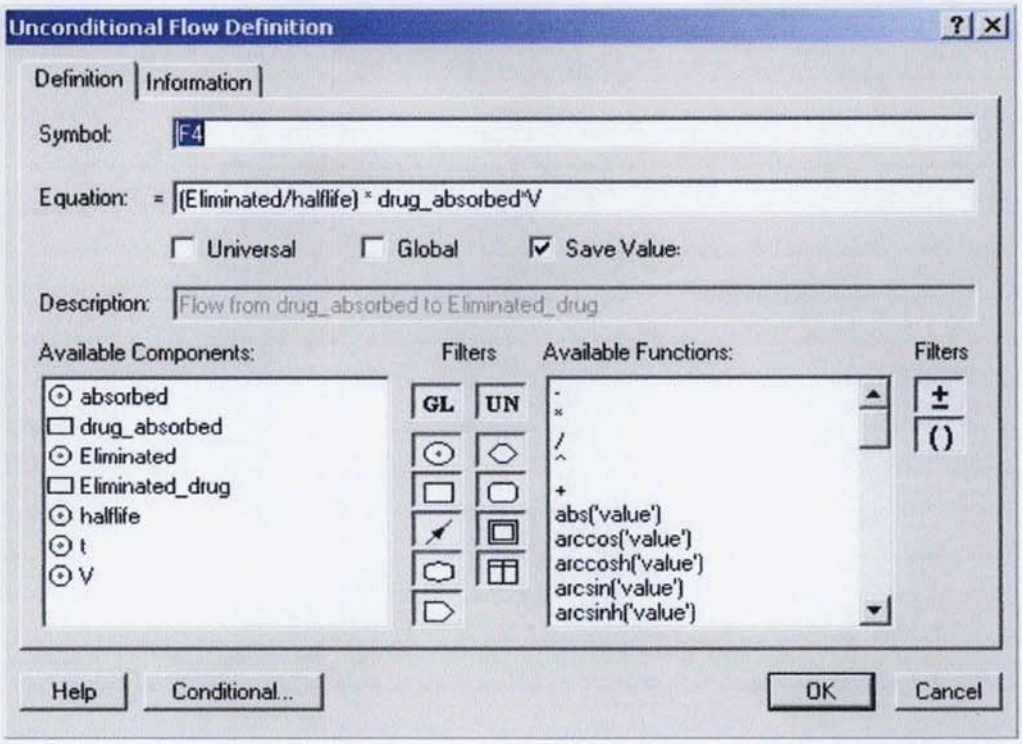

The absorption constant (k_a) and the elimination constant (k_{el}) for troglitazone have not been published. This, therefore, highlights one of the main limitations of the model, that these values may not be physiologically relevant. If it was required to be calculated k_{el} can be calculated by equation 4.1 (where $t_{1/2}$ is

the half life of elimination, *i.e.* the time taken for the drug plasma concentration to fall to half it original value). The half life can be obtained by administering the drug by parental means and measuring the plasma concentration over time.

Equation 4-1

$$K_{el} = \frac{\ln 2}{t_{1/2}}$$

The calculation of K_a is a little more difficult, and there are various methods for obtaining it: least squares regression of the plasma-time curve and the Wagner-Nelson approach (Pidgeon and Pitlick 1977) For both methods it is required that a plasm-time curve is obtained, and in the case of the Wagner-Nelson approach the K*el* data is required from parental administration.

4.5.7 Using the model to predict the *in vivo* performance of the solid dispersions based upon the *in vitro* dissolution in FaSSIF

4.5.7.1 Dissolution kinetics

As discussed in section 4.5.5 the dissolution of the dispersions in the intestine was described using the Hixson-Crowell model. The model was applied over the first twenty minutes of the dissolution profiles; this was due to the dissolution of the majority of the dispersions reaching a plateau at 20 minutes (section 3.1.1.3). Table 4-4 shows the derived dissolution rates for each of the dispersions using the Hixson-Crowell model, and it was these rates that were used in the model. It can be seen that these dissolution rates do not correlate with the polynomial rates shown in table 3-2, for example the HPMCP has the highest polynomial rate at 9 and 17% polymer loading, whereas PVP has the highest dissolution rates when the Hixson-Crowell model is applied. It is seen, however that that the Hixson Crowell dissolution rates correlate better with the AUC_{20} results (table 3-2), thus supporting the fact that they give a better indication of the dissolution over a longer period of time than the polynomial rates. This means that the Hixson-Crowell dissolution rate is better suited to the model than the polynomial dissolution rates. Figures 4-16 to 4-36 illustrate the similarity of the data obtained from the dissolution tests to those obtained from the derived dissolution rates. These figures show that the rates

derived from the Hixson-Crowell model generally do underestimate the dissolution of troglitazone from the solid dispersions. Therefore, to evaluate the effectiveness of the model, the f_2 similarity test (discussed in section 1.4.6) was used to establish how significant this underestimation is. The f_2 value, in this instance, is being used as estimation of the similarity of experimental data and the predicted data. It is only being used as an estimation of similarity, as not all of the criteria for the use of the f_2 value has not been met, so although there are enough data points (*i.e.* 3 points not including zero), there are not enough replicates for each time point (*i.e.* twelve replicates are required for each time point). It is being used, though, as it can give a rapid indication as to whether the profiles are similar. Ideally a paired t-test on each time point could be used to ascertain whether the profiles are statically similar.

Table 4-4 Derived Hixson-Crowell dissolution cube root rates for each of the dispersions over the initial twenty minutes of dissolution (units = $mg^{1/3}/h$)

	Concentration of polymer in dispersion						
	9%	17%	29%	50%	71%	83%	91%
HPMC	0.780	0.994	0.699	1.348	2.032	0.274	0.127
HPMCP	0.637	1.099	1.530	4.238	8.348	5.925	5.666
PVP	1.080	1.386	1.310	1.702	1.224	0.161	0.672

Figure 4-16 Comparison of the actual data with the data derived from the Hixson-Crowell fit for the 9% HPMCP dispersion. Results are the mean of three replicates, error bars ± SD.

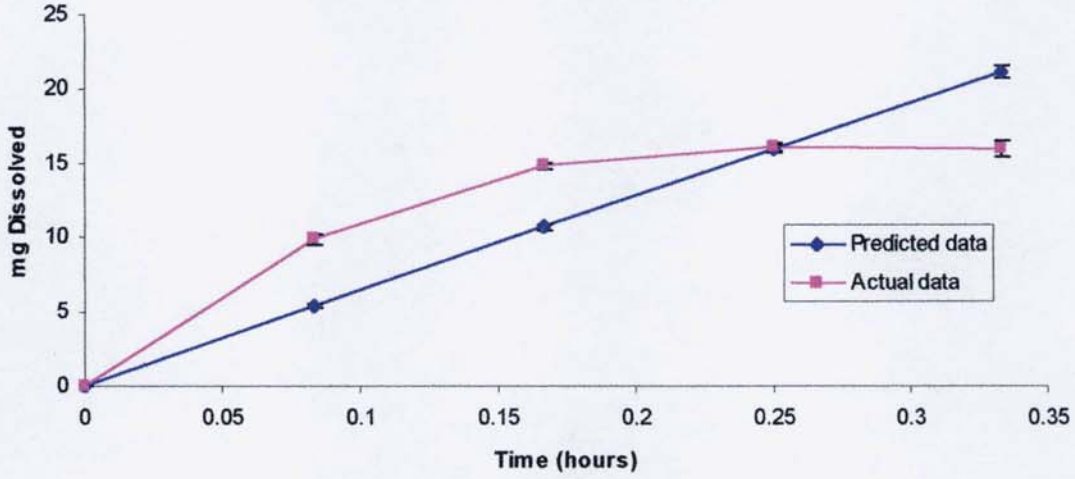

Figure 4-17 Comparison of the actual data with the data derived from the Hixson-Crowell fit for the 17% HPMCP dispersion. Results are the mean of three replicates, error bars ± SD.

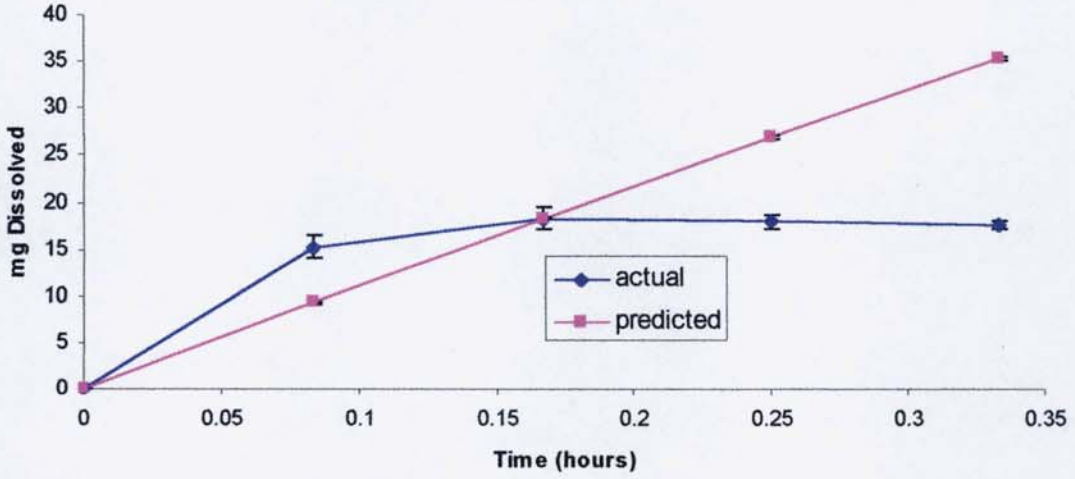

Figure 4-18 Comparison of the actual data with the data derived from the Hixson-Crowell fit for the 29% HPMCP dispersion. Results are the mean of three replicates, error bars ± SD.

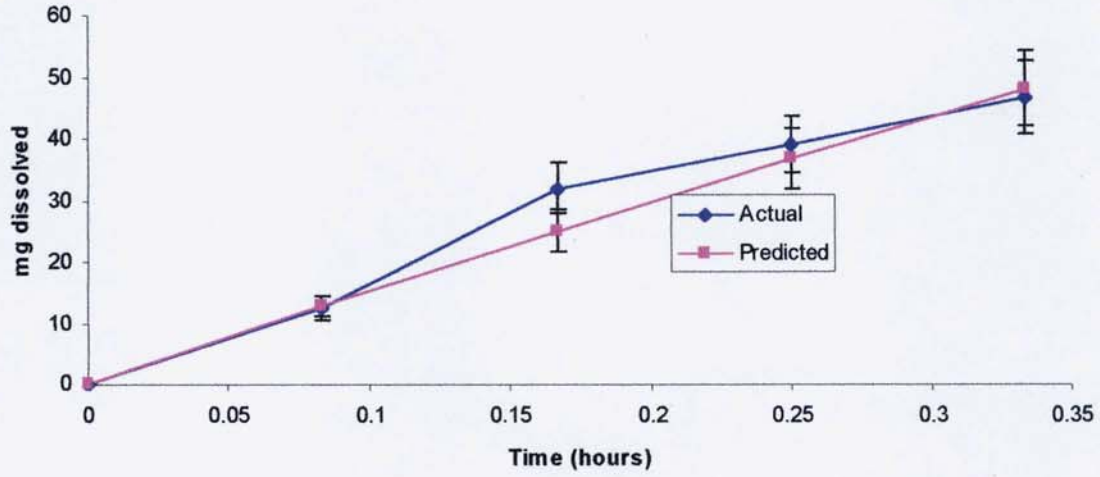

Figure 4-19 Comparison of the actual data with the data derived from the Hixson-Crowell fit for the 50% HPMCP dispersion. Results are the mean of three replicates, error bars ± SD.

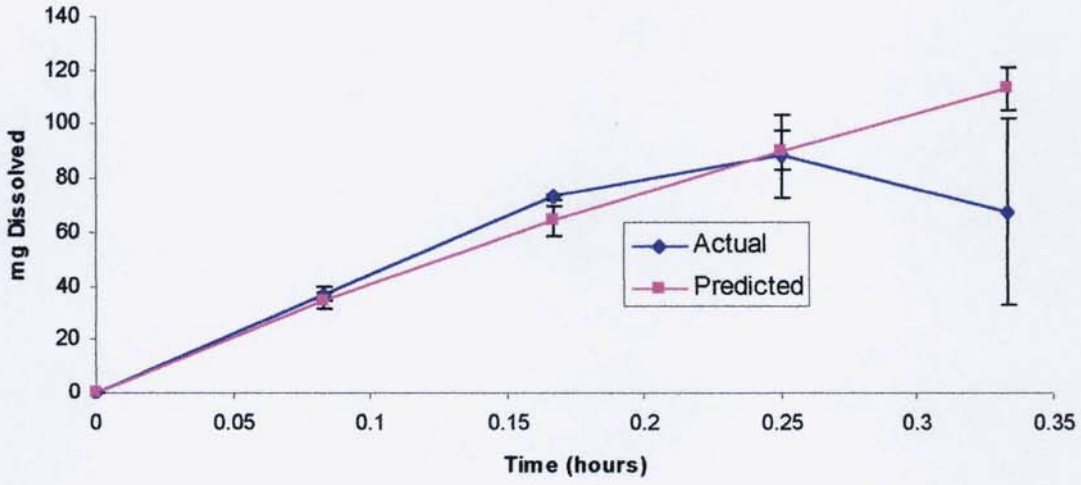

Figure 4-20 Comparison of the actual data with the data derived from the Hixson-Crowell fit for the 71% HPMCP dispersion. Results are the mean of three replicates, error bars ± SD.

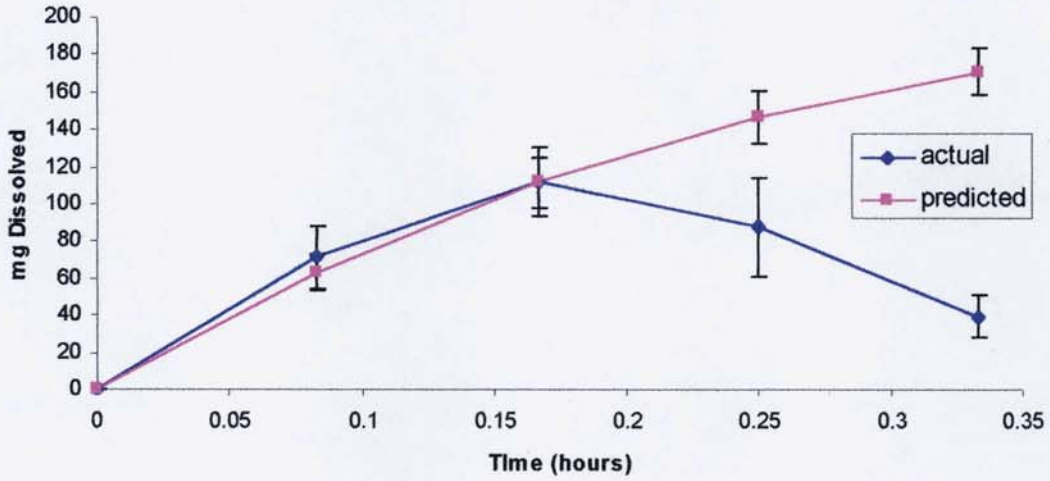

Figure 4-21 Comparison of the actual data with the data derived from the Hixson-Crowell fit for the 83% HPMCP dispersion. Results are the mean of three replicates, error bars ± SD.

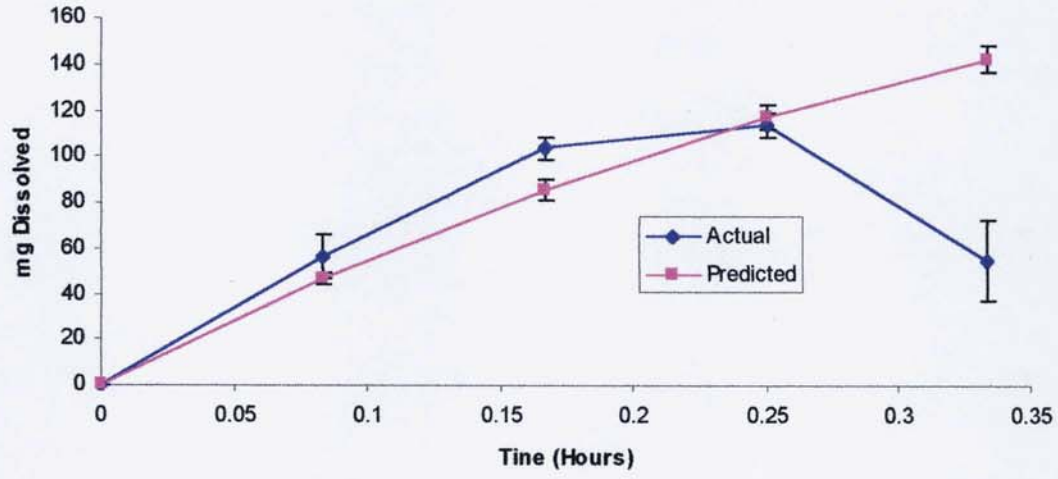

Figure 4-22 Comparison of the actual data with the data derived from the Hixson-Crowell fit for the 91% HPMC dispersion. Results are the mean of three replicates, error bars ± SD.

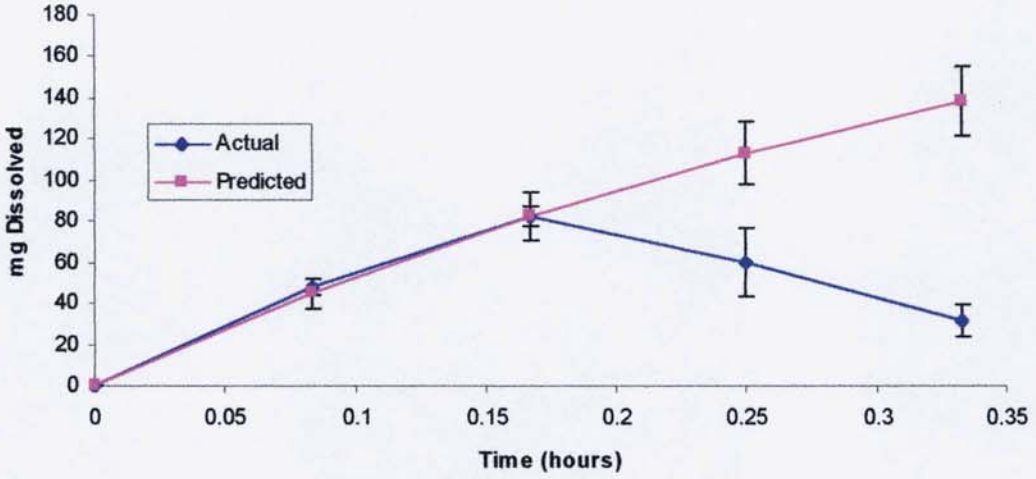

Figure 4-23 Comparison of the actual data with the data derived from the Hixson-Crowell fit for the 9% HPMC dispersion. Results are the mean of three replicates, error bars ± SD.

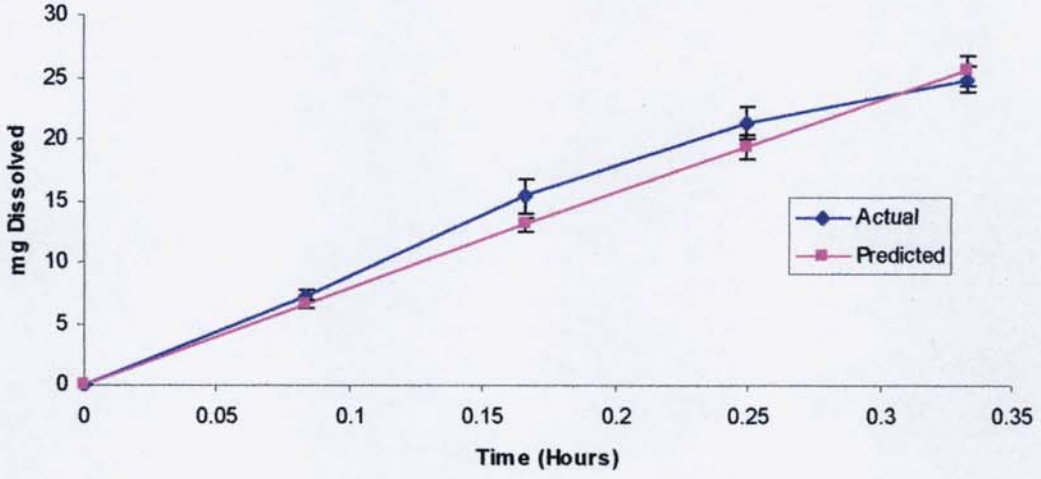

Figure 4-24 Comparison of the actual data with the data derived from the Hixson-Crowell fit for the 17% HPMC dispersion. Results are the mean of three replicates, error bars ± SD.

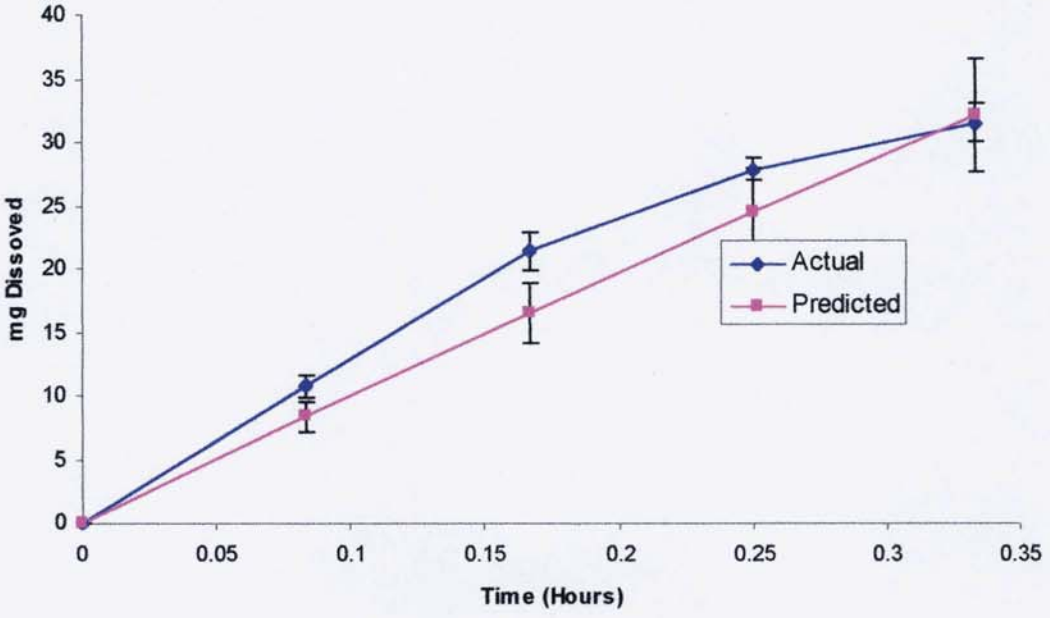

Figure 4-25 Comparison of the actual data with the data derived from the Hixson-Crowell fit for the 29% HPMC dispersion. Results are the mean of three replicates, error bars ± SD.

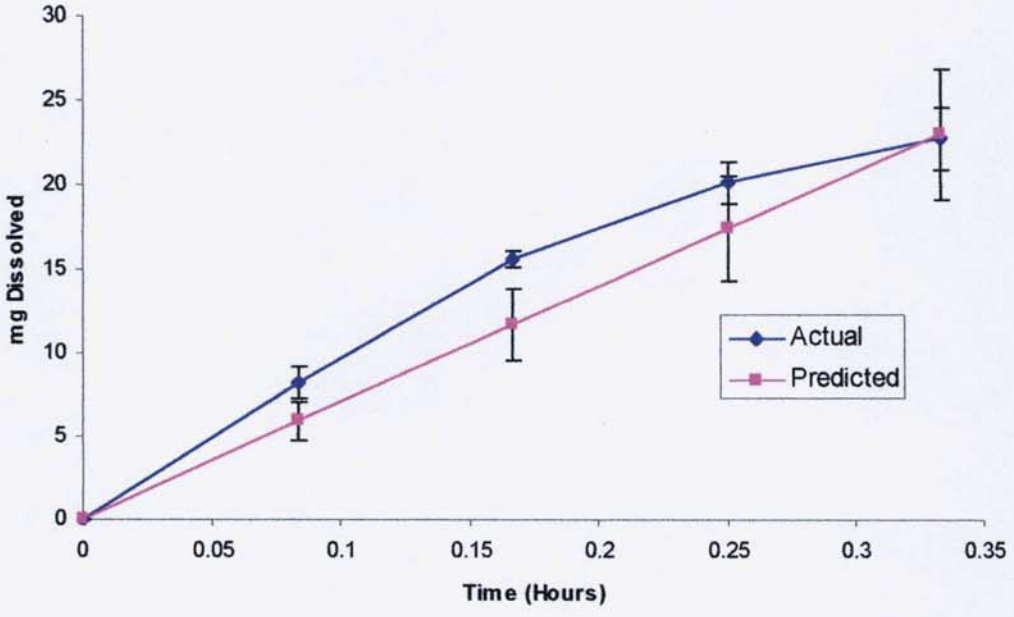

Figure 4-26 Comparison of the actual data with the data derived from the Hixson-Crowell fit for the 50% HPMC dispersion. Results are the mean of three replicates, error bars ± SD.

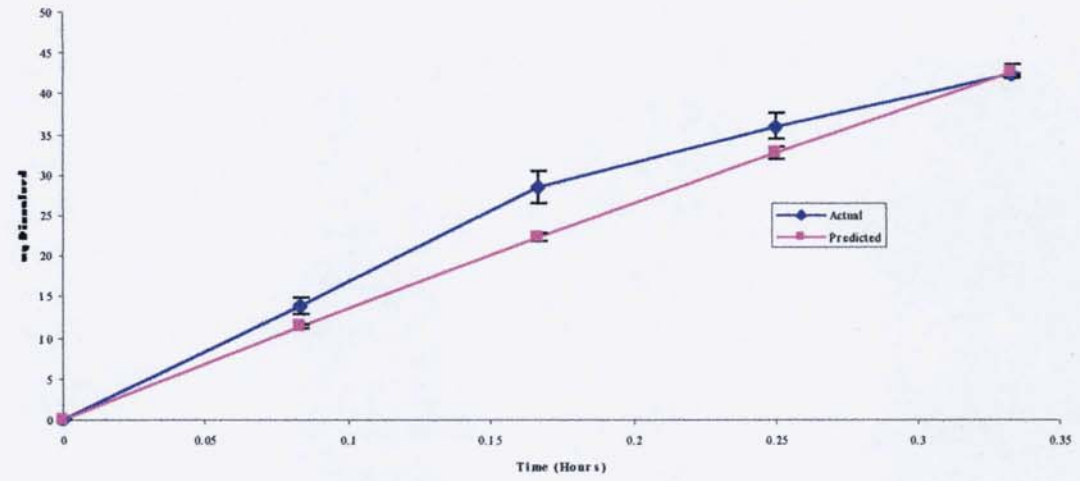

Figure 4-27 Comparison of the actual data with the data derived from the Hixson-Crowell fit for the 71% HPMC dispersion. Results are the mean of three replicates, error bars ± SD.

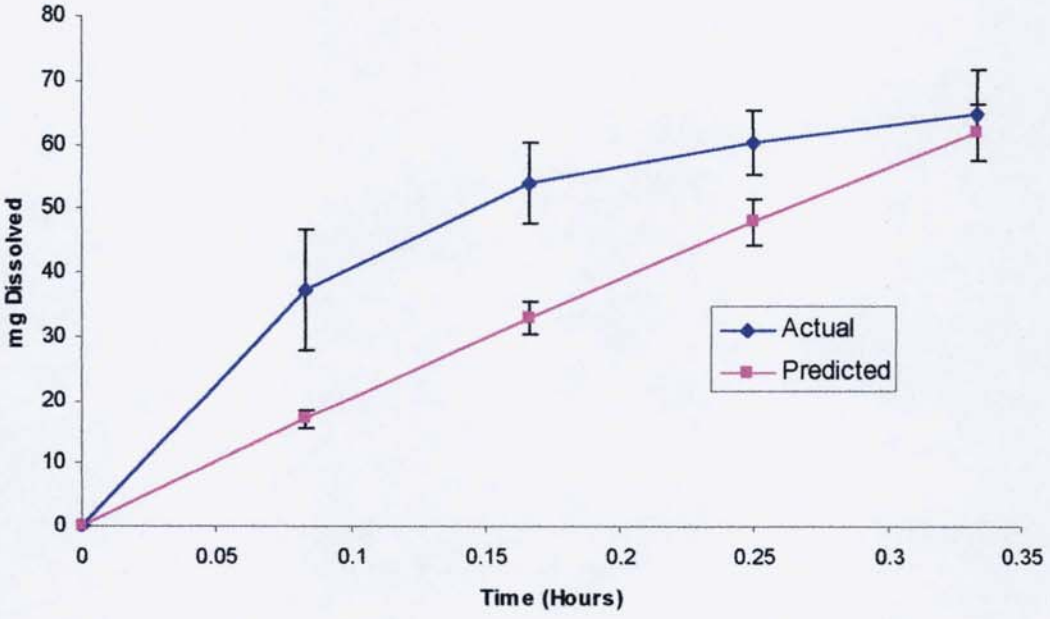

Figure 4-28 Comparison of the actual data with the data derived from the Hixson-Crowell fit for the 83% HPMC dispersion. Results are the mean of three replicates, error bars ± SD.

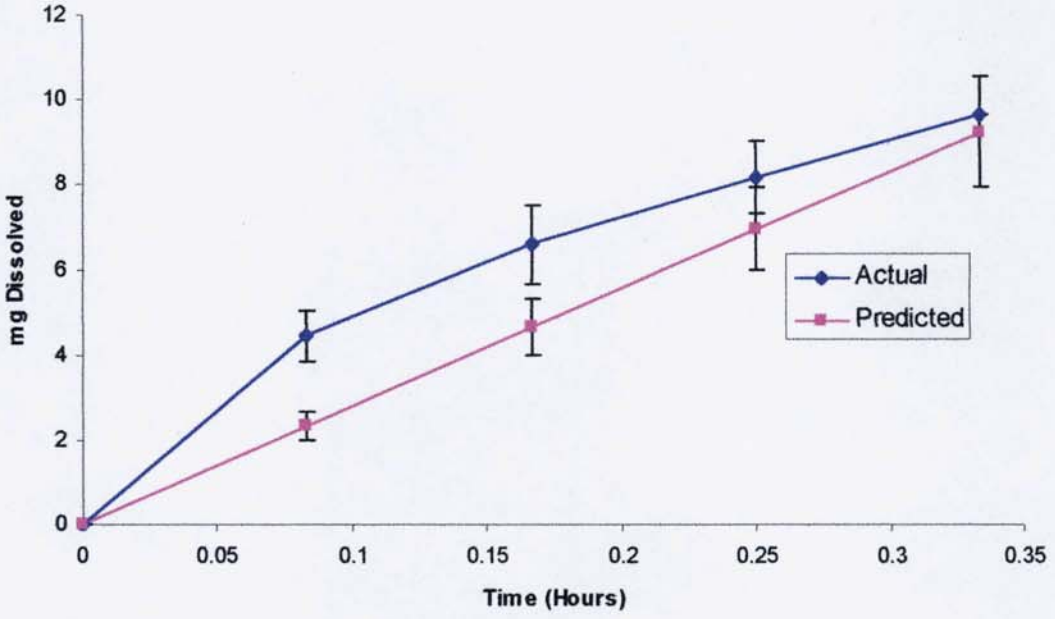

Figure 4-29 Comparison of the actual data with the data derived from the Hixson-Crowell fit for the 91% HPMC dispersion. Results are the mean of three replicates, error bars ± SD.

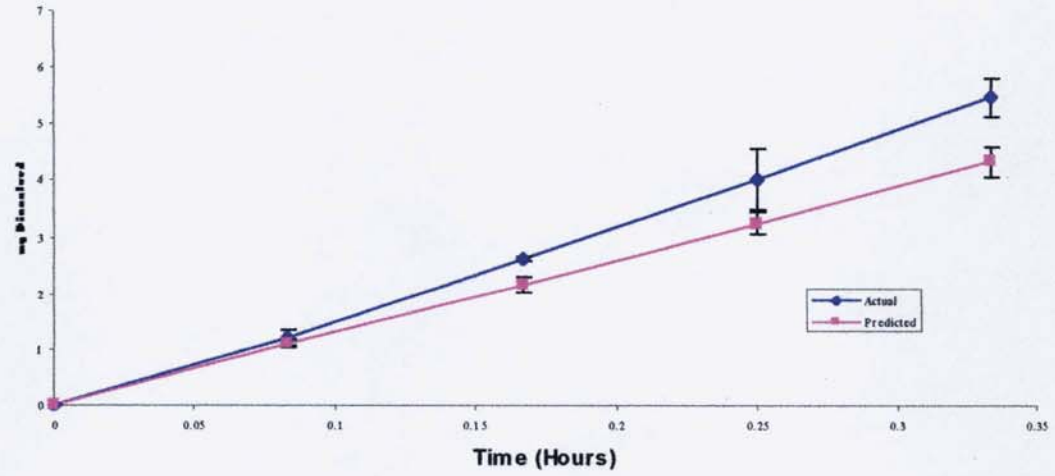

Figure 4-30 Comparison of the actual data with the data derived from the Hixson-Crowell fit for the 9% PVP dispersion. Results are the mean of three replicates, error bars ± SD.

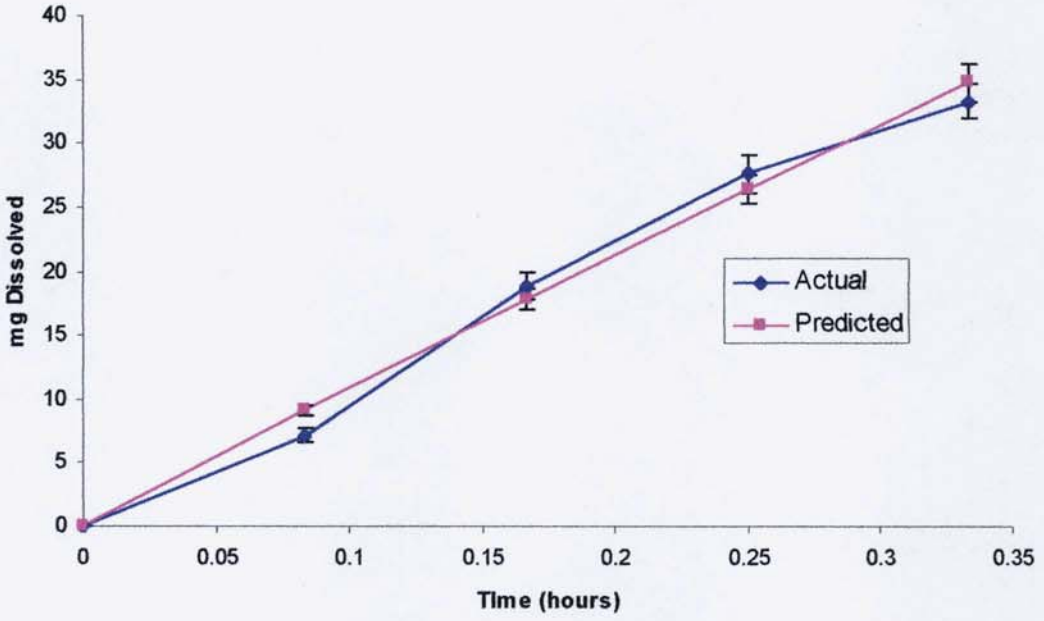

Figure 4-31 Comparison of the actual data with the data derived from the Hixson-Crowell fit for the 17% PVP dispersion. Results are the mean of three replicates, error bars ± SD.

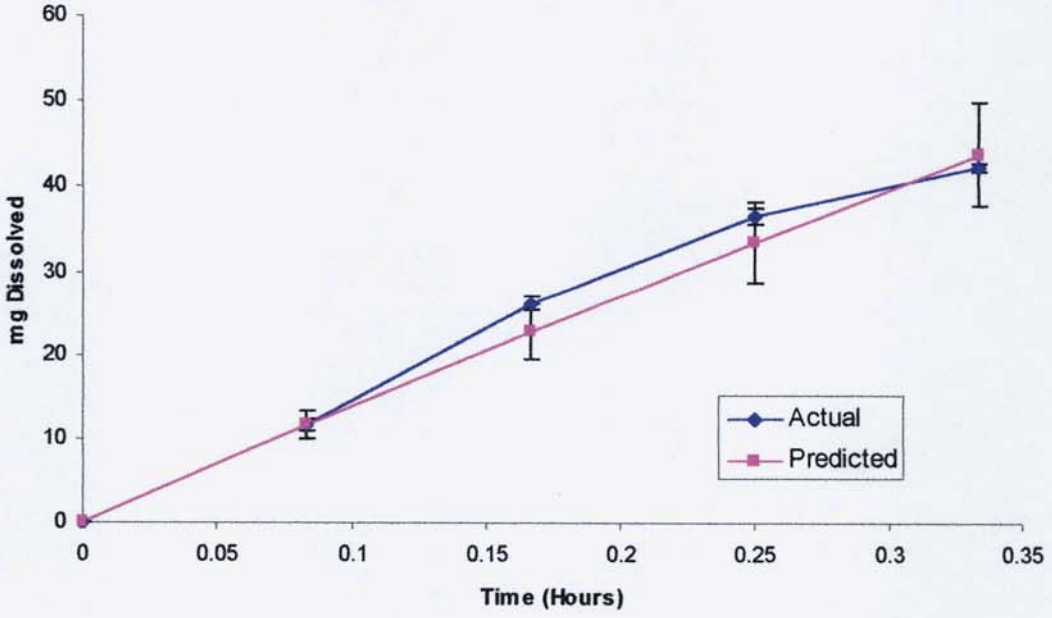

Figure 4-32 Comparison of the actual data with the data derived from the Hixson-Crowell fit for the 29% PVP dispersion. Results are the mean of three replicates, error bars ± SD.

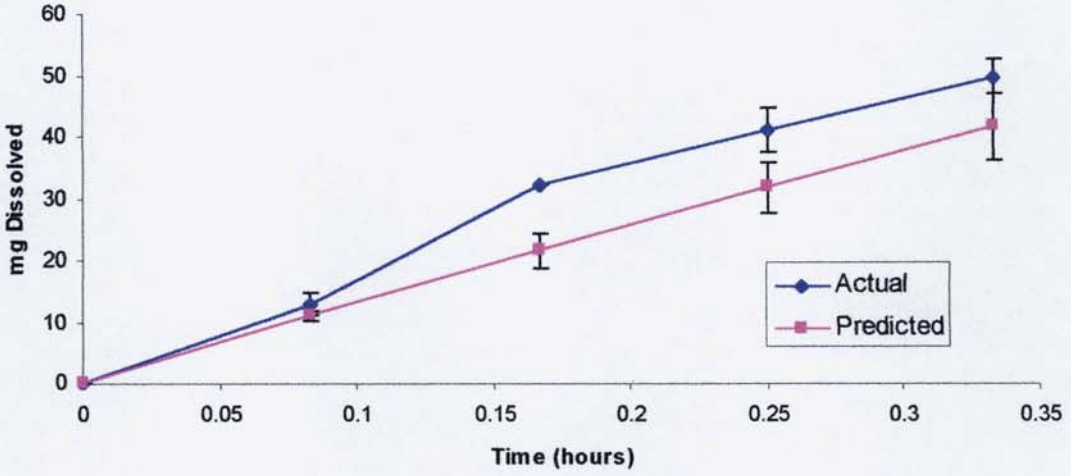

Figure 4-33 Comparison of the actual data with the data derived from the Hixson-Crowell fit for the 50% PVP dispersion. Results are the mean of three replicates, error bars ± SD.

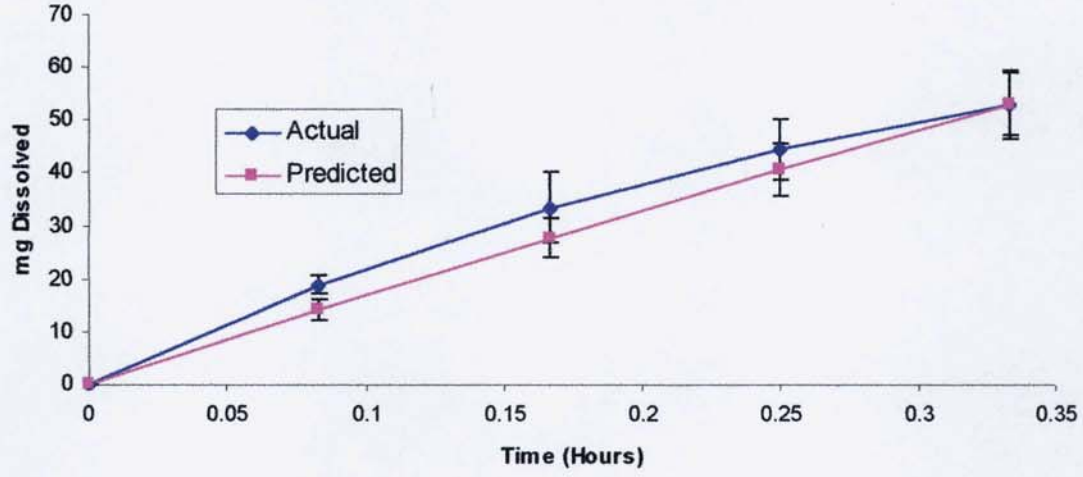

Figure 4-34 Comparison of the actual data with the data derived from the Hixson-Crowell fit for the 71% PVP dispersion. Results are the mean of three replicates, error bars ± SD.

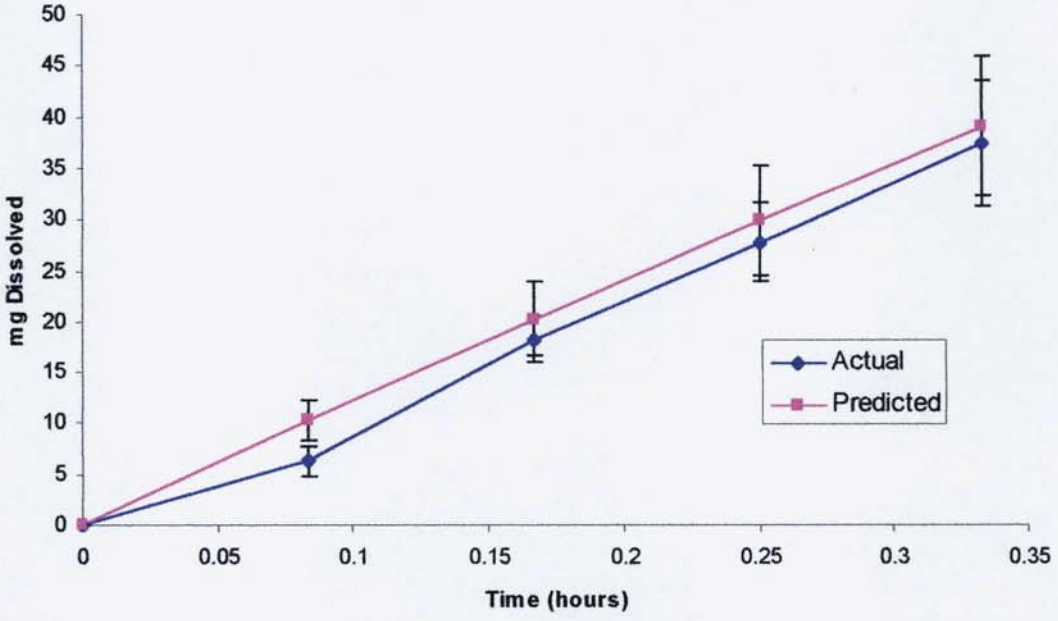

Figure 4-35 Comparison of the actual data with the data derived from the Hixson-Crowell fit for the 83% PVP dispersion. Results are the mean of three replicates, error bars ± SD.

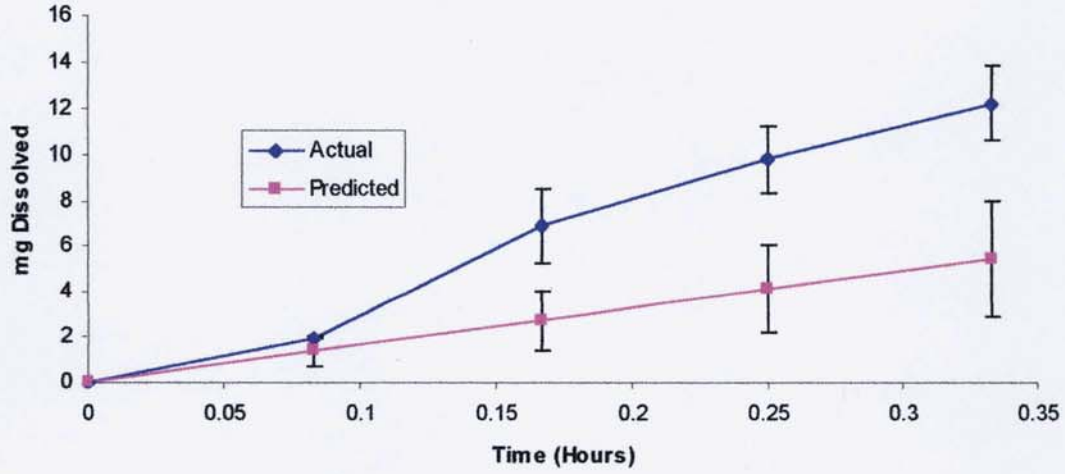

Figure 4-36 Comparison of the actual data with the data derived from the Hixson-Crowell fit for the 91% PVP dispersion. Results are the mean of three replicates, error bars ± SD.

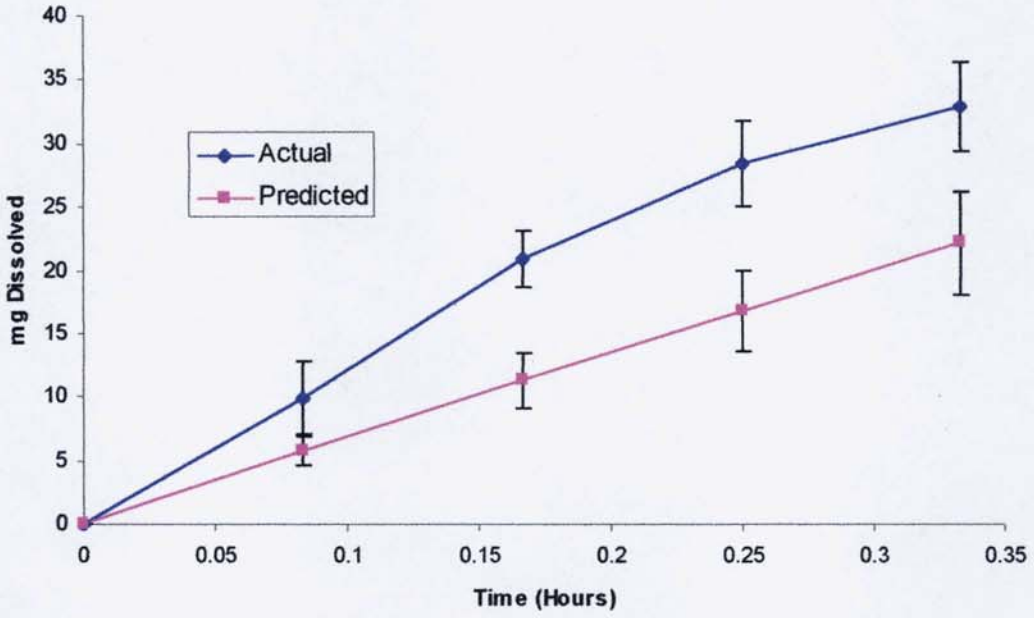

Table 4-4 shows that for the HPMC and PVP dispersions (with the exception of the 71% HPMC dispersion) experimental data and the calculated data are similar, with all the results being above 50. Examination of the curve for the 71% HPMC dispersion (figure 4-27) shows that the derived rate is severely underestimating the amount of drug that is dissolved. This will have an impact upon the data obtained from the final model. The possible reason for the low f_2 value could be due to the lack of fit when the data is modelled, an r^2 value of 0.859 is obtained. In contrast the 91% dispersion has a f_2 value of 95.46, and an r^2 value of 0.999 when the data is modelled. The poor fit could be due to the rapid initial dissolution experienced by the 71% HPMC dispersion (it has the highest AUC_{20} and polynomial rate of the HPMC dispersions (table 3-2)), that the dissolution begins to plateau at 15 minutes. Therefore this dispersion will not be used within the model due to the failure of the dissolution model to predict an appropriate rate of dissolution. This means that the obtained result is not used in any final discussion, and highlights the pitfalls of developing such a model.

Poor predictability by the model is also evident with the following HPMCP

dispersions: 17%, 50%, 71%, 83% and 91% (table 4-4). This was however anticipated due to the precipitation of the drug after 15 – 20 minutes (depending upon the system, see figure 3-1). A decision was made to utilise the HPMCP dispersion within the model based upon examination of the obtained curves (figures 4-27 to 4-34). Prior to the precipitation of the drug a good fit is obtained with these dispersions, an example being the 50% HPMCP dispersion having an f_2 value of 62 when applied to only the first three points (0.08, 0.17, 0.25 hours). It should be emphasised again that the f_2 test is only being used as an estimation of fit, and that more than twelve replicates are required for the test to be valid. It is hypothesised that the precipitation experienced *in vitro* will not be experienced *in vivo* as troglitazone is a rapidly absorbing drug.

Table 4-5 Derived f_2 values for experimental data versus calculated data (shaded cells highlight the curves where a poor fit was obtained)

	Concentration of polymer in dispersion						
	9%	17%	29%	50%	71%	83%	91%
HPMC	86.31	73.64	77.47	70.35	39.77	86.55	95.46
HPMCP	69.52	49.08	70.81	31.67	7.06	17.38	11.29
PVP	88.05	79.06	54.30	68.41	77.92	65.15	51.02

4.5.7.1.1 Prediction of the *in vivo* performance of the dispersions using the final model

In order to verify that the model functioned correctly the model was developed using the dissolution results of three troglitazone batches, the formulations of which were not disclosed (M94/058C, D157/155B, D157/155D), obtained in FaSSIF fluid (Galia 2000), pharmacokinetic data for these batches was also made available. For each curve that was derived (and the provided data) the following three pharmacokinetic parameters were derived: AUC, C_{max} and T_{max}.

Firstly it was attempted to derive a single model that could predict the performance of all three batches, with one set of parameters that could be used (*i.e.* volume of distribution, half life). Due to the variable pharmacokinetic performance of troglitazone (section 1.5), this proved difficult to do as it was found that each batch performed very differently (*i.e.* volume of distribution $t_{1/2}$ has been found to vary between 7-24 hours). It was, therefore, decided to derive individual parameters for each batch (figures 4-37, 4-36 and 4-38). The predicted *in vivo* performance of each dispersion was then calculated using each set of parameters, this meant that the predicted *in vivo* performance of the dispersions is the mean curve.

Figure 4-37 Comparison of *in vivo* derived data with that obtained through the model for batch M94/058C

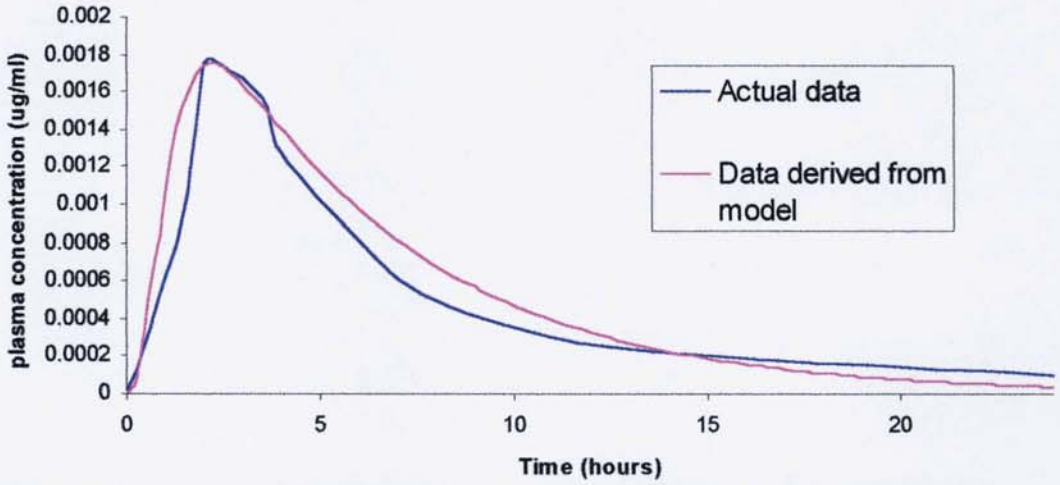

Figure 4-38 Comparison of *in vivo* derived data with that obtained through the model for batch D157/155B

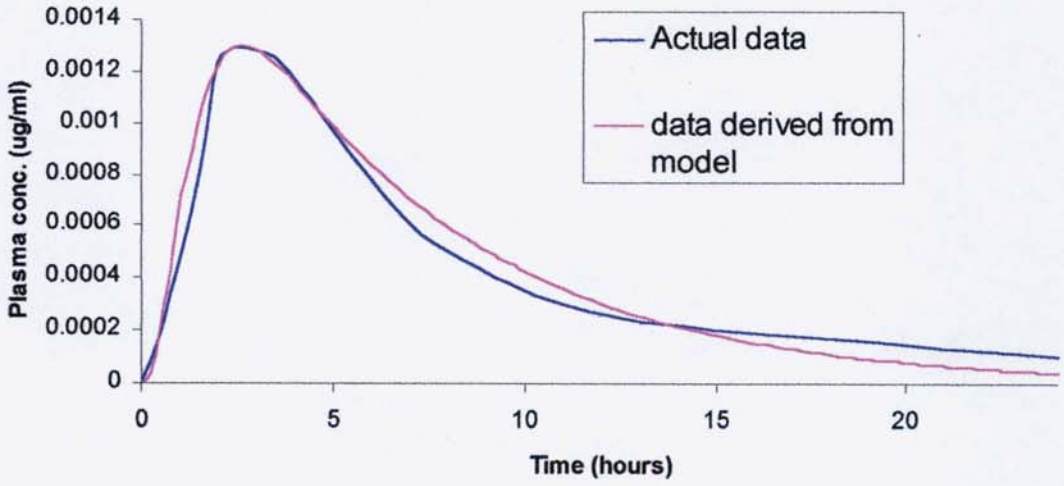

Figure 4-39 Comparison of *in vivo* derived data with that obtained through the model for batch D157/155D

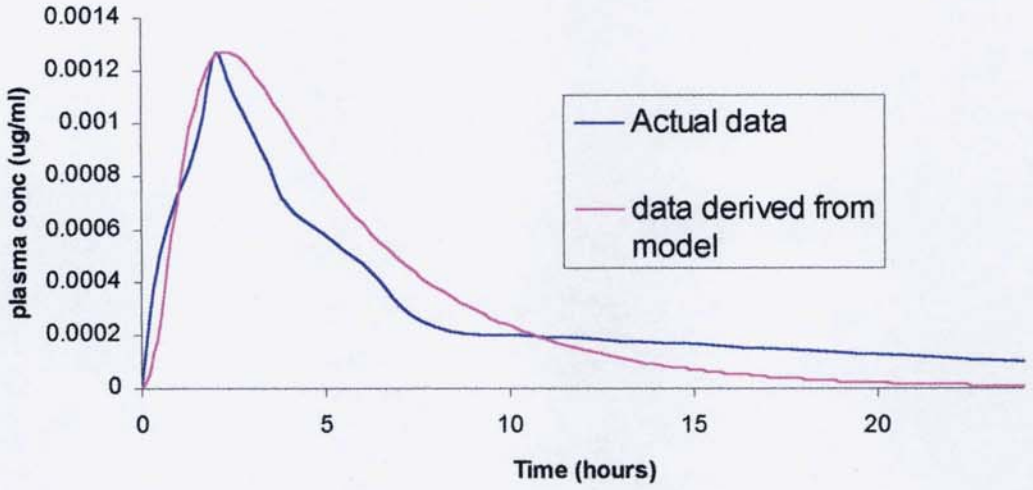

Table 4-6 shows the derived and actual pharmacokinetic data for the three commercial batches of troglitazone. In order to assess the ability of each model to predict the *in vivo* performance for each batch an f_1 test was applied to the plasma-time data obtained from the model and that obtained from the *in vivo* data, this was applied successfully to assess the differences between *in vivo* and model derived profiles by Nicolaides *et al.* (2001). When using f_1 values it is considered that values of > ±15% are considered to be non-equivalent (FDA, 1997). It is shown in table 4-9 that for each batch the f_1 value is less than ± 15%. It can, therefore, be said that each curve derived using the model is equivalent to those obtained through *in vivo* methods. Due to the results obtained here the model was then used to assess the potential *in vivo* performance of the solid dispersions, based on the FaSSIF dissolution.

Table 4-6 f_1 fit factors for the model derived data compared to the *in vivo* data

Batch	f_1 value (%)
M94/058C	-10.08
D157/155B	-3.14
D157/155D	-10.83

To further establish the relevance of the model to *in vivo* data, the following three pharmacokinetic parameters were calculated (using the PK functions for Excel add in (Usansky *et al.* 1999)): AUC, T_{max} and C_{max}. The results, from

both model and the *in vivo* data, are displayed in table 4-7. It is seen that each model is able to predict the trends that are seen with the actual data, *i.e.* M94/058C has a larger AUC than D157/155D. Due the variable nature of troglitazone absorption and that each batch provides different parameters and different models, each dispersion was evaluated using all three models.

Table 4-7 Comparison of model derived pharmacokinetic parameters with those derived *in vivo*

Batch	Source of data	Pharmacokinetic parameter		
		AUC µg/ml.hr	T_{max} (hours)	C_{max} µg/ml
M94/058C	Actual data	11.73	2.00	0.0018
	Model derived	12.65	2.16	0.0018
D157/155B	Actual data	10.49	2.50	0.0013
	Model derived	10.41	2.64	0.0013
D157/155D	Actual data	7.73	2.00	0.0013
	Model derived	7.77	2.40	0.0013

Figures 4-40, 4-41 and 4-42 show the mean derived curves, and tables 4-8, 4-9 and 4-10 show the derived pharmacokinetic parameters for each of the solid dispersions. The model predicts that the dispersions will act differently from each other *in vivo*. It is also expected that the higher polymer concentration HPMCP dispersions will have a higher mean AUC than the other dispersions. This implies that in an *in vivo* scenario that the dispersions with a high concentration of HPMCP would give the high bioavailability. What is also apparent from the data shown in tables 4-9 to 4-11 is that although a higher AUC and C_{max} can be obtained by altering the polymer and polymer concentration the T_{max} remains relatively unaffected. In the case of the HPMCP dispersions only the 71% dispersion sees any improvement, and this is by 4 minutes.

Figure 4-40 Mean model derived plasma-time curves for the HPMC:troglitazone dispersions

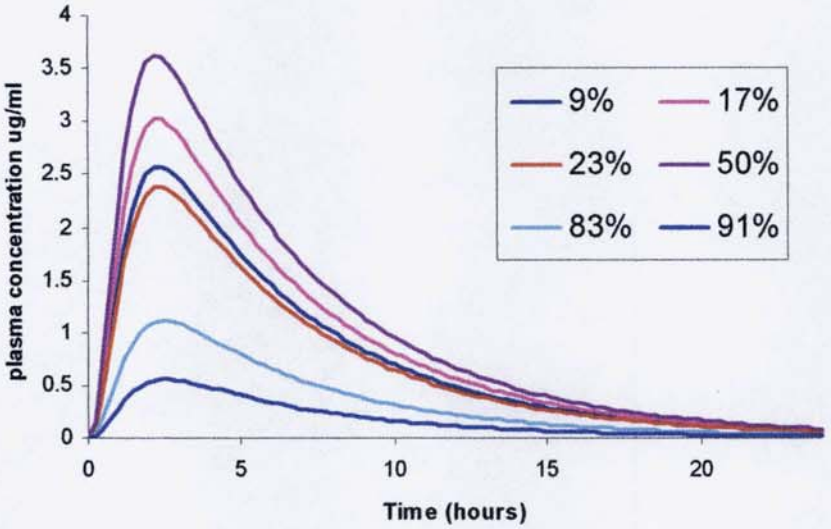

Table 4-8 Pharmacokinetic parameters from the model derived plasma-time profile of the HPMC dispersions

Dispersion	Tmax (hours)	AUC (ug.ml.hr)	Cmax (µg/ml)
9%	2.32 ± 0.14	18.64 ± 8.31	2.58 ± 1.09
17%	2.32 ± 0.14	21.81 ± 9.68	3.03 ± 1.28
23%	2.32 ± 0.14	17.28 ± 7.71	2.38 ± 1.01
50%	2.32 ± 0.14	25.95 ± 11.49	3.62 ± 1.53
83%	2.48 ± 0.14	8.23 ± 3.73	1.11 ± 0.48
91%	2.56 ± 0.14	4.14 ± 1.89	0.55 ± 0.24

Figure 4-41 Mean model derived plasma-time curves for the HPMCP:troglitazone dispersions

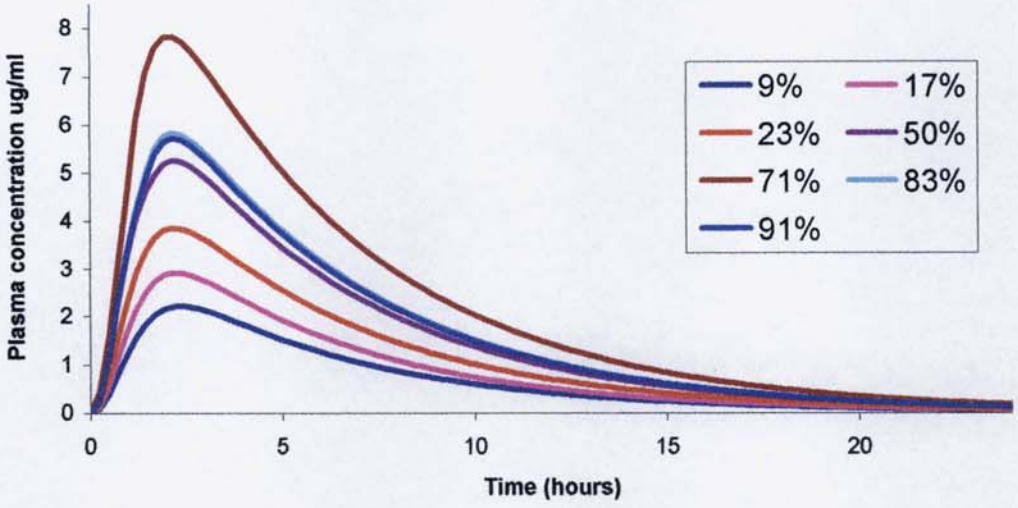

Table 4-9 Pharmacokinetic parameters from the model derived plasma-time profile of the HPMC dispersions

Dispersion	Tmax (hours)	AUC (ug.ml.hr)	Cmax (µg/ml)
9%	2.32 ± 0.14	16.18 ± 7.23	2.23± 0.94
17%	2.32 ± 0.14	20.63 ± 5.23	2.93± 1.09
23%	2.16 ± 0.24	27.64 ± 12.22	3.86± 1.63
50%	2.16 ± 0.24	37.66 ± 16.32	5.27± 2.21
71%	2.08 ± 0.14	55.58 ± 17.35	7.86± 2.17
83%	2.16 ± 0.24	41.5 ± 16.50	5.85± 2.22
91%	2.16 ± 0.24	40.7 ± 16.47	5.74± 2.22

Figure 4-42 Mean model derived plasma-time curves for the PVP:troglitazone dispersions

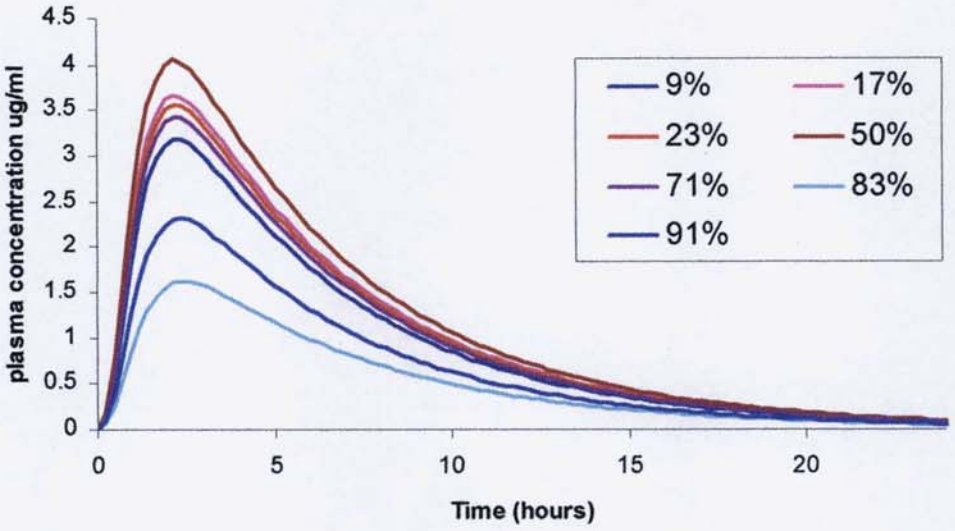

Table 4-10 Pharmacokinetic parameters from the model derived plasma-time profile of the HPMC dispersions

Dispersion	Tmax (hours)	AUC (ug.ml.hr)	Cmax (µg/ml)
9%	2.32 ± 0.14	22.94 ± 10.17	3.19
17%	2.32 ± 0.14	26.32 ± 11.65	3.67
23%	2.32 ± 0.14	25.56 ± 11.32	3.56
50%	2.16 ± 0.24	29.06 ± 12.84	4.06
71%	2.32 ± 0.14	24.64 ± 10.92	3.43
83%	2.40 ± 0.00	12.52 ± 9.69	1.62
91%	2.32 ± 0.14	16.81 ± 7.51	2.32

As discussed in section 1.4 the absorption potential was proposed by Dressman *et al.*, (1985) as a method of predicting the potential of the drug to be absorbed through the GI tract. A relatively good correlation was found between the absorption potential and the pharmacokinetic performance of a series of drugs. For the purpose of this study the solubility of the drug is substituted by the maximum amount of drug dissolved from the dispersion during dissolution, in the absorption potential equation.

It is shown in figure 4-43 that a satisfactory correlation has been obtained between the absorption potentials and AUCs of each dispersion. Although the absorption potential model has its limitations (section 1.3) it does give some extra confidence that the derived models are showing results that have some relevance to the potential *in vivo* performance of the dispersions.

Figure 4-43 Plot of calculated absorption potential vs obtained AUC from model

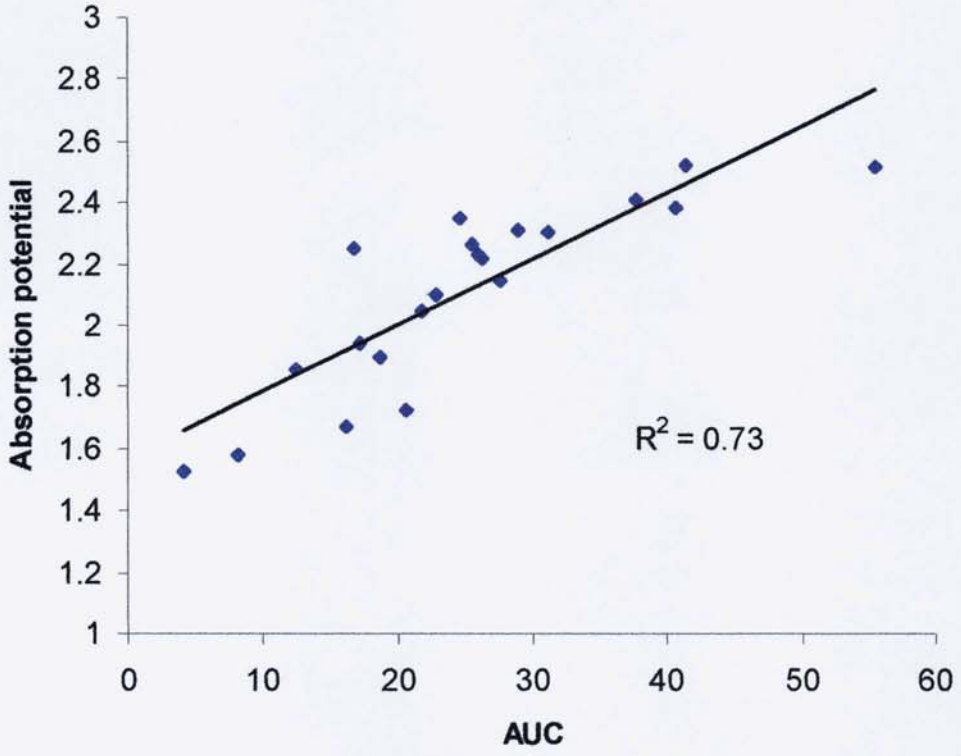

One aspect that comes out of this is that the the solid dispersions are predicting much higher bioavailabilty than the marketed troglitazone samples (figures 4-37 – 4-41), this could be due to the fact that there are differences in the ways the formulations were added to the *in vitro* dissolution vessel. The marketed troglitazone would have been added in tablet form, whereas the solid dispersions were added as free powder. This means that prior to any troglitazone being released from the marketed formulation the tablet would have to disintegrate before the drug is available for dissolution, thus a slower initial dissolution rate would occur. In the case of the solid dispersions there would have to be no disintigration occurring and there would be a much larger surface area from the onset of dissolution. Therefore, it would be advisable to perform some bioavailability studies upon the solid dispersions to ensure that

the model is full optimised.

The other aspect is that the *in vitro* dissolution of the solid dispersions was performed at 75 rpm. It was shown in section 3.2 that the paddle speed has a significant effect upon the dissolution rate of the solid dispersion. It would therefore, as recommended in section 3.2, to perform bioavailability studies in order to fully optimise the *in-vitro* dissolution test.

However, it has been shown that if *in vivo* data is available it is possible to design a model that could give an early indication as to the performance of a formulation *in vivo*. Such a model, once made, would allow for a quick and easy early assessment of a potential formulations performance *in vivo*.

5 Investigation of the underlying mechanisms controlling release of the drug from solid dispersions

5.1 Introduction

There are various theories as to why solid dispersions enhance dissolution of sparingly soluble drugs (these are covered in section 1.3.2.3). In section 3.1 it was shown that the polymer used in the dispersion had a large effect upon the dissolution of troglitazone, and to a lesser extent on atovaquone. The behaviour of the drugs with each polymer, in liquid phase, were investigated, due to it being apparent from the mechanism described by Craig (2002) that the dissolution of the drug into the polymer layer is a critical step that determines the mechanism by which the drug dissolves into the bulk solution. It was proposed that slow dissolution into the polymer results in the dissolution being controlled by the properties of the drug (*I.e.* drug-controlled mechanism); and rapid dissolution of the drug into the polymer results in the carrier-controlled mechanism. Three mechanisms have been proposed; by the possible wetting effects of the carrier, the polymer inhibiting the precipitation of the drug from the supersaturated state and the effect of the polymer dissolution rate. In order to understand the potential mechanisms by which the solid dispersions enhance the dissolution of drugs it is useful to investigate the interactions between the drugs and the polymers in liquid phase.

5.1.1 Increased wetting of the drug by the carrier

As discussed in section 1.3.2.3, one of the earliest proposed mechanisms for the enhancement of dissolution by solid dispersions was that the polymer could aid the wetting of the drug (Chiou and Reigelman, 1971). This link between enhanced dissolution and solubility was first discovered with solubility studies conducted with chloramphenicol in urea solutions (Goldberg *et al.* 1966). As the concentration of urea increased in the aqueous solutions, the solubility of choloramphenicol increased (at 0% urea the solubility was approximately 5 mg/ml and at 45% urea the solubility was approximately 25 mg/ml). This paralleled dissolution of the solid solution, which demonstrated a 3.5-fold increase of drug dissolved compared to the pure drug. It was also found that the rate of dissolution of the drug from the physical mixture and

from the eutectic mixture was higher than the drug alone. This enhanced dissolution rate was attributed to the fact that the drug dissolves into the micro-environment of urea (a saturated urea solution), in which it is far more soluble. The enhanced dissolution rate of the physical mixtures and eutectic mixture, however, cannot be attributed to the fact that urea improves the wettability of the chloramphenicol as urea increases the surface tension of water (Bresslow and Guo, 1990). Although the actual mechanism by which urea enhances the solubility of hydrophobic materials is unclear there is a potential mechanism which attempts to explain this observation. This model is known as the Frank and Frank model (Grdadolnik and Maréchal 2002), and in this model the urea disrupts the water structure around the solute, thus forming cavities within the water for the hydrophobic materials to dissolve into. Studies have shown that urea does indeed have the ability to break up the tetrahedral structure of the water by forming hydrogen bonds (using the amine and carbonyl functional groups on the urea molecule) with the water molecules (Idrissi, 2005).

Other studies have found a similar pattern with regards to the enhancement of dissolution using physical mixtures. A study investigating reserpine-PVP solid dispersions found that the physical mixture of the two components improved the dissolution rate when compared to the drug alone (Bates, 1969). This, again, was attributed to the drug dissolving into the polymer-rich micro-environment, with the possible mechanism being through complexation. The idea of complexation fits with the information found when the surface tensions and contact angles of polymer solutions are investigated. It is found that, in solutions of HPMC, the contact angle of the solution increases, thus reducing the spreading of the solution (see section 1.2.3) (Riedl *et al.* 2000). This early observation fits in with the carrier-controlled mechanism proposed by Craig (2002) (section 1.3), which attributed the dissolving (or diffusion) of the drug into the diffusion layer as the rate determining step for solid dispersions.

5.1.2 Crystal-growth inhibition by the carrier

Studies show that the presence of a polymer, whether in the solid state or present in a liquid, can help prevent the recrystallisation of a drug from an

unstable state, for example the amorphous state (Van der Mooter *et al.* 2001), or a supersaturated state (Tanno *et al.* 2004).

PVP has been shown to inhibit crystal growth. One study investigated the ability of PVP to inhibit precipitation from super-saturated systems (Sekikawa *et al.* 1978). In the study by Sekikawa *et al.* (1978) super-saturated solutions were prepared from solutions of the drug in absolute ethanol, at an elevated temperature (50°C). These solutions were then allowed to cool at a controlled rate (12°C/h), thus promoting re-crystallisation at lower temperatures. It was found that adding PVP to the super-saturated solutions slowed the rate of recrystallisation of sulphisosoxazole, sulphamethizole and sulphamerazine. The effect was also found to be additive, so the more PVP added the more pronounced the effect. The mechanism proposed by Sekikawa *et al.* (1978) was that the polymer and the drugs formed *in situ* complexes with the PVP; this was backed up by calculation that indicated that relatively stable complexes can be formed with PVP. The PVP did not, however, have the same effect upon the other drugs tested (caffeine and nalidixic acid); this was determined to be due to these drugs being unable to interact with the PVP.

The PVP-sulphathiazole system was investigated some years earlier with regard to the growth of the crystal (Simonelli *et al.* 1970). It was noted that PVP alters the shape of the growing crystal, which it was concluded was the main reason behind the inhibition. Figure 5.1 shows a schematic representation of the growth of the sulphathiazole crystals, illustrating the change in growth due to the addition of PVP. It was postulated that the PVP can form a mesh-like structure over the crystal (figure 5.2), and the crystal growth continues through the pores in the mesh, thus explaining the crystal structural change at the addition of PVP. This model was supported by the fact that the diffusional rate of the PVP to the crystal surface was the determining factor, coupled with the proposal that a strong interaction between PVP and drug must be involved due to the small amount of PVP required to inhibit the growth. This model could possibly be applied to theory of solid dispersions, in so much that it could explain the apparent wetting that has been reported to be caused by the polymers (section 5.1.1).

Figure 5-1 Appearance of the crystal surface of sulfathiazole: A, original crystal at time 0: B, after normal growth (note the straight edge): C, after the addition of PVP (note the jagged edge, indicating polymer inhibition. Adapted from Simonelli *et al.* 1970).

Figure 5-2 Highlighting the crystal growth through the polymer net (Adapted from Simonelli *et al.* 1970)

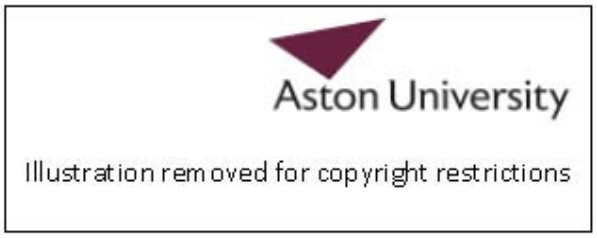

It has been suggested, that some polymers are better at inhibiting the re-crystallisation of a drug from a super-saturated solution than others. This can be used to explain the differences, in dissolution rate of the same drug, observed between solid dispersions of different polymers (Tanno *et al.* 2004). This study investigated the ability of several polymers to inhibit the precipitation of naproxen from super-saturated solutions. The results showed a strong correlation between the level of protection of recrystallisation from the supersaturated system and the dissolution of the drug from the polymer. This extends earlier data, which suggested that there is a physico-chemical interaction between the polymer and drug when in solution (Hasegawa *et al.* 1985). The findings of this study, similar to Simonelli *et al.* (1970), were that whilst in solution the drug nuclei adsorbs to the surface of the polymer, thus forming an *in situ* complex. This inhibits the re-crystallisation of the drug from solution. The differences observed in the re-crystallisation rate of the naproxen from the super-saturated solutions, was the only difference found between the polymers. Infra-red spectroscopy carried out on the solid dispersions showed no differences between the polymers (Tanno *et al.* 2004).

The suggestion that the increased dissolution of the dispersion due to the carrier's ability to inhibit the re-crystallisation of the drug is an interesting

concept and one to which attention has been paid. It could well be that in the early stages of dissolution of a dispersion, it would be easy for recrystallisation to occur. This would be due to the high local concentration of freshly released drug (from the dispersion), in an environment of lower viscosity than is found within the solid dispersion (one of theories behind the stability of solid solutions is that the viscosity is sufficient to prevent re-crystallisation of the drug within the dispersion (Van der Mooter *et al.* 2001) so the likelihood of drug-drug interaction and crystal growth is a lot higher than it was in the dispersion.

5.1.3 Dissolution of the carrier

As previously discussed in section 1.3.2 it has been postulated that there are two principal mechanisms controlling the release of drug from the solid dispersion: the carrier-controlled, and the drug-controlled (Craig 2002). One method for investigating whether or not these mechanisms are occurring is to examine the behaviour of the carrier during dissolution.

So far in the literature, there have been few examples of the carrier dissolution being followed during the dissolution of solid dispersions. The most prominent example was by Corrigan (1985), where the dissolution rate of PEG was followed colormetrically from different drug-polymer systems. Alternatively the prediction of the carrier dissolution from solid dispersions has been done by using the disintegration time as a way of approximating the polymer dissolution. This has the advantage in that it is a simple method to perform, and gives a way of comparing one dispersion to another. It does not on the other hand represent what is occurring within a dissolution bath, and gives neither rate data nor profile data.

There have been various methods proposed to study the dissolution behaviour of polymers; these include differential refractometry, optical microscopy, fluorescence and gravimetry (Miller-Chou & Koenig 2003). This section provides a review of these techniques, together with their advantages, disadvantages and their possible usefulness in following the dissolution of a carrier from a solid dispersion.

The method of differential refractometry exploits the fact that, as the polymer concentration increases within the solution, the refractive index changes; this is one of the earliest methods used to follow polymer dissolution. This method can be used for detecting an increase in the polymer concentration and appears sensitive to change in the concentration. It has, though, some disadvantages, it can only be used for high concentrations of polymer and is not very sensitive for small concentrations of polymer (Miller-Chou & Koenig, 2003). It can, also, only be used to detect solutions of polymer alone, as if anything else added to the solution, *e.g.* a drug, will affect the refractive index.

The process of optical microscopy allows for direct observation of the dissolution of the polymer within a given solvent. This, therefore, makes it a practical technique for establishing how the polymer dissolves, *e.g.* the formation of the gel layer and the penetration of the solvent into the matrix. This technique, in theory, would be able to follow the behaviour of a solid dispersion and allow information to be obtained on the surfaces of the polymer in question. The main issue is that no quantitative information can be obtained. This means that it would not be possible to obtain dissolution profiles of the polymer.

It would be possible to measure dissolution rates of a polymer using laser inferometry (Rodriguez *et al* 1985). This involves the placing of a polymer film between two mirror lenses (within the solvent), and then passing monochromatic light through the film. The dissolution of the polymer can then be calculated based upon the interference lines from the monochromatic light. The disadvantages with this method are that it can only be used with a transparent film of polymer, no dissolution profile can be obtained and, finally, the sensitivity of the method is very much dependent upon the uniformity of the film surface.

An alternative to optical methods is the use of gravimetric methods to follow the dissolution of a polymer. One such method is to prepare pellets of the polymer and perform a dissolution test using these pellets. The dissolution run

is stopped at predetermined time points to weigh the pellet. One of the issues against using this method is that preparation of the pellet involves compression and these forces may be sufficient to destroy the structure of the solid dispersion.

A technique called microviscometry has been shown to successfully follow the dissolution of PVP from a solid dispersion (Esnaashari *et al.* 2005). This method exploits the fact that as a polymer dissolves into solution the viscosity of that solution increases, and that the instrument is capable of distinguishing the viscosity between low polymer concentration solutions, as shown by the calibration curves. The benefits of such a method are that samples can be taken during the dissolution run (so that drug concentration and polymer concentration can be examined concurrently), and that only a small sample is required – typically 1 – 2 ml.

5.2 Dissolution of the drug with the polymer pre-dissolved into dissolution media

5.2.1 Introduction

It is the aim of this study is to investigate the effect that the polymers have upon the dissolution of pure troglitazone. The concentrations of polymer that are relevant to the levels found when full dissolution of the 9% (which would relate to 0.04 mg/ml) and 91% (which would relate to 4 mg/ml) dispersion were examined. Polynomial fit is reported for the dissolution profiles, as this (section 3) allows the estimation of an initial dissolution rate that is important when examining the effect of wetting. The other parameter investigated is the peak level of drug dissolved after ninety minutes, as it has been reported that increased viscosity of PVP solutions, drug solubility can increase (de Schmidt *et al.* 1991).

5.2.2 Experimental

5.2.2.1 Materials

The materials used in this experiment are described in sections 2.2.2.1, 2.4.2.1 and 2.6.1.1.

5.2.2.2 Equipment

Dissolution was performed using the equipment described in section 2.6.1.2. Analysis was performed on the HPLC system described in section 2.2.2.2.

5.2.2.3 Method

The FaSSIF fluid was prepared as previously described in section 2.6.1.3 except that sufficient HPMC/HPMCP or PVP was added to make a polymer concentration of 0.04 or 4.0 mg/ml. These concentrations are representative of 100% polymer dissolution from a 9% or 90% polymer dispersion. The dissolution testing was carried out as described in section 2.6.1.3. The samples were then analysed using the HPLC method described in section 2.2.2.3.2. ANOVA tests were performed using Graphpad's Instat 3 software package.

5.2.2.4 Results and discussion

The dissolution of troglitazone in the presence of the three polymers is shown in figures 5-3, 5-4 and 5-5 (figures 5-6, 5-7 and 5-8 show the first 10 minutes of the dissolution, so that differences in the dissolution found by the polynomial rates can be more clearly seen). The rates, derived from the polynomial fit of the curves (described in section 3.1.3.7), are in table 5.1 and indicate that the presence of the polymer can affect the dissolution of troglitazone. There are large increases in this derived rate, especially when the polymer concentration is 4 mg/ml. What is also seen from the data is that although there is this increase in the initial dissolution rate, there is no overall effect upon the amount of drug dissolved. The results of an ANOVA on the AUC after twenty minutes show no significant difference ($p<0.05$) between any of the AUCs. The data in table 5.2 show that compared to troglitazone there is no significant difference in AUC when the polymers are added, except for the HPMCP 4 mg/ml.

Figure 5-3 Dissolution of troglitazone in FaSSIF containing varying levels of PVP. Results are the mean of three replicates, error bars ± SD.

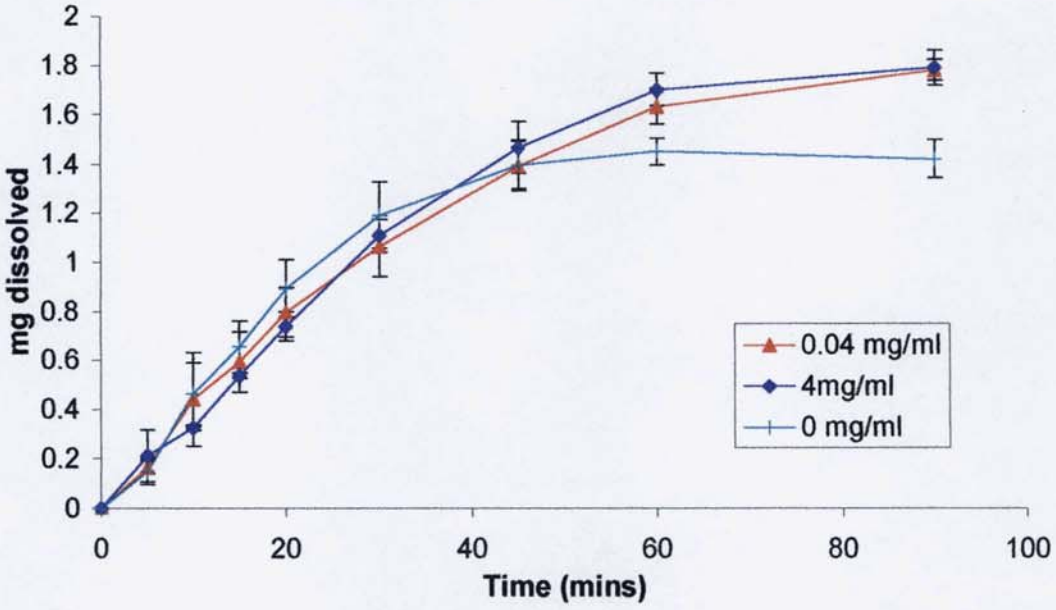

Figure 5-4 Dissolution of troglitazone in FaSSIF containing varying levels of HPMCP. Results are the mean of three replicates, error bars ± SD.

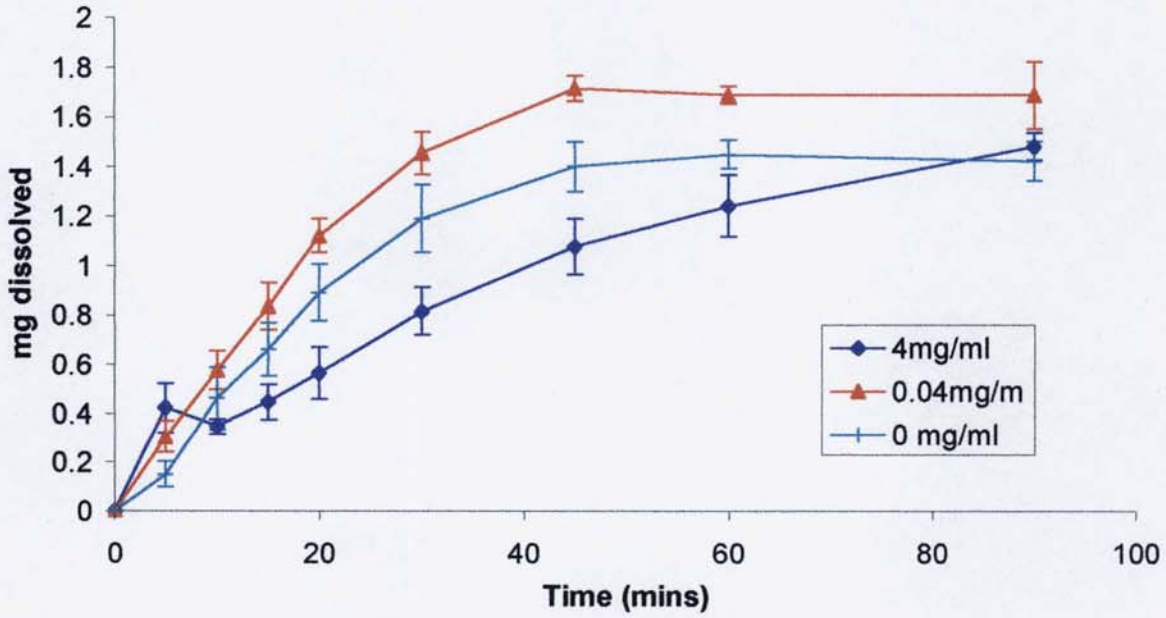

Figure 5-5 Dissolution of troglitazone in FaSSIF containing varying levels of HPMC. Results are the mean of three replicates, error bars ± SD.

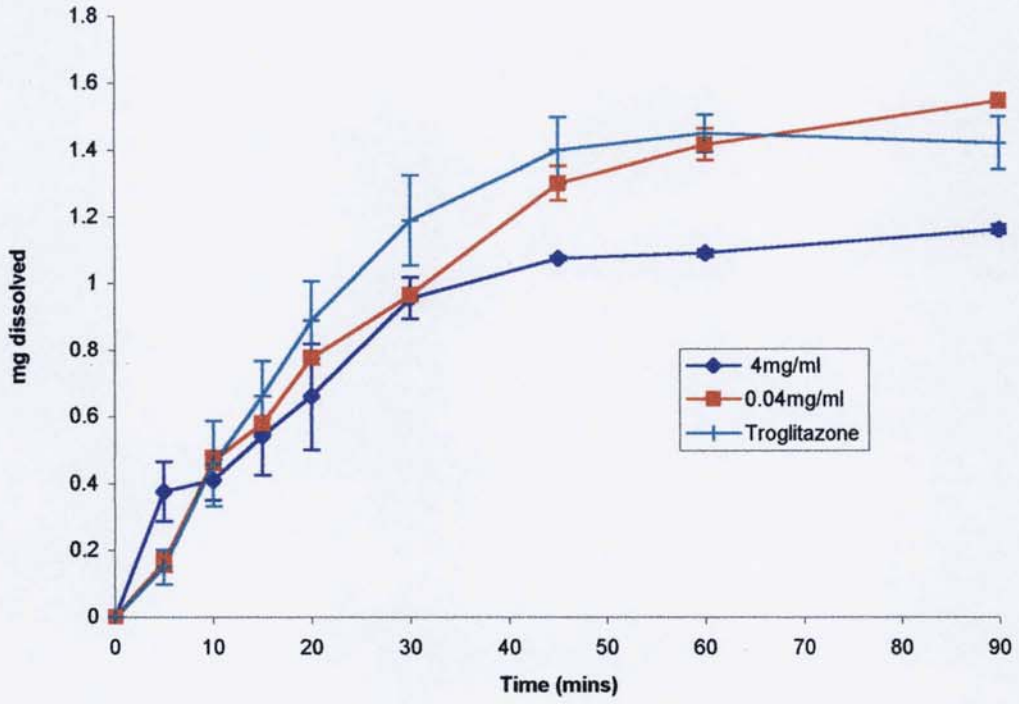

Figure 5-6 Dissolution of troglitazone in FaSSIF, over the first ten minutes, containing varying levels of HPMC. Results are the mean of three replicates, error bars ± SD.

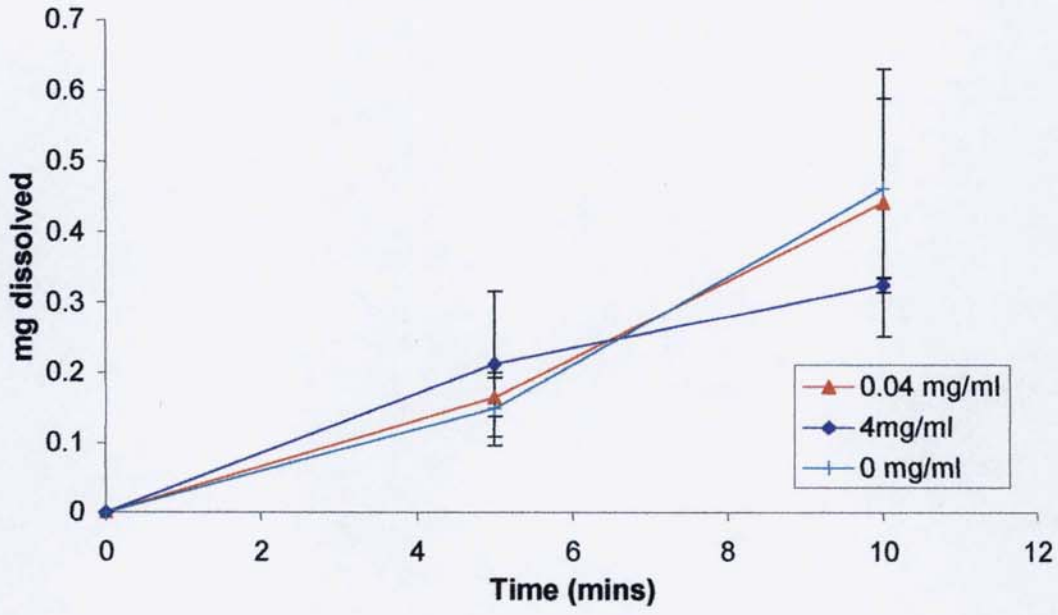

Figure 5-7 Dissolution of troglitazone in FaSSIF, over the first ten minutes, containing varying levels of HPMCP. Results are the mean of three replicates, error bars ± SD.

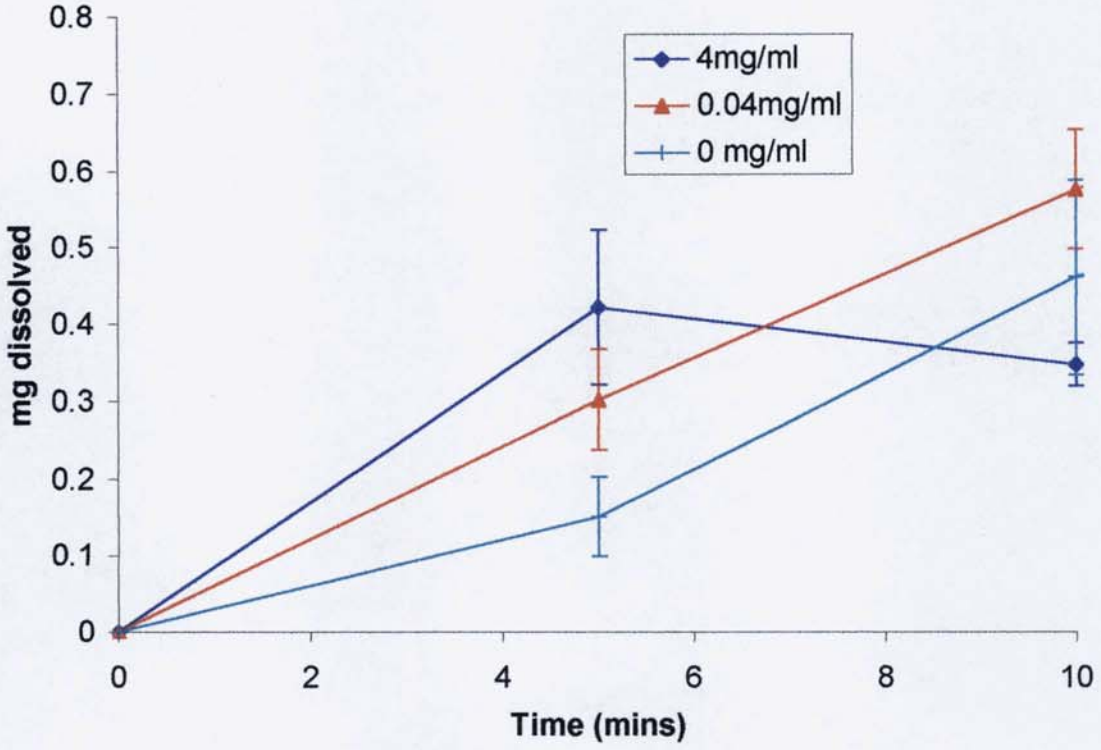

Figure 5-8 Dissolution of troglitazone in FaSSIF, over the first ten minutes, containing varying levels of HPMC. Results are the mean of three replicates, error bars ± SD.

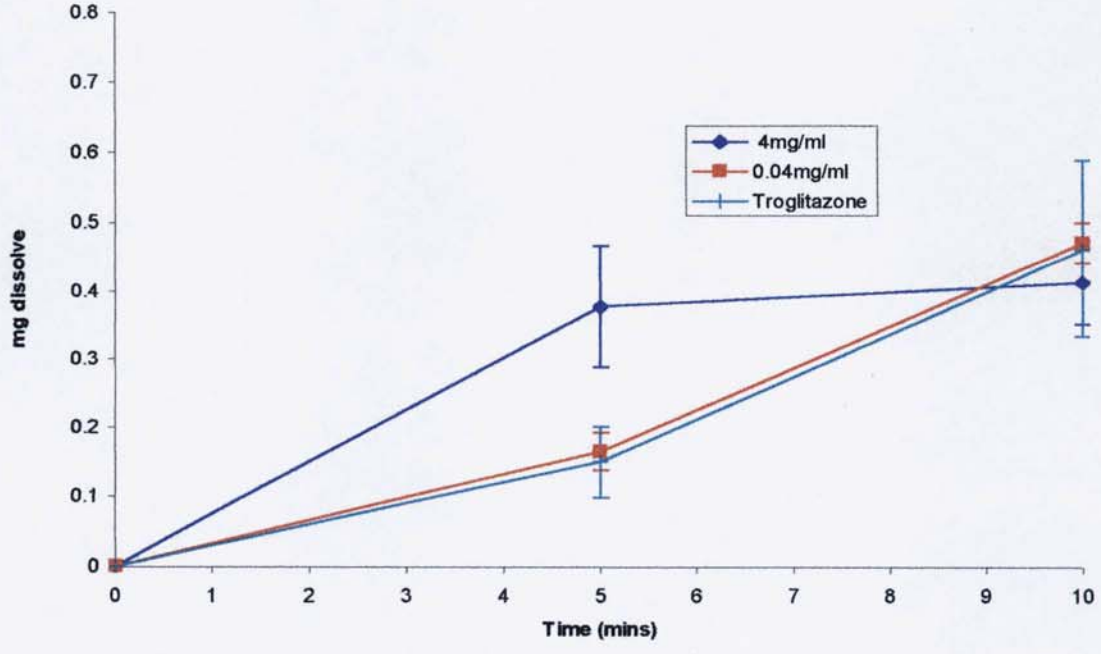

Table 5-1 AUC and polynomial rate data from the dissolution of troglitazone in FaSSIF with either HPMC, PVP or HPMCP pre-dissolved in it

	AUC 20 ($mg.ml^{-1}.min$)	AUC 90 ($mg.ml^{-1}.min$)	Rate (mg/min)
No polymer	8.56 ± 2.54	102.77 ± 10.76	0.032 ± 0.004
PVP (0.04 mg/ml)	9.23 ± 3.89	110.77 ± 8.69	0.047 ± 0.015
PVP (0.4 mg/ml)	7.22 ± 0.68	111.82 ± 4.81	0.112 ± 0.035
HPMCP (0.04 mg/ml)	11.34 ± 1.34	124.09 ± 3.10	0.066 ± 0.015
HPMCP (4 mg/ml)	7.32 ± 0.35	77.24 ± 16.81	0.195 ± 0.072
HPMC (0.04 mg/ml)	9.25 ± 2.12	99.79 ± 4.02	0.044 ± 0.007
HPMC (4 mg/ml)	8.31 ± 0.79	81.64 ± 2.27	0.166 ± 0.086

It is, though, the rate that is the interesting parameter, as this is an indicator to the effect of the polymer as a wetting agent of the drug. As discussed in section 3.1, the polynomial fit provides an estimation of the initial dissolution rate of the drug. It is noticeable from table 5-1 that as the amount of polymer is increased the rate of dissolution of the drug increases. Examination of figures 5-6 to 5-8 shows that in the case of PVP (figure 5-6) this rate increase is not significant, when compared to troglitazone (as the SD bars are all overlapping). In the case of HPMCP (figure 5-7), the addition of polymer at any level gives a significant increase when compared to FaSSIF alone, however the increase between polymer levels cannot be considered significant. With HPMC (figure 5-8), only the high level of polymer (4.0 mg/ml) shows a significant increase upon FaSSIF alone. This effect could be due to an enhancement in the wetting of the drug by each of the polymers, with HPMCP showing the best improvement in wetting. Although the effect is very minimal, it could though have an impact upon the behaviour of the solid dispersions. If the carrier controlled dissolution method is considered (section 1.3.2.3) the rate limiting step in the mechanism is the dissolution of the drug into the polymer. It follows that the carrier with the superior wetting properties of a drug will undoubtedly allow a drug to dissolve into it quicker. As already discussed the effects in this experiment are minimal, and it was stated that it is assumed that the polymer diffusion layer is very concentrated in the carrier

and drug-controlled mechanisms (Craig 2002).

Table 5-2 The results of Tukey analysis of the AUC_{90} data of the dissolution of troglitazone in FaSSIF containing varying concentrations of polymer (shaded boxes indicate those that are considered similar to each other)

	Troglitazone	HPMCP 0.04	HPMCP 0.4	HPMC 0.04	HPMC 0.4	PVP 0.04
Troglitazone						
HPMCP 0.04	>0.05					
HPMCP 0.4	<0.05	<0.001				
HPMC 0.04	>0.05	<0.05	>0.05			
HPMC 0.4	>0.05	<0.001	>0.05	>0.05		
PVP 0.04	>0.05	>0.05	<0.01	>0.05	<0.05	
PVP 0.4	>0.05	>0.05	<0.01	>0.05	<0.05	>0.05

The results of the dissolution rates of troglitazone in the polymer solutions were compared to the dissolution of troglitazone from the solid dispersions. The dispersions containing 29% (w/w) of polymer were selected as it is predicted that these dispersions undergo dissolution *via* a drug-controlled mechanism. Despite the upper polymer concentration (4 mg/ml) representing the dissolution of the polymer from a 91% solid dispersion the 71% (w/w) dispersions were selected. This was due to the difficulties found with the 91% HPMC solid dispersion, *i.e.* the polymer forming a gelatinous layer on top of the dissolution medium. The parameters examined from the dispersions are the rate (calculated from the polynomial fit), maximum concentration obtained, M_{max} and AUC_{20}.

When the rank orders (solid dispersion data obtained from table 3-2), for the solid dispersions, were compared with those obtained for troglitazone in polymer solutions there are some noticeable patterns emerging (table 5-3). For all the parameters examined for the solid dispersions the HPMCP 71% (w/w) dispersions is the best performing dispersion, this is mirrored by the dissolution rate of troglitazone is at its fastest in the 0.4 mg/ml HPMCP solution. It is also noticeable that the HPMC 29% dispersion is found to be the

poorest performing dispersion, it is also found that troglitazone had the lowest dissolution rate 0.04 mg/ml, when compared to the other polymer solutions.

Table 5-3 Rank order comparison of the dissolution of troglitazone in polymer solutions with the dissolution of troglitazone from solid dispersions of either PVP, HPMCP or HPMC

Polynomial rate of troglitazone in polymer solution (mg/ml)	Polynomial rate of troglitazone from the solid dispersions (w/w)	AUC_{20} of troglitazone from solid dispersions	M_{max} of troglitazone after dissolution from solid dispersions
HPMCP 0.4	HPMCP (71%)	HPMCP (71%)	HPMCP (71%)
HPMC 0.4	HPMC (71%)	HPMC (71%)	PVP (71%)
PVP 0.4	HPMCP (29%)	HPMCP (29%)	HPMC (71%)
HPMCP 0.04	PVP (29%)	PVP (29%)	PVP (29%)
PVP 0.04	HPMC (29%)	PVP (71%)	HPMCP (29%)
HPMC 0.04	PVP (71%)	HPMC (29%)	HPMC (29%)

The position of the dissolution rate of troglitazone in the 0.04 mg/ml HPMCP solution in the rank order mirrors the performance of the 29% (w/w) HPMCP solid dispersions. Examination of the dissolution rate of troglitazone from the 29% dispersion shows that this dispersion has the fastest initial rate of the low polymer concentration dispersions, and the highest AUC_{20}. When the dissolution rate of troglitazone in the 0.04 mg/ml solution is considered it is also found that the highest increase in rate, compared to pure troglitazone, is found.

The way that the AUC_{20} and the initial dissolution rate, of the dispersions, mirror that of the dissolution of troglitazone, in polymer solutions, indicates that the presence of the polymer has a positive effect upon the dissolution of troglitazone. As discussed in section 5.1.1 there are two possible mechanisms as to how this is accomplished; I) increased wetting by the polymer, or II) by some complexation mechanism. As shown by Riedl *et al.* (2000) the addition of HPMC to a solution increases the contact angle, thus reducing the spreading and wetting of the solution, which would serve to reduce the

dissolution rate. Results presented in section 5.3, show that the HPMCP is the most efficient polymer at inhibiting the precipitation of troglitazone from a super-saturated solution. It was suggested by Hasegawa *et al.* (1985) that a polymer inhibits precipitation by a physico-chemical interaction between the polymer and the drug. Further work would have to be performed to establish the extent at which each polymer complexes with troglitazone. This could be achieved by preparing suspensions of troglitazone using each polymer, removing the powder, by centrifuging, and then measuring the concentration of polymer in the supernatant. A mass balance is then performed between the original polymer concentration and the supernatant concentration.

5.3 Effectiveness of the polymers at protecting re-crystallisation

5.3.1 Introduction

It was highlighted in section 5.1.2 that the performance of a dispersion in enhancing the dissolution of a drug could be linked to the ability of a carrier to inhibit precipitation of the drug from a super-saturated solution. It was, therefore, the aims of this study to evaluate the ability of HPMCP, PVP and HPMC to inhibit the precipitation of troglitazone from supersaturated alcohol solutions, and to investigate the effect of polymer concentration on the rate of polymer precipitation.

5.3.2 Experimental

5.3.2.1 Materials

See sections 2.2.2.1, 2.4.2.1 2.6.1.1 for details of the materials used. Ethanol was supplied in-house.

5.3.2.2 Equipment

HPLC equipment is described in section 2.2.2.2.

5.3.2.3 Methods

5.3.2.3.1 Solubility investigation

The following aqueous solutions of ethanol were prepared 20%, 40%, 60%, 80% 100% (v/v) in distilled water. Troglitazone was then added in excess to

10 ml of aqueous ethanol solution into vials, the vials were sealed using laboratory film to minimise evaporation of the ethanol. These samples were then placed on the flask shaker for ten minutes, setting 4. These samples were then place in the water bath (set to 37°C), agitator-setting 4 (60 cycles per minute) for twelve days, samples were checked on a daily basis and troglitazone added to any sample where complete dissolution had occurred. Aliquots were taken on the twelfth day; 5 ml was withdrawn and filtered into a HPLC vial (with the first 3 ml discarded), using a 0.45 μm cellulose acetate syringe filter.

HPLC analysis was carried out as described in section 2.2.2.3.1

5.3.2.3.2 Precipitation experiment

A ninety percent solution of aqueous ethanol was prepared. 50 mg of troglitazone and 50 mg of polymer were dissolved into 25 ml of the aqueous ethanol. These were placed into water bath overnight at 37°C. An aliquot of 5 ml was extracted and diluted 100 times in ethanol and analysed to give the initial concentration. The remaining 20ml was added to 40ml of distilled water in order to make a thirty percent aqueous ethanol solution (this enabled a supersaturated solution of a degree of 66).

Samples were taken at the following intervals 15, 30, 60, 90, 120, 180, 240 mins and 48 hours. 5 ml aliquots were taken using 5 ml syringes and then the samples were centrifuged for one minute at 500rpm. 1 ml was then extracted and diluted 1:1 with ethanol prior to HPLC analysis.

HPLC analysis was carried out as described in section 2.2.2.3.1

5.3.2.4 Results and discussion

The results are shown in figure 5-9 and illustrate the expected increase in solubility as the alcohol content increases. In order to predict the solubility of troglitazone at different concentrations of ethanol a semi-log plot can be plotted (as shown in figure 5-10), thus enabling a linear plot to be obtained. Using the derived equation of the line it then possible to calculate % of co-

solvent required to dissolve the required amount of drug.

Figure 5-9 Solubility of troglitazone in the presence of ethanol. Results are the mean of three replicates, error bars ± SD.

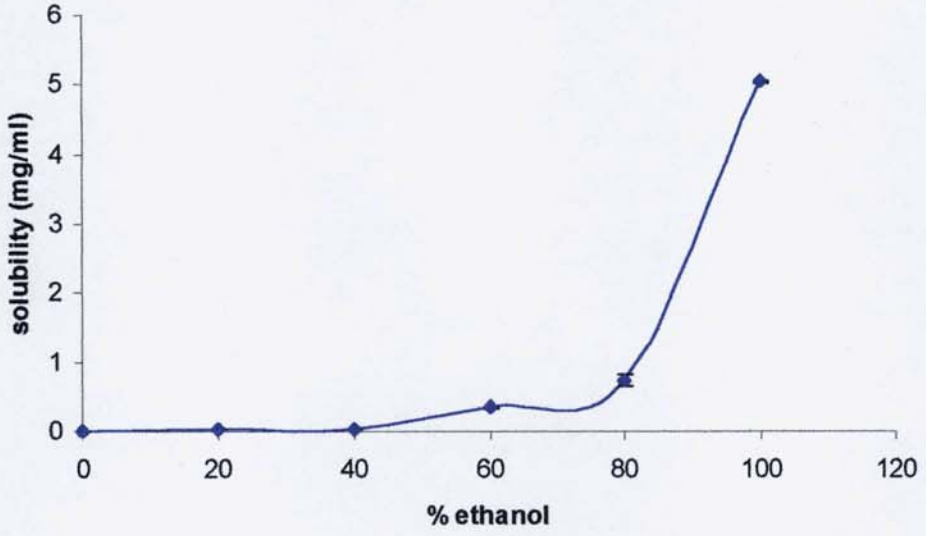

Figure 5-10 Ln plot of solubility of troglitazone in the presence of ethanol. Results are the mean of three replicates, error bars ± SD.

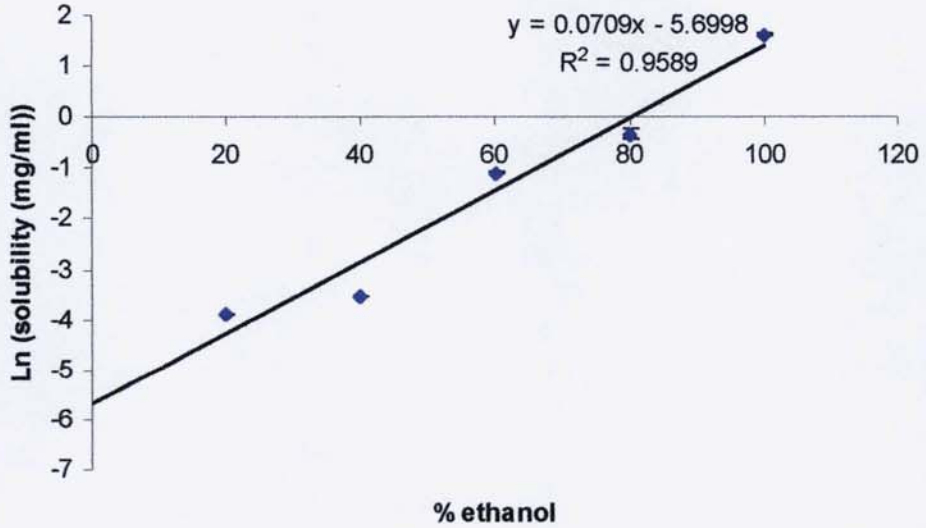

The results displayed in figure 5-11 and table 5-4 show that the polymer HPMCP appears to have the best ability to inhibit the re-precipitation of troglitazone from a supersaturated system. Even after 48 hours there is still the presence of a super-saturated system in the presence of 1 mg/ml HPMCP. Cellulose polymers appear more effective at preventing

recrystallisation. This was reported by Tanno *et al.* (2004), for troglitazone with the same three polymers.

Table 5-4 Rate of precipitation of troglitazone from supersaturated solutions containing 1mg/ml polymer

Polymer	Slope (mg/min)	Conc. of drug after 48 hrs (mg/ml)
No Polymer	1.06E-03 ± 1.13E-04	0.028 ± 0.004
PVP	9.89E-04 ± 2.94E-04	0.026 ± 0.007
HPMC	6.14E-04 ± 1.22E-04	0.037 ± 0.008
HPMCP	1.88E-04 ± 8.20E-05	0.085 ± 0.006

Figure 5-11 Protection of drug precipitation from solutions containing 1mg/ml of polymer

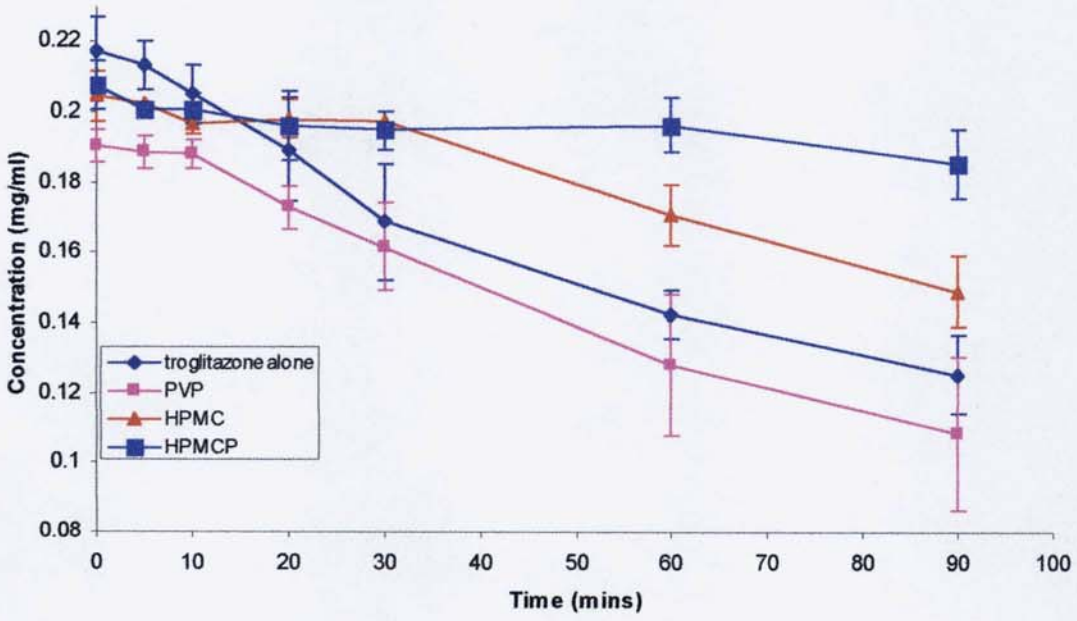

If the results in table 5-4 and the polynomial dissolution rates for the 50% polymer troglitazone dispersions (table 3-2) are considered, a similar rank order becomes apparent. The initial dissolution rate of the 50% HPMCP dispersions is quicker than that of either the 50% HPMC or PVP dispersions, with the HPMC being quicker than the PVP. This same relationship is found in the precipitation study; the HPMCP being more effective than the HPMC and

PVP, with again the HPMC working better than PVP. This correlates with the results found by Tanno *et al.* (2004), where it was suggested that this behaviour could explain why certain polymers release quicker than others. If the mechanism for the inhibition of precipitation proposed by Simonelli *et al.* (1971) (section 5.2) is considered it could be said that the HPMCP has a higher affinity for the troglitazone than either PVP or HPMC. It is hypothesised that the nature of this affinity could be due hydrogen bonding formation between the polymer and the troglitazone,methods for investigating this are outlined in section 3.1.3.4. This could have two possible impacts upon the performance of the solid dispersion;

1) A higher percentage of the troglitazone is incorporated fully in the solid dispersion when HPMCP is used.
2) In the dissolution mechanism proposed by Craig (2002) the rate determining step for the dissolution of a drug from a solid dispersion is the dissolution of the drug into the polymer diffusion layer. If the troglitazone has a higher affinity for HPMCP it is more likely that dissolution into the HPMCP diffusion layer will occur quicker than with PVP or HPMC.

Either one of or both of these could explain the higher dissolution rate experienced with troglitazone in HPMCP dispersions.

What the results in this study do not explain is the precipitation that occurs from the high polymer concentration HPMCP dispersions. It has been seen in section 3.1 that immediately after the peak drug concentration is obtained for HPMCP dispersions, the amount of drug rapidly decreases. Although it has been shown that the rate of precipitation from a super-saturated system is dependent on stirring speed, the same pattern is not observed with the PVP and HPMC dispersions. The issue of this precipitation is dealt with in more detail in section 3.

The next stage in the study investigated the effect of increasing concentration has on the degree of protection offered by HPMCP. It is seen from figure 5-11 and table 5-5 that the inhibition protection is additive, i.e. the more polymer that is added the more protection offered. Examination of figure 5-11 shows

that this effect eventually plateaus, thus indicating that that there is an optimum amount of polymer that can be added to a solution for this effect to occur.

Table 5-5 Rate of precipitation of troglitazone from supersaturated solutions containing varying amounts of HPMCP (HP-55)

Polymer conc. (mg/ml)	Slope (mg/ml/min)
0.04	9.85E-04 ± 4.05E-05
0.08	6.21E-04 ± 7.35E-05
0.16	5.37E-04 ± 3.82E-05
0.40	2.71E-04 ± 2.42E-04
1.00	1.88E-04 ± 8.20E-05
2.00	4.27E-05 ± 6.56E-05
4.00	4.41E-05 ± 1.37E-04

Figure 5-12 Protection from precipitation of troglitazone from supersaturated solutions containing varying amounts of HPMCP (HP-55)

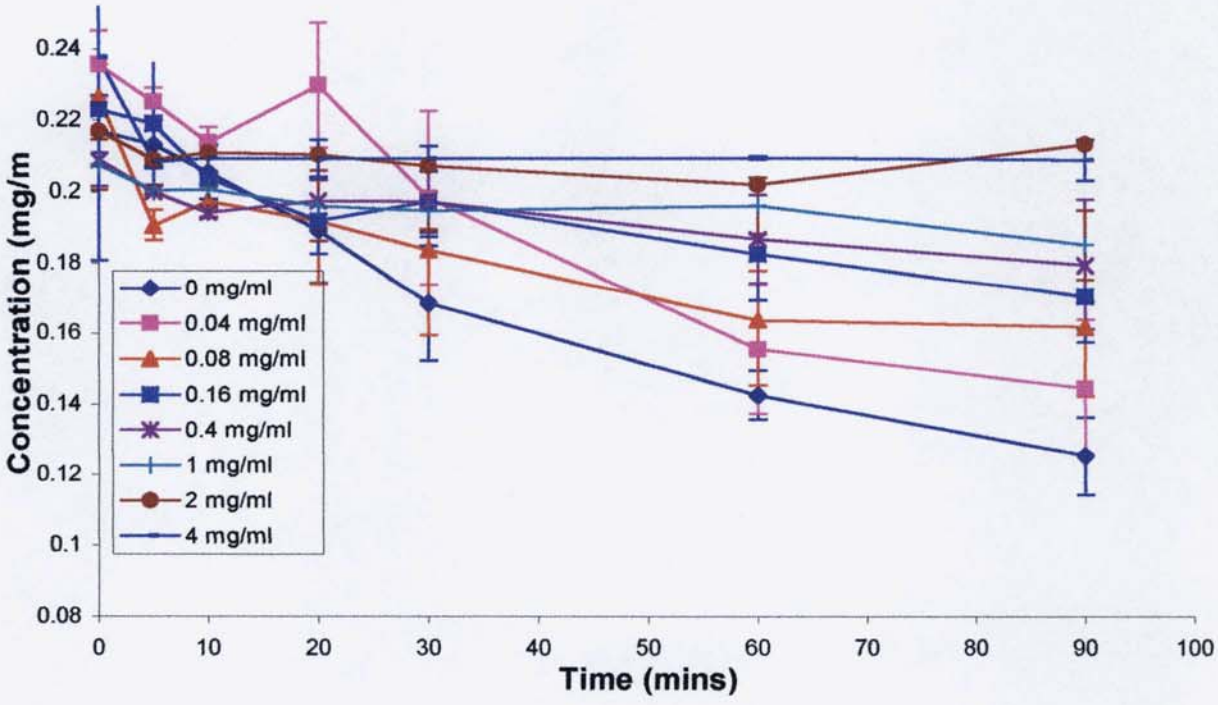

Figure 5-13 Rate of precipitation of troglitazone from supersaturated solutions containing varying amounts of HPMCP (HP-55)

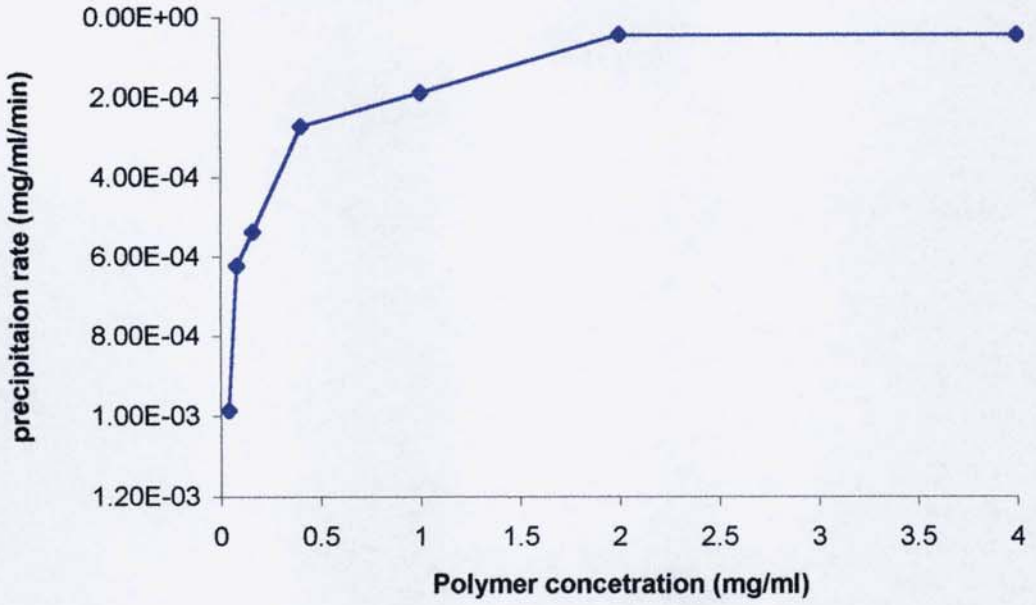

5.4 Investigation into the carrier dissolution

5.4.1 Introduction

As previously discussed in section 5.1.3 there have been many methods that have been suggested for the analysis of the dissolution of a polymer. The shortcomings of these methods were also noted, especially with regards to the analysis of carrier dissolution from a solid dispersion. It is therefore the intention to investigate two new methods for the analysis of polymer dissolution. One method will utilise the fact that some polymers do in fact have a chromophore, so will therefore be suitable for ultra violet spectroscopy, the other method will utilise the fact that as a polymer dissolves into a solution it will cause some increase in the viscosity of the solution.

5.4.2 The validation of an ultra violet spectroscopy method for following the dissolution of the carrier

5.4.2.1 Introduction

Assessment of the structures of the polymers used yielded information that two of the polymers (PVP and HPMCP) would have a chromphore. It was

therefore decided to exploit this fact by developing an ultra violet spectroscopy method to analyse the concentration of polymer within the dissolution medium.

One of the main concerns with doing this is that the solution, after dissolution, would contain troglitazone as well as the polymer. The Beer Lambert Law is, though, an additive effect. So utilising simultaneous equations would yield the concentrations of both components within the mixture.

5.4.2.2 Experimental

5.4.2.2.1 Materials

See sections 2.2.2.1, 2.4.2.1, and 2.6.1.1 for details of the materials used.

5.4.2.2.2 Equipment

The ultra violet spectrometer is described in section 2.1. Dissolution was performed using the equipment described in section 2.6.1.2.

5.4.2.3 Experimental

Working standards of PVP was prepared by serial dilution of a stock solution to encompass a range of 0.05 – 1 mg/ml, in FaSSIF. Working standards of troglitazone were prepared by serial dilution of a stock solution to encompass a range of 0.005-0.1 mg/ml, in FaSSIF. Mixtures of drug and polymer were then prepared at concentrations within the calibration range, in order to validate the method. All standards and mixtures were produced in triplicate. A UV scan was then produced on one of the standards (from each polymer and troglitazone), using the conditions described in section 2.1, in order to select appropriate wavelengths for the calculation of the molar absorbtivity constant. Each standard was then scanned at the selected wavelengths to obtain an absorbance reading. Beer-Lambert plots were then constructed and the molar absorbtivity constants calculated.

The following mixtures were prepared and then examined at the appropriate wavelengths:

- Mixture 1 = 0.5mg/ml PVP, 0.025mg/ml troglitazone

- Mixture 2 = 0.25mg/ml PVP, 0.01mg/ml troglitazone
- Mixture 3 = 0.1mg/ml PVP, 0.005mg/ml troglitazone

To analyse the obtained data a spreadsheet was set up (using Excel©).

5.4.3 Results

Table 5-6 shows the calculated absorbtivity constants for both troglitazone and PVP K-30 at 225 nm and 230 nm. These were then used in the spreadsheet with the absorbance data that was obtained from the prepared mixtures. Table 5-7 shows that the developed method was able to measure the polymer concentration with some degree of accuracy.

Table 5-6 Absorbtivity constants for troglitazone and PVP in FaSSIF

	Absorptivity constant 225 nm ($ml.mg^{-1}.cm^{-1}$)	Absorptivity constant 230 nm ($ml.mg^{-1}.cm^{-1}$)
Troglitazone	52.817	45.677
PVP K-30	1.673	0.600

Table 5-7 Results of the analysis of troglitazone:PVP mixtures. Results are a mean of 3 samples, ± SD.

	PVP K30 mg/ml	Troglitazone mg/ml
Mixture 1	0.473 ± 0.06	0.0209±0.0003
Mixture 2	0.222 ± 0.04	0.0077±0.001
Mixture 3	0.09 ± 0.03	0.007±0.0004

5.4.4 Dissolution of the carrier from a solid dispersion

5.4.4.1 Experimental

5.4.4.1.1 Materials

See sections 2.2.2.1, 2.4.2.1 and 2.6.1.1 for details of the materials used.

5.4.4.2 Equipment

Dissolution was performed using the equipment described in section 2.6.1.2. Analysis was performed on the HPLC system described in section 2.2.2.2. See section 2.1 for details on the UV spectrometer used.

5.4.4.2.1 Method

Solid dispersions were prepared as described in section 2.4.1.1. The dissolution method was carried out as described in section 2.5. Samples once extracted were diluted 1:1 with 0.01M NaOH, to prevent any recrystallisation. Samples were then scanned on the UV spectrometer, at the relevant wavelengths, using the method described in section 2.1.

5.4.4.3 Results and Discussion

Figure 5-14 shows that reproducible data was obtainable between replicates, this coupled with the data in table 5-7 shows that this could be a useful method for the analysis of the dissolution of PVP when used as a carrier. It was discussed in section 3.1.3.4 that, as the PVP concentration increases (from 0% to 100%) the dissolution rate of the drug also increases, until a maximum dissolution rate is obtained from which the dissolution rate steadily decreases (Ford 1986). From this maximum onwards (as polymer concentration increased) it was predicted that the drug dissolution was polymer controlled (from now on known as the 'carrier-controlled dissolution region'), and that after this point, the increased levels of polymer caused a reduction in the dissolution rate due to reasons such as increased viscosity. This carrier-controlled dissolution region was approximated to be between 45 – 75% (depending on the polymer). This relationship is in evidence in the results shown in figure 5-14, 5-15 and 5-16, as it is shown that up to 30 – 40 minutes the dissolution of troglitazone from the 50% sample is quicker than that from the 71% sample. After the 40-minute time point (figure 5-16), the dissolution of troglitazone from the 71% dispersion surpasses that of the 50% dispersion. This ties in with what is seen with the dissolution of the polymer; it is about at the 40-minute point that the dissolution of the polymer from the 50% dispersion effectively plateaus. It is also after the 40-minute time point that the dissolution of the polymer from the 71% dispersion surpasses that of

the 50% dispersion, and does not effectively reach a plateau point.

When the dissolution of the 50% and the 91% dispersions are considered it is seen that, as predicted by the model, there is a region where the rate of dissolution of the polymer becomes less controlling upon the dissolution of the drug. It is seen that the dissolution of the polymer from the 91% dispersion is slightly quicker than that of the 50% dispersion over the first 20 minutes of dissolution. This, however, is not reflected in the dissolution of the troglitazone, where the dissolution of troglitazone from the 91% dispersion is slower and to a lesser extent than the 50% dispersion. This, therefore, indicates that the dissolution of the polymer is not the only contributing factor to the release of troglitazone from PVP dispersions with over 50% PVP.

It was noted in section 3.2.1 that the dissolution of troglitazone from the 83% PVP dispersion is considerably less when compared to the other dispersions. Figure 6-11 shows that there is nothing significantly different in the dissolution of the PVP from this dispersion when compared to that of the PVP dispersions, having a similar dissolution rate and profile to that of the 71% dispersion. It is interesting to note that there is less polymer in the 83% dispersion than there is in the 91% dispersion, but the dissolution of troglitazone is slower in the 83% dispersion than in the 91% dispersion. This potentially rules out any viscosity changes influencing the dissolution of troglitazone from PVP dispersions. Referring to the DSC data presented in section 3.1.3.4 it is evident that the 83% dispersion was not as 'clean' as the other dispersions, with various peaks and possible glass transitions being present.

It is predicted by the Higuchi two component model that in a true carrier controlled system that if 70% of a carrier dissolves then it is expected that approx 70% of the less soluble component will dissolve. In all instances this has not happened (not only the 83%); the amount of troglitazone dissolved is approximately 50 – 60% of that of the carrier. For example the amount of polymer dissolved from the 71% sample is approximately 75%, whereas in the case of the troglitazone from the same dispersion only 45% of the drug

content enters the solution. This indicates that other mechanisms could be at work, controlling the amount of drug released from a solid dispersion. It is hypothesised that this could be due to two possible reasons; 1) as troglitazone is dissolving, some troglitazone is precipitating from the solution, and 2) not all of the troglitazone is fully incorporated into the solid dispersion.

As it is shown in section 5.3, the PVP is not the most effective polymer at inhibiting the precipitation of troglitazone from a super-saturated system. As the dissolution profiles show in section 3 the troglitazone from the solid dispersions is in a super-saturated solution. The protection offered by the PVP against the troglitazone precipitating from the solution is minimal, not much more effective than drug alone. It could be possible that precipitation of troglitazone is occurring as the dissolution run continues. The possible explanation as to why the concentration of troglitazone plateaus instead of precipitating out of solution as is seen with the HPMCP dispersions is that there is still some troglitazone being released from the solid dispersions. It is seen from figure 6-9 that even after 90 minutes there is still some dissolution of the polymer occurring, so some drug is still entering solution (although after 60 minutes it is evident that precipitation is occurring 65-14, 5-15).

Figure 5-14 Dissolution of PVP K30 from PVP:troglitazone (%polymer) dispersions, in FaSSIF. Results are the mean of three replicates, error bars ± SD.

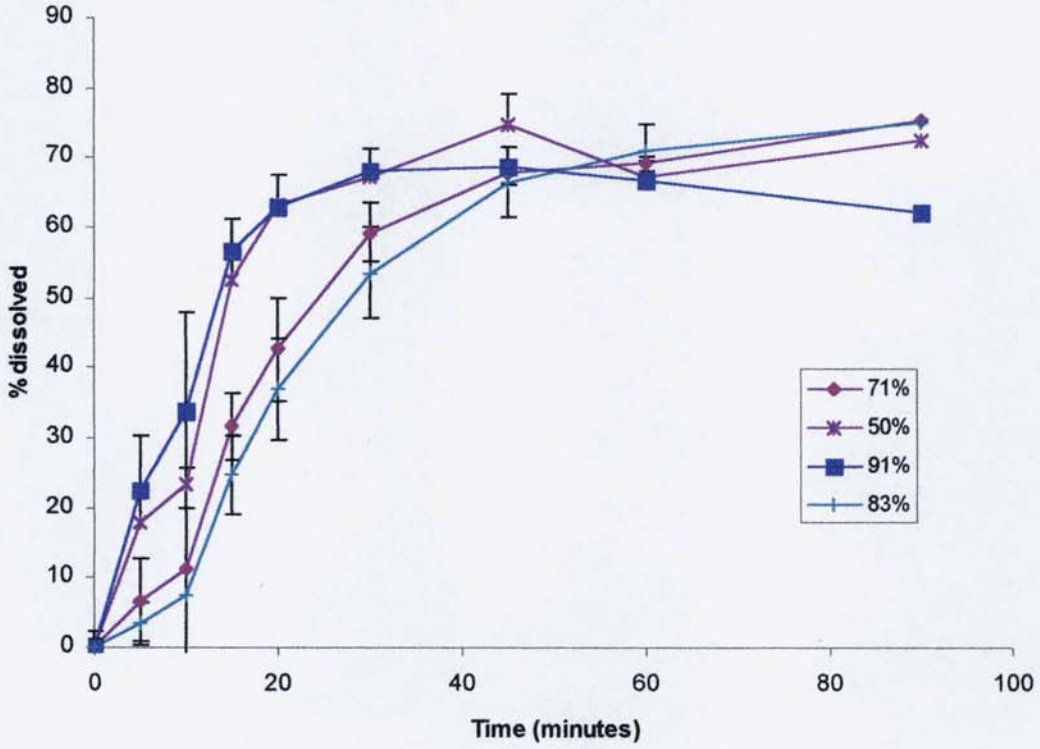

Figure 5-15 Dissolution of troglitazone from PVP solid dispersion, derived from the UV analysis. Results are the mean of three replicates, error bars ± SD.

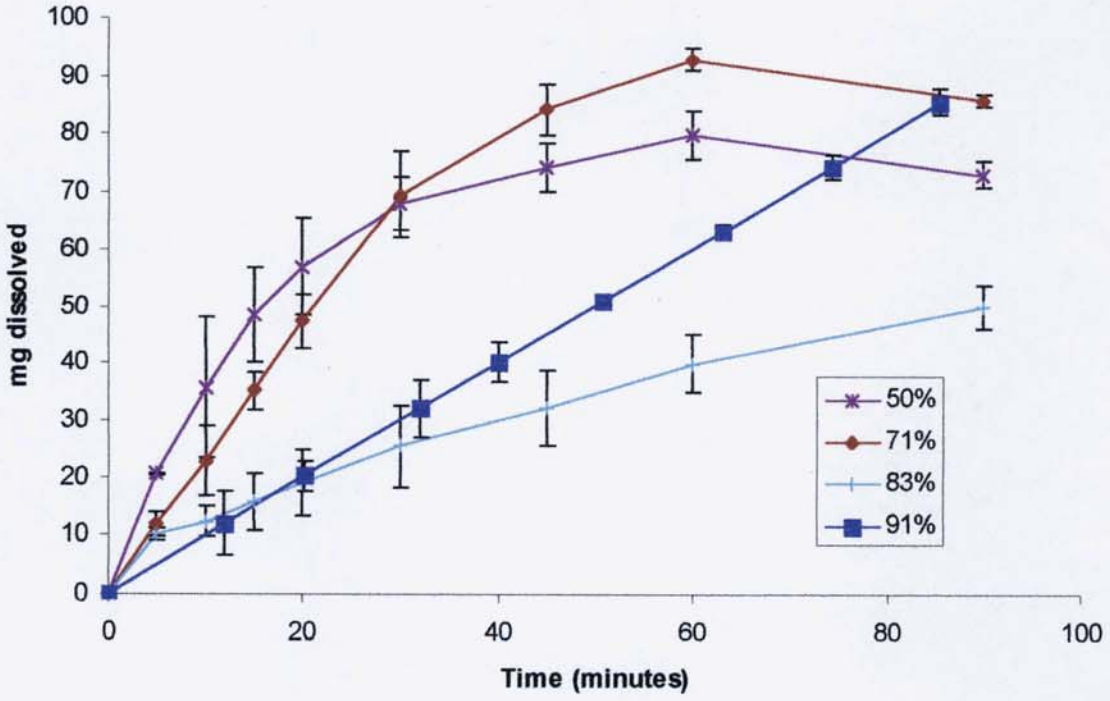

Figure 5-16 Dissolution of troglitazone from PVP solid dispersion, derived from the HPLC analysis. Results are the mean of three replicates, error bars ± SD.

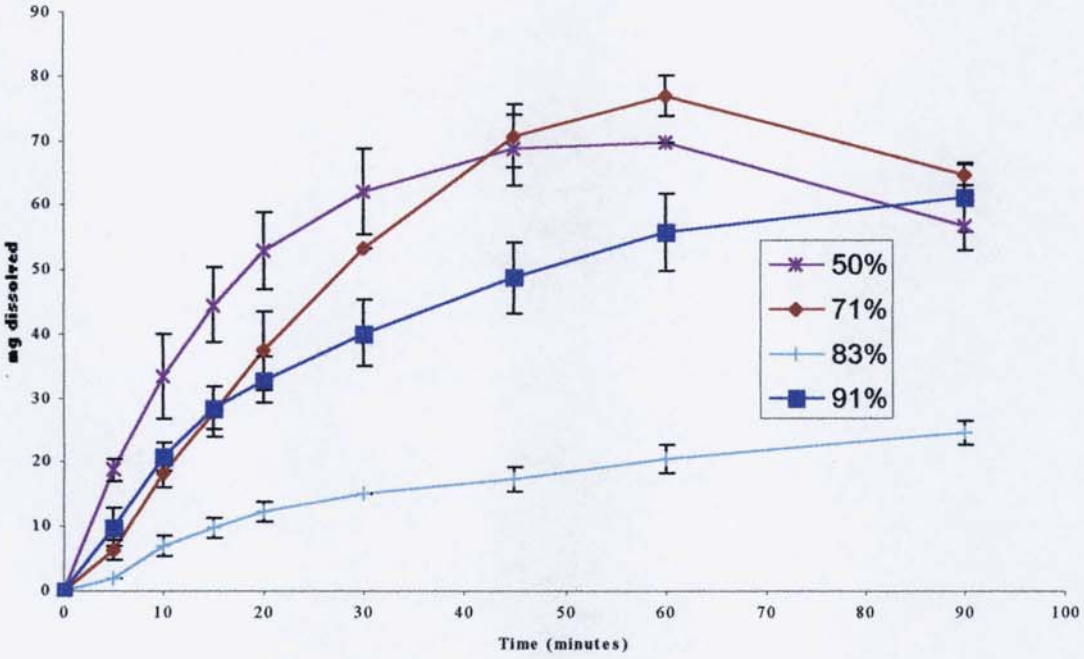

The other reason for the dissolution of troglitazone not obeying the model described by Higuchi is possibly the physical state of the drug within the solid solution. Work utilising electron-probe microanalysis and micro-thermal analysis has shown that it is possible within a troglitazone:PVP solid dispersion (1:2) to have up to 36% crystallinity (Hasegawa *et al.* 2005). There is no reason, based on DSC data, to suspect that the dispersions prepared for this study have such a high quantity of crystallinity, but it is a possibility that some crystallinity could be present (especially the 83% dispersion). What could be more likely is that rather than the entire bulk drug being fully incorporated within the solid dispersion it may be in pockets of amorphous drug. It has been discussed that within a solid dispersion a drug can be found within three phases; crystalline drug, amorphous drug and drug incorporated into a solid solution. The dispersions that contained the highest amount of drug incorporated into the solid solution obtained the fastest dissolution rate and were more complete (Sertsou *et al.* 2002).

5.4.5 Using viscometry to measure the dissolution of the carrier

5.4.5.1 Introduction

It was discussed in section 5.1.3 the use of microviscometry as a method of following the dissolution of the carrier from a solid dispersion. One of the problems that has prevented viscometry being used is that the concentrations of polymer at 100% dissolution are very low (the maximum being 4 mg/ml in the case of the dispersions prepared in section 3.1). It is predicted that at these sort of concentrations will have very little impact upon the overall viscosity of the solution, and will be beyond the capacity of conventional methods for measuring viscosity (U- tube, and Brookfield).

It is therefore suggested to use an instrument called an Anton Parr microviscometer. This instrument has the capability of measuring accurately viscosities as low as 0.3 mPa.S, and also allows for temperature control (as viscosity being affected by temperature). The instrument works by measuring the amount of time it takes for a small sphere to roll through a cylindrical tube under the influence of gravity, with the measuring principle being based upon stokes law (Anton-Parr 2004)

5.4.5.2 Experimental

5.4.5.2.1 Materials

See sections 2.2.2.1, 2.4.2.1 and 2.6.1.1 for details of the materials used.

5.4.5.2.2 Equipment

The samples were measured on an Anton-Parr AMVn, equipped with the visolab software. Dissolution was performed using the equipment described in section 2.6.1.2. Analysis was performed on the HPLC system described in section 2.2.2.2.

5.4.5.2.3 Methods

Working standards of either polymer were prepared by serial dilution of a stock solution to encompass a range of 0.05 – 1mgml, in FaSSIF. Viscosity of standards measured using micro-viscometer, and a calibration plot was

constructed. Control standards prepared to check the reliability of the calibration plots.

Solid dispersions were prepared as described in section 2.4.1.1. The dissolution method was carried out as described in section 2.5. Samples once extracted were diluted 1:1 with 0.01M NaOH, to prevent any recrystallisation. Viscosity of the samples was then measured. ANOVA tests were performed using Graphpad's Instat 3 software package.

5.4.6 Results and discussion

Figure 5-15 shows the calibration curves that were obtained from the analysis of the stock solutions that were prepared in section 5.4.4.5.3. As it can be seen, good linearity (r^2 = 0.9991 and 0.9944) was achieved from the analysis over the desired range. The instrument also has the sensitivity to distinguish between very small increases in polymer concentration, with the entire range of the viscosity encompassing 0.06 mPa.s. This means that the method has promise for the analysis of the carrier dissolution.

Figure 5-17 Calibration curves for HPMCP and HPMC using the micro-viscometer. Results are the mean of three replicates, error bars ± SD.

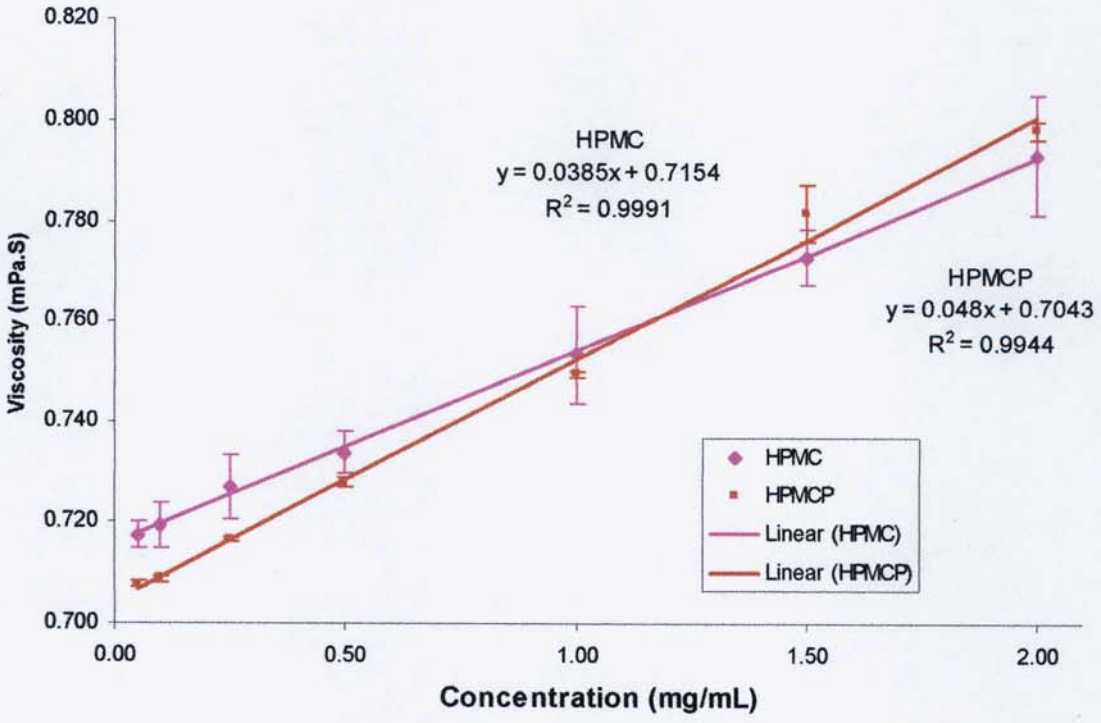

The dissolution profiles of the spray-dried polymers is shown in figure 5-16, and it is shown that the dissolution of HPMCP is quicker and more complete than the dissolution of the spray-dried HPMC. Using the AUC at twenty minutes as an indication of the amount of polymer dissolved, it is shown that the dissolution of HPMCP is in fact nearly twice as fast as that HPMC (table 6-10). This is supported by the rate data obtained for both polymers (table 6-9). This is probably to be expected, as HPMCP is, as discussed in section 1.4, an enterically soluble polymer. It is, therefore, designed to dissolve at the higher pH, the grade used in this study is HP-55 where the 55 signifies the pH (x10) at which the HPMCP begins to dissolve, *i.e.* pH 5.5 (Kibbe 2000). It has been shown that the dissolution rate of HPMCP nears its peak dissolution rate between pH 6.0 – 7.0. At pH 6.5, the pH of FaSSIF (table 1-5), the HPMCP ionises and is therefore more soluble (Guo 2002). When used as a tablet coating HPMC is designed to dissolve at a range of pHs, and it is shown not to affect the dissolution rate at various pHs for the dissolution of vitamin B_2, when it was used a tablet coating (section 1.4). Figure 5-13 shows that over the ninety minutes the dissolution of the HPMC was not complete, it was found after the dissolution run was completed that some undissolved HPMC was found in each dissolution vessel. It was not possible to quantify the amount as it was in the form of 'fisheyes', *i.e.* small gelatinous aggregates, this evidence of a hydrocolloid that is not sufficiently hydrated (Weiner, 2005).

Figure 5-18 Comparison of the dissolution of spray dried HPMC and HPMCP (% dissolved based upon maximum polymer added). Results are the mean of three replicates, error bars ± SD.

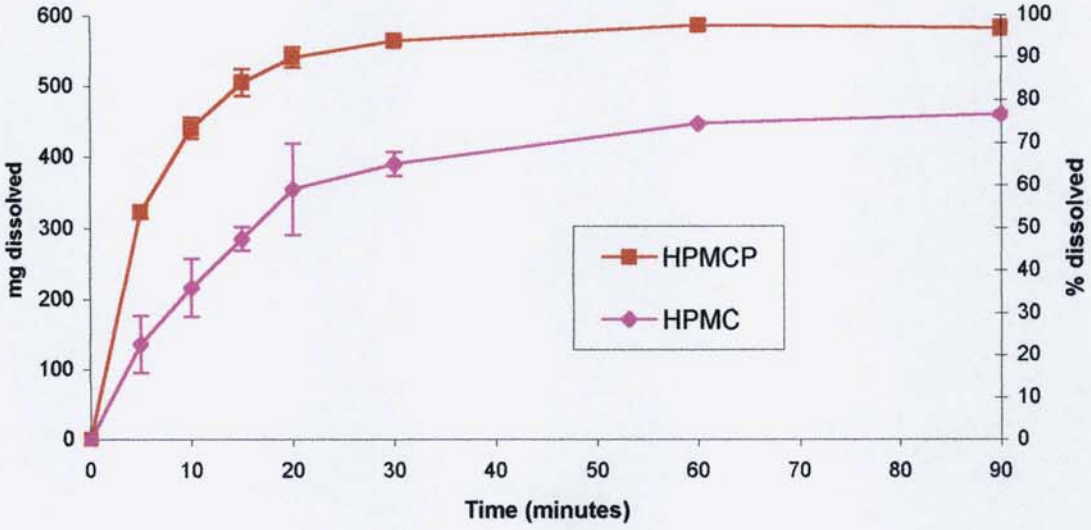

When the dissolution of the polymers from the solid dispersions is considered, it is seen that, like the dissolution of the polymers alone, that the dissolution of HPMCP is quicker and more complete than HPMC (table 5-8 and table 5-9). It is noticeable from the Tukey analysis (table 5-10 and 5-11 that the dissolution of the polymers from the 71% dispersions is comparable to that of the spray-dried polymers for both polymers (p= >0.05 for both polymers). This is observed for both the twenty-minute and ninety-minute time points. These observations parallel the dissolution of troglitazone, with the dissolution of troglitazone being faster and reaching a higher concentration from the HPMCP dispersion. This, therefore, indicates that the dissolution of troglitazone from these dispersions is controlled to some extent by the behaviour of the polymer. It could, therefore, be expected that the 71% dispersion will follow the two-compartment dissolution model (discussed in section 1.3.2.3), and that the rate of the drug dissolution could be predicted from the dissolution rate of the polymer. Table 5-9 shows the polynomial-rates of the polymers, the polymers from the dispersions and the drugs from the dispersions. When the two-compartment dissolution model is applied (table 5-9) to the 71% dispersions, it is seen that there is a discrepancy between the experimental and theoretical rate. The model predicts that theoretical rate of

the drug is higher than the experimentally determined rates. This indicates that the dissolution of the drug from these solid dispersions is not completely controlled by the action of the polymer and that there is another aspect controlling the dissolution of the drug.

Table 5-8 Area under the curve data for the dissolution of the polymers (based on % dissolved)

System	AUC_{20} ($mg.ml^{-1}.min$)	AUC_{90} ($mg.ml^{-1}.min$)
Spray-dried HPMC	679 ± 100	5661 ± 204
Spray-dried HPMCP	1283 ± 41	7995 ± 122
HPMC:Troglitazone 71%	760 ± 43	5320 ± 55
HPMCP:Troglitazone 71%	1278 ± 52	7786 ± 141
HPMC:Troglitazone 91%	89 ± 18	2620 ± 300
HPMCP:Troglitazone 91%	941.9 ± 52	7621 ± 312
HPMC:Atovaquone 71%	934 ± 11	5932 ± 116
HPMCP:Atovaquone 71%	1533	8427

Figure 5-19 Dissolution of HPMC and HPMCP from 71% (polymer solid dispersions). Results are the mean of three replicates, error bars ± SD.

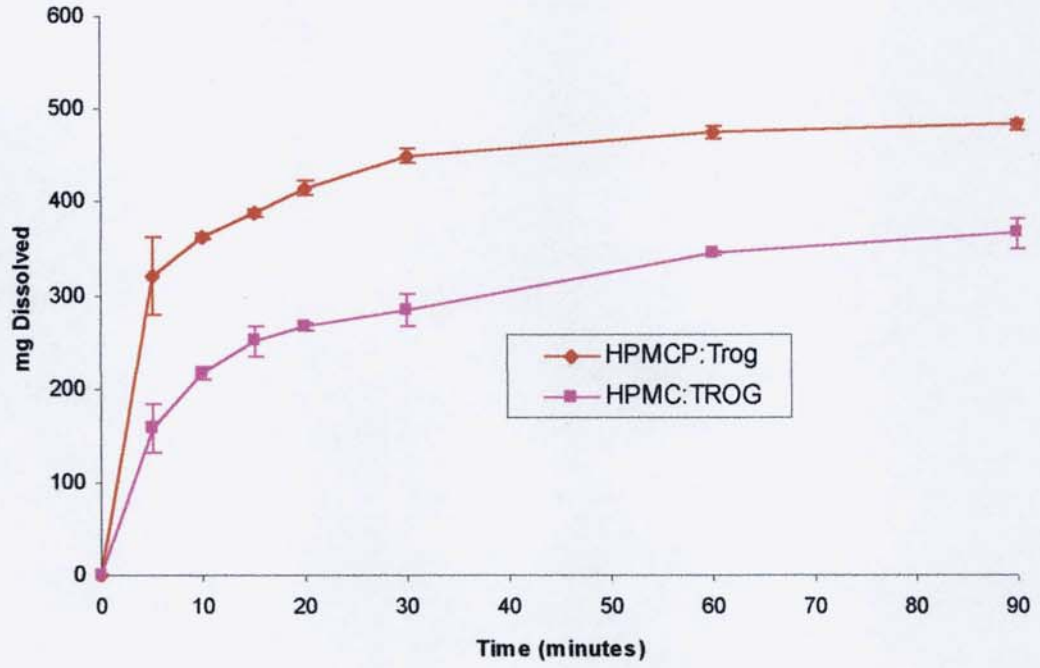

Figure 5-20 Dissolution of troglitazone from 71% (polymer) solid dispersions. Results are the mean of three replicates, error bars ± SD.

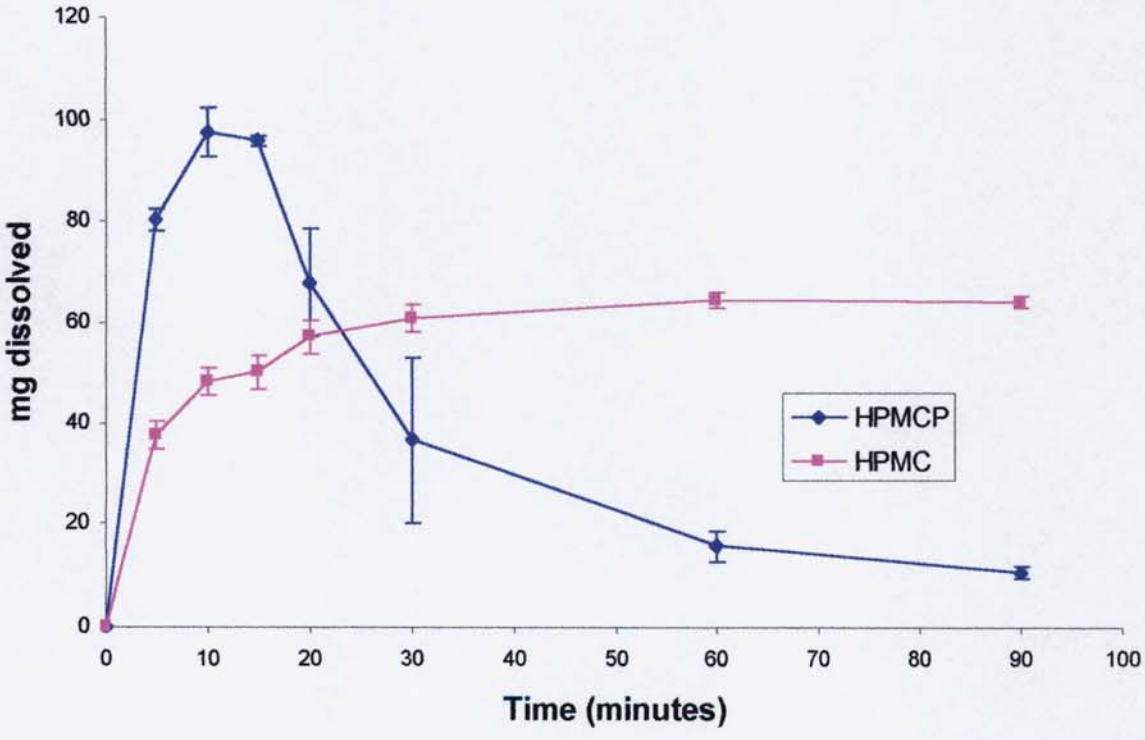

Table 5-9 Rate data calculated between 0-5 mins

System	Polymer rate ($mgmin^{-1}$)	Experimental drug rate ($mgmin^{-1}$)	Theoretical drug rate ($mgmin^{-1}$)
HPMCP:Troglitazone 71%	121 ± 31	28	49
HPMC:Troglitazone 71%	50 ± 17	12	20
HPMCP:Troglitazone 91%	132 ± 27	5	13
HPMCP:Troglitazone 91%	Not measurable		
HPMCP:Atovaquone 71%	101	2	41
HPMC:Atovaquone 71%	49	2	20

Figure 5-21 Dissolution of HPMCP and HPMC from 91% (polymer) troglitazone dispersions

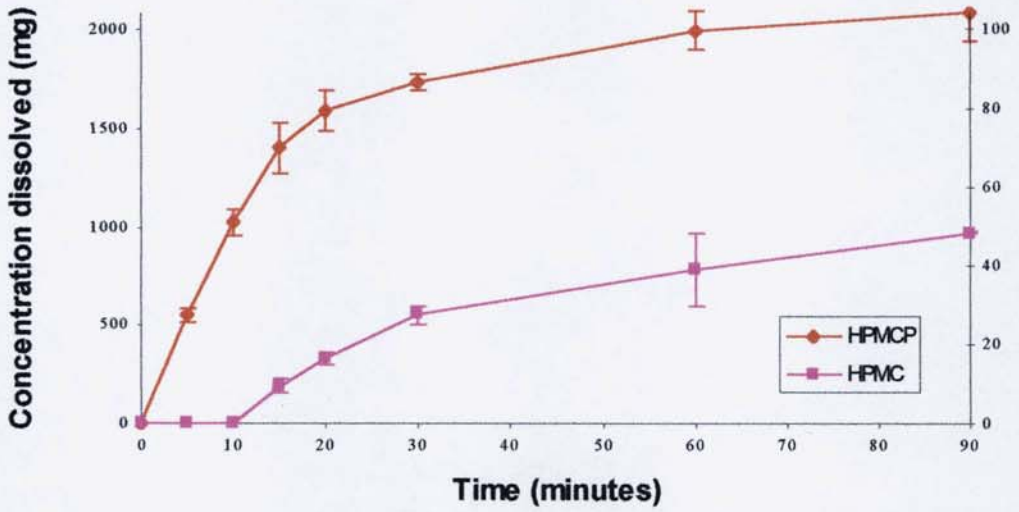

When the dissolution of the polymers from the 91% dispersions are considered, it is noted, that within the first twenty minutes, the amount of polymer released for both polymers is lower than that for the 71% dispersions (based on AUC table 5-8). The amount of HPMCP dissolved within the first 20 minutes, from the 91% dispersion, is significantly less ($p=<0.001$) than the amount of HPMCP from the 71% dispersion. This difference in polymer dissolution is also experienced with HPMC dispersions, with $p=<0.001$. This is also found for both polymers over the 90-minute period (table 5-8). This mirrors the dissolution of the troglitazone from the solid dispersions, after twenty minutes the dissolution of troglitazone from the 91% HPMCP

dispersion is slower than the 71% dispersion, with the rate of troglitazone being 45 (71%) compared to 35 (91%). This relationship between the dissolution of troglitazone and the polymer over the two concentrations is also observed for the HPMC dispersions with the polymer dissolution being very slow. As outlined in section 3.1.3.4 the 91% HPMC troglitazone dispersion formed a gelatinous layer on top of the dissolution medium, this reduction in the wetting in the polymer will have the effect of reducing the dissolution of the polymer from the solid dispersion.

Figure 5-22 Dissolution of troglitazone from 91% (polymer) dispersion

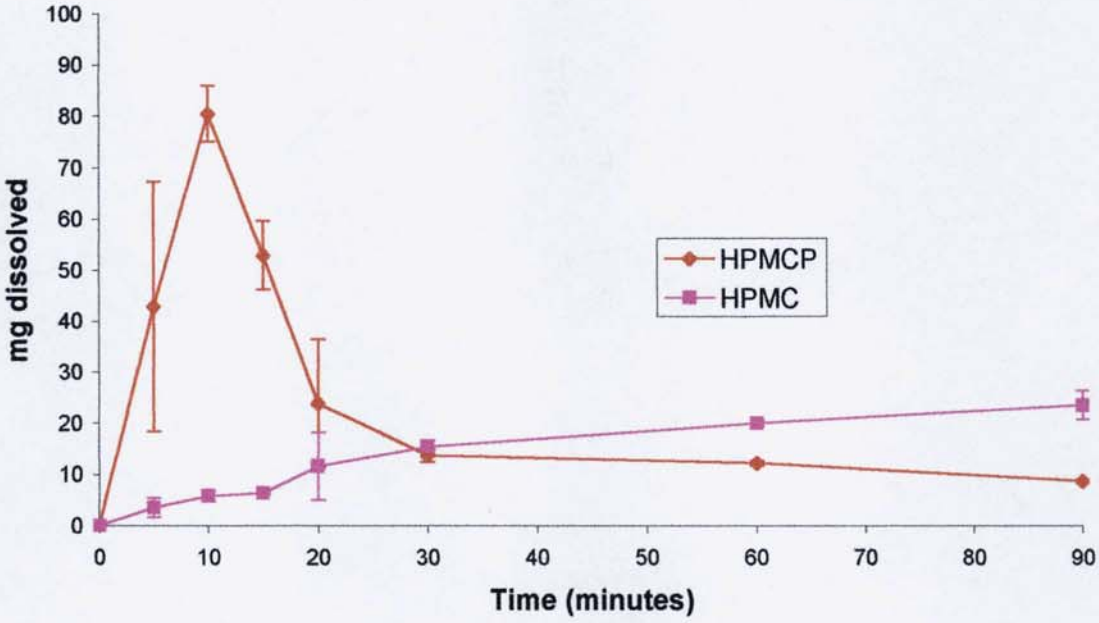

The precipitation of the troglitazone from the HPMCP dispersion could be explained by the results discussed in this section (figure 5-17 to 5-22). After 20 minutes, the dissolution of the HPMCP 9from both the 71% and 91% dispersions) effectively plateaus, which means that, from this point forward, it could be expected that no more troglitazone is being released from the dispersion. This corresponds with the point at which the troglitazone begins to precipitate from the super-saturated solution. Up to this point, it could be considered that any troglitazone that is precipitating from the solution is effectively masked due to the rapid dissolution from the solid dispersion. Although it has been shown (section 5.3) that the precipitation of the

troglitazone is effectively inhibited by the presence of HPMCP, with the concentration of HPMCP being what would be expected after 100% dissolution of the solid dispersion. The experiments in section 5.3, however, were conducted in an effectively static solution, whereas, with a dissolution bath, there is agitation, which may aid precipitation of the troglitazone. The ability of the HPMCP to inhibit the precipitation of troglitazone may also explain the high release of troglitazone from the dispersion. This is because, whilst the drug is undergoing dissolution, the polymer may slow down the rate of precipitation that would normally be expected, thus enabling a higher amount of drug to dissolve.

With the dissolution of the atovaquone dispersions the effect is far more pronounced. Again the dissolution of the polymers show similar rates and AUC data (after 90 minutes $p>0.05$) when compared to the polymers alone. This time, there is no significant difference between the dissolution of the drugs from the different polymers. It is also found, for the atovaquone dispersions that the two-compartment model fails to predict the dissolution rate, with the prediction being twenty and ten times higher for the HPMCP and HPMC respectively (table 5-7). Thus dissolution of the polymer is not the driving force behind the dissolution of the drug from the solid dispersions, but dissolution is drug-controlled. Dissolution is not controlled completely by the physical properties of the drug because there is a third aspect to be considered, and this is the solid state of the dispersions. As previously discussed in section 3.4.4.3 not all of the atovaquone is incorporated into the solid dispersion, and it exists in the different phases described by Sertsou *et al* (2002). This is because the DSC data showed a lot of re-crystallisation of the drug upon heating. It is; therefore, felt that the dissolution of these dispersions is controlled more by the amount of drug incorporated as a solid solution.

Figure 5-23 Dissolution of HPMC and HPMCP from 71% (polymer) atovaquone dispersion

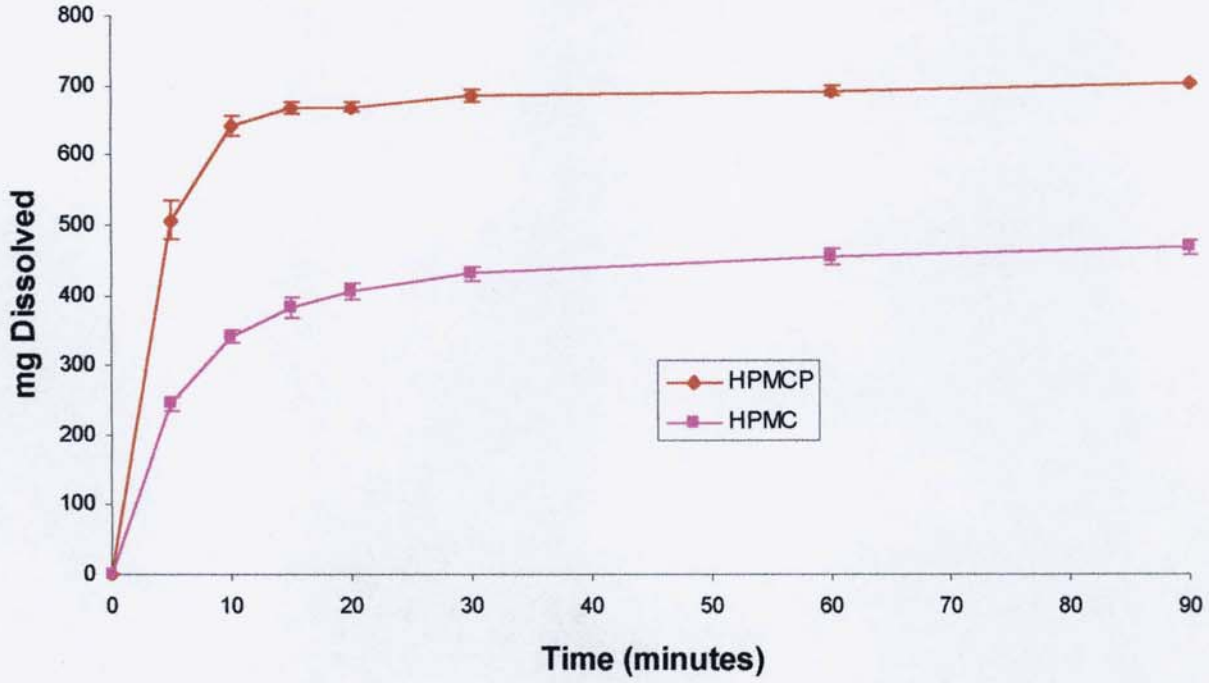

Figure 5-24 Dissolution of atovaquone from 71% (polymer) dispersions

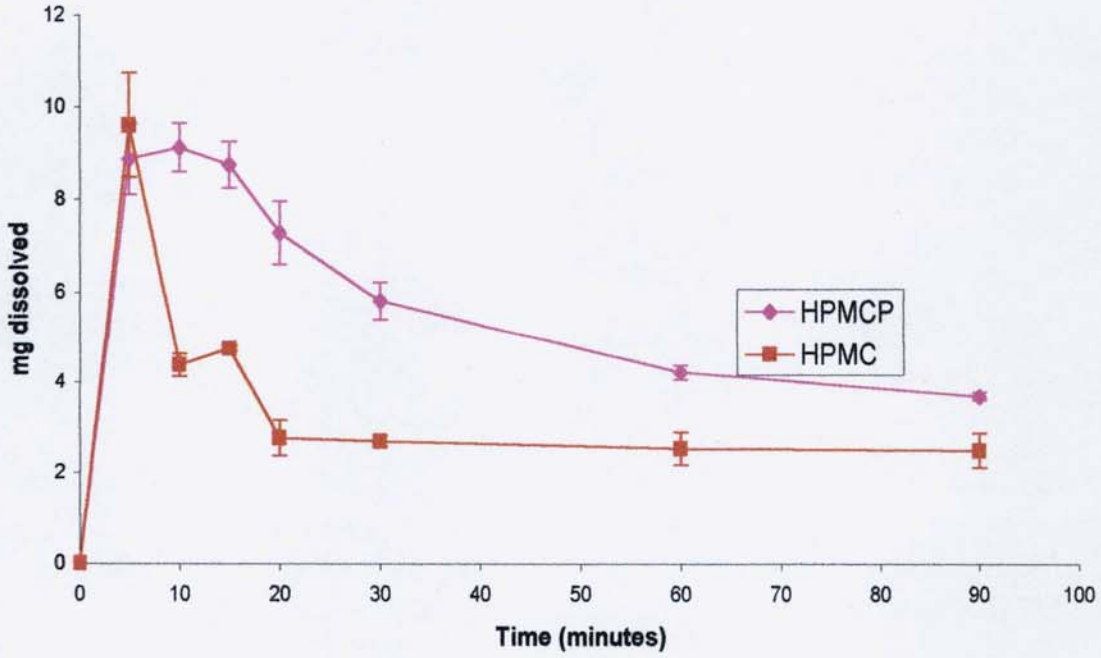

Table 5-10 Tukey analysis of AUC (20 minutes) of polymers (figures bracket indicate the mean difference (row – column))

	Spray-dried HPMC	Spray-dried HPMCP	HPMC:Troglitazone 71%	HPMCP:Troglitazone 71%	HPMC:Troglitazone 91%	HPMCP:Troglitazone 91%	HPMC:Atovaquone 71%	HPMCP:Atovaquone 71%
Spray-dried HPMC								
Spray-dried HPMCP	<0.001							
HPMC:Troglitazone 71%	>0.05	<0.001						
HPMCP:Troglitazone 71%	<0.001	>0.05	<0.001					
HPMC:Troglitazone 91%	<0.001	<0.001	<0.001	<0.001				
HPMCP:Troglitazone 91%	<0.01	<0.001	<0.05	<0.001	<0.001			
HPMC:Atovaquone 71%	<0.01	<0.001	<0.05	<0.001	<0.001	>0.05		
HPMCP:Atovaquone 71%	<0.001	<0.01	<0.001	<0.01	<0.001	<0.001	<0.001	

Table 5-11 Tukey analysis of AUC (20 minutes) of polymers (figures bracket indicate the mean difference (row – column))

	Spray-dried HPMC	Spray-dried HPMCP	HPMC:Troglitazone 71% polymer	HPMCP:Troglitazone 71% polymer	HPMC:Troglitazone 91% polymer	HPMCP:Troglitazone 91% polymer	HPMC:Atovaquone 71% polymer	HPMCP:Atovaquone 71% polymer
Spray-dried HPMC								
Spray-dried HPMCP	<0.001							
HPMC:Troglitazone 71%	>0.05	<0.001						
HPMCP:Troglitazone 71%	<0.001	>0.05	<0.001					
HPMC:Troglitazone 91%	<0.001	<0.001	<0.001	<0.001				
HPMCP:Troglitazone 91%	<0.001	>0.05	<0.001	>0.05	<0.001			
HPMC:Atovaquone 71%	>0.05	<0.001	<0.05	<0.001	<0.001	>0.001		
HPMCP:Atovaquone 71%	<0.001	>0.05	<0.001	<0.05	<0.001	<0.01	<0.001	

Table 5-12 AUC data for the two drugs from the solid dispersion (* calculated mg dissolved, ** calculated using % dissolved)

System	Area under the curve (20 mins) ($mg.ml^{-1}.min$) (polymer)	Area under the curve (90 mins) ($mg.ml^{-1}.min$) (polymer)	**Area under the curve (20mins)** ($mg.ml^{-1}.min$) (drug)	**Area under the curve (90 mins)** ($mg.ml^{-1}.min$) (drug)	**Tmax (min)**
HPMC:Troglitazone 71% polymer	3799 ± 213	26601 ± 276	760 ± 43	5320 ± 55	60
HPMCP:Troglitazone 71% polymer	6389 ± 258	38932 ±	1278 ± 52	7786 ± 141	10
HPMC:Troglitazone 91% polymer	1777 ± 277	52398 ± 5996	89 ± 18	2620 ± 300	90
HPMCP:Troglitazone 91% polymer	18839 ± 1040	152429 ± 6250	941.9 ± 52	7621 ± 312	10
HPMC:Atovaquone 71% polymer	5839 ± 68	37074 ± 727	934 ± 11	5932 ± 116	5
HPMCP:Atovaquone 71% polymer	10734	58991	1533	8427	5

6 Conclusions

Quantitative methods for comparing supersaturated dissolution data was developed, allowing for both the comparison of the overall dissolution of the product (*i.e.* AUC) and the derivation of an initial dissolution rate. These two methods have proved effective at describing differences found in the dissolution profiles of formulations, which do not conform to the usual conventional methods (*i.e.* f_2 comparative test, and Hixson-Crowell model).

The incorporation into solid dispersions, with HPMC, HPMCP or PVP, was effective at enhancing the dissolution of both troglitazone and atovaquone in FaSSIF, when compared to the drug alone and physical mixtures. The enhancement in the dissolution was found to be more pronounced with those dispersions prepared with troglitazone compared to those prepared with atovaquone, with both the initial dissolution rate and the overall dissolution being superior with troglitazone. The differences experienced between atovaquone and troglitazone appeared to be due to the physical structure of the dispersions formed, with the troglitazone showing more incorporation into the solid dispersions than the atovaquone dispersions. This work shows that it would be prudent to screen a range of potential carriers with the drug intended for a solid dispersion.

The dissolution of troglitazone was affected by the concentration of polymer that was used in the formulation. It was found that at as the concentration of the polymer, up to 83% (w/w), increased the dissolution of the drug increased. Beyond 83% (w/w) polymer, especially with troglitazone, the dissolution of the drug began to reduce in comparison to 71% (w/w) dispersions. Examination of the polymer dissolution, at 71% and 91% polymer (HPMC or HPMCP), showed that the dissolution of the polymer begins to influence the dissolution rate of the drug. With less dissolution of the polymer occurring at the higher polymer loading (indicated by the AUC_{90}), and in the instance of HPMC a severe drop in the polynomial rate of the polymer was experienced when the polymer loading was over 83%.

The selection of polymer is also shown to be an important factor when deciding upon the formulation of a solid dispersion. It was found, for both atovaquone and troglitazone, that HPMCP was more efficient at releasing either drug from at high polymer ratios. The effect was more pronounced with the troglitazone dispersions. Examination of the polymer dissolution found that HPMCP, in FaSSIF, had consistently faster dissolution rates than HPMC, whether alone or incorporated in a solid dispersion. This mirrored the dissolution of troglitazone from the solid dispersion, indicating that troglitazone solid dispersion undergo dissolution via the carrier-controlled dissolution mechanism. With atovaquone there is evidence that the polymer selection has an impact upon the dissolution, but this is not as significant as with troglitazone. Analysis of the dissolution of the polymer showed that the dissolution of atovaquone was, in fact, irrespective of the polymer at a given ratio.

The effect of reducing the paddle speed from 75 to 25 rpm had the following two effects: a) changing the rank order by which the dissolution occurred, and b) reducing the amount of drug released from the solid dispersions. The changing of the rank order of contrasted what had been reported earlier, showing that even when using biorelevant dissolution medium care should still be taken when developing a discriminatory dissolution test.

An effective method for examining the effect of pre-exposure to bio-relevant gastric fluid upon the eventual dissolution of a solid dispersion in bio-relevant intestinal fluid was successfully developed. This method showed, in the case of an acidic drug, that it is advantageous to use an enteric polymer, over a gastric soluble polymer; to obtain higher dissolution rates in the intestinal fluids. The method could also have a use in early development of new pharmaceutical products; aiding understanding into the impact exposure to the gastric fluids will have upon the formulation.

It was shown that, in the case of troglitazone, the behaviour of the drug with polymer, when in solution, shows a relationship with the dissolution of a drug,

the nature of which was not fully established.

Micro-viscometry has shown to be a practical and effective method for measuring the dissolution of the carrier from the solid dispersions. It is found that the instrument is sensitive to differentiate between the dissolution of two different polymers (HPMC and HPMCP). It was shown to be effective and repeatable for the two polymers, and enabling an understanding of how the whole dispersion behaved whilst undergoing dissolution.

The analysis of polymer dissolution has also been achieved using UV analysis. This method proved capable of measuring both the drug and polymer dissolution; however it was not as effective as microviscometry at measuring the dissolution of the polymer. This was mainly due to the UV method only being capable of following the dissolution of specific polymers. It was unsuitable for measuring the dissolution of HPMC, as this polymer has no chromophore. Regarding HPMCP it appears this polymer had too strong a chromophore, which interfered with the troglitazone chromophore. Therefore, the method of choice for measuring polymer dissolution would be microviscometry.

6.1 Future Work

It was proposed that the main difference between the atovaquone dispersions and the troglitazone dispersions was due to differences found between the physical structures of the dispersions. As a consequence of this it is suggested that further work could be undertaken to try and understand the interactions that take place between the carriers and the drugs. Such testing could involve the use of techniques such as solid state NMR, which would allow an understanding as to whether there are any chemical interactions occurring between the drug and the carrier. Another technique, which could be used, would be Electron probe microanalysis (this works by examining x-rays emitted from the sample when it is probed with an electron beam, which allow an insight as to how the drug is distributed within the carrier, and in which form the drug is in (crystalline or amorphous).

Further work should be done to fully elucidate the extent of the interactions of the drug and carrier, when in solution. It is felt that there is a link between the interactions of polymers at this stage and the overall dissolution, and further understanding of this would enable better prediction of dispersions properties. It also felt that further work could be performed to characterise the dissolution media after the polymer has been dissolved into it. Such tests that could be performed are viscosity (using microviscometry), surface tension and contact angle analysis.

Bioavailability studies should be conducted to assess whether the dissolution data obtained using the FaSSIF dissolution medium is meaningful in the case of solid dispersions. This is driven by the fact that large differences are seen in the dissolution of the dispersions at different paddle speeds.

7 References

Adams, E., Coomans, D., Smeyers-Verbeke, J. and Massart, D. L., Application of linear mixed effects models to the evaluation of dissolution profiles. Int. J. Pharm., 226(2001) 107-125.

Atkinson, R.M., Bedford, C., Child, K.J. and Tomich, E.G., Effect of particle size on blood griseofulvin-levels in man. Nature, 193(1962) 588–589.

Aldén, M., Tegenfeldt, J. and Sjökvist, E., Structure of solid dispersions in the system polyethylene glycol-griseofulvin with additions of sodium dodecyl sulphate. Int. J. Pharm., 83(1992) 47-52.

Aldén, M., Tegenfeldt, J. and Sjökvist Saers, E., Structures formed by interactions in solid dispersions of the system polyethylene glycol-griseofulvin with charged and non charged surfactants added. Int. J. Pharm., 94(1993) 31-38.

Amidon, G.L., Sinko, P.J. and Fleisher, D., Estimating oral fraction dose absorbed: a correlation using rat intestinal membrane permeability for passive and carrier mediated compounds. Pharm. Res., 5(1988) 651-654.

Amidon, G.L., Lennernäs H., Shah, V. P. and Crison, J.R., A theoretical basis for a biopharmaceutics drug classification: The correlation of *in vitro* drug product dissolution and *in vivo* bioavailability. Pharm. Res., 12(1995) 413-420.

Anderberg, E.K., Bisrat, M. and Nystrom, C., Physicochemical aspects of drug release. VII. The effect of surfactant concentration and drug particle size on solubility and dissolution rate of felodipine, a sparingly soluble drug, Int. J. Pharm., 47(1988) 67–77.

Arias, M.J., Ginés, J.M., Moyano, J.R., Pérez-Martínez J.I., and Rabasco, A.M., Influence of the preparation method of solid dispersions on their dissolution rate: study of triamterene-D-mannitol system. Int. J. Pharm., 123(1995) 25–31.

Aulton, M.E., Pharmaceutics: The science of dosage form design. Churchill Livingstone. 2000 (pp. 38–173).

Aulton, M.E., Pharmaceutics: The science of dosage form design. 2nd ed. Churchill Livingstone. 2005 (pp. 88-89).

Bates, T. R., Dissolution characteristics of reserpine-polyvinylpyrrolidone co-precipitates. J. Pharm. Pharmac., 21(1969) 710-712.

Behme, Brooke, D., Farney, R.F. and Kensler T.T., Characterization of polymorphism of geprione hydrochloride. J. Pharm. Sci., 74(1985) 1041-1046.

Bhaskar, R. K., Garik, P., Turner, S.T., Bradley, J. D., Bansil, R., Stanley, H. E. and Lamont, T. J., Viscous fingering of HCl through gastrin mucin. Nature, 360(1992) 458 -461.

Blum patient and family learning centre. http://healthgate.partners.org/images/si55551448_ma.jpg (accessed November 2006).

Breslow, R. and Guo, T. Surface tension measurements show that chaotropic salting-in denaturants are not just water-structure breakers. Proc. Natl. Acad. Sci. USA, 87(1990) 167-169.

Broman, E., Khoo, C. and Taylor, L. S., A comparison of alternative polymer excipients and processing methods for making solid dispersions of a poorly water soluble drug. Int. J. Pharm., 222(2001) 139-151.

Chiou, W.L., and Riegelman, S., Pharmaceutical applications of solid dispersion systems. J. Pharm. Sci., 60(1971) 1281 - 1302.

Corrigan, O. I., Mechanisms of dissolution of fast release solid dispersions. Drug Dev. Ind. Pharm. 11(1985) 697-724.

Corrigan, O. I., Retardation of polymeric carrier dissolution by dispersed drugs: factors influencing the dissolution of solid dispersions containing polyethylene glycols. Drug Dev. Ind. Pharm. 12(1986), 1777-1793.

Craig, D.Q.M., The mechanisms of drug release from solid dispersions in water-soluble polymers. Int. J. Pharm., 231(2002) 131-144.

Curtis, H. and Barnes, S. Invitation to Biology. 5th Edition. New York: Worth, 1994. pp. 529

Davis, S.S., Hardy, J.G. and Fara, J.G., Transit of pharmaceutical dosage forms through the small intestine. Gut, 27(1986) 886-892.

Dawson, M., Braithwaite, P.A., Roberts M.S. and Watson T.R., The pharmacokinetics and bioavailability of a tracer dose of [3H]-mebendazole in man. Br. J. Clin. Pharmacol. 19(1985) 79–86.

Desai, M. A. and Vadgama, P. M., Biocarbonate and other buffer systems can enhance the rate of hydrogen ion diffusion through mucus *in vitro*. Biochim. Biophys. Acta., 1116(1992) 43-49.

Diem, K. and Lentner, Documents Geigy: Scientific Tables Geigy Pharmaceuticals, Ardsley, New York, 7th edition, 1970, p. 651.

Dillard R.L., Eastman H. and Fordtran J.S., Volume-flow relationship during the transport of fluid through the human small intestine. Gastroenterology, 49(1965) 58-66.

Dressman, J.B., Amidon, G.L. and Fleisher D., Absorption potential: estimating the fraction absorbed for orally administered compounds, J. Pharm. Sci. 74(1985) 588–589.

Dressman, J.B. and Fleisher, D., Mixing tank model for predicting dissolution rate control of oral absorption. J. Pharm Sci., 75(1986) 109-116.

Dressman, J.B., Berardi, R.R., Dermentzoglou, L.C., Russell, T.L., Schmaltz, S.P., Barnett, J.L. and Jarvenpaa, K.M., Upper gastrointestinal pH in young, healthy men and women, Pharm. Res., 7(1991) 756–761.

Dressman, J.B., Amidon, G.L., Reppas, C., Shah, V.P., Dissolution testing as a prognostic tool for oral drug absorption: Immediate release dosage forms. Pharm. Res., 15 (1998) 11-22.

Dressman, J.B., Repas, C., In vitro-in vivo correlations for lipophilic, poorly water-soluble drugs. Eur. J. Pharm. Sci., 11(2000) S73-S80.

Dubois, J. and Ford, J. L., Similarities in the release rates of different drugs from polyethylene glycol 6000 solid dispersions. J. Pharm. Pharmacol., 37(1985) 494-496.

Efentakis, M. and Dressman, J.B., Gastric juice as a dissolution medium: Surface tension and pH. Eur. J. Drug Metab. Pharmacokin., 23(1995) 97–102.

Esnaashari. S., Javadzadeh Y., Batchelor H.K. and Conway, B.R., The use of microviscometry to study polymer dissolution from solid dispersion drug delivery systems. Int. J. Pharm., 292(2005) 227-230.

Evans, D.F., Pye, G., Bramley, R., Clark, A.G., Dyson, T.J. and Hardcastle, J.D., Measurement of gastrointestinal pH profiles in normal ambulant human subjects, Gut, 29(1988) 1035–1041.

Eve, K., Patel, N., Luk, S.Y., Ebbens, S.J. and Roberts, C.J., A study of single drug particle adhesion interactions using atomic force microscopy, Int. J. Pharm., 238(2002) 17–27.

FDA (1997). Guidance for industry – Dissolution testing of immediate release solid oral dosage forms: U.S Department of Health and human services, Food and Drug Administration, Center for Drug Evaluation and Research (CDER).

FDA (1998). Guidance for industry - Immediate release oral dosage forms. Scale-up and post-approval changes: Chemistry, manufacturing and controls, in-vitro dissolution testing, and in vivo bioequivalence: U.S Department of Health and human services, Food and Drug Administration, Center for Drug Evaluation and Research (CDER).

FDA (2000). Guidance for industry - Waiver of In Vivo Bioavailability and Bioequivalence Studies for Immediate-Release Solid Oral Dosage Forms Based on a Biopharmaceutics Classification System. , Food and Drug Administration, Center for Drug Evaluation and Research (CDER).

Feinblatt, T.M. and Ferguson Jr., E.A., Timed disintegration capsules: an *in vivo* roentgenographic study. N. Engl. J. Med., 254(1956) 940-945.

Fell, J. T. and Mohammad, H. A. H., The wetting of powders by bile salt solutions and gastric juice. Int. J. Pharm., 125(1995) 327-330.

Fleisher, D., Bong. R. and Stewart, B.H., Improved oral drug delivery: solubility limitations overcome by the use of prodrugs. Adv. Drug Deliver. Rev., 19(1996) 115-130.

Florence, A.T. and Attwood, D., Physicochemical principles in pharmacy. Basingstoke: Macmillan Press 1988 (pp. 121–170).

Ford J.L. and Rubenstein M.H., The effect of composition and ageing on the dissolution rate of chlorpropamide-urea solid dispersion. J. Pharm. Pharmacol., 29(1977) 688–694.

Ford, J. L. and Rubenstein, M. H., Phase equilibria and dissolution rates of indomethacin-polyethylene glycol 6000 solid dispersions. Pham. Acta Helv., 53(1978) 327-332.

Ford, J.L., The current status of solid dispersions. Pharm. Acta Helv., 61(1986). 69 - 88.

Forster, A. Hempenstall, J. and Rades T., Internet J. Vib. Spec., http://www.ijvs.com/volume5/edition2/section3.html (accessed on November 2006)

Fox, S. I., Human Physiology. WCB Publishers, 5th edition, 1996 (pp.543–552)

Galia, E., Nicolaides, E., Hörter, D., Löbenberg, R., Reppas, C., Dressman, J. B., Evaluation of various dissolution media for predicting *in vivo* performance of class I and class II drugs. Pharm. Res., 15(1998) 698-705.

Galia, E., Horton, J. and Dressman, J. B., Albendazole generics – a comparative *in vitro* study. Pharm. Res., 16(1999) 1871-1875.

Galia, E., Physiologically based dissolution tests- experiences with poorly soluble drugs. PhD thesis, Johann Wolfgang Goethe-Universität Frankfurt am Main 1999.

Goldberg, A.H., Gibaldi, M., Kanig, J.L., Increasing dissolution rates and gastrointestinal absorption of drugs via solid solutions and eutectic mixtures I - theoretical considerations and discussion of the literature. J. Pharm. Sci., 54(1965) 1145 - 1148.

Goldberg, A. H., Gibaldi, M., Kanig, J. L. and Mayersohn, M., Increasing dissolution rates and gastrointestinal absorption of drugs *via* solid solution and eutectic mixtures IV chloramphenicol-urea system. J. Pharm. Sci., 55(1966) 581-583.

Grass, M., Simulation models to predict oral drug absorption from in vitro data. Adv. Drug Deliv. Rev., 23(1997) 199–219.

Grassi, M., Colombo, I. and Lapasin R., Drug release from an ensemble of swellable crosslinked polymer particles. J. Control. Release, 68(2000) 97-113.

Grdadolnik, J. and Maréchal, Y., Urea and urea – water solutions – an infrared. J. Mol. Struct., 615(2002) 177-189.

Hasegawa, A., Kawamura, R., Nakagawa, H. and Sugimoto, I., Dissolution mechanism of solid dispersions of nifedipine with enteric coating agents. J. Pharm. Sci. Technol., 106(1985) 586-592.

Hasegawa, S., Hamaura, T., Furuyama, N., Kusai, A., Yonemochi, E. and Terada, K., Effects of water content in physical mixture and heating temperature on crystallinity of troglitazone-PVP K30 solid dispersions prepared by closed melting method. Int. J. Pharm., 302(2005) 103-112.

Hidalgo, M., Reinecke, H. and Mijangos, C., PVC containing hydroxyl groups II. Characterisation and properties of crosslinked polymers. Polymer, 40(1999) 3535-3543.

Higuchi, W.I., Mir, N.A. and Desai, D.J., Dissolution rates of polyphase mixtures. J. Pharm. Sci., 54(1965) 1405-1410.

Higuchi, W.I., Diffusional models useful in biopharmaceutics. J. Pharm. Sci., 56(1967) 315-324.

Hirayama, F., Wang, Z. and Uekama, K., Effect of 2-hydroxypropyl-B-cyclodextran on crystallisation and polymorphic transition of nifedipine in solid state. Pharm. Res., 11(1994) 1766 – 1770.

Hilton, J. E., Summers, M. P., The effect of wetting agents on the dissolution of indomethacin solid dispersion systems. Int. J. Pharm., 31(1986) 157 - 164.

Hino, T., and Ford, J.L., Characterisation of the hydroxypropylmethylcellulose-nicotinaamide binary system. Int. J. Pharm., 219(2001) 39-49.

Hörter, D. and Dressman, J.B., Influence of physicochemical properties on dissolution of drugs in the gastrointestinal tract. Adv. Drug Deliv. Rev., 46(2001) 75-87.

Hourston, D.J., Song, M., Schafer, F.-U., Pollock, H.M. and Hammiche, A., Modulated-temperature differential scanning calorimetry: 15. Crosslinking in polyurethane-poly(ethyl methacrylate) interpenetrating polymer networks. Polymer, 40(1999) 4769-4775.

Hunter, E., Fell, J.Y. and Sharma, H., The gastric emptying of pellets in hard gelatine capsules. Drug. Dev. Ind. Pharm., 8(1982) 751-757.

Idrissi, A., Molecular structure and dynamics of liquids: aqueous urea solutions. Spectrochim. Acta, A, 61(2005) 1–17.

Itai, S., Nemoto, M., Kouchiwa, S., Murayama H. and Nagai, T., Influence of wetting factors on the dissolution behavior of flufenamic acid. Chem. Pharm. Bull., 33(1985) 5464–5473.

Iwanaga, K., Ono, S., Narioka, K., Morimoto, K., Masawo, K., Yamashita, S., Nango, M. and Oku, N., Oral delivery of insulin using surface coating liposomes. Improvement of stability of insulin in GI tract, Int. J. Pharm., 157(1997) 73–80.

Jachowicz, R., and Nürenburg, E., Enhanced release of oxapam from tablets containing solid dispersions. Int. J. Pharm., 159(1997) 149 – 158.

Jung, J., Yoo, S.D., Lee, S., Kim, K., Yoon, D., and Lee, K., Enhanced

solubility of itraconazole by a solid dispersion technique. Int. J. Pharm., 187(1999) 209 – 218.

Kerlin, P. and Phillips, S.F., Diffential transit of liquids and solid residue through the human ilieum., Am. J. Physiol. 245(1983) G38-G43.

Kai, T., Akiyama, Y., Nomura, S. and Sato, M., Oral absorption improvement of poorly soluble drug using solid dispersion technique. Chem. Pharm. Bull., 44(1996) 568-571.

Kalampokis, A., Argyrakis P. and Macheras P., Heterogeneous tube model for the study of small intestinal transit flow. Pharm. Res., 16(1999) 87–91.

Kanig, J.L. (1964). Properties of fused mannitol in compressed tablets. J. Pharm. Sci., 53(1964)188 - 192.

Katori, N., Aoyagi, N. and Terao, T., Estimation of agitation intensity in the GI tract in humans and dogs based on *in-vitro in vivo* correlation. Pharm. Res. 12(1995) 237-243.

Kobayashi, M., Sada, N., Sugawara, M., Iseki K. and Miyazaki, K., Development of a new system for prediction of drug absorption that takes into account drug dissolution and pH change in the gastro-intestinal tract. Int. J. Pharm., 221(2001) 87–94.

Kondo, N., Iwao, T., Hirai, K., Fukuda, M., Yamanouchi, K., Yokoyama, K., Miyaji, M., Ishihara, Y., Kon, K., Ogawa Y. and Mayumi, T., Improved oral absorption of enteric coprecipitates of a poorly soluble drug. J. Pharm. Sci., 83(1994) 566–570.

Kukura, J., Baxter J.L. and Muzzio, F.J., Shear distribution and variability in the USP apparatus 2 under turbulent conditions. Int. J. Pharm. 26(2004) 9–17.

Lane, M.E., Levis, K.A. and Corrigan, O.I., Effect of intestinal fluid flux on ibuprofen absorption in the rat intestine. Int. J. Pharm., 309(2006) 60-66.

Levis, K.A., Lane, M.E. and Corrigan, O.I., Effect of buffer media composition on the solubility and effective permeability coefficient of ibuprofen. Int. J.

Pharm., 253(2003) 49-59.

Lin, S., Menig, J. and Lachman, L., Interdependence of physiological surfactant and drug particle on the dissolution behaviour of water insoluble drugs. J. Pharm. Sci., 57(1968) 2143-2148.

Lennernas, H., Human intestinal permeability. J. Pharm. Sci., 87(1998) 403-410.

Leuner, C., Dressman, J., Improving drug solubility for oral delivery using solid dispersions. Eur. J. Pharm. and BioPharm., 50(2000) 47-60.

Lheritier, J., Chauvet, A., Abramovici B. and Masse J., Improvement of the dissolution kinetics of SR 33557 by means of solid dispersions containing PEG 6000. Int. J. Pharm., 123(1995) 273–279.

Löbenberg, R. and Amidon, G.L., Modern bioavailability, bioequivalence and biopharmaceutics classification system. New scientific approaches to international regulatory standards. Eur. J. Pharm. Biopharm., 50(2000) 3-12.

Löbenburg, R., Krämer, J., Shah, V.P., Amidon, G.L. and Dressman, J.B., Dissolution Testing as a Prognostic Tool for Oral Drug Absorption: Dissolution Behavior of Glibenclamide. Pharm.Res., 17(2000) 439-444.

Luner, P.E., Babu, S.R. and Mehta, S.C., Wettability of a hydrophobic drug by surfactant solutions. Int. J. Pharm., 128(1996) 29-44.

Luner, P. E. and Van Der Kamp, D., Wetting behaviour of bile salt-lipid dispersions and dissolution media patterned after intestinal fluids. J. Pharm. Sci., 90(2001) 348-359.

Malagelada, J.R., Robertson, J.S., Brown, M.L., Remmington, M., Duenes, J.A. and Thomforde, G.M., Intestinal transit of solid and liquid components of a meal in health. Gastroenterology, 87(1984) 1255-1263.

Marizo, L., Neri, F., Capone, F., Di Felice, F., De Angelis, C., Mezzeti, A. And Cuccurullo, F., Gallbladder contraction and its relationship to interdigestive duodenal motor activity in normal human subjects. Digest. Dis. Sci., 33(1988)

540-544.

McGregor, C., Saunders, M.H., Buckton, G. and Saklatvala, The use of high-speed differential scanning calorimetry (Hyper-DSC™) to study the thermal properties of carbamazepine polymorphs. Thermochim. Acta, 417(2004) 231-237.

Moore, J. W. and Flanner, H. H., Mathematical comparison of dissolution profiles. Pharm. Technol., 20(1996) 64-74.

Morris, K. R., Knipp, G. T. and Serajuddin, A. T. M., Structual properties of polyethylene glycol-polysorbate 80 mixture, a solid dispersion vehicle. J. Pharm. Sci., 81(1992) 1185-1188.

Mura, P., Manderioli, A., Bramanti G. and Ceccarelli L., Properties of solid dispersions of naproxen in various polyethylene glycols. Drug. Dev. Ind. Pharm., 22(1996) 909–916.

Mura, P., Faucci, M. T., Manderioli, A., Bramanti, G. and Parrini, P., Thermal behaviour and dissolution properties of naproxen from binary and ternary solid dispersions. Drug Dev. Ind. Pharm., 25(1999) 257-264.

Mosharraf M., Sebhatu T. and Nystrom C., The effects of disordered structure on the solubility and dissolution rates of some hydrophilic, sparingly soluble drugs. Int. J. Pharm., 177(1999) 29–51.

Newarkbioweb. http://newarkbioweb.rutgers.edu/bio360/cholesterol.htm. (accessed 2006)

Nielsen L.S., Sløk F. and Bundgaard H., *N*-alkoxycarbonyl prodrugs of mebendazole with increased water-solubility. Int. J. Pharm., 102(1994) 231–239.

Norris, D. A., Leesman, G. D., Sinko, P. J. and Grass, G. M. Development of predictive pharmacokinetic simulation models for drug discovery. J. Control. Release, 65(2000) 55-62.

Nicolaides E, Symillides M, Dressman JB, Reppas C.Biorelevant dissolution

testing to predict the plasma profile of lipophilic drugs after oral administration. Pharm Res., 18(2001) 380-388.

Oberle, R.L., Chen, T.S., Lloyd, C., Barnett, J.L., Owyang, C., Meyer J. and Amidon G.L., The influence of the interdigestive migrating myoelectric complex on the gastric emptying of liquids. Gastroenterology, 99(1990) 1275–1282.

Pandit, J.K. and Khakurel, B.K., In vitro and in vivo evaluation of some fast release dosage forms of hydrochlorothiazide. Drug Dev Ind Pharm., 10(1984) 1709–1724.

Pantoja, J.L., Defilippi, C., Valenzuela, J.E. and Csendes, A., Nonsteroidal antiinflammatory drugs: Effect on pyloric sphincter and duodenogastric reflux. Digest. Dis. Sci., 24(1979) 217-220.

Paradkar, A., Ambike, A. A., Jadhav, B.K., and Mahadik, K.R., Characterization of curcumin-PVP solid dispersion obtained by spray drying. Int. J. Pharm., 271(2004) 281-286.

Parker, J. C., Troglitazone: the discovery and development of a novel therapy for the treatment of Type 2 diabetes mellitus. Adv. Drug Deliver. Rev., 54(2002) 1173-1197.

Peters, T.L., Vantrappen, G. and Janssens, J., Bile acid output and the interdigestive migrating motor complex in normals and in cholecystectomy patients. Gastroenterology., 79(1980) 678-681.

Pidgeon, C. and Pitlick, W.H., Unique approach for calculation of absorption rate constant. Res. Commun. Chem. Path., 18(1977) 467-475.

Pitha, J. and Pitha, J., Amorphous water soluble derivatives of cyclodextrins: nontoxic dissolution enhancing excipients. J. Pharm. Sci., 74(1985) 987-990.

Polli, J.E., Rekhi, G.S., Augsburger, L.L. and Shah, V.P., Methods to compare dissolution profiles and a rationale for wide dissolution specifications for metoprolol tartate tablets. J. Pharm. Sci., 86(1997) 690-696

Rees, W. D. W., Mucus-biocarbonate barrier-shield or sieve. Gut, 28(1987) 1553-1556.

Riedl, Z., Szklenárik, Gy., Zelkó, R., Marton, S. and Rácz, I., The effect of temperature and polymer concentration on dynamic surface tension and wetting ability of hydroxypropylmethylcellulose solutions. Drug Dev. Ind. Pharm., 26(2000) 1321-1323.

Russell, T.L., Berardi, R.R., Barnett, J.L., Dermentzoglou, L.C., Jarvenpaa, K.M., Schmaltz, S.P. and Dressman, J.B., Upper gastrointestinal pH in 79 healthy, elderly, North American men and women, Pharm. Res., 10(1993) 187–196.

Sanford, P. A., Digestive system physiology, Edward Arnold, 1st edition, 1982 (pp. 36–38).

Schachter, D.M., Xiong, J. and Tirol, G.C., Solid state NMR perspective of drug–polymer solid solutions: a model system based on poly(ethylene oxide). Int. J. Pharm., 281(2004) 89-101.

Sekiguchi, K. and Obi, N., Studies on absortion of eutectic mixture. I. A comparison of the behaviour of eutectic mixture of sulfathiazole and that of ordinary sulfathiazole in man. Chem. Pharm. Bull., 9(1961) 866-872.

Sekiguchi, K., Obi, N. and Ueda, Y., Studies on absorption of eutectic mixtures II. Absorption of fused conglomerates of chloramphenicol and urea in rabbits. Chem. Pharm. Bull., 12(1964) 134–144.

Sekikawa, H., Nakano., M. and Arita, T., Inhibitory effect of polyvinylpyrrolidone on the crystallization of drugs. Chem. Pharm. Bull., 26(1978) 118- 126.

Serajuddin, A. T. M., Improved dissolution of a poorly water-soluble drug from solid dispersions in polyethylene glycol:polysorbate 80 mixtures. J. Pharm Sci., 79(1990) 493-484.

Serajuddin, A.T. M., Solid dispersions of poorly water soluble drugs: early

promises, subsequent problems, and recent breakthroughs. J. Pharm. Sci., 88(1999) 1058-1065.

Sertsou, G., Butler, J., Scott, A., Hempenstall, J. and Rades, T., Factors affecting incorporation of drug into solid solution with HPMCP during solvent change co-precipitation. Int. J. Pharm., 245(2002) 99-108.

Sertsou, G., Butler, J., Hempenstall, J. and Rades, T., Solvent change co-precipitation with hydroxypropyl methylcellulose phthalate to improve dissolution characteristics of a poorly water-soluble drug. J. Pharm. Pharma, 54(2002) 1041-1047.

Shah, P., Tsong, Y., Sathe, P. and Lie, J., *In vitro* dissolution profile comparison—statistics and analysis of the similarity factor, f_2, Pharm. Res., 15(1998) 889–896.

Sheen, P. C.; Kim, S. I.; Petillo, J. J.; Serajuddin, A. T. M. Bioavailability of a poorly water-soluble drug from tablet and solid dispersion in humans. J. Pharm. Sci., 80(1991) 712-714.

Shibata, M., Kokubo, H., Morimoto, K., Morisaka, K., Ishida T. and Inoue, M., X-Ray structural studies and physicochemical properties of cimetidine polymorphism. J. Pharm. Sci., 72(1983) 1436–1442.

Shriver, D.F. and Atkins, P.W., Inorganic chemistry. W.H. Freeman & Company; 3rd edition 1999 (pp. 154).

Simonelli, A. P., Metha, S. C., Higuchi, W. I., Dissolution rates of high energy polyvinylpyrrolodine (PVP) - sulfathiazole coprecipitates. J. Pharm. Sci., 58(1969) 538 - 549.

Simonelli, A. P., Metha, S. C., Higuchi, W. I., Inhibition of sulfathiazole crystal growth by polyvinylpyrrolidone. J. Pharm. Sci., 59(1970) 633-637.

Simonelli, A.P., Mehta, S.C. and Higuchi, W.I., Dissolution rates of high energy sulfathiazole-povidone coprecipitates II: characterization of form of drug controlling its dissolution rate via solubility studies. J. Pharm. Sci.,

65(1976) 355–361.

Sjökvist E. and Nyström, C., Physicochemical aspects of drug release. VI. Drug dissolution rate from solid particulate dispersions and the importance of carrier and drug particle properties, Int. J. Pharm., 47(1988) 51–66.

Sjökvist, E., Nyström, C. and Aldén, M., Physicochemical aspects of drug release. XIII. The effect of sodium dodecyl sulphate additions on the structure and dissolution of a drug in solid dispersions. Int. J. Pharm., 69(1991) 53-62.

Sjökvist Saers, E., Craig, D. Q. M., An investigation into the mechanisms of dissolution of alkyl *p*-aminobenzoates from polyethylene glycol solid dispersions. Int. J. Pharm., 83(1992) 211-219.

Smith, A., Use of thermal analysis in predicting drug-excipient interactions. Anal. Proc., 19(1982) 559–561.

Suzuki, H. and Sunada, H., Influence of water soluble polymers on the dissolution of nifedipine solid dispersions with combined carriers. Chem. Pharm. Bull., 46(1998) 482-487.

Suzuki, N., Kasahara, K., Hasegawa, H. and Kawasaki, T., Physical property of troglitazone, an equal mixture of four stereoisomers. Int. J. Pharm., 248(2002) 71-80.

Tangerman, A., van Schaik, A. and van der Hoek, E.W., Analysis of conjugated and unconjugated bile acids in serum and jejunal fluid of normal subjects. Clin. Chim. Acta, 159(1986) 123-132.

Tanno, F., Nishiyama, Y., Kokubo H. And Obara S., Evaluation of hypromellose acetate succinate (HPMCAS) as a carrier in solid dispersions. Drug Dev. Ind. Pharm., 30(2004) 9-17.

Tantishaiyakul, V., Kaewnopparat, N. and Ingkatawornwong, S., Properties of solid dispersions of piroxicam in polyvinylpyrrolidone. Int. J. Pharm. 30(1999) 143–151.

Taylor, L.S. and Zografi, G., Spectroscopic characterization of interactions

between PVP and indomethacin in amorphous molecular dispersions. Pharm. Res., 14(1997) 1691 - 1698.

Tejwani, R. W., Joshi, H. N., Varia, S. A. and Serajuddin, A. T. M., Study of phase behaviour of poly(ethylene glycol)-polysorbate 80 and poly(ethylene glycol)-polysorbate 80-water mixtures. J. Pharm. Sci., 89(2000) 946-950.

USA (1995). The United States Pharmacopia (USP 23). Rockville USA: United States Pharmacopeial Convention (pp. 1927-1929).

Usansky, J.I., Desai, A., and Tang-Liu, D., PK Functions for Microsoft Excel, Department of Pharmacokinetics and Drug Metabolism, http://www.boomer.org/pkin/soft.html, accessed on November 2006.

Usui, F., Maeda, K., Kusai, A., Ikeda, M., Nishimura K. and Yamamoto, K., Inhibitory effects of water-soluble polymers on precipitation of RS-8359. Int. J. Pharm., 154(1997) 59–66.

Valenzuela, J.E. and Defilippi, C., Pyloric-sphincter studies in peptic-ulcer patients: Pylorus in peptic ulcer, Diges. Dis. Sci., 21(1976) 229-232.

Valsami, G., Dokoumetzidis, A. and Macheras P., Modeling of supersaturated dissolution data. Int. J. Pharm., 181(1999) 153-157.

van Berge Henegouwen, G.P. and Hofmann., Nocturnal gallbladder storage and emptying in gallstone patients and healthy subjects. Gastroenterology, 75(1978) 879-885.

Van den Mooter, G., Wuyts, M., Blaton, N., Busson, R., Grobet., Augustijns, P. and Kinget, R., Physical stabilistaion of amorphous ketoconazole in solid dispersions with polyvinylpyrrolidone K25. Eur. J. Pharm. Sci., 12(2001) 261-269.

Vertzoni, M., Dressman, J., Butler, J., Hempenstall, J. and Reppas, C., Simulation of fasting gastric conditions and its importance for the in vivo dissolution of lipophilic compounds. Eur. J. Pharm. Biopharm., 60(2005) 413-417.

Walking, W.D. Povidone. In: A. Wade and P.J. Weller, Editors, Handbook of Pharmaceutical Excipitients, American Pharmaceutical Association/The Pharmaceutical Press, Washington, DC/London 1994 (pp. 392–399).

Washington, N., Washington, C., and Wilson, C.G., Physiological Pharmaceutics-Barriers to Drug Absorption. Taylor and Francis, New York. 2001 (pp. 75-144).

Watanabe, T., Ohno, I., Wakiyama, N., Kusai, A., Isobe, T. and Senna, M., Stabilization of amorphous indomethacin by co-grinding in a ternary mixture. Int. J. Pharm., 241(2002) 103–111.

Wikipedia. http://en.wikipedia.org/wiki/Chenodeoxycholic_acid. (accessed on November 2006)

Wikipedia. http://en.wikipedia.org/wiki/Cholic_acid. (accessed on November 2006)

Williams, S.E., and Turnberg, L.A., Demonstration of a pH gradient across mucus adherent to rabbit gastric mucosa evidence for a 'mucus-biocarbonate' barrier. Gut, 22(1981) 94-96.

Wilson, C. G., Washington, N., Greaves, J. L., Washington, C., Wilding, I. R., Hoadley, T. and Sims E. E., Predictive modeling of the behavior of a controlled release buflomedil HCl formulation using scintigraphic and pharmacokinetic data. Int. J. Pharm., 72(1991) 79-86.

Young, D., Devane, J.G., and Butler, J., Editors, In Vitro–In Vivo Correlations. Advances in Experimental Medicine and Biology. Plenum Press, New York 1997 (pp. 275-277).

Appendix 1 – HPLC trace of troglitazone

JCL6000 for Windows 2.0 Chromatography Data System

Date : 22/11/2001 Time : 18:12:51 Date Acquired : 22/11/2001 Time Acquired : 18:5:59
Channel : 2 Sample Type : Unk Data File : c:\jcldata\SOLUB1.WD2 Configuration : C:\JCLMETH\NEWTROG
Run Number 1 of 33 Chan 2 Desc. : Detector1, Channel #2
Sample Name : STD1

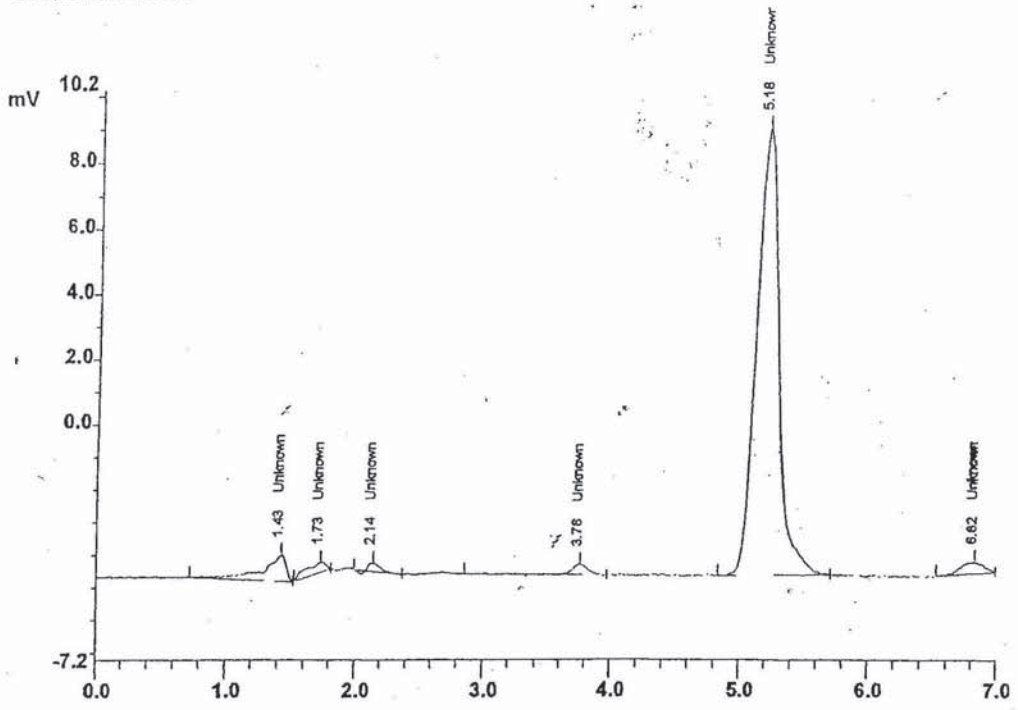

Pk #	Ret. Time	Hgt.	Height %	Area	Area %	Modified Response	Response Ratio	Solution Conc.	Qfy	Derived Result	Component Name
1	1.42	415	5.02	10324	5.24	N/A	0	N/A		N/A	UNKNOWN
2	1.73	158	1.91	3690	1.87	N/A	0	N/A		N/A	UNKNOWN
3	2.14	137	1.65	1780	0.90	N/A	0	N/A		N/A	UNKNOWN
4	3.76	166	2.01	3074	1.56	N/A	0	N/A		N/A	UNKNOWN
5	5.18	7193	87.11	173332	88.01	N/A	0	N/A		N/A	UNKNOWN
6	6.82	189	2.29	4755	2.41	N/A	0	N/A		N/A	UNKNOWN

Total Height % 100.00
Total Area % 100.00
Total Height 8257
Total Area 196955

Area used for calculations.
Modified response has been scaled to internal standard.

Appendix 2 – HPLC trace of atovaquone

Appendix 3 – Performance testing of troglitazone HPLC method – method 1

Day	Measured concentration of samples (mg/ml)				
	Sample 1	Sample 2	Sample 3	Sample 4	Sample 5
1	0.075	0.075	0.076	0.076	0.076
2	0.075	0.076	0.075	0.073	0.076
3	0.076	0.073	0.075	0.074	0.074

Day 1

Mean: 0.076 mg/ml

Standard Deviation: 0.001

Relative standard deviation ((SD/Mean)*100): 0.72%

Day 2

Mean: 0.075 mg/ml

Standard Deviation: 0.001

Relative standard deviation ((SD/Mean)*100): 1.63%

Day 3

Mean: 0.074 mg/ml

Standard Deviation: 0.001

Relative standard deviation ((SD/Mean)*100): 1.53%

Combained days

Mean: 0.075 mg/ml

Standard Deviation: 0.001

Relative standard deviation ((SD/Mean)*100): 1.43%

Appendix 4 – Performance testing of troglitazone HPLC method – method 2

Day	Measured concentration of samples (μg/ml)				
	Sample 1	Sample 2	Sample 3	Sample 4	Sample 5
1	5.51	5.54	5.44	5.52	5.47
2	5.55	5.57	5.47	5.46	5.5
3	5.52	5.46	5.51	5.52	5.53

Day 1

Mean: 5.50 mg/ml

Standard Deviation: 0.04

Relative standard deviation ((SD/Mean)*100): 0.73%

Day 2

Mean: 5.51 mg/ml

Standard Deviation: 0.05

Relative standard deviation ((SD/Mean)*100): 0.88%

Day 3

Mean: 5.51 mg/ml

Standard Deviation: 0.03

Relative standard deviation ((SD/Mean)*100): 0.50%

Combained days

Mean: 5.50 mg/ml

Standard Deviation: 0.04

Relative standard deviation ((SD/Mean)*100): 0.68%

Appendix 5 – Performance testing of atovaquone HPLC method

Day	Measured concentration of samples (µg/ml)				
	Sample 1	Sample 2	Sample 3	Sample 4	Sample 5
1	3.54	3.62	3.48	3.57	3.45
2	3.38	3.47	3.52	3.51	3.42
3	3.44	3.48	3.56	3.58	3.55

Day 1

Mean: 3.53 µg/ml

Standard Deviation: 0.07

Relative standard deviation ((SD/Mean)*100): 1.93%

Day 2

Mean: 3.46 µg/ml

Standard Deviation: 0.06

Relative standard deviation ((SD/Mean)*100): 1.72%

Day 3

Mean: 0.074 µg/ml

Standard Deviation: 0.06

Relative standard deviation ((SD/Mean)*100): 1.68%

Combained days

Mean: 3.50 µg/ml

Standard Deviation: 0.07

Relative standard deviation ((SD/Mean)*100): 1.90%

Appendix 6 – Comparison of solid dispersion dissolution (HPMCP) to physical mixtures and troglitazone alone, in FaSSIF

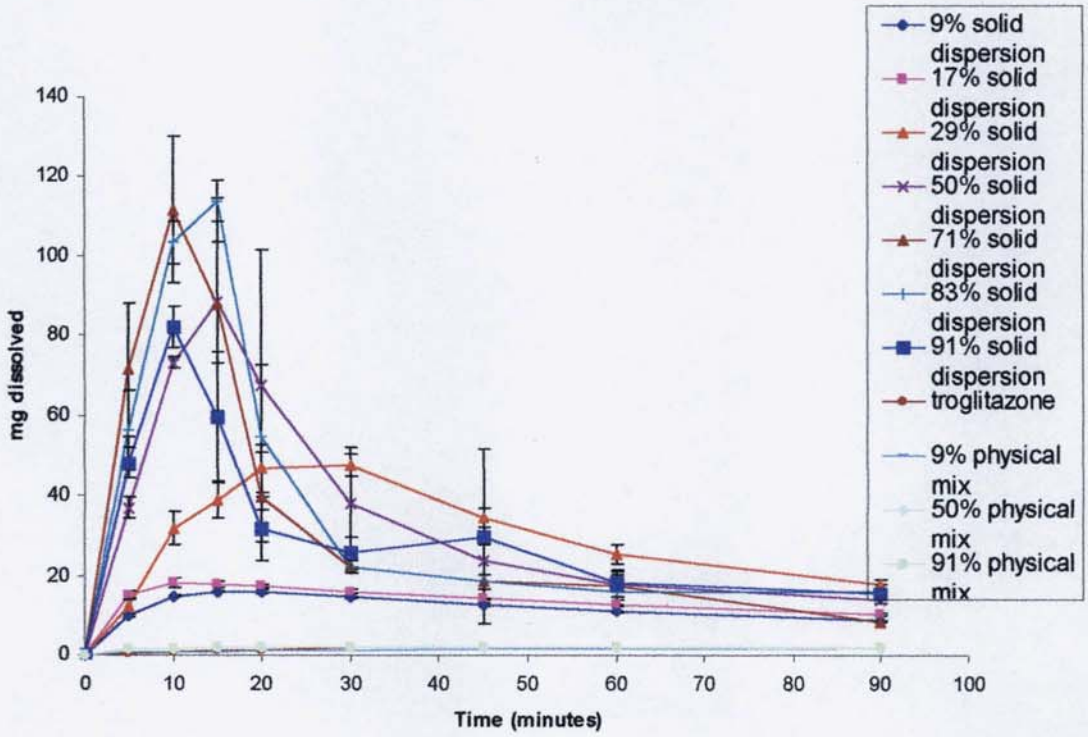

Appendix 7 – Comparison of solid dispersion dissolution (HPMC) to physical mixtures and troglitazone alone, in FaSSIF

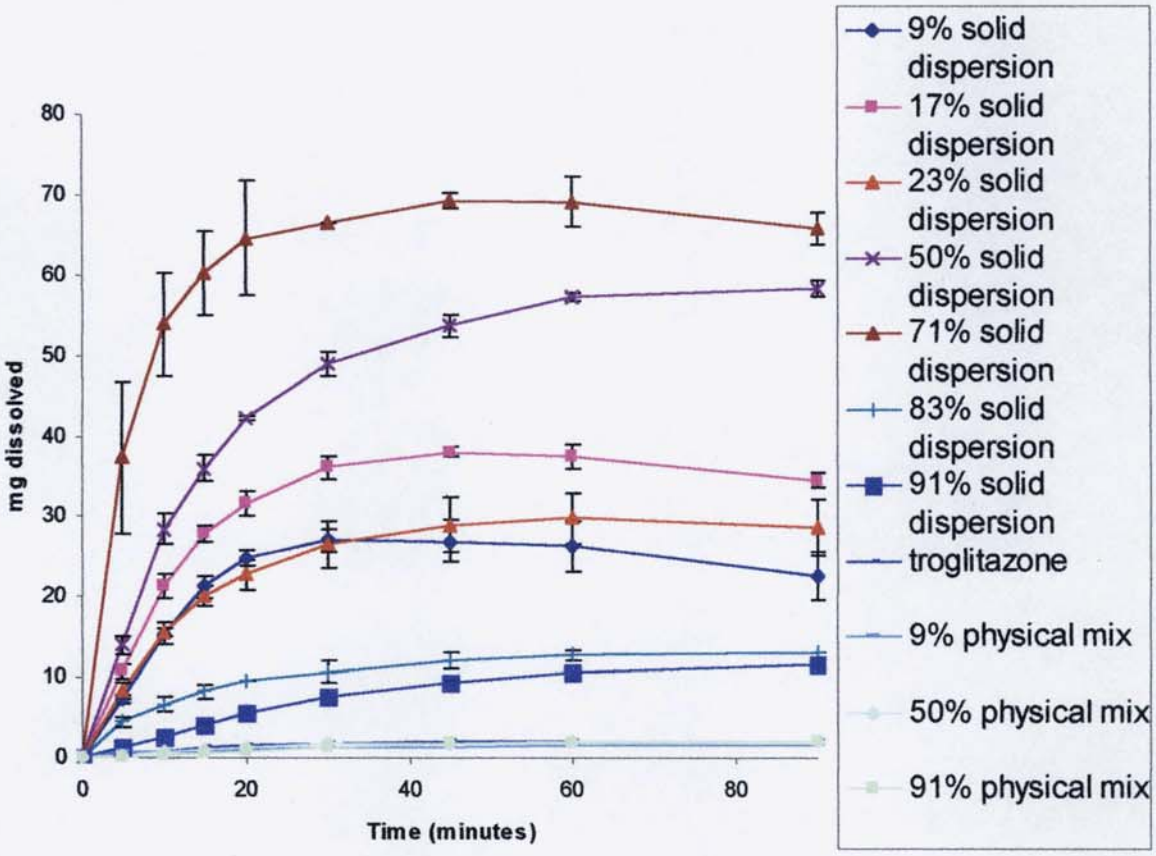

Appendix 8 – Comparison of solid dispersion dissolution (HPMCP) to physical mixtures and troglitazone alone, in FaSSIF

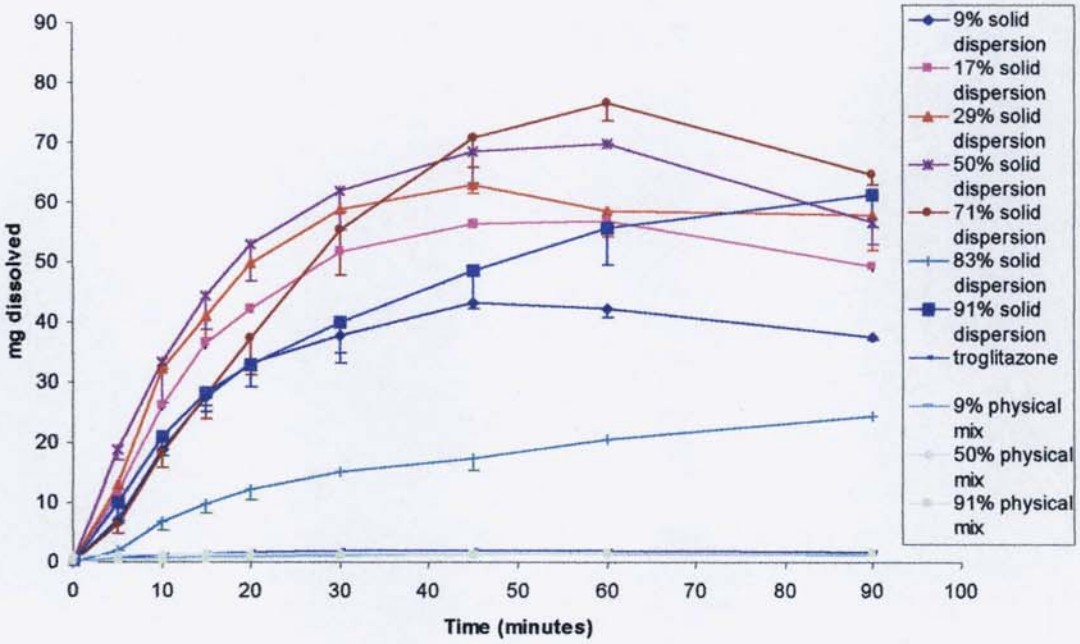

Appendix 9 – Sample spreadsheet for the calculation of dissolution results

Conc mg/ml	Peak area
0.005	
0.025	
0.05	
0.1	
0.15	
0.2	

				Slope	=SLOPE(F4:F9,E4:E9)
				Intercept	=INTERCEPT(F4:F9,E4:E9)
				R^2	=CORREL(F4:F9,E4:E9)
time	peak	conc mg/ml	conc mg/500ml	AUC	AUC
0		=($C15-$G$12)/$G$11	0		
5		=(($C16-$G$12)/$G$11)*2	=500*$D16	=(E16+E15)*(B16-	=F16+G15
10		=(($C17-$G$12)/$G$11)*2	=500*$D17+(4*SUM(D10:D16))	=(E17+E16)*(B17-	=F17+G16
15		=(($C18-$G$12)/$G$11)*2	=500*$D18+(4*SUM(D11:D17))	=(E18+E17)*(B18-	=F18+G17
20		=(($C19-$G$12)/$G$11)*2	=500*$D19+(4*SUM(D12:D18))	=(E19+E18)*(B19-	=F19+G18
30		=(($C20-$G$12)/$G$11)*2	=500*$D20+(4*SUM(D13:D19))	=(E20+E19)*(B20-	=F20+G19
45		=(($C21-$G$12)/$G$11)*2	=500*$D21+(4*SUM(D14:D20))	=(E21+E20)*(B21-	=F21+G20
60		=(($C22-$G$12)/$G$11)*2	=500*$D22+(4*SUM(D15:D21))	=(E22+E21)*(B22-	=F22+G21
90		=(($C23-$G$12)/$G$11)*2	=500*$D23+(4*SUM(D16:D22))	=(E23+E22)*(B23-	=F23+G22

Appendix 10 – Calculation of the f_2 value

Time point	1	2	3	4	5	6	7	8
Rn-Tn	=C6-C5	=D5-D6	=E5-E6	=F5-F6	=G5-G6	=H5-H6	=I5-I6	=J5-J6
$(Rn-Tn)^2$	=C7^2	=D7^2	=E7^2	=F7^2	=G7^2	=H7^2	=I7^2	=J7^2
$\sum (Rn-Tn)^2$								=SUM(D8:G8)
1/n								=1/4
$1/n \sum(Rn-Tn)^2$								=J9*J10
$1+(1/n \sum(Rn-Tn)^2)$								=J11+1
$(1+(1/n \sum(Rn-Tn)^2))^{-0.5}$								=J12^-0.5
$(1+(1/n \sum(Rn-Tn)^2))^{-0.5}*100$								=J13*100
Log **$((1+(1/n \sum(Rn-Tn)^2))^{-0.5}*100)$**								=LOG(J14)
F_2=50 Log **$((1+(1/n \sum(Rn-Tn)^2))^{-0.5}*100)$**								=50*(J15)